THE ROLE OF CLAUDIN-5 IN THE PROGRESSION OF HUMAN BREAST CANCER

by

Astrid Escudero-Esparza

A dissertation submitted to Cardiff University in candidature for the degree

of

Doctor of Philosophy

Metastasis and Angiogenesis Research Group,

University Department of Surgery,

Cardiff School of Medicine,

Cardiff University.

September 2010

ProQuest LLC
789 East Eisenhower Parkway
P.O. Box 1346
Ann Arbor, MI 48106-1346

APPENDIX 1:

DECLARATION

This work has not previously been accepted in substance for any degree and is not concurrently submitted in candidature for any degree.

Signed ..... (candidate) Date 18/11/10

STATEMENT 1

This thesis is being submitted in partial fulfillment of the requirements for the degree of PhD.

Signed ..... (candidate) Date 18/11/10

STATEMENT 2

This thesis is the result of my own independent work/investigation, except where otherwise stated.
Other sources are acknowledged by explicit references.

Signed ..... (candidate) Date 18/11/10

STATEMENT 3

I hereby give consent for my thesis, if accepted, to be available for photocopying and for inter-library loan, and for the title and summary to be made available to outside organisations.

Signed ..... (candidate) Date 18/11/10

STATEMENT 4: PREVIOUSLY APPROVED BAR ON ACCESS

I hereby give consent for my thesis, if accepted, to be available for photocopying and for inter-library loans **after expiry of a bar on access previously approved by the Graduate Development Committee.**

Signed ..... (candidate) Date .....

DEDICATION

I dedicate this thesis to my family for their endless love, support and much needed patience throughout the period of study.

ACKNOWLEDGEMENTS

I would like to thank my supervisors Professor W.G. Jiang and Dr. Tracey Martin for the patient guidance, encouragement and advice they have provided throughout my time in the Metastasis and Angiogenesis Research group. I would also like to express my sincere thanks to Dr. Jane Lane and Dr. Andrew Sanders for their encouragement and for proof reading the thesis.

PUBLICATIONS

Full papers

Escudero-Esparza A, Martin TA, Davies ML, Jiang WG. PGF isoforms, PLGF-1 and PGF-2, in colorectal cancer and the prognostic significance. Cancer Genomics Proteomics. 2009 Jul-Aug;6(4):239-46.

Kang H; **Escudero-Esparza A,** Douglas-Jones A, Mansel RE, Jiang WG. Transcript analyses of stromal cell derived factors (SDFs): SDF-2, SDF-4 and SDF-5 reveal a different pattern of expression and prognostic association in human breast cancer. Int J Oncol. 2009 Jul;35(1):205-11.

Escudero-Esparza A, Martin TA, Douglas-Jones A, Mansel RE, Jiang WG. PGF isoforms, PLGF-1 and PGF-2 and the PGF receptor, neuropilin, in human breast cancer: prognostic significance. Oncol Rep. 2010 Feb;23(2):537-44.

Escudero-Esparza A, Martin TA, Jiang WG. The Claudin family and their role in cancer and metastasis. Frontiers in Bioscience (in press).

Escudero-Esparza A, Martin TA, Jiang WG. The role of Claudin-5 in human breast cancer cells (in preparation).

Escudero-Esparza A, Martin TA, Jiang WG. The role of Claudin-5 in human endotheliai cells (in preparation).

Poster presentations

Escudero-Esparza A, Martin TA, Jiang WG. The Role of Claudin-5 and the Paracellular Barrier Function in Endothelial Cells during Invasion of Breast Cancer Cells. 32nd Annual San Antonio Breast Cancer Symposium, Date: DEC 09-13, 2009 San Antonio TX, Cancer Research 2009;69(24): 879S-879S.

Escudero-Esparza A, Martin TA, Jiang WG. Prognostic Significance of Placenta Growth Factor(PIGF)-1 and PGF-2 Expression in Human Breast Cancer. 32nd Annual San Antonio Breast Cancer Symposium, Date: DEC 09-13, 2009 San Antonio TX, Cancer Research 2009;69(24): 659S-659S.

Escudero-Esparza A, Martin TA, Davies ML, Jiang WG. PLGF1 and 2 as prognostic indicators in human colorectal carcinoma. National Cancer Research Institute (NCRI), Oct 2008, Birminham, UK.

Escudero-Esparza A, Martin TA, Jiang WG. Prognostic significance of PlGF-1 and -2 expression in human breast cancer.Wales Cancer Conference 2008. May 2008, Cardiff, UK.

ABBREVIATIONS

ABC	-	avidin biotin complex
AF6	-	MLLT4 (myeloid/lymphoid or mixed-lineage leukemia)
AJ	-	adherens junctions
ANOVA	-	analysis of variance
Arp 2/3	-	actin related protein complex
BBB	-	blood-brain barrier
BBMVC	-	bovine brain microvascular endothelial cells
BRCA	-	breast cancer
BSA	-	bovine serum albumin
BSS	-	balanced salt solution
cAMP	-	cyclic adenosine monophosphate
C-CPE	-	C-terminal fragment of Clostridium perfringens enterotoxin
CCR7	-	chemokine (C-C motif) receptor 7
CDX	-	transcription factor protein
cEND	-	murine brain endothelial cells
Cip1	-	COP1-interactive protein 1
CNS	-	central nervous system
CPE	-	carboxypeptidase E
c-src	-	c-src tyrosine kinase
c-yes	-	Yamaguchi sarcoma viral oncogene homolog
CXCR4	-	chemokine (C-X-C motif) receptor 4

DAB	-	diaminobenzidine
DEPC	-	diethylpyrocarbonate
DMEM	-	dulbecco's modified eagle medium
DMSO	-	dimethylsulphoxide
DTA	-	*diphtheria* toxin A
ECIS	-	electrical cell-substrate impedance sensing
EDTA	-	ethylene diamine tetra-acetic acid
EGF	-	epidermal growth factor
EMT	-	epithelial/ mesenchymal transition
ERβ	-	estrogen receptor beta
ERK1/2	-	extracellular signal-regulated kinase type ½
ES	-	embryonic stem cells
EtOH	-	ethanol
FGF	-	fibroblast growth factor
Flt-IFc	-	vascular endothelial growth factor inhibitor
FoxO1	-	forkhead box O1transcription factor
FRET	-	fluorescence resonance energy transfer
GAPDH	-	glyceraldehyde-3-phosphate dehydrogenase
GATA4	-	GATA binding protein 4
GEF H1	-	Rho/Rac guanine nucleotide exchange factor (GEF) 2
GLA	-	gamma linoleic acid
GTPase	-	guanosine triphosphatase

hCG	-	human chorionic gonadotrophin
HDAC1	-	histone deacetylase 1
HECV	-	human endothelial cell vascular
HGF	-	hepatocyte growth factor/scatter factor
HIV	-	human immunodeficiency virus
HNF-1α	-	hepatocyte nuclear factor-1α
HRP	-	horseradish peroxidase
HUVEC	-	human umbilical vein endothelial cells
I	-	iodate
IGF	-	insulin-like growth factor
IHC	-	immunohistochemistry
ITCH	-	itchy E3 ubiquitin protein ligase homolog
JAMs	-	junctional adhesion molecules
JEAP	-	junction-enriched and -associated protein
LGC	-	luteinized granulosa cells
MAGI	-	membrane associated guanylate kinase
MAGUK	-	membrane associated guanylate kinase
MAPK	-	mitogen-activated protein kinase
MARVEL	-	membrane associated and related proteins for vesicle trafficking and membrane link
MBEC1	-	mouse brain endothelial cell 1
MCF-7	-	Michigan Cancer Foundation-7 cells

MDCK	-	Madin-Darby canine kidney cells
MT1-MMP	-	matrix metallopeptidase 14
MUPP-1	-	multiple PDZ domain protein 1
MyEND	-	microvascular endothelial cells
NPI	-	Nottingham prognostic index
NSCLC	-	non-small cell lung cancer
N-WASP	-	neuronal- Wiskott-Aldrich syndrome protein (human)
OHSS	-	ovarian hyper stimulation syndrome
p16INK4A	-	cyclin-dependent kinase inhibitor 2A (melanoma, p16, inhibits CDK4)
p21IWaf1	-	COP1-interactive protein 1
p27kip1	-	cyclin-dependent kinase inhibitor 1B
Pals	-	protein associated with Lin7
Par	-	protease activated receptor
PATJ	-	Pals1 associated tight junction protein
PCR	-	polymerase chain reaction
PDGF	-	platelet-derived growth factor
PDZ	-	PSD-95/Discs-large/ZO-1
PEG	-	polyethylene glycol oligomers
Pilt	-	pilus retraction motor
PKA	-	cAMP dependent protein kinase
PKC	-	Protein kinase C

PSIF	-	protein synthesis inhibitory factor
PTEN	-	phosphatase and tensin homolog
Rab	-	Ras related protein
Rac	-	Ras-related C3 botulinum toxin substrate
Raf-1	-	v-raf-1 murine leukemia viral oncogene homolog
Rho	-	Ras homologue gene
RLE	-	rat lung endothelial cells
ROCK	-	Rho-associated serine-threonine protein kinase
RT-PCR	-	reverse transcription polymerase chain reaction
RT-QPCR	-	quantitative reverse transcription polymerase chain reaction
SCRIB	-	scribbled homolog
SDS-PAGE	-	sodium dodecyl sulfate polyacrylamide gel electrophoresis
Se	-	selinium
SH3	-	Src-homology domain 3
SOC	-	super optimal broth catabolite repression
SOX18	-	SRY (sex determining region Y)-box 18
TAMP	-	tight junction–associated MARVEL protein
TBE	-	tris-boric acid-EDTA
TBS	-	tris buffered saline
TEMED	-	tetramethylethylenediamine
TER	-	trans-epithelial/endothelial resistance
TJ	-	tight junction

TMVCF	-	transmembrane protein deleted in velo-cardio-facial syndrome
TNFα	-	tumour necrosis factor alpha
TNM	-	tumour node metastasis
Tris	-	Tris (hydroxymethyl) aminomethane
TRITC	-	Tetramethyl Rhodamine Iso-Thiocyanate
TTBS	-	TBS containing TWEEN
TWEEN	-	polysorbate detergent
UICC	-	Union for International Cancer Control
VCF	-	Velo-Cardio-Facial/ DiGeorge syndrome
VEGF	-	vascular endothelial growth factor
WASP	-	Wiskott-Aldrich syndrome protein (murine)
WNK4	-	WNK lysine deficient protein kinase
ZAK	-	Leucine-zipper and sterile-alpha motif kinase
ZO	-	Zona Occludens
ZONA B	-	ZO-1 associated nucleic-acid-binding protein

SUMMARY

A key step in metastasis is the interaction and penetration of the vascular endothelium by cancer cells. Tight Junctions (TJ) are located between the cancer epithelial cells themselves functioning in an adhesive manner, and between the endothelial cells. They represent a critical barrier which the cancer cells must overcome in order to penetrate and initiate metastasis. The Claudin family are TJ proteins expressed in both endothelial and epithelial cells. They participate in the formation of tissue barriers between different tissue compartments by regulating the efflux of molecules through TJ complexes.

This thesis examined the level of expression and distribution of Claudin-5 in human breast cancer tissues and analysed them against clinical parameters. The effect of knockdown and forced expression of Claudin-5 in the MDA-MB-231 aggressive breast cancer cell line and in the HECV human endothelial cell line was also examined. Results revealed that Claudin-5 is aberrantly expressed in human breast cancer and has a link to the clinical outcome of the patient. Patients who died from breast cancer had higher levels of Claudin-5 compared with patients who remained disease-free. Furthermore, patients whose tumours expressed high levels of Claudin-5 had shorter survival than those with low levels.

Investigating *in vitro* the effect of altering levels of expression of Claudin-5 in MDA-MB-231and HECV cells revealed that the role of Claudin-5 was not primarily in keeping the cell barrier tight suggesting little function in the TJ of these cells, in fact a link was identified between Claudin-5 and cell motility. Furthermore, a possible link between Claudin-5 and N-WASP, and Claudin-5 and ROCK was demonstrated when interactions between these proteins were seen in both cell lines. Moreover, cell motility was assessed following treatment with N-WASP inhibitor, Arp2/3 inhibitor and ROCK inhibitor. Results show that the knockdown of Claudin-5 in HECV cells masked their response to N-WASP inhibitor, Arp2/3 inhibitor and ROCK inhibitor. A parallel response was observed in the knockdown of Claudin-5 in MDA-MB-231 after treatment with N-WASP inhibitor and Arp2/3 inhibitor; however treatment with ROCK inhibitor did not reveal any differences in motility in this particular cell line.

This study portrays a very new and interesting role for Claudin-5 in cell motility involving the N-WASP and ROCK signalling cascade indicating a possible role for Claudin-5 in the metastasis and progression of human breast cancer.

List of Figures:

List of Tables

CONTENTS

Chapter 1

Introduction

1.1 Breast cancer

1.1.1 Breast cancer incidence and risk factors

Breast cancer is by far the most frequent cancer in women; more than a million women are diagnosed with breast cancer every year. More than half the cases are in industrialized countries, with about 426,900 new cases of breast cancer occurring each year in Europe (in 2006 there were 45,822 new cases diagnosed in the UK: 45,508 woman and 314 men) and an estimated 182,460 in the USA (Figure 1.1A) (Office for National Statistics, 2006).

It is widely recognised that the high incidence of breast cancer in the more affluent world areas, with the highest age-standardised incidence in North America, is due to the presence of screening programs that detect early invasive cancers, some of which would otherwise have been diagnosed later or, in the worst case, not at all. Although there is a high incidence of breast cancer, the relatively good prognosis means that it is the most prevalent cancer in the world today; there are an estimated 4.4 million people alive who have had breast cancer diagnosed within the past 5 years (compared with just 1.4 million survivors from lung cancer). Between 1989 and 2007 in the UK, the breast cancer mortality rate fell by 41% in women aged 40-49 years; by 41% in women aged 50-64; by 38% in women aged 65-69; by 35% in women aged 15-39; and by 20% in women over 70 (Figure 1.1B) (Office for National Statistics, 2006).

There has been however, a general increase in incidence rates of about 0.5% annually worldwide. At this pace of growth, there would be around 1.4 million new

cases in 2010. The incidence of breast cancer shows considerable geographic cancer variation. In China, there are annual increases in incidence of 3% to 4%, and in other parts of Asia increases are also very similar, whilst in the UK the number of cases has increased by 14% over the last ten years (Parkin *et al.*, 2005).

Genetic factors, including 'high risk' breast cancer susceptibility genes BRCA1 and BRCA2, genes encoding growth factors and receptors, intracellular signalling molecules, cell cycle regulators, apoptosis regulators and adhesion molecules may account for up to 10% of breast cancer incidence in developed countries, but their occurrence in the population is too low to explain the differences in risk worldwide. Therefore, the vast majority must be a consequence of different environmental exposures. This is evident from studies of migrants from Japan to Hawaii showing that the incidence of breast cancer in migrants assumes the rate in the host country within the first generation, indicating the magnitude of the influence of the environmental surroundings (Kolonel *et al.*, 2004).

A large number of risk factors have been suggested as playing a role in the development of breast cancer. These include age, reproductive factors (first pregnancy, breastfeeding), lifestyle (physical activity, diet, alcohol intake and smoking), oral contraceptives and hormone replacement therapy (McPherson *et al.*, 2000).

A

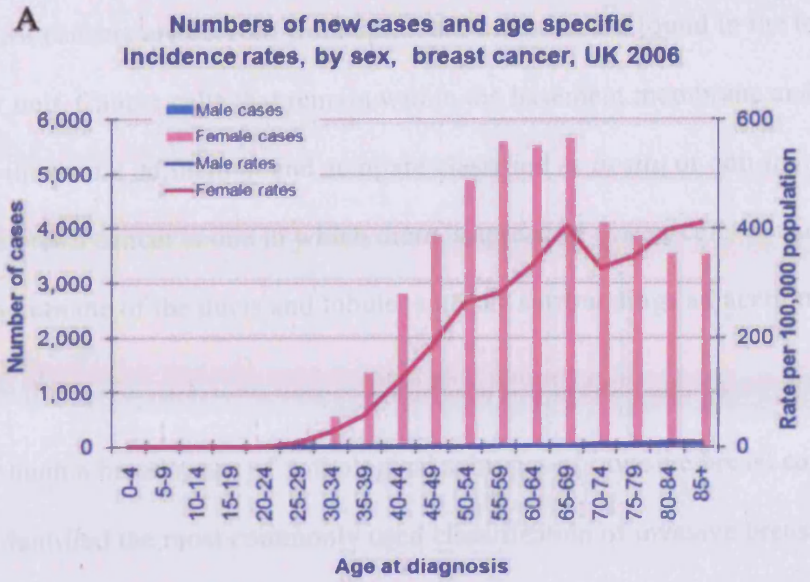

B

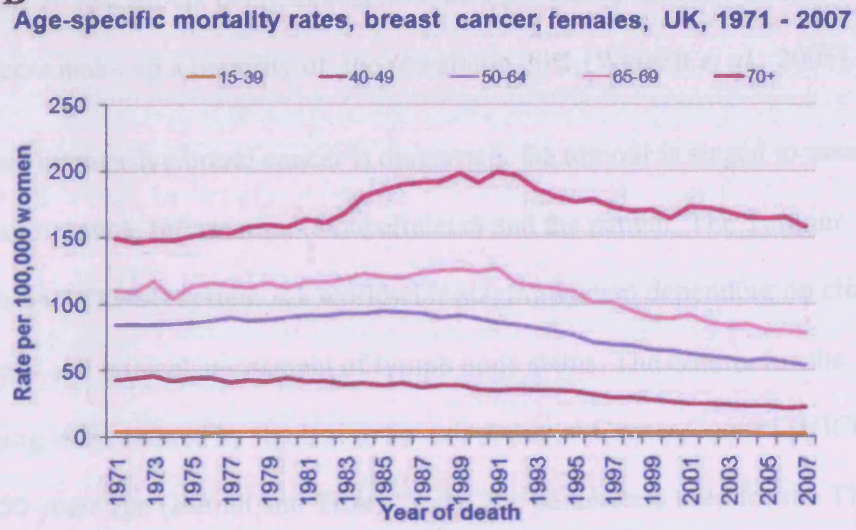

Figure 1.1: (A) Number of new cases diagnosed and age specific incidence in the UK (Source: Office for National Statistics, 2006). (B) A decrease in breast cancer mortality in all age groups between the late 1980s and 2007 (Source: Office for National Statistics, 2006).

Breast cancers are derived from epithelial cells that are found in the terminal duct lobular unit. Cancer cells that remain within the basement membrane and are confined to the ductal epithelium and acini are classified as *in situ* or non-invasive. An invasive breast cancer is one in which there is spread of cancer cells outside the basement membrane of the ducts and lobules into the surroundings adjacent normal tissue.

Although a broad range of pathological subtypes of invasive breast cancer have been identified the most commonly used classification of invasive breast cancers divides them into ductal and lobular types. Invasive ductal carcinoma represents the largest group, being almost 80% of the invasive cancers. Invasive lobular cancers make up a majority of the remaining 20% (Weigelt *et al.*, 2005).

When an invasive breast cancer is diagnosed, the tumour is staged to assess the cancer and provide information to the clinician and the patient. The Tumour Node Metastases (TNM) system is a worldwide staging system depending on clinical measurements and clinical assessment of lymph node status. The criteria for the cancer staging were defined by the Union for International Cancer Control (UICC) more than 50 years ago (Berndt and Titze, 1969). The parameters used for the TNM include size of tumour (T) followed by a number from 0 to 4; spread to the axilary lymph node (N) followed by a number from 0 to 3; and its spread to distant sites (M) followed by a 0 or 1. Once the T, N, and M categories have been determined, this information is combined in a process called stage grouping (Table 1.1). With modern advances in breast cancer diagnosis, UICC have reviewed the system to introduce changes that will improve TNM classification (Gospodarowicz *et al.*, 2004).

Stage	T (tumour size)	N (node status)	M (metastasis)
0	Pre- cancerous		
I	T-1	N-0	M-0
II	T-1	N-1	M-0
	T-2	N-0 or N-1	
	T-3	N-0	
III	T-Any	N-1	M-0
	T-3	N-0 or N-1	
	T-4	N-0	
IV	T-Any size	N-Any status	M-1

Table 1.1: TNM staging system for breast cancer. Where T, N and M means: T=tumour size: T-1= 0-2cm, T-2=2-5cm, T-3= >5cm; T-4= ulcerated or attached. N= node status: N-0= clear or negative nodes, N-1= cancerous or positive nodes. M=metastasis: M-0= no metastasis, M-1= metastasis.

1.1.2 Breast cancer metastasis

Metastasis is the presence of disease at distant sites due to the spread of cancer cells which results in overwhelming mortality in patients with cancer. It is a complex, multi-staged process determined by a large number of different factors and involving a number of sequential steps and events which must be completed for the cancer cell to successfully metastasise and form a secondary tumour in a distant organ, the so called metastatic cascade.

The most widely accepted model for metastasis is the "seed and soil" hypothesis postulated by Stephen Paget in 1889. He suggested that malignant tumour cells are shed from the primary tumour and disseminated in the entire body though they will only metastasise when the seed (disseminated tumour cells) and soil (secondary organ) are compatible. Ever since, the knowledge in this area has expanded significantly. However, the mechanisms underlying the whole process are still unclear and currently the available therapies are mainly palliative.

The metastatic cascade is thought to consist of the following steps: invasion, intravasation and extravasation (Figure 1.2). Invasion occurs when tumour cells gain the ability to dissociate from the primary tumour and penetrate the surrounding tissues through degradation of the basement membrane and the extracellular matrix, leading to intravasation as the detached cells enter the circulatory or lymphatic system. Once the tumour cell arrives at a possible point of extravasation, it interacts and attaches at the new site to penetrate the endothelium and the basement membrane to produce a secondary tumour, this is called extravasation.

In order to activate the metastastatic cascade, cancer cells must acquire a motile phenotype. Cell motility is orchestrated by a variety of complicated signal pathways, most of which are just starting to be unravelled. Understanding cell motility not only requires knowledge of the signal pathways regulating actin polymerisation, but also details concerning their dynamics.

Cell motility and migration occur in response to chemokines or growth factor signals. In response to these stimuli, changes in the cytoskeleton, in the cell-cell adhesion structures, in the cell-substrate adhesion and in the extracellular matrix (ECM) take place resulting in a motile cell capable of gaining access to the systemic circulation and ultimately metastasis. Cell migration is initiated by the development of cellular extensions such as filopodia and lamellipodia that define the front of the migrating cells driven by actin polymerisation and filament elongation (Ridley *et al.*, 1992). The activation of Rho, Rac1 and Cdc42, all members of the small GTPases familiy, has been reported to result in the formation of actin stress fibres, membrane ruffles, lamellipodia and filopodia respectively in *in vitro* studies (Hall, 1998). It has been shown that Cdc42 interacts with Wiskott-Aldrich syndrome protein (WASP) and N-WASP (a homologue of WASP) resulting in an active conformation of the Arp2/3 complex (Actin related protein) responsible for inducing the assembly of branching networks of actin filaments to push the cell membrane forward (Cory and Ridley, 2002).

Rho GTPases and their most common effector, ROCK, are important regulators of cellular processes including cell motility. Furthermore, Rho-ROCK interactions have been demonstrated to be involved in tumour invasion and

metastasis by increasing cell motility in breast cancer cells through the regulation of actin cytoskeletal reorganisation and the formation of focal adhesions (Nishimura *et al.*, 2003) (Figure 1.3).

Extensive interactions between tumour cells and surrounding tissues during their dissemination complicate the analysis of signalling events during this cascade. Due to its complex nature, the understanding of the cellular and molecular factors is limited. The most important questions arising are focused to define the genetic and epigenetic changes conferring such behaviours on these cells (Yang *et al.*, 2006).

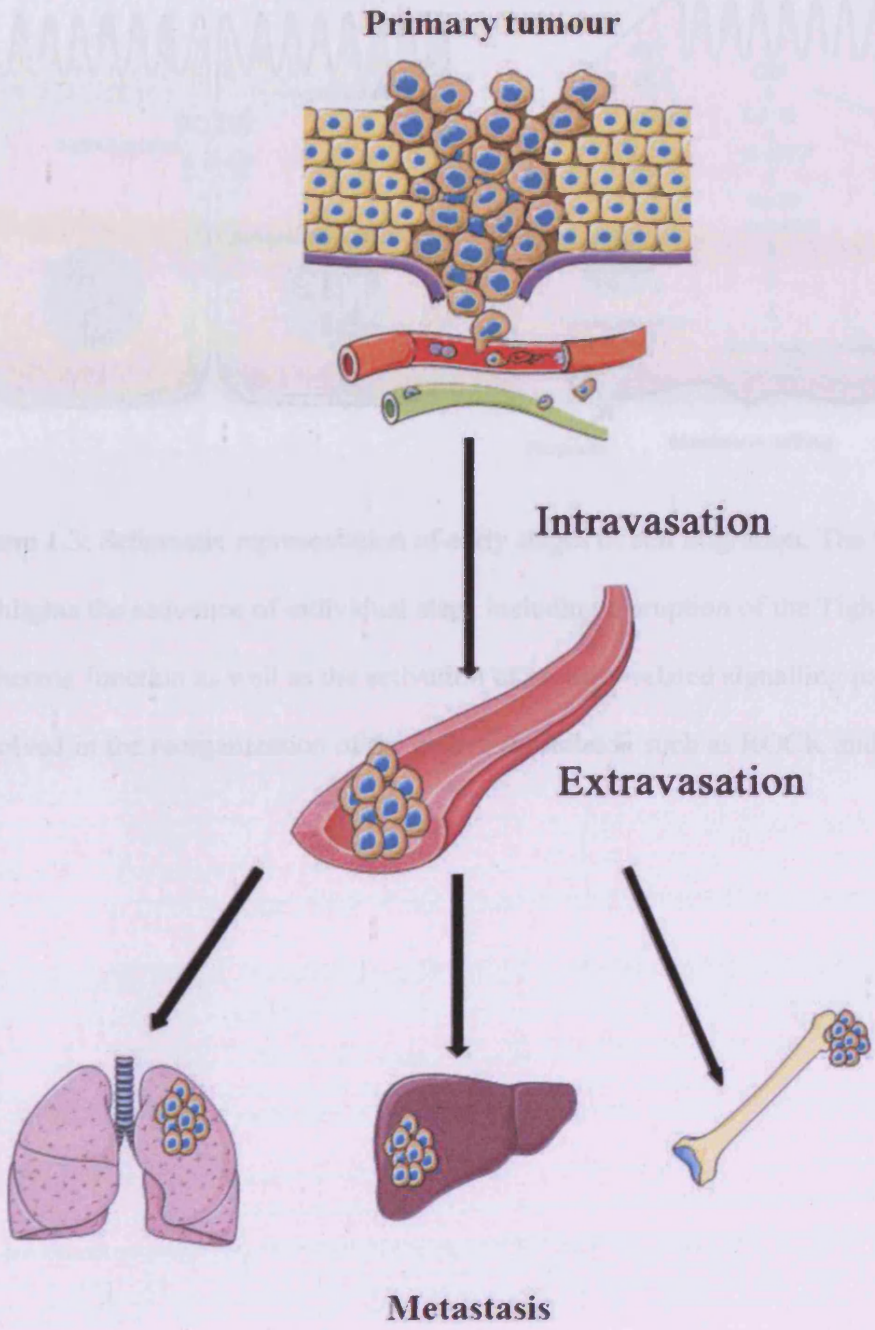

Figure 1.2: Major steps in the metastatic cascade.

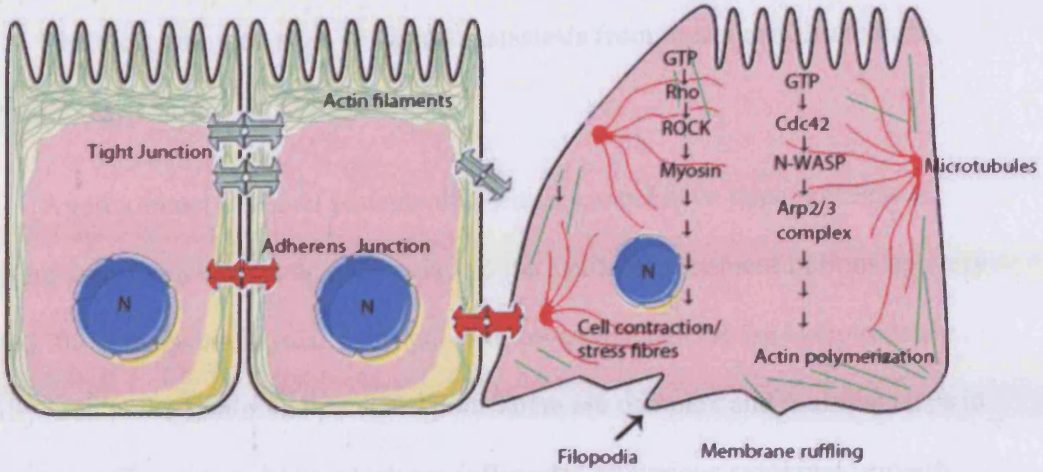

Figure 1.3: Schematic representation of early stages of cell migration. The figure highlights the sequence of individual steps including disruption of the Tight and Adherens Junction as well as the activation of motility-related signalling pathways involved in the reorganization of the actin cytoskeleton such as ROCK and N-WASP.

The most common sites of distant metastasis from breast cancer are bone, liver and lung (Carty *et al.*, 1995).

Approximately 70% of patients with breast cancer have bone metastases. They are associated with poor prognosis and the available treatment options are very limited. Bone metastases usually present with severe pain and these symptoms are usually seen in the femur and pelvic region. There are complex and multiple steps in the process of bone metastasis which are influenced by various cytokines, growth factors and cellular signals. There are two types of breast cancer bone metastasis: Osteolytic lesions are the most common form and cause destruction of the bone; Osteoblastic lesion that are less common and cause new bone formation. Most patients have components of both bone resorption and bone formation (Akhtari *et al.*, 2008).

The liver is the second most common site to be colonised during breast cancer metastasis. About 40-50% of women with metastatic breast cancer have metastasis to the liver during the course of the disease. Hepatic disease related to breast cancer can be consequential to the metastatic spread of the tumour to the liver, or as a result of regular treatment with chemotherapeutic agents or endocrine therapy. Both cases are associated with a poor prognosis among patients (Diamond *et al.*, 2009).

Pulmonary metastases are also common features in patients with breast cancer. As cancer cells arrive at the pulmonary capillaries, they became physically trapped and restricted by the narrowing blood vessels in the lung. Several studies have shown that the adhesion and extravasation of cancer cells in the lung is

mediated by specific surface adhesion molecules on the cancer cells and the endothelium like the chemokine receptors CXCR4 and CCR7 (Lu and Kang, 2007).

The diverse nature of breast cancer metastasis makes not only finding a cure for the disease complicated, but also assessing risk factors for metastasis. Improving the understanding of the molecular mechanisms of the metastatic cascade will also provide quality in management of the disease.

Since Tight Junctions (TJs) are located between the cancer epithelial cells, themselves functioning in an adhesive manner, and between the endothelial cells, as a barrier through which molecules and inflammatory cells can travel, they represent a critical barrier which the cancer cells must overcome in order to penetrate and initiate metastasis. If any microorganism or cancer cell can gain access to the systemic circulation, there exists a wealth of nutrients and an ideal environment for many to proliferate. Therefore, TJ integrity is a key step in the metastatic cascade (Martin *et al.*, 2004b).

1.2 Tight Junction molecular structure

As the proverb states: "Good fences make good neighbours", this humble and intelligent statement is not just applicable to the property market; it is indeed a reality seen in nature, in all species, in evolution and in development.

A single cell in the ocean can exchange nutrients and waste products constantly. However, when a single cell is part of a multicellular organism this

changes; moving from an easy movement of substances to a complicated and extremely organized exchange system with the external environment.

A defining characteristic of multicellular organisms is the capability of forming TJ that seal the intercellular space between neighbouring cells and transform the layer of individual cells into an effective permeability barrier. Barriers not only separate fluids, but they also perform thermodynamic work by reabsorbing solutes from compartment A to B, or secreting others from B to A, thus establishing gradients across themselves.

TJs are highly regulated areas of adhesion between epithelial and endothelial cells. They are the most apical component of the lateral plasma membrane and they are connected to the actin cytoskeleton. They create a regulated paracellular barrier to the movement of ions, solutes and immune cells between the cells and signalling pathways that communicate cell position, limit growth and apoptosis.

The morphology of TJ has been intensively analysed using transmission electron microscopy, where the TJ appear as a sequence of very close points as fusions of the plasma membrane of both cells, and by freeze fracture electron microscopy where these contacts are shown as rows of intra-membrane strands and complementary grooves that encircle cells (Staehelin, 1973).

Physiological studies of the past decades have demonstrated that the TJ barrier is not absolute, and permeability to small and macro-molecules varies amongst different tissues. Moreover, barrier assembly and permeability characteristics are influenced by different cellular signalling mechanisms.

TJs have been proposed to have two equally exclusive functions: 1. A fence function by forming an apical/basolateral intra-membrane diffusion barrier which prevents the mixing of membrane proteins; and 2. A gate function by controlling the breadth and selectivity of diffusion along the paracellular pathway (Cereijido *et al.*, 2008). These functions will be explained more fully in section 1.3.

The number of TJ strands is an important factor in determining the barrier properties of the TJ. There is not a linear relationship between the complexity of the TJ strand network and their measured electrical resistance (trans epithelial/endothelial resistance, or TER), in other words, the number of TJ strands does not correlate with the tightness of the barrier, in fact the relationship is an exponential one (Claude, 1978). Such results led to the prediction that TJ must contain aqueous pores lined by proteins. Subsequently, it was reported that the strands do indeed contain aqueous pores and that the pores oscillate between open and closed states (Tsukita *et al.*, 2001). Therefore, it has been accepted that the tightness of the TJ is remarkably dynamic and finely regulated in individual cells.

Although the details of how intracellular signals may influence these proteins are not understood, many signalling messengers, including prostaglandins, cAMP, and protein kinase C, have been seen to regulate the actin cytoskeleton in epithelial cells (Anderson and Van Itallie, 1995).

Several types of proteins have been identified as components of TJ (Table 1.2), depending on their distribution within the junction (Figure 1.4):

1. **Transmembrane proteins** such as the MARVEL/TAMP proteins (Occludin, Tricellulin and MARVEL D3), the Claudin superfamily and Junctional Adhesion Molecules (JAMs). These proteins span the cell membrane and are anchored into position by links to the cytoplasmic/plaque proteins.

2. **Cytoplasmic plaque** such as the Zonula Occludens family, ZO-1,-2,-3, AF6, MUPP-1, MAGI-1,-2,-3, Cingulin, Angiomotin family and Symplekin. These proteins link TJ to the actin-cytoskeleton and the adherens junction to the regulatory proteins.

3. **Associated/regulatory proteins** such as the Rho subfamily proteins, Rab-13, Rab-3B, heterotrimeric G proteins like Gαi-2 and Gα0 etc.

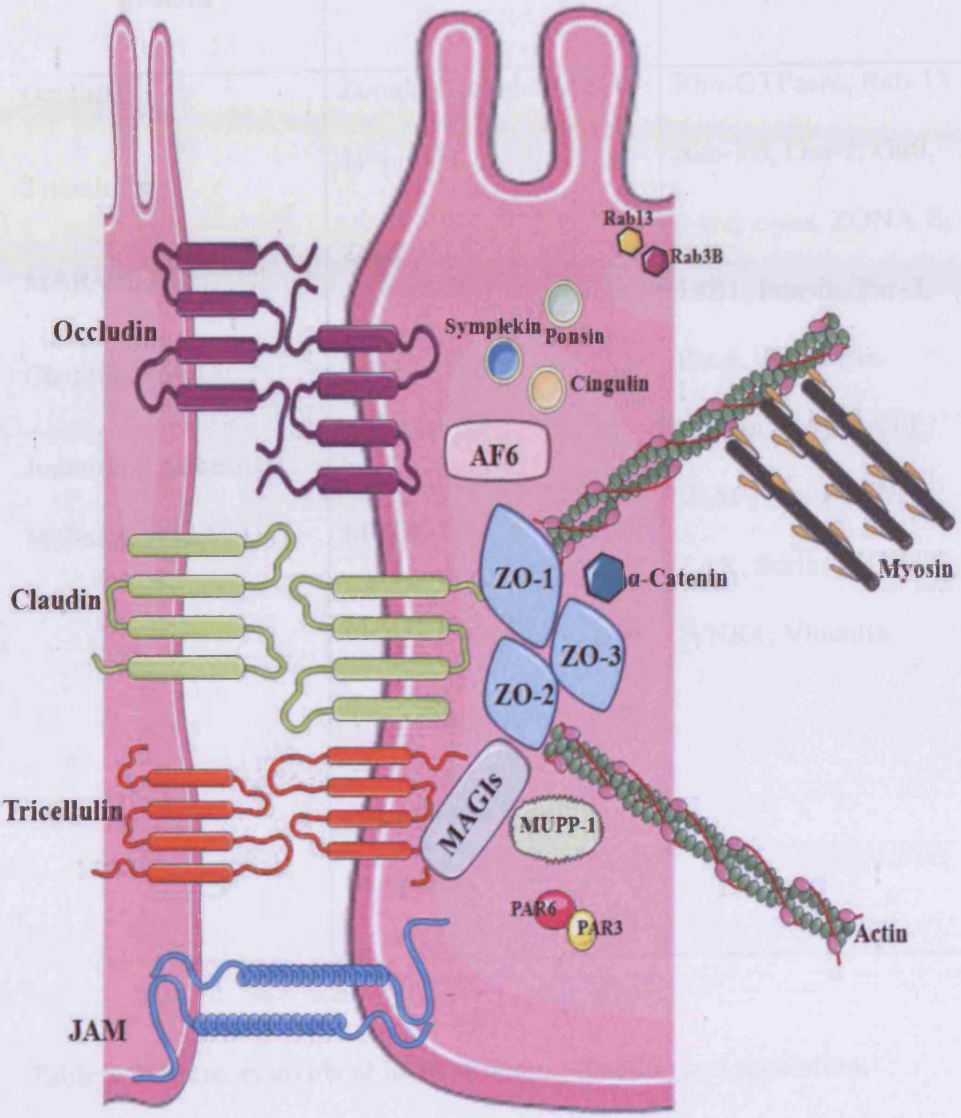

Figure 1.4: Molecular structure of TJ.

Transmembrane protein	Cytoplasmic plaque	Associated/regulatory proteins
Occludin Tricellulin MARVEL D3 Claudin 1-24 Junctional Adhesion Molecules (JAM 1-4)	Zonula Occludens (ZO-1) ZO-2 ZO-3 AF6 MUPP-1 MAGI-1,-2,-3 Cingulin Angiomotin family Symplekin	Rho-GTPases, Rab-13, Rab-3B, Gαi-2, Gα0, *c-src, c-yes,* ZONA B, 19B1, Ponsin, Par-3, Par-6, Afadin, α-catenin, Pals, PATJ, JEAP, Pilt, PTEN, ZAK, Scrib, ITCH, WNK4, Vinculin

Table 1.2: Proteins involved in TJ structure, function and regulation.

1.2.1 Transmembrane proteins

TJs contain two principal types of transmembrane components: tetraspan and single-span transmembrane proteins. The tetraspan proteins are the TAMP family (Occludin, Tricellulin and MARV3D) and the Claudin family (1-24), all of which share the same membrane topology, with their N- and C-termini domains within the cytoplasm and two extracellular loops implicated in establishing contact with homotypic molecules located in the TJ region of the neighbouring cell. The single-span transmembrane proteins are the Junctional Adhesion Molecules (JAM1-4 and JAM-like) that belong to the immunoglobulin superfamily and mediate homotypic cell-cell adhesion.

All these proteins share a common feature, the presence of a PDZ domain. This feature is key for the establishment of protein-protein interaction in the Tight Junction. PDZ domains contain 80-90 amino acid residues and are named after the proteins in which they were initially identified: PSD-95, Dlg, and ZO-1 (Daniels *et al.*, 1998). These mediate intermolecular homotypic interactions between PDZ domains, like the ones established between ZO-1and ZO-2 and also ZO-1 and ZO-3, as well as heterotypic interactions by association to specific motifs found at the carboxyl terminal ends of several proteins including Claudins, JAMs and ZO-2 and ZO-3.

1.2.1.1 Occludin

Occludin, the first-discovered and probably most abundant tetraspan TJ protein is an approximately 60 kDa tetraspan membrane protein (Furuse *et al.*, 1993),

depending on phosphorylation status. There are two different isoforms that result from alternative mRNA splicing, but there is no clear difference in their tissue distribution and functions (Muresan *et al.*, 2000). Its localisation in the Tight Junction is regulated by phosphorylation in both epithelial and endothelial cells, whereas the non-phosphorylated Occludin is localised to both the basolateral membrane and in cytoplasmic vesicles.

Although both domains interact with components of the cytosolic plaque, they have been shown to have different functionality. The N- terminal domain regulates neutrophil transmigration (Oshima *et al.*, 2003), whereas the C-terminal domain interacts with various intracellular proteins of the TJ including ZO-1,-2 and -3. This interaction is essential for the localisation of Occludin at the TJ (Furuse *et al.*, 1994) .

Mice genetically altered to express reduced levels of Occludin have previously been generated in a study by Saitou *et al.* These mice showed the presence of normal TJ in the intestinal epithelium (Saitou *et al.*, 2000). This data suggested that Occludin may play a role in the regulation of TJ rather than in the assembly of the structure itself and may also suggest that Occludin is not the only key protein in the making of TJ.

In addition, over-expression in several cancer cells results in increased sensitivity to apoptotic factors via modulation of the expression of genes involved in apoptotic pathways like mitogen activated protein kinase (MAPK), and thus contributes to reduce tumour progression and metastasis. These findings support the idea of a regulatory role for Occludin rather than a simple structural one,

demonstrating that Occludin acts as a signal transmitter in the TJ (Osanai *et al.*, 2006).

1.2.1.2 Tricellulin

Tricellulin is a tretraspan transmembrane protein localised in tricellular TJs, the meeting points of three cells, but it is also seen in bicellular TJ. It is down-regulated by the zinc-finger transcription factor Snail. The suppression of Tricellulin expression by RNA interference impairs the barrier function of the TJ, suggesting that Tricellulin might have a pivotal function for junction assembly and barrier function (Ikenouchi *et al.*, 2005).

Four isoforms of human Tricellulin have been described by Riazuddin *et al.*, In addition, the same study revealed that Tricellulin-a (TRIC-a) mutations lead to non-syndromic deafness (Riazuddin *et al.*, 2006).

1.2.1.3 Claudins

The Claudin superfamily consists of at least 24 tretraspan protein members all believed to be expressed in a tissue-specific manner. Claudins are capable of forming TJ strands and thus are thought to be the backbone of the TJ (Furuse and Tsukita, 2006). This will be discussed in full in section 1.5.3.

1.2.1.4 Junctional Adhesion Molecules (JAMs)

Junctional Adhesion Molecules (JAMs) are single-span transmembrane proteins that are associated with TJ. They belong to the immunoglobulin (Ig) superfamily and consist of two extracellular Ig-like domains, a single transmembrane

domain and a C-terminal cytoplasmic domain. Four JAMs, JAM-1(JAM-A), -2 (VEJAM/JAM-B), -3 (JAM-C) and –4, have been described (Bazzoni, 2003). V-set/VSISI/GPA34 is also a member of the family (Scanlan *et al.*, 2006). JAMs regulate adhesion between leukocytes and endothelial cells, as well as the paracellular transmigration of leukocytes across the endothelium (Weber *et al.*, 2007).

1.2.2 Cytoplasmic plaque proteins

A very important feature of TJs is that they include a cytoplasmic plaque, which forms a link between the junctional membrane and the cytoskeleton. The cytoplasmic plaque also recruits a variety of signalling components that includes kinases and phosphatases as well as proteins that are involved in signalling in and from the nucleus. The cytoplasmic plaque contain two principal types of proteins: MAGUK proteins that contain a PDZ domain like ZO proteins, MAGI and MUPP-1, and those non-PDZ proteins like Cingulin, Angiomotin family proteins, small GTPases and Symplekin (Guillemot *et al.*, 2008). Of all these proteins mentioned above, the ZO proteins are the most studied in the TJ cytoplasmic plaque.

1.2.2.1 ZO proteins

ZO-1, ZO-2 and ZO-3 are members of the MAGUK (membrane associated guanylate kinase homologs) family. The MAGUK family is characterised by their PDZ domain, in particular ZO proteins have three, an SH3 domain and a guanylate kinase homologous domain. They are at the core of a network of protein interactions. The first PDZ domain of ZO-1, ZO-2 and ZO-3 binds directly to the C-terminal domain of Claudins. In fact, a study by Umeda *et al.*, demonstrated that the

interaction between the first PDZ domains of ZO-1 and ZO-2 and Claudins plays a crucial role in the assembly of the TJs (Umeda *et al.*, 2006).

1.2.3 Associated/regulatory proteins

A large number of associated proteins like small GTP-binding proteins of the Rho subfamily have been involved in the control of Actin organization. Protein tyrosine kinases like c-*src* and c-*yes*, are also represented in this group of proteins acting as regulators of junction assembly and actin dynamics. Other small GTP-binding proteins like, Rab-13 and Rab-3B, have been seen to be involved in vesicle targeting rather than in cytoskeletal activity (Mitic and Anderson, 1998). Cingulin is not directly required for TJ formation and cell polarity but it has been proposed to regulate RhoA signalling, through its interaction with the RhoA activator GEF-H1 (Citi *et al.*, 2009).

Other members of the TJ associated proteins are: ZONAB, 19B1, Ponsin, Rab 3B, PKC, Par-3, Par-6, Afadin, α-Catenin, Pals, PATJ, JEAP, Pilt, PTEN, ZAK, Scrib, ITCH, WNK4 and Vinculin (Martin and Jiang, 2009).

1.3 Tight Junctions functions

Until the early nineties, TJs were mainly seen as paracellular seals. The subsequent vast amount of studies that have been done on TJ has changed our view in such a way that TJ are now considered as being active participants in the regulation of cell proliferation, gene transcription and cellular differentiation. In

other words, TJs are not static structures that simply seal two neighbouring cells; they are implicated in a variety of events that occur in the cell.

This section will summarize the most important roles that TJs have been associated with so far.

1.3.1 Tight Junction as gate and fence

One of the major functions of TJs is the construction of a diffusion barrier by tight control of the paracellular pathways, so called the gate function, and to create a physical barrier preventing the movement within the cytoplasm of lipids and proteins, the fence function (Figure1.5). The paracellular diffusion gate represents a semi-permeable barrier that limits diffusion depending on the charge and the size of the solute. The ion and size selectivity differs among tissues and it is regulated by different physiological and pathological stimuli.

Occludin and the Claudins are the main TJ proteins responsible for the paracellular permeability. Several studies have pointed at Claudins as being the major determinant of the permeability properties. For example, mutant mice lacking Claudin-1 die after birth due to water loss through the skin (Furuse and Tsukita, 2006). On the contrary, the fence function requires the cooperation and coordination between integral membrane proteins, TJ scaffolding proteins and signalling molecules (Umeda *et al.*, 2006).

In epithelial and endothelial cells, "polarity" refers to an asymmetric allocation of macromolecules such as, proteins, lipids and carbohydrates, within the cell conferring a subdivision in the plasma membrane creating two well

differentiated areas: the apical and the basolateral domains. TJs between neighbouring cells allow the separation of apical and basolateral membranes, a necessary state for normal cell functions (Tsukita *et al.*, 2001).

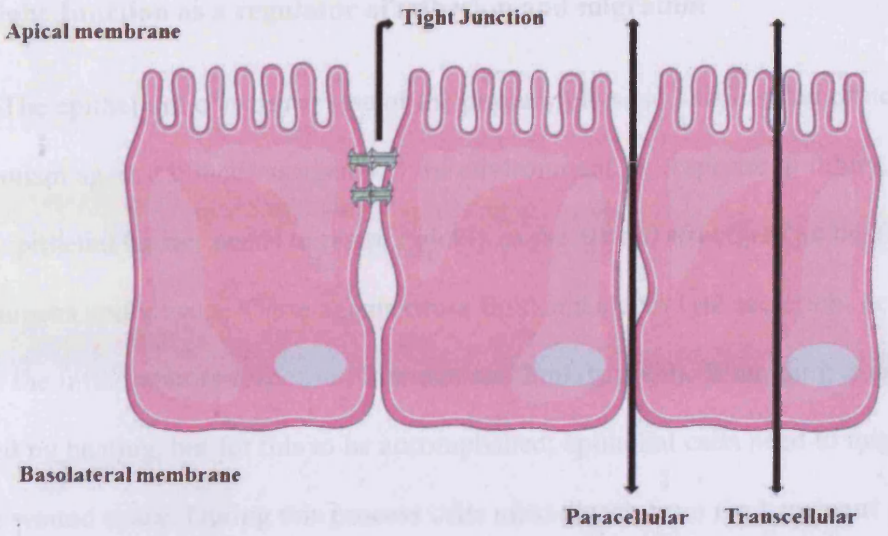

Figure 1.5: TJs serve to separate the apical and basolateral domains, thus acting as a gate and fence.

1.3.2 Tight Junction as a regulator of adhesion and migration

The epithelium constitutes one of the primary physical barriers that protects the organism against infectious agents in the environment. In response to injury, the broken epithelial barrier needs to reseal quickly as the altered structure can be a gate for pathogens and viruses. These agents cause fluid and electrolyte secretion, or activate the inflammatory response (Guttman and Finlay, 2009). Wounding is usually followed by healing, but for this to be accomplished; epithelial cells need to migrate into the wound space. During this process cells must detach from the basement membrane due to disruption of the actin cytoskeleton, and extend their body through polarized protrusion extensions in the direction of the movement which results in TJ disruption. As explained above, TJs play a fundamental role in cell polarisation. The apical-basolateral polarity is disrupted in this process and protein complexes are redistributed in the cell. The Par3-Par6-aPKC, PAJT-PLAS-CRB, and Scrib-Dlg-Lgl complex are crucial for the polarity of the cell and for directional movement. Those complexes relocate within the cell after wounding, leaving proteins associated with TJ structure towards the migration borders (Shin *et al.*, 2007). A recent study in Madin-Darby canine kidney (MDCK) epithelial cell, showed that Occludin accumulates on the migration edge membrane suggesting that it might intercede in the recruitment of Par3-aPKC/PATJ during healing (Du *et al.*, 2010).

1.3.3 Tight Junctions as regulators of cell-surface polarity, proliferation and differentiation

Cell proliferation and polarisation are tightly regulated processes which are essential for the development of differentiated tissues. As mentioned in section 1.3.1,

TJs are necessary for cell polarisation, however several studies have also linked these structures to cell proliferation and differentiation, all of which are fundamental steps in cancer progression.

The recruitment of leukocytes is an important part of wound healing and the angiogenesis processes. It is a complicated mechanism involving leukocyte activation, selectin-mediated rolling, integrin-mediated adhesion and diapedeis. Leukocytes need to leave the vasculature passing through the barrier that endothelial cells form. To achieve this transmigration, interactions between leukocytes and the endothelial cells needs to occur. Several studies have implicated JAM-1,-2 and –3 in leukocyte trafficking during inflammation and angiogenesis. In particular, JAM-1 was seen to participate in the process by undergoing homophilic binding interactions, as well as heterophilic interactions to the β2-integrin LFA. JAM-2 has been suggested to interact with β1-integrin VLA-4 in T-cells. JAM-3 has been shown as a receptor for Mac-1, a member of the β2-integrin family, contributing to leukocyte Transendothelial transmigration (Keiper *et al.*, 2005). Taking into account all this evidence, it is clear that JAMs, as members of the TJ structure, participate in leukocyte migration.

Recent evidence has pointed to TJs as being regulators of cell proliferation, gene expression, differentiation and morphogenesis. One interesting study by Katsuno *et al.*, showed the critical role that ZO-1 may play in tissue organisation and remodelling. ZO-1 knockdown mice died at the embryonic stage of 10.5 days, with embryonic and extraembryonic imperfections, such as impaired angiogenesis in the yolk sac or disorganized notochord areas (Katsuno *et al.*, 2008). To complement

these results, ZO-2 has been seen to form a complex with c-*myc* and HDAC1 which appears to be able to down-regulate the transcription of cyclin D1, a pivotal regulator of cell cycle (Huerta *et al.*, 2007).

High cell density increases expression of Cingulin in MDCK cells and this has been linked to lower levels of active Rho A, a member of the Rho GTPase family and vice versa, with reduced expression of Cingulin in low density cell growth causing higher levels of active Rho A. Unexpectedly, levels of GEF-H1 (a guanine nucleotide exchange factor for Rho A) remains constant, suggesting that Cingulin might interact with GEF-HI and together inactivate Rho A (Aijaz *et al.*, 2005).

Such results provide a molecular mechanism whereby the development of Tight Junctions in epithelial cells participate in the down-regulation of Rho A by GEF-H1 in a Cingulin-dependent way.

Several studies have also linked TJs to the suppression of proliferation. Raf-1, a downstream effector of the *ras* oncogene which is associated with the control of proliferation and differentiation, appears to down-regulate the expression of Occludin in epithelial cells. But when Occludin is forcibly expressed lacking its first extracellular loop, the normal polarized state of the cell is recovered. However, when the second extracellular loop is knocked down, the proliferation of tumour growth progresses. This suggests that the second extracellular loop may play an important role in recovering the normal phenotype of the cell while its absence allows tumour growth *in vivo* (Wang *et al.*, 2005).

In the case of ZO-1, different studies point to this protein as fundamental in epithelial morphogenesis and differentiation due to its interaction with ZONAB (ZO-1 associated nucleic-acid-binding protein), a Y-box transcription factor that promotes proliferation and differentiation (Matter and Balda, 2007).

1.4 Tight Junction and cancer

The link between altered TJs and epithelial tumour development has been confirmed by earlier studies placing TJs in the spotlight of cancer research. These studies showed dysregulation in TJ structures of several epithelial cancers including breast cancer.

Most cancers originate from epithelial tissues and are characterised by irregular growth and aberrant tissue morphology. It is absolutely necessary for tumour cells to have distinct adhesion behaviour; being significantly weaker in cancer cells. Thus, the communication between cells is highly affected and disorders in the signal transduction pathways that connect cell to cell arise. This change in cell surroundings encompasses a wide spectrum of changes, revealed in early and late stages of tumour growth, when the lost of polarity and uneven growth, as well as invasion and metastasis are a reality in cancerous epithelia. As tumour epithelial cells were examined in different types of cancer, early evidence was found of disorganized structure of TJs (Swift *et al.*, 1983) or even a lack of them in hepatocellular carcinoma, and reductions in the number of TJs strands when seen by freeze fracture in breast carcinoma (Robenek *et al.*, 1981). Decreased transepithelial resistance

(TER) and consequently increased TJ permeability has also been reported in TJs of colon tumours (Soler *et al.*, 1999). In normal kidney epithelial cells, structural adjustments in TJs were observed during mitosis. However cell division itself does not increase epithelial TJ permeability, therefore inducing leakiness in the epithelial barrier. These results indicate that altered permeability may be due to disease states like cancer (Soler *et al.*, 1993).

Taken together all this evidence from different cancer types appears to clearly indicate that a decrease in the epithelial barrier function and loss of TJ function are correlated. An extensive number of studies have shown that different protein members of TJs are directly or indirectly related to cancer progression, some of those have also been shown to correlate with staging and metastatic potential in various cancers (Table 1.3).

In bladder cancer the expression of Claudin-1, -4 and -7 was analysed by Boireau *et al.*, Claudin-4 expression appears to be modified in 26/39 tumours compared with the exceptional modifications found in Claudin-1 and -7. Over-expression of Claudin-4 was found in different carcinomas followed by remarkable down-regulation in invasive/high grade tumours. Delocalisation of Claudin-1 and -4 was seen in most human bladder tumours as well as in the bladder cell line HY-1376 (Boireau *et al.*, 2007).

In colorectal cancer, Resnick *et al.*, studied the expression pattern of Claudin-1, -4, Occludin and ZO-1 and their possible role in prognosis of disease was evaluated in a cohort of 129 TNM stage II tumours using tissue microarray technology. They found that in that order 75%, 58%, 56% and 44% of the tumours

examined displayed normal to elevated expression levels of Claudin-1, -4, Occludin and ZO-1 respectively. Low expression levels of Claudin-1 and ZO-1 were related to high tumour grade. Taking all these results together, it was confirmed that loss of Claudin-1 might be a strong candidate for disease recurrence and poor patient survival in stage II colorectal cancer (Resnick *et al.*, 2005). An earlier study by Tokunaga *et al.* examined the expression of Occludin in a cohort of 40 rectal carcinoid tumours using an anti-Occludin monoclonal antibody. The results showed that Occludin was not found in most of the rosette-like or trabecular structures in carcinoid tumours, however 20% presented a small number of rosette-like tubular structures presented Occludin as a dot or short line. These studies indicate that Occludin could be a useful marker of polarized glandular structures, a helpful tool to distinguish true glands from rosettes in human rectal carcinoid tumours (Tokunaga *et al.*, 2004). The levels of expression of Claudin-1 and -2 were examined in adenocarcinoma tissues as well as normal mucosa by Kinugasa *et al.* Immunohistochemistry and quantitative reverse transcription-polymerase chain reactions (RT-PCR) were used in the study. Results showed up-regulation in both Claudins at mRNA level as well as at protein level clearly linking these results to tumour invasion (Kinugasa *et al.*, 2007). The expression of Claudin-3, -4 and -7 was identified upregulated in gastric carcinoma when gene expression was analyzed by microarrays in three oesophageal adenocarcinomas, one case of Barrett's oesophagus, and three normal oesophagi. Claudin -3 showed a marked increase in mRNA expression compared with normal oesophagus while Claudins- 4 and -7 were moderately up-regulated. Claudin-4 and -7 protein expressions were highly up-regulated in Barrett's oesophagus but minimally in squamous and gastric mucosa.

Claudin-3, -4 and -7 expressions showed high-grade in dysplasia, adenocarcinoma, and metastases specimens using Immunohistochemical staining. All these findings suggested that alterations in Claudin proteins are an early event in tumorigenesis of oesophageal adenocarcinoma (Montgomery *et al.*, 2006). Usami *et al.* analyzed the expression of Claudin-7 in squamous cell carcinoma of the oesophagus showing that Claudin-7 levels at the metastatic lymph nodes are significantly reduced compared to expression levels at the invasive front of the primary tumours. This suggests that the reduction may be linked to tumour progression and subsequent metastatic events (Usami *et al.*, 2006).

An early study from Kimura *et al.*, investigated Occludin in combination with ZO-1 in normal epithelia and cancers in the human digestive tract by immunostaining. In normal epithelium ZO-1 and Occludin were expressed together as a single line at the apical cell border. However, in the oesophagus only ZO-1 was expressed. When looking at cancer tissues, both proteins followed the same pattern of expression in normal epithelium as in differentiated adenocarcinoma cells. Conversely, in poorly differentiated adenocarcinomas both expressions were reduced indicating a correlation between tumour differentiation and expression of Occludin and ZO-1 (Kimura *et al.*, 1997).

Disruptions in the TJ structure have also been seen in lung cancer. An early study of 68 lung carcinomas and surrounding normal tissue found strong staining of Occludin in the apico-luminal borders of the branchial epithelia and bronchial glands as dots or short lines. When looking at cancer tissue, staining of Occludin was found in all cells that faced lumen in all adenocarcinomas including bronchioalveolar

carcinomas and followed the same staining pattern as that of the normal epithelia. This suggests that Occludin could be an ideal indicator to differentiate those glands that form tubulo-papillary structures in human lung carcinoma tissues (Tobioka *et al.*, 2004b). Using semi-quantitative reverse transcription-PCR on 27 pairs of lung squamous cell carcinomas and normal lung tissue, Liu *et al.*, confirmed differential expression of Claudin-1 in 82.1% (23/28) of lung tumour tissue (Liu *et al.*, 2007). Paschoud *et al.*, investigated different patterns of expression of a large panel of TJ proteins in lung squamous cell carcinomas and adenocarcinomas using quantitative RT-PCR. Significant changes in transcript levels were found when looking at squamous cell carcinomas in JAM-1, Occludin, Claudin-1, -3, -4, -7, Cingulin, ZO-2 and -3. Only Claudin-1 was shown to be down-regulated while the other proteins were up-regulated. In adenocarcinomas, transcript levels were compared to bronchial cells and a significant down-regulation in the levels of Claudin-1, -3, -4, -7, ZO-2 and -3 was observed (Paschoud *et al.*, 2007).

In prostate cancer, down-regulation of Occludin was seen in polygonal cells of Gleason grades 4 and 5, however, Occludin expression still occurred in cells facing the lumen in all grades of cancer. These results suggest that Occludin in prostate cancer is associated with loss of cell polarity and occurs at the same time as the formation of the complex glandular architecture of Gleason grade 4 pattern or complete loss in Gleason grade 5 pattern (Busch *et al.*, 2002). A study from Sheehan *et al.*, shows the pattern of expression of several Claudins in prostatic adenocarcinomas from 141 tissues samples. Decreased expression of Claudin-1 correlated with high tumour grade and biochemical disease recurrence, Claudin-7 appears to be decreased and also correlated with high tumour grade. However,

Claudin-3 correlated with advanced tumour stage and recurrence, while Claudin-4 correlated with advanced stage (Sheehan *et al.*, 2007).

Normal endometrium glands, endometrial hyperplasia and endometroid carcinoma grade 1 samples were analyzed by Tobioka *et.al.* All samples were seen to express Occludin. However, in endometrioid carcinomas grades 2 and 3, Occludin is not present in solid areas. Occludin expression was decreased in parallel with the increase in carcinoma grade, and the decrease in expression correlated with myometrial invasion and lymph node metastasis (Tobioka *et al.*, 2004a). Claudin-4 was over-expressed in epithelial ovarian cancer, although this expression did not correlate with survival or other clinical endpoints. However, Claudin-4 over-expression was correlated with changes in barrier function after treatment with *Clostridium perfringes* enterotoxin in a dose-Claudin-4 dependent non-cytotoxic manner (Litkouhi *et al.*, 2007). When Claudin-4 protein and transcript level were analyzed in 110 patients with different histological types of epithelial ovarian carcinomas Tassi *et al.*, found them to be significantly up-regulated in both primary and metastatic tumours compared to normal human ovarian surface epithelium cell lines. At protein level, Claudin-7 appears to be significantly higher in tumours of primary and metastatic origin when compared to normal ovaries, despite grade of differentiation, histologic type and pathological state. Complementary results show Claudin-7 to be over-expressed in all main histological types of epithelial ovarian carcinomas, in single neoplastic cells dispersed in the peritoneal cavity and pleural effusions. The data presented in this study suggested that Claudin-7 may be a useful novel marker in the disease (Tassi *et al.*, 2008).

The blood-testis barrier is composed of TJ, Adherens Junctions and Gap Junctions. Of all these structures, TJ is the main structural component in the Sertoli cell barrier. A study by Fink *et al.*, found an association between ZO-1 and -2 with the blood-testis barrier region in men with normal spermatogenesis. ZO-1 and -2 immunostaining were observed in normal tubules and at different stages of human testicular carcinoma in situ. When looking at carcinoma in situ tubules, the staining appears to be cytosolic, scattered and weaker. This data was complemented with Western blot and RT-PCR confirming that the disruption of Sertoli cell barriers in carcinoma in situ is linked to aberrant distribution of ZO-1 and ZO-2 (Fink *et al.*, 2006).

In human pancreatic endocrine tumours and ductal carcinomas, the protein and mRNA expression of different members of the Claudin family was analysed by Borka *et al.* Claudin-1, -2, -3, -4 and -7 revealed strong staining while Claudin-2 stained diffusely in normal acini and ducts. Langerhans islands presented only for Claudin-3 and -7 expression. The majority of endocrine tumours were negative for Claudin- 1, -2 and -4. Claudin-2 was present in half of the ductal adenocarcinomas whereas Claudin-3 was totally negative. Claudin-3 and -7 were detected in all endocrine tumours. When looking at the level of expression, differences were seen between endocrine tumours and ductal adenocarcinomas, worth mentioning is the high expression of Claudin-3 in endocrine tumours and Claudin-7 in ductal carcinomas making those proteins suitable targets for adjuvant therapy (Borka *et al.*, 2007). When ZO-1 expression level was investigated in pancreatic cancer, Kleeff *et al.*, found that it was higher in pancreatic ductal carcinomas when compared to normal pancreas. Under the confocal microscope, ZO-1 was present in the apical and

apicolateral areas of ductular cells in the normal pancreas and in chronic pancreatitis. However, pancreatic ductal carcinomas displayed ZO-1 regardless of expression in cancer cell forming duct-like structures. In lymph nodes, metastatic pancreatic cancer cells displayed a random pattern of distribution of ZO-1. It appears to be presented from apical to apicolateral areas including diffuse staining in the membrane. All these findings suggested that in pancreatic ductal carcinomas over-expression of ZO-1 might help pancreatic cancer cells to metastasise (Kleeff *et al.*, 2001).

1.4.1 Tight Junctions and breast cancer

An increasing number of studies have described the dysregulation of the TJ proteins and how these changes also affect breast cancer progression.

When looking at transmembrane proteins in the TJ, results have revealed that Occludin expression is down-regulated in several cancers including breast. When Occludin was over-expressed in the murine breast carcinoma cells AC2M2, results showed that Occludin promotes detachment-induced apoptosis (anoikis) via regulation of a set of apoptosis-associated genes (Osanai *et al.*, 2006). Further experiments from the authors have also shown that Occludin is associated with premature senenscence in AC2M2 cells through the up regulation of negative cell cycle regulators such as p16INK4A, p21IWaf1/Cip1 and p27Kip. However, p53 was not affected. Taking all these findings together, loss of Occludin appears to be partially involved in the senescence-promoting program during mammary tumourigenesis (Osanai *et al.*, 2007b). JAM-A has been implicated in the development of breast cancer. Niak *et al.*, showed that levels of JAM-A were down-regulated in metastatic breast tumours. *In vitro* studies with breast cancer cell lines

MCF-7, MDA-MB-231 and MDA-MB-468 revealed that over-expression of this protein results in a decrease in migration as well as invasion, whereas its knockdown promotes invasiveness (Naik *et al.*, 2008). However, McSherry *et al.*, recently studied the role of JAM-A in MCF-7 and MDA-MB-213, revealing a link between high levels of JAM-A and poor prognosis in patients with breast cancer. An *in vivo* study has been reported, revealing that knockdown of JAM-A in MCF-7 cells significantly decreases migration (McSherry *et al.*, 2009).

A number of studies have also implicated the Claudin family in breast cancer. Claudin-1 protein level has been reported to be reduced in breast tumours as well as in breast cancer cell lines such as MDA-MB-231 and MDA-MB-435. In these cell lines no genetic alterations were seen in the promoters or coding sequences with no explanation for the loss of expression of Claudin-1, therefore rejecting any tumour-suppressor effect for this protein (Kramer *et al.*, 2000). In similar breast cancer cell lines, Hoevel *et al.*, found no signal of expression of Claudin-1 nor Occludin, however, when Claudin-1 retrovirus was transduced into these cells, expression of Claudin-1 was found at the usual location at cell-cell contact sites, suggesting that other proteins might be responsible for targeting Claudin-1 in the TJ. In addition the paracellular permeability was altered in the transduced cells. The authors suggested that Claudin-1 over expression might be sufficient to exert TJ paracellular barrier function in metastatic breast cancer cells in the absence of other transmembrane proteins such as Occludin. These results agree with the study by Kramer *et al.*, suggesting that even though there is no evidence of any genetic changes, there must be some epigenetic or regulatory factors involved in the down-regulation of Claudin-1 (Hoevel *et al.*, 2002). Furthermore, Claudin-1 has been seen to be a useful

prognostic marker in breast cancer patients. Morohashi *et al.*, have revealed a correlation between recurrent breast tumours and low levels of Claudin-1 expression compared to primary tumours. Decreased expression of Claudin-1 was also associated with the lymph node metastasis-positive group and short-disease free patient group (Morohashi *et al.*, 2007).

Examination of Claudin-16 in breast cancer cells, *in vitro* and *in vivo* studies, have shown that when Claudin-16 is over expressed in the human breast cancer cell line MDA-MB-231, cells were significantly less motile and displayed reduced aggressiveness, with an increase in TJ function as the colonies became tighter. To complement this study, patient data revealed low expression of Claudin-16, mainly in patients who displayed high mortality (Martin *et al.*, 2008a). Studies of Claudin-7 have revealed the loss of expression in preneoplastic and invasive ductal carcinoma and this loss was mostly seen in high-grade lesions. The same situation was seen in lobular carcinoma where Claudin-7 was also absent. The authors suggested a link between the lack of Claudin-7 expression and cancer progression due to the increased cellular discohesion that is frequently seen in high-grade lesions, proposing that Claudin-7 might help tumour progression and increases metastatic potential. Moreover, when the breast cancer cell lines MCF-7 and T47D, which express high levels of Claudin-7, were treated with HGF, there was a resultant loss of Claudin-7 after 24 hours of treatment as well as dissociation of these cell lines in culture, linking the loss of Claudin-7 and cell cohesion in breast cancer (Kominsky *et al.*, 2003). In concordance with the above mentioned study, Sauer *et al.*, showed an inverse correlation between Claudin-7 level of expression and tumour grading. Grade 2 and -3 invasive carcinoma revealed reduced expression of protein. This data

correlates with metastatic disease, including loco-regional recurrences and with heterogeneous staining pattern. However, these results do not correlate with tumour size or subtype (Sauer *et al.*, 2005). Osani *et al.*, demonstrated that the knock down of Claudin-6 in MCF-7 cells increases cell migration and invasion (Osanai *et al.*, 2007a). In agreement with Osani's results, a recent study by Wu *et al.*, revealed that over expression of Claudin-6 in the MCF-7 cell line resulted in a decrease in cell growth rate as well as migration and invasion. However, the transepithelial resistance was increased in the transfected cells, suggesting a possible role in breast cancer progression acting as a cancer suppressor (Wu *et al.*, 2010).

Soini *et al.* analysed the pattern of expression of Claudin-2, -3, -4 and -5 protein levels in breast carcinoma. The study revealed that Claudin-2 and -4 were highly expressed in non-neoplastic breast tissue whereas Claudin-3 and -5 appear to show high expression in ductal and acinar cells. Levels of expression in breast carcinoma were for Claudin-2 in 52%, Claudin-3 in 93%, Claudin-4 in 92% and Claudin-5 in 47% of the samples respectively. It is important to mention that there was no correlation between level of expression of these Claudin members and tumour grade or oestrogen receptor status. Levels of expression between different Claudins were seen to be associated, strong Claudin-2 expression was linked to Claudin-5 and -3. In the same way, strong Claudin-3 expression was associated to Claudin-5 and -4 (Soini, 2004). A similar study analysing levels of mRNA compared to protein levels for Claudin-1, -3 and -4 in malignant breast tumours and benign lesions was carried out by Tokes *et al.*, revealing that whereas Claudin-3 and -4 mRNA and protein levels did not show any difference in expression between invasive tumour and the surrounding normal tissue, Claudin-1 mRNA appeared to be

highly down-regulated when compared with the control group. However, Claudin-3 and -4 proteins were detected in all primary breast carcinomas in one study by Kominsky *et al.*, in addition, when compared to normal epithelium, these two Claudin members were over-expressed in 62% and 26% of samples respectively (Kominsky *et al.*, 2004). Additionally, Claudin-1 was located in the membrane of ductal cells and in some of the ductal carcinoma in situ, whereas in invasive tumours Claudin-1 was not presented or its distribution was diffuse in the tumour cells. This data provided further evidence of how Claudin-1 is involved in invasion and metastasis of breast cancer. High levels of Claudin-4 distribution was seen in normal epithelial cells and was almost lost in mucinous, papillary, tubular breast carcinoma as well as in areas of apocrine metaplasia (Tokes *et al.*, 2005).

Studies focusing in cytoplasmic plaque proteins of the TJ have revealed how ZO-1 staining was found to be decreased or even lost in 69% of breast cancer using immunohistochemistry, whereas normal breast tissue showed intensive staining in the area where TJs were localized. When infiltrating ductal carcinoma was analysed Hoover *et al.*, found a fall in staining of 42% when tissue was well differentiated, in 83% of moderately differentiated and 93% when tumours were hardly differentiated. In addition to these results, it was reported that staining for ZO-1 correlated with tumour differentiation, and particularly with the glandular differentiated tumours implying that down-regulated level of ZO-1 might be a link to cancer progression (Hoover *et al.*, 1998). Martin *et al.*, investigated levels of expression of ZO-1, -2, -3 and MUPP-1 in patients with primary breast cancer. Immunohistochemical staining for ZO-1, -2 and -3 revealed low intensity in tumour samples when compared with paired background sections and a delocalisation of ZO-1 in the TJ. Looking at

mRNA levels, the level of expression of all these proteins was reduced in tumour tissues; however the differences were not statistically significantly. This study also reported a decrease of ZO-1 and MUPP-1 expression in patients with poor prognosis and with increasing tumour grade (Martin *et al.*, 2004b). A study from Polette *et al.*, suggested a link between ZO-1 and cell invasion in breast cancer cells by modulating membrane-type 1 matrix metalloproteinase (MT1-MMP) which appears to be over-expressed in many types of cancer including breast. In invasive breast cancer cell lines, MDA-MB-435, BT549, and Hs578T, ZO-1 was localized in the cytoplasm whereas Occludin was absent. Quite the opposite happened in non-invasive cell lines, MCF-7 and BT20, which exhibited membrane staining for ZO-1 as well as for Occludin and did not express MT1-MMP. This data also suggested a possible role for ZO-1 in the regulation of MT1-MMP through the β-catenin/TCF/LEF pathway which regulates the transcription of different genes implicated in tumour invasion (Polette *et al.*, 2005). ZO-2 has also been seen to be down-regulated in breast adenocarcinoma (Chlenski *et al.*, 2000). Glaunsinger *et al.*, reported the importance of ZO-2 in the tumour-inducing capacity of the adenovirus type 9 (Ad9) E4 protein. Expression of mutant ZO-2 protein with no E4 binding site inhibits Ad9 E4- induced transformation (Glaunsinger *et al.*, 2001).

Similar studies, looking at associated/regulatory proteins have reported that the level of expression of Ponsin and Vinculin correlates with poor prognosis in patients with breast cancer (Martin and Jiang, 2009). The Par complex (Par3-Par6-aPKC) has been related to breast cancer progression. In particular the level of expression of Par6B appeared to be up-regulated in breast cancer tissues. Over expressing Par6 in the breast epithelial cell line MCF-10A resulted in higher

proliferation rates which depended on interactions between Par6, aPCK and Cdc42. Down-regulation of aPCK or Cdc42 inhibits the capacity of Par6 to enhance proliferation, demonstrating that Par6 promotes cell proliferation in breast cancer cells (Nolan *et al.*, 2008). Opposite to Par6, Par3 has been reported to be down-regulated in squamous cell carcinomas showing a correlation with positive lymph node metastasis and poor differentiation (Zen *et al.*, 2009). Immunohistochemistal staining for Scrib, member of the Scribble complex, appeared to be reduced and mislocalised in human breast cancer tissues (Navarro *et al.*, 2005). A study by Zhan *et al.*, suggested a role for Scrib in breast cancer development, where knockdown of Scrib in the MCF-10 cell line altered cell polarity and caused inhibition of the capacity of the oncogene *c-myc* to induce apoptosis in breast epithelial cells (Zhan *et al.*, 2008).

To evaluate how different agents could induce changes in TJ functions, Martin *et al.*, studied the effect of selenium (Se), gamma linolenic acid (GLA) and iodate (I) in two different breast cancer cell lines, MDA-MB-231 and MCF-7. Even though the cell lines have different responses to the agents the study revealed how I, Se and Gla, independently or in combination, can induce changes in the TJ enhancing the transepithelial resistance. In addition to this, these three agents were also able to reverse the effect of the hormone 17-β estradiol on this cell line, which also causes modifications in the paracellular permeability of the endothelial cell line HUVEC decreasing the transepithelial resistance of the TJ (Ye *et al.*, 2003). A remodelling of the structure of TJs after treatment has also been reported, where the proteins Occludin and ZO-1 showed increased intensity when immunofluorescence staining was analysed as well as relocation in the cell membrane (Martin *et al.*, 2007).

Hepatocyte growth factor (HGF) is a cytokine that has been involved in cell motility, mitogenesis and morphogenesis in a broad range of cells including cancer cells. Treatment of cancer cells with HGF was seen to induce invasiveness as well as angiogenesis *in vitro* and *in vivo* (Jiang *et al.*, 2005). In the host laboratory, HGF has also been reported to disrupt the TJ in endothelial cells (Jiang et al., 1999b),an effect that can be reversed by highly unsaturated lipids (Jiang *et al.*, 1998). When breast cancer cell lines MDA-MB-231 and MCF-7 were treated over time with HGF, different TJ proteins such us Occludin, JAM-1 and -2, and Claudin-1 and -5 appeared to be regulated both at mRNA and protein levels as well as did their localisations inside the TJ (Martin *et al.*, 2004a).

All these results certainly indicate the potential involvement of different TJ proteins in the cascade of events related to breast cancer progression. Further studies will provide greater understanding of the role of these proteins in breast cancer and will clarify their contributions to tumour development.

Cancer type	Claudin type	Changed expression	Reference
Breast	Claudin-16	Down-regulated	(Martin *et al.*, 2008a)
	Claudin-7	Down-regulated	(Kominsky *et al.*, 2003)
	Claudin-1	Down-regulated	(Kramer *et al.*, 2000),(Hoevel *et al.*, 2002; Morohashi *et al.*, 2007), (Tokes *et al.*, 2005)
	Claudin-3, -4	Up-regulated	(Kominsky *et al.*, 2004)
Colon	Claudin-3,-4,-7	Up-regulated	(Montgomery *et al.*, 2006)
	Claudin-1,-2	Up-regulated	(Kinugasa *et al.*, 2007)
	Claudin-1	Down-regulated	(Resnick *et al.*, 2005)
	Claudin-7	Down-regulated	(Usami *et al.*, 2006)
	Claudin-1,-4	Up-regulated	(Resnick *et al.*, 2005)
Ovarian	Claudin-1,-2,-4	Down-regulated	(Litkouhi *et al.*, 2007)
	Claudin-7	Up-regulated	(Tassi *et al.*, 2008)
	Claudin-5	Up-regulated	(Turunen *et al.*, 2009)
Pancreatic	Claudin-4	Down-regulated	(Borka *et al.*, 2007)
	Claudin-3,-7	Up-regulated	(Borka *et al.*, 2007)
Prostate	Claudin-1,-7	Down-regulated	(Sheehan *et al.*, 2007)
	Claudin-5	Up-regulated	(Seo *et al.*, 2010)
Bladder	Claudin-4	Up-regulated	(Boireau *et al.*, 2007)
Lung	Claudin-1	Down-regulated	(Paschoud *et al.*, 2007)
	Claudin-3,-4,-7	Up-regulated	(Paschoud *et al.*, 2007)
	Claudin-5	Up-regulated	(Paschoud *et al.*, 2007)
	Claudin-5	Down-regulated	(Paschoud *et al.*, 2007)
Hepatocellular	Claudin-5	Down-regulated	(Sakaguchi *et al.*, 2008)

Table 1.3: Changes in expression levels of different Claudin members in human cancers.

1.5 Claudins, a multi-gene family

1.5.1 Structure of Claudins

To date the Claudin family is composed of 24 members in mammals having molecular weights ranging from 22 to 27 kDa (Table 1.4). There have been 54 Claudins identified in the fish *Takifugu* and 15 in *Danio rerio.* Invertebrates also express Claudins despite their lack of TJs, e.g. *Drosophila melanogaster* appears to have 6 Claudins. Claudins were originally thought to be simple sealing proteins at TJ. In fact, the name of *Claudin* derives from the latin word "claudere" which means to close.

Claudins were first identified by Furuse *et al.*, using the same isolated fraction from chicken liver from which Occludin was first identify by Tsukita's group in 1989 (Tsukita, 1989). They showed for the first time that a group of proteins existed with similar sequence to each other and with four transmembrane domains where the N- and C- terminal domains are orientated towards the cytoplasm, but with no similarity to Occludin. Claudin members have since been divided into two groups. The so called "Classic Claudins", which include members with high sequence homology like Claudin-1 to -10, -14,-15, -17 and -19. And the "Non-classic" Claudins which include Claudin-11, -13, -16, -18, and -20 to -24 (Krause *et al.*, 2008).

The cytoplasmatic C-terminal domain in Claudin varies between members in length and sequence, ranging from 21 to 63 residues. While the N-terminal domain is relatively short, 7 amino acid sequence, the intracellular loop is composed of 12

amino acids. The first extracellular loop is a 52 amino acid sequence which is highly conserved in different members with two conserved cysteines that influences parcellular charge selectivity [Gly-Leu-Trp-x-x-Cys-(8-10 aa)-Cys]. Some studies suggest that this loop determines the charge selectivity of the paracellular transport (Figure 1.6). The second extracellular loop is shorter, ranging from 16 to 33 amino acid residues. It is worth mentioning that this loop might fold in a helix-turn-helix motif which seems to be a participant in the Claudin-Claudin interactions (Piontek *et al.*, 2008) . It has been observed that this loop functions as a receptor for the *Clostridium perfringens* enterotoxin or CPE (section 1.5.2).

The cytoplasmic tails have the most varied sequences in the topology of the Claudins, their lengths range from 21 to 63 amino acid residues, suggesting the involvement of this structure in isoform-dependent paracellular selectivity. All members have a PDZ domain in their COOH- terminal tail (as already stated in section 1.2.1) that allows them to interact with other proteins in the TJ such as ZO-1, -2, and -3, MUPP, and PATJ. The interaction with cytoplasmic plaque proteins as ZO-1 links Claudins to the actin cytoskeleton (Van Itallie and Anderson, 2006). To date, there is no information about the function of the NH_2 domain.

Claudin name	Alternative name	Gene location
CLDN1	Senescence-associated epithelial membrane protein 1 (SEMP1)	3q28-q29
CLDN2	-	Xq22
CLDN3	Clostridium Perfringens Enterotoxin Receptor 2; CPETR2	7q11
CLDN4	Clostridium Perfringens Enterotoxin Receptor 1; CPETR1	7q11
CLDN5	Transmembrane Protein Deleted In Velocardiofacial Syndrome; TMVCF	22q11
CLDN6	-	16p13
CLDN7	-	17p13
CLDN8	-	21q22
CLDN9	-	16p13
CLDN10	-	13q3
CLDN11	Oligodendrocyte Transmembrane Protein; OTM	3q26
CLDN12	-	7q21
CLDN13	-	21q2
CLDN14	deafness, autosomal recessive 29, included; DFNB29, INCLUDED	21q22
CLDN15	-	3q28
CLDN16	Paracellin-1	21q2
CLDN17	-	3q34
CLDN18	-	3q21-q23
CLDN19	-	1p34
CLDN20	-	6q25
CLDN21	-	11q2
CLDN22	-	4q35
CLDN23	-	8p23
CLDN24	-	4q35

Table 1.4: The Claudin gene family. Information on gene location.

Figure 1.6: Model of Claudin protein structure.

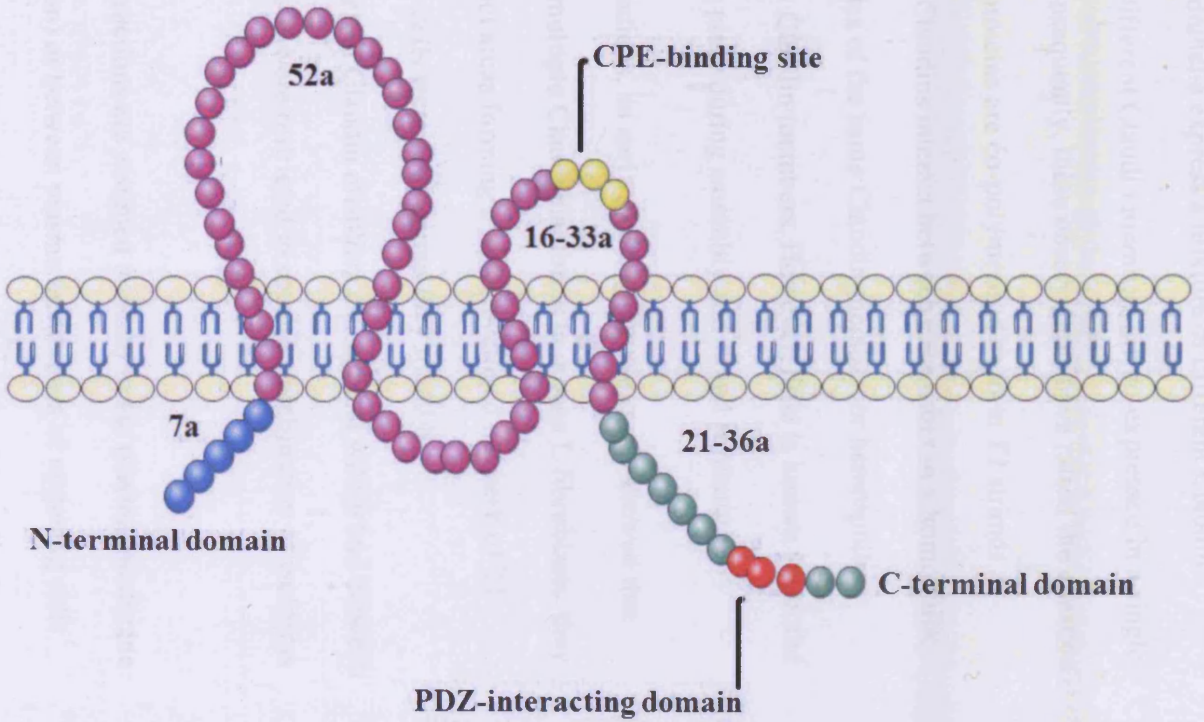

1.5.2 Claudin interactions

Most epithelia and endothelia express a mixture of different Claudin members and more than two different Claudin members are co-expressed in a single cell (Morita *et al.*, 1999a). Consequently, these observations have raised the question of whether different Claudin proteins are co-polymerised to form TJ strands as heteropolymers, and whether Claudins interact between each other in a homophilic manner, between two molecules of the same Claudin member, or heterophilic manner between two different Claudin members. However, little is known about the molecular mechanisms taking place during assembly and strand formation.

To assess all these questions, an early study by Furuse *et al.*, showed that when using co-expression of multiple Claudin isoforms in mouse L fibroblasts, they concentrated at cell-cell contact areas forming a well-developed network of TJ strands. However, when these cells were co-cultured they found by immunoprecipitation that different Claudin members can interact within and between TJ strands, but these interactions were restricted to specific combination of isoforms (Furuse *et al.*, 1999).

These heterotypic interactions are assumed to occur in the plasma membrane of the same cell (*cis*-interaction) or between plasma membranes of opposing cells (*trans*-interaction), in a similar way these interactions were defined in cadherins (Ahrens *et al.*, 2002).

Homophilic *trans*-interactions, also named homotypic interactions (Daugherty *et al.*, 2007), have been seen for Claudin-1,-2,-3 (Furuse *et al.*, 1999),

Claudin-5 (Morita *et al.*, 1999c), Claudin-6,-9, -14 (Nunes *et al.*, 2006), Claudin-11 (Morita *et al.*, 1999b), and Claudin-19 (Miyamoto *et al.*, 2005). All these Claudin isoforms were able to form TJs when transfected into TJ free cells. Homophilic *cis*-interaction, or homomeric interaction (Daugherty *et al.*, 2007), has been described for Claudin-5 and -5 using fluorescence resonance energy transfer (FRET) and electron microscopy (Piontek *et al.*, 2008).

Heterophilic *trans*- interactions, also termed as heterophilic interactions (Daugherty *et al.*, 2007), have been observed for Claudin-1 and -3, Claudin-2 and -3 (Furuse *et al.*, 1999) and for Claudin-3 and -5 (Daugherty *et al.*, 2007). The heterophilic interactions for at least these isoforms require compatible structural features in both extracellular loops. It has not been possible to demonstrate a heterophilic trans-interaction for Claudin-1 and -2 (Furuse *et al.*, 1999), Claudin-1 and -4 , Claudin-3 and -4, and Claudin-4 and -5 (Daugherty *et al.*, 2007). These results demonstrated that only specific Claudins are able to interact with each other. Heterophilic *cis*- interactions, or heteromeric interactions (Daugherty *et al.*, 2007), were found for Claudin-2 and -3, Claudin-3 and -4 and assumed for Claudin-1 and -2, respectively (Furuse *et al.*, 1999).

1.5.3 Physiological functions of Claudins

Paracellular transport through pores in the TJ differs in several important features from transcellular transport across the membrane. Firstly, it happens through the intercellular space of neighbouring cells. Secondly, this transport is passive and dependent on an electrochemical gradient. As discussed before (section 1.3), TJs play a central role in the intercellular space in epithelia and endothelia, and therefore

the key factor of paracellular transport. These pores, now known to be formed by Claudins are the major determinants of paracellular transport processes (Tsukita and Furuse, 2000).

The role of different Claudin members has been studied by three different approaches: by over-expression or down-regulation of Claudins in different cell lines, by knockdown of Claudin genes in mice and by the study of the phenotype of human diseases arising due to Claudin mutation (see section 1.5.5) (Angelow *et al.*, 2008). Taking together all the data from these studies, it is more than evident that the combination and mixing ratios of different Claudin isoforms determine the selectivity of paracellular transport across epithelia and endothelia.

To study the effect of different Claudins on conductance, monolayers of Madin-Darby canine kidney (MDCK) epithelial cells expressing a single type of Claudin have been used. There are two types of MDCK cell based on transepithelial electrical resistance, type I or "tight" cells, and type II or "leaky" cells.

A clear outline of results has been revealed, showing that the expression of Claudin-1,-4,-8,-14 and -15 significantly increases resistance when expressed in low-resistance MDCK type II cells. Whereas, the expression of Claudin-2 in high resistance MDCK type I cells decreases resistance (Van Itallie and Anderson, 2004). A Claudin-19 study in the same cell line has reported an increase in resistance and decrease in permeability to monovalent and divalent cations, but anions and urea were unaffected (Angelow *et al.*, 2007). Over-expression of Claudin-7 in the renal epithelial cell line of porcine proximal tubule LLC-PK1 has revealed an increase in resistance and a dramatic reduction of dilution potentials compared to wild type cells

(Alexandre *et al.*, 2005). Claudin-4, over-expression in the ovarian cancer cell line OVCA433, containing a mutation simulating its phosphorylated state, decreases the TJ strength (D'Souza *et al.*, 2005). Claudin-5 transfected in the human colonic cell Caco-2, low transepithelial resistance cell line, showed a significant increase in barrier function (Amasheh *et al.*, 2005).

The knockout of specific Claudin genes in mice also indicates that Claudins are the major participants of the selective size, charge, and conductance properties of the paracellular pathway. A very significant example has been seen in the Claudin-1 knockout mice, which die within 1 day of birth from dehydration (Furuse *et al.*, 2002). Claudin-11 null mice exhibit neurological and reproductive problems, showing the importance of this isoform in forming the paracellular physical barrier of the TJ required for spermatogenesis and normal central nervous system (Gow *et al.*, 1999). Claudin-14 knockout in mice showed a rapid degeneration of cochlear outer hair cells leading to deafness, suggesting the role of Claudin-14 as a cation-restrictive barrier in the maintenance of the ionic composition in this type of cells (Ben-Yosef *et al.*, 2003).

Colegio *et al.*, have shown, by swapping the first, second and both extracellular domains between Claudin -2 and -4 in MDCK type II cells, that charged amino acid residues on the first extracellular domain of Claudins mediates the paracellular permeability for ions (Colegio *et al.*, 2003). However, a recent study using chimeras of Claudin-2 and -4 in MDCK type II cells suggested that the extracellular domains are sufficient to increase the permeability, but the participation of the carboxy-terminal PDZ binding motif is also necessary indicating that an

interaction with other TJ cytoplasmic plaque proteins like as ZO-1, ZO-2, ZO-3 or MUPP-1 are also needed in order to form pores (Van Itallie *et al.*, 2009).

Examples of cation pore-forming Claudins are Claudin-2 (Amasheh *et al.*, 2009) as well as Claudin-16 that forms a Mg^{2+}-selective channel in the thick ascending limb of Henle (Schneeberger, 2003).The confirmation for anion pore-forming Claudins is less clear, nevertheless Claudin-10 has been identified as an anion-selective paracellular pore (Van Itallie *et al.*, 2006). Using polyethylene glycol oligomers (PEGs), small uncharged solutes, with increasing radii, Van Itallie *et al.*, measured the size of the pore formed by Claudin-2. This study has revealed that this pore has a high capacity for compounds charged and uncharged below 4Å and a lower capacity for larger solutes (Van Itallie *et al.*, 2009). To date there are no other studies on the sizes of pores formed by other Claudin isoforms.

The particular role played by a number of Claudin family members are yet to be identified. Examples are Claudin-6, -9, -12, -13,-17, -18, and 20-24. Claudin-6, -9 and -13 studies have closely linked these isoforms to the maturation of the epidermis or the barrier function in different cell types such as embryonic stem cells (ES) (Krause *et al.*, 2008). Studies for Claudin-12 showed that it is expressed in endothelia and epithelia of the mouse intestine (Fujita *et al.*, 2006) as well as in the inner ear and brain endothelial cells. Claudin-18 has also been identified in the inner ear (Kitajiri *et al.*, 2004). For other Claudin family member such as Claudin-17, -20, -22 and -23, only the mRNA expression levels have been identified in the duodenum of rats (Charoenphandhu *et al.*, 2007). The existence of Claudin-23 and -24 has only been established from the analysis of the human genome (Gerhard *et al.*, 2004).

1.5.4 Regulation of Claudins

The paracellular barrier modulated by Claudin members could be affected by a wide range of physiologic factors including cell signalling pathways, hormones, cytokines, and disruption of the cell-cell contacts. This field is still emerging and little is known about the mechanism that regulates the Claudin family. However, post-translational modifications, including phosphorylation, lipid modification and removal of Claudins by endocytosis, appear to be potential mechanism for the regulation of Claudins.

A number of studies have revealed that Claudin function can be highly regulated by phosphorylation. It is widely accepted that most Claudin members have potential serine and/or threonine phosphorylation sites in their cytoplasmatic COOH-terminal domain. Results after phosphorylation contribute in some cases to increase the barrier function of the TJ and in other cases to reduce it. For example, Protein Kinase-A (PKA) phosphorylation of Claudin-5, probably at the amino acid site around Thr207, results in an increase of the barrier function in porcine blood-brain barrier endothelial cells treated with cyclic AMP (cAMP) (Ishizaki *et al.*, 2003). However, PKA-dependent phosphorylation of Claudin-3, at the amino acid site Thr192 in the cytoplasmatic COOH-terminal domain, in the ovarian cancer cell line OVCA433 resulted in a decrease of the TJ strength (D'Souza *et al.*, 2005). Yamauchi *et al.*, found in MDCK type II cells that the threonine-serine kinase WNK4, binds and phosphorylates endogenous Claudin-1,-2,-3 and -4 and that the human disease-causing mutant of WNK4 is associated with increased paracellular chloride permeability without increasing sodium permeability (Yamauchi *et al.*, 2004). A

different study showed similar results and revealed that Claudin-7 is also a substrate to WNK4 on Ser206 in its cytoplasmatic COOH-terminal domain (Tatum *et al.*, 2007). Different studies have reported how other kinases are also linked to Claudin members such as MAPK (mitogen-activated protein kinase) phosphorylating Claudin-1 (Fujibe *et al.*, 2004), Claudin-4,-7,-8 and -9 (Carrozzino *et al.*, 2009). Rho kinase phosphorylating Claudin-4 (Tanaka *et al.*, 2005) and EphA2 phosphorylating Claudin-5 (Yamamoto *et al.*, 2008).

Endocystosis is a critical step in the remodelling of the TJ structure. To assure the correct sealing of the intercellular space of epithelial and endothelial cells this process has to be thoroughly regulated. Live observation and electron microscopy have revealed, in confluent Eph cells, that the endocytosis of Claudins was aided when wounding the cellular sheet and that other TJproteins such as Occludin and ZO-1 appeared to be detached from Claudins before this process occurred (Ikenouchi *et al.*, 2003).

Other potential post-translational modification is palmitoylation. Van Itallie *et al.*, shown that mutation of palmitoylation sites in MDCK type II cells alter the localization of Claudin-14, however, the stability and assembly of the TJ strands were not affected, indicating that alterations in transepithelial resistance in mutants might be due to the translocation of Claudin-14 (Van Itallie *et al.*, 2005).

When looking at the level of gene expression, the zinc finger-containing transcription factor Snail, which plays a pivotal role in epithelial-to-mesenchymal transition (EMT), emerged as a regulator of the Claudin gene expression binding directly to Claudin promoters. Claudin genes, as well as E-Cadherin and Occludin,

contain E-box motifs that trigger Snail and thus repress transcription (Ikenouchi *et al.*, 2003). A study in MDCK type II cells by Ohkubo *et al.* reported a possible second mechanism for Snail, finding that Snail down-regulates protein levels of Claudin-1 however, mRNA was unaffected, suggesting that Snail may regulate Claudin translation (Ohkubo and Ozawa, 2004).

Further experiments using MDCK type II cells expressing Snail showed an increase in the paracellular permeability for chloride and sodium. They also reported a slight decrease in Claudin-2 expression but a significant decrease in Claudin-4 and -7 (Carrozzino *et al.*, 2005). These results suggest that the increase in Snail expression has different effects in different Claudin members, resulting in selective changes in the cell barrier function.

Other transcription factors have also been reported. An early study by Niimi *et al.*, showed that one isoform lacking the C-terminal cytoplasmatic domain of Claudin-18 is regulated by the T/EBP/NKX2.1 homeodomain transcription factor which is expressed in the lung, thyroid and stomach (Niimi *et al.*, 2001). The transcription factor GATA-4 is also connected to one Claudin member, Claudin-2. GATA-4 binds to the promoter of Claudin-2 when the transcription factors CDX or HNF-1α are present suggesting that GATA-4 is totally necessary for the expression of Claudin-2 (Escaffit *et al.*, 2005).

Hepatocyte growth factor (HGF) and epidermal growth factor (EGF), have been seen to regulate Claudin family members. Both are cytokines that are involved in cell motility, mitogenesis and morphogenesis in a broad range of cells including

cancer cells where HGF can induce invasiveness as well as angiogenesis *in vitro* and *in vivo* (Jiang *et al.*, 2005)

Two different studies revealed that both cytokines have similar effects when treating MDCK type II cells with HGF and EGF. Both increased the transepithelial resistance linked to a reduction in the expression of Claudin-2 and activation of the extracellular signal-kinase (ERK) 1/2. ERK 1/2 inhibitor, U0126, induces Claudin-2 expression in MDCK type I cells which showed no levels of Claudin-2, in contrast to MDCK type II, which seems to have high levels of this Claudin isoform (Lipschutz *et al.*, 2005). In addition to this EGF, aside from increasing the transepithelial resistance in MDCK type II, induces cellular remodelling and enhances the expression levels of Claudin-1, -3 and -4 (Singh and Harris, 2004). All these results indicate the importance of ERK 1/2 in determining the paracellular permeability in MDCK cells. Peter *et al.*, studied the effect of EGF in the non-small cell cancer lung (NSCLC) cell line, their results showed that after treatment with EGF, levels of Claudin-2 expression is increased however, transepithelial resistance is reduced (Peter *et al.*, 2009).

HGF decreases transepithelial resistance and increases paracellular permeability in human endothelial cells HUVEC after treatment. The level of expression of Claudin-1 seems to be reduced overtime whereas no changes were observed in the levels of Claudin-5 (Martin *et al.*, 2002). When breast cancer cells, MDA-MB-231 and MCF-7, were treated with HGF, the transepithelial resistance was once more reduced. Claudin-1 transcripts levels were reduced in MDA-MB-231 cells through time, whereas changes in MCF-7 cells were less significant. When

looking at Claudin-5, significant changes in expression were seen in both cell lines (Martin *et al.*, 2004a).

Overall, it is clear that HGF and EGF modulate changes in expression of different Claudin family members and therefore altering the physiological function of TJs in different cell types including breast cancer cells.

1.5.5 Diseases involving Claudins

The effect of the disease progression on epithelial and endothelial barriers is almost always to make them leakier. In normal differentiated cells, a high degree of cellular organization is typically observed, but tumour cells exhibit abnormal structure and behaviour. This reflects a change in the TJ itself, such that it either disappears entirely or its permeability increases significantly. Usually in disease situations, the TJ barriers do not become "tighter".

It is increasingly apparent that changes in TJ functions are found in cancer development, as thoroughly reviewed in section 1.4. But in addition to cancer disease, there are a growing number of diseases reported to involve changes in the TJ functions. These include autoimmune diseases, infections and allergies (Table 1.5). This section will focus on Claudins and their aberrant expressions in diseases other than cancer.

A number of Claudins have been implicated in mutations leading to human diseases. Much of the information provided by these studies is currently helping to elucidate the role of Claudins and their importance in the development of severe diseases. For instance, mutation in Claudin-16 that introduces a premature stop

codon resulting in cleavage of the C-terminal cytosolic tail leads to recessive renal hypomagnesemia causing failure of the kidney (Muller *et al.*, 2006). Claudin-19 presented a similar deficiency in regulating magnesium reabsorption as well as retina development (Konrad *et al.*, 2006). Mutations provoking a premature stop codon in Claudin-1 caused severe chronic disease characterized by inflammation and fibrosis of the bile ducts named Neonatal Ichthyosis and Sclerosing Cholangitis Syndrome (NISCH), leading to liver failure (Hadj-Rabia *et al.*, 2004). Moreover, these patients also suffer from dry ichthyotic skin and thicker stratum corneum, a similar phenotype to Claudin-1 knockout mice in which animals died after dehydration due to "leaky" TJs (Zimmerli *et al.*, 2008). Claudin-11 (Gow *et al.*, 2004) and -14 (Wilcox *et al.*, 2001) mutations were associated with congenital deafness in mice and humans respectively, suggesting the role of these proteins in the cation-restrictive barrier that maintains the normal ionic concentration in the ear. Velo-Cardio-Facial/ DiGeorge syndrome (VCF), which is characterized by a broad range of phenotypes including conotruncal heart as well as facial dysmorphology, has been associated with mutations in chromosome 22q11, which maps to Claudin-5. It has been demonstrated that 80% of the patients displaying these syndromes have a deletion in the region coding for Claudin-5 (Sirotkin *et al.*, 1997).

Diseases provoked by mutations	Claudin type	Reference
Hypomagnesemia with hypercalciuria and nephrocalcinosis	Claudin-16	(Muller *et al.*, 2006)
Hypomagnesis and visual impairment	Claudin-19	(Konrad *et al.*, 2006)
Congenital deafness	Claudin-11,-14	(Gow *et al.*, 2004; Wilcox *et al.*, 2001)
Neonatal Ichthyosis and Sclerosing Cholangitis Syndrome (NISCH)	Claudin-1	(Hadj-Rabia *et al.*, 2004; Zimmerli *et al.*, 2008)
Velo-Cardio-Facial/ DiGeorge syndrome (VCF)	Claudin-5	(Morita *et al.*, 1999a; Sirotkin *et al.*, 1997)

Immunity-related Disease	Claudin type	Reference
Crohn's disease and ulcerative colitis	Claudin-2,-5,-8	(Zeissig *et al.*, 2007)
Multiple Sclerosis	Claudin-11	(Gow *et al.*, 1999)
Dermatophagoides pteronyssinus	Claudin-1	(Wan *et al.*, 1999)
Helicobacter pylori	Claudin-4,-5	(Fedwick *et al.*, 2005)
Clostridium perfringens	Claudin-3,-4	(Fujita *et al.*, 2000)
Rotavirus, HIV	Claudin-1,-7	(Dickman *et al.*, 2000; Zheng *et al.*, 2005)

Table 1.5: Claudin proteins involved in genetic and immune-related diseases.

Claudin expression has also been seen to be altered in response to inflammation and to pathogens resulting in changes to paracellular permeability. These changes in the TJ structure offer a perfect route for antigen penetration. Virus and pathogens have evolved numerous strategies to enter the cell cycle, however, before they can start to replicate and cause infection they firstly have to reach the apical surface of polarized epithelial cells. Recent studies have shown that *Clostridium perfringens* food poisoning, which is released into the intestinal lumen, binds directly to the second extracellular loop domain of Claudin-3 and -4 resulting in a inhibition of TJ reorganization as well as promoting endocytosis (Fujita *et al.*, 2000). Infection causing by *Helicobacter pylori* in the stomach alters the gastric epithelial barrier by activating myosin light chain kinase reducing levels of expression of Claudin-4 and -5, therefore increasing the permeability in the cell (Fedwick *et al.*, 2005). Rotavirus infections were also responsible for altering paracellular permeability by decreasing transepithelial resistance and changing the localization of Claudin-1 in Caco-2 cell line (Dickman *et al.*, 2000). Claudin-7 has been involved with Human inmmunodeficiency virus (HIV). CD4 is a primary receptor used by HIV to penetrate the epithelium. Zheng.*et al.*, have revealed that Claudin-7 enhances the viral susceptibility of CD4(-), suggesting that HIV can penetrate across the epithelial barrier through a direct interaction with TJ proteins (Zheng *et al.*, 2005)

Allergens like *Dermatophagoides pteronyssinus* can cause disruption in the TJ structure by increasing paracellular permeability allowing the pathogen to cross the epithelial barrier and by cleaving the extracellular domains of Claudin-1 (Wan *et al.*, 1999). Multiple sclerosis, an inflammatory demyelinizing disorder of the central

nervous system (CNS), has been linked to Claudin-11. Claudin-11 is presented in the CNS as well as in the testis and plays a pivotal role in the paracellular barrier of both as implied through the neurological and reproductive failures seen in Claudin-11 knockdown mice (Gow *et al.*, 1999). Another example of Claudin misregulation has been seen in Crohn's disease and ulcerative colitis, which provokes not only gastric problems but inflammatory too. The TJ structure is altered as Claudin-5 and -8 were down-regulated as well as the pores formed by Claudin-2 which in this case was highly up-regulated (Zeissig *et al.*, 2007).

1.5.6 Claudins as emerging targets for cancer

Due to the high specificity of expression patterns of Claudins in cancer, the possibility of Claudins being utilised as useful molecular markers has been raised. Regardless of their exact functions in cancer cells, Claudin protein expression may have a significant clinical relevance. Research in the past has been focused on the expression of members of the Claudin family in a number of cancer types as described in section 1.4. Studies have revealed how some of the Claudins were up-regulated in cancer progression while others were down-regulated. This data opens up the possibility of the potential value of Claudins as targets for therapeutic intervention. A number of key points have arisen from various studies into targeting Claudins for cancer therapy.

1. Claudins are cell surface proteins that contain two extracellular domains which are accessible as target sites for therapy.

2. Claudin members have been found to be over-expressed in a number of different cancers showing different expression patterns between normal and tumour cells.

3. Claudins could be more accessible in tumour cells due to an increase in TJ permeability compared with normal cells (Soler *et al.*, 1999) even if Claudins are not over-expressed in that tumour type.

As previously stated, Claudins, are transmembrane proteins with two relatively large extracellular loops, and present themselves as promising targets for antibody therapy. This therapy is based on antibodies against Claudins that will specifically recognize one of these loops and therefore induce leaky TJ or even destroy them (Tsukita *et al.*, 2008); or antibodies that will simply, after specific binding to the C-terminal domain of the Claudins, provide evidence for the antibody-based therapy approach (Kominsky, 2006).

Cell tumour lysis can be achieved by attachment of toxins to the cell surface, or by stimulating a response from the immune system. The second extracellular loop of some Claudins have appeared to be a receptor for the *Clostridium perfringens* enterotoxin (CPE), usually associated with *Clostridium perfringens* type A, which is known for causing cytolisis in mammalian cells due to its effects on membrane permeability. This binding allows the formation of a large multiprotein membrane-pore complex, which alters the osmotic equilibrium in the cell causing lysis. Although several Claudins have shown binding affinity to CPE like Claudin-4, -6, -7, -3, -14, -8 (Fujita *et al.*, 2000) only Claudin-3 and -4 have been seen to form this complex. Taking these results in consideration, and based on the evidences from different studies that revealed over expression of these two Claudins members in

breast, pancreatic, colon, lung as well as ovarian cancers (see table 1.3), Claudin-3 and -4 might be perfect candidates for CPE-based therapy. More recently Kominsky *et al.*, performed similar experiments treating several breast cancer cell lines expressing Claudin-3 and -4, such as MCF-7, SKBr3 and T47D, as well as cell lines lacking both proteins, such as HS578T and MDA-MB-435, with CPE. Results revealed that breast cancer cell lines lacking these particular Claudin proteins were totally resistant to the cytotoxic effects caused by the enterotoxin but not the Claudin-expressing cells, resulting in complete cytolysis. To complement the *in vitro* study, they investigated the cytolytic effects of CPE on the T47D breast cancer cell line *in vivo,* resulting in a significant reduction in tumour volume as well as cell necrosis (Kominsky *et al.*, 2004). Recent studies have used *Pseudomonas aeruginosa* exotoxin as a method of cancer-targeting therapy. The exotoxin binds to the cell surface, enters the cytosol by endocytosis, releasing PSIF which inhibits protein synthesis. Saeki *et al.*, have reported that the artificial complex C-CPE- PSIF interacts with Claudin-4 through C-CPE binding domain and shows *in vivo* anti-tumour activity against the 4T1 breast cancer cell line, causing a significant reduction in tumour growth (Saeki *et al.*, 2009). Similar results were obtained when studying metastasis in the lung using the Claudin-4 expressing cell line B16, where the treatment with the complex C-CPE- PSIF revealed reduction in tumour growth and metastasis without any side effects in the mice (Saeki *et al.*, 2010). A related study by Kakutani *et al.*, reported the fusion between C-CPE and the *diphtheria* toxin A (DTA) which also inhibits proteins synthesis in gastrointestinal L cells expressing different Claudin proteins. Results revealed specificity from the DTA-C-CPE complex to Claudin-4 expressing cells (Kakutani *et al.*, 2010).

Therefore, exhaustive administration of the enterotoxin CPE to cancer cells might be a potential approach for cancer therapy. The key question to be addressed in the near future is how to avoid cellular toxicity in the surrounding normal cells caused by the administration of CPE, or whether there are other toxin displaying affinity to different Claudin proteins in the cell.

Claudins are indeed unusual proteins in the TJs structure as they are presented in a variety of tissues with different properties. Their mixture and different ratios between the 24 members confers specific barrier properties to each cell. These special features make the modulation of Claudins a promising method to deliver and enhance absorption of drugs to a target tissue through the paracellular pathway as 60% of these targets are located at the cell surface (Kondoh and Yagi, 2007).

Overall these findings indicate that further study and preclinical testing are required to assess the usefulness of Claudins as emerging targets for cancer.

1.6 Claudin-5

Claudin-5 was firstly described by Morita and colleagues in 1999 (Morita *et al.*, 1999a). It was initially identified as a deleted protein in patients who suffer from the velo-cardio-facial syndrome hereditary disease and was termed TMVCF (transmembrane protein deleted in velo-cardio-facial syndrome) and the gene was mapped to chromosome 22q11 (Sirotkin *et al.*, 1997). A different group described, in the same year as Morita, the expression of Claudin-5 in brain capillary endothelial cells and originally termed this protein MBEC1 (mouse brain endothelial cell 1) (Chen *et al.*, 1998). In both studies the concentration of TMVCF/ MBEC1 were not

examined. Claudin-5, TMVCF and MBEC1 have been identified as the same protein (Morita *et al.*, 1999c). Morita *et al.*, subsequently developed a specific antibody against Claudin-5 revealing a high level of expression in the brain, lung and endothelial cells of the blood vessels concluding that Claudin-5 was an endothelial-specific component of the TJ strand (Morita *et al.*, 1999c). However, several studies have reported Claudin-5 to be expressed in certain epithelial TJs, such as, the stomach, rat liver and pancreas (Rahner *et al.*, 2001) as well as in cell lines like HT-29/B6, an epithelial cell derived from human colon (Amasheh *et al.*, 2005). Surprisingly, when looking at the level of expression of Claudin-5 in the human colonic cell Caco-2, Claudin-5 was not present although it is present in the human intestine. Similar results were seen in MDCK-C7 (presenting "tight" TJ) and MDCK-C1 (presenting "leaky" TJ). To complement the study, they measured the transepithelial resistance in Caco-2 and MDCK-C7 following transfection with FLAG-Claudin-5 cDNA. The results revealed an obvious increase in resistance of Caco-2 transfected cells, but no differences were seen in MDCK-C7. These results suggested a role for Claudin-5 as a "sealing" protein in the TJs of epithelial cells as the over-expression caused changes in the paracellular barrier of this particular cell line (Caco-2) making it tighten, whereas in cells that exhibit high transepithelial resistance (MDCK-C7) no changes to the barrier properties were observed (Amasheh *et al.*, 2005). Studies focusing on blood-brain barrier (BBB) also have proposed a "sealing" role for Claudin-5 (Wolburg *et al.*, 2003) (Nitta *et al.*, 2003). BBB protects the brain from the blood surroundings within the central nervous system (CNS), and most importantly maintains homeostasis of the brain environment, which is crucial for neural activity and function. Extremely close TJs between endothelial cells of

brain capillaries prevent the passage of hydrophilic molecules from blood to brain and vice versa. Mice genetically altered to lack Claudin-5 were generated in a study by Nitta *et al.* These mice have shown a normal development and morphology of blood vessels in the brain, however, in terms of the barrier function, these endothelial cells showed an unexpected feature: a size-selective loosening of the BBB, in other words, only small molecules (<800Da) were allowed to pass across the TJ but no larger molecules were affected. Moreover, Claudin-5 deficient mice die within 10 hours of birth (Nitta *et al.*, 2003). Therefore, it appears that loss of Claudin-5 from the TJ complexes in the brain can compromise barrier function making it "leakier" while keeping their structural integrity, demonstrating that Claudin-5 specifically tightens the BBB for molecules <800Da. The majority of the drugs in clinical use are included in this range, subsequently Claudin-5 might be interesting in terms of drug delivery to brain tumours or neurodegenerative disease.

Not much is known regarding the transcriptional regulation of Claudin-5. In porcine blood-brain barrier endothelial cells, cyclic AMP (cAMP) increases Claudin-5 gene expression in a protein kinase A (PKA) independent and dependant way. PKA activation by cAMP enhances the signal of Claudin-5 along cell borders and in the cytoplasm as well as increasing the TER in dependent and independent pathways. It was also reported that the amino acid site Thr^{207}in the cytoplasmatic COOH-terminal domain is the phosphorylation site for PKA (Ishizaki *et al.*, 2003). A parallel study in the rat lung endothelial cell line (RLE) which displays failed TJs, revealed that when mutations in the Thr^{207} of Claudin-5 were introduced, the barrier function was altered while in the forced expression of Claudin-5 the TJ structure was partially formed allowing only the passage of the small molecules. These results

highlight how the phosphorylation of Thr^{207} site by PKA provokes changes in the Transendothelial resistance of the cells as well as loosening of the Claudin-5 barrier against small molecules (Soma *et al.*, 2004). Studies examining the effect of Ethanol (EtOH) in the BBB have revealed that the permeability of the BBB is altered via structural alterations of the TJ (Jonsson and Palmblad, 2001). When bovine brain microvascular endothelial cells (BBMEC) were treated with EtOH, a decrease in the transepithelial resistance was observed. Claudin-5 staining was decreased and phosphorylation of myosin light chain (MLC) as well as Claudin-5 and occludin were confirmed. This suggests that EtOH activates myosin light chain kinase (MLCK) leading to Claudin-5 phosphorylation. These results reported a different phosphorylation pathway from the one suggested by Ishizaki *et al.*, (Haorah *et al.*, 2005). A more recent study in brain endothelial cells bEnd3 has shown another possible Claudin-5 kinase. Yamamoto *et al.*, using a recombinant of Claudin-5 and Occludin, have reported that Rho kinase (RhoK) directly phosphorylates site Thr^{207} on Claudin- 5. As a result, reduced Transepithelial resistance was observed (Yamamoto *et al.*, 2008). As mentioned in section 1.5.2, HGF regulates the level of expression of Claudin-5 in breast cancer cells MDA-MB-231 and MCF-7 (Martin *et al.*, 2004a).

It has been reported that endothelial vascular protein VE-cadherin expression and aggregation at the TJ appears to be a requirement for the transcriptional up-regulation of Claudin-5. Taddei *et al.*, have proposed a pathway in the absence of VE-cadherin through which the inactivation of the complex formed by the forkhead box transcription factor FoxO1 and β-catenin results in down-regulation of Claudin-5 gene. However, when VE-cadherin is expressed in the cell FoxO1 becomes

phosporylated whereas β-catenin is sequestered at the plasma membrane. Nevertheless, it is important to notice that the lack of VE-cadherin and therefore of Claudin-5 expression did not alter the structure of the TJ although the paracellular permeability was significantly decreased (Taddei *et al.*, 2008). The description of the murine Claudin-5 promoter region has already been reported. The murine Claudin-5 gene is mapped on chromosome 16 and the complete nucleotide sequence of the promoter was found to be 1131bp. The promoter constructs were transfected into the murine brain cEND and microvascular MyEND endothelial cells. The study examined the influence of the inflammatory cytokine TNFα and the synthetic glucocorticoid dexamethasone on Claudin-5 promoter activity and in Claudin-5 mRNA levels. Treatment with TNFα resulted in a decrease in the promoter activity as well as strong down-regulation of Claudin-5 mRNA levels in both cells. Conversely, treatment with dexamethasone revealed an increase in the promoter activity and therefore in Claudin-5 mRNA levels. This effect was more noticeable in cEND cells, suggesting a tissue-specific regulation of Claudin-5 via glucocorticoids (Burek and Forster, 2009). A recent study on HUVEC, human umbilical vein endothelial cells, revealed that the human Claudin-5 gene is regulated by the sex determining region Y-box SOX18, a specific-regulatory factor in endothelial cells. Over-expression of SOX18 induced an increase in Claudin-5 expression at mRNA and protein level in confluent culture cells of HUVEC whereas the effect on single isolated cells was not evident. Silencing SOX18 resulted in a significant decrease of Claudin-5 mRNA and protein levels whereas in other proteins of the TJ such as Occludin levels remain unaltered. These results indicate that SOX18 is specifically involved in the regulation of Claudin-5 and is dependent on cell density (Fontijn *et*

al., 2008). A recent study *in vitro* and *in vivo* has described Claudin-5 as a novel oestrogen target in vascular endothelium. Treatment of murine brain and heart endothelial cells, cEND and MyEND respectively, with 17β-Estradiol (E2) has revealed an increase in transepithelial resistance and up-regulation of Claudin-5 levels. Similar results were obtained *in vivo* after E2 treatment. However, in ERβ knockout mice significantly lower levels of Claudin-5 were detected. Thus, this data suggested Claudin-5 as a new oestrogen target in vascular endothelium (Burek *et al.*, 2010).

Martin *et al.*, studied the effect of selenium (Se), gamma linolenic acid (GLA) and iodate (I) in HECV, human umbilical vein endothelial cells. Se, GLA and I in combination or individually can induce changes in the TJ enhancing the transepithelial resistance via regulation of Claudin-5 as well as Occludin and ZO-1. Claudin-5 showed an increase in staining intensity after treatment. This effect was more evident when I was present, in particular when combined with Se after 0.5h of treatment. These three agents were able to reverse the effect of the hormone 17-β estradiol on this cell line (Martin *et al.*, 2006).

Claudin-5 has been linked to the follicular development in the marmoset ovary. The study *in vivo* on this primate has revealed that vascular endothelial growth factor (VEGF) inhibition might induce changes in expression of Claudin-5 thus compromising the follicular development as a result of alterations in the TJ structure (Rodewald *et al.*, 2007). Subsequently an *in vitro* study using a co-culture of human umbilical vein endothelial cells (HUVEC) and luteinized granulosa cells (LGC) has examined the paracrine effect of human chorionic gonadotrophin (hCG),

and its relation with ovarian hyper stimulation syndrome (OHSS), a disease characterized by increased capillary permeability. Results, after treatment with hCG, have revealed down-regulation of Claudin-5 protein expression, an increase in endothelial permeability as well as an increase in VEGF concentration. However, when cells were treated with VEGF inhibitor, down-regulation of Claudin-5 and changes in permeability were not seen. These results suggested that hCG does not directly regulate Claudin-5. Instead hCG might be involved in the regulation of VEGF which appears to be responsible for the reduction in Claudin-5 expression and subsequent changes in cell permeability (Rodewald *et al.*, 2009).

Studies of fluorescent tagged Claudin-5 in the HEK-239 cells (human embryonal kidney cell line 239) and the MDCK cell line have shown that Claudin-5 is able to form homodimers in the plasma membrane of the same cell, moreover it was demonstrated that the second extracellular loop is responsible for the self-association (Blasig *et al.*, 2006). A subsequent study, using fluorescence resonance energy transfer (FRET) and electron microscopy, demonstrated that homophilic *cis*-interaction occurs for Claudin-5 and -5 (Piontek *et al.*, 2008).

1.6.1 Role of Claudin-5 in breast cancer progression

Currently, within the literature there are a limited number of studies examining Claudin-5 in human cancer, with very few focusing on breast cancer.

Increased Claudin-5 expression has been associated with aggressive behaviour in serous ovarian carcinomas. Turune *et al.*, studied 85 serous ovarian cancer tissue samples. Immunostaining results revealed strong Claudin-5 staining in

advanced stage and high grade carcinomas. When looking at Claudin-5 expression, only 25-30% of patients who were Claudin-5 positive were still alive at 5 years follow-up compared to 60% of patients who were Claudin-5 negative (Turunen *et al.*, 2009). Examination of Claudin-5, as well as Claudin-1,-3 and -4, in 118 cases of gastric carcinoma revealed that the lowest expression of all these Claudin members was in Claudin-5. Nevertheless, strong Claudin-5 expression was associated with levels of E-cadherin, high levels of cell proliferation and apoptosis. The results also revealed that expression of these Claudin members was lower in diffuse-type gastric carcinoma (Soini *et al.*, 2006). A similar study in human lung squamous cell carcinoma and adenocarcinoma has reported high levels of Claudin-5 in cylindric cells, pneumocytes and adenocarcinamas, and low or even undetectable levels of expression in basal cells and squamous cell carcinoma. These results indicate the possible role of Claudin-5 as a diagnostic tool to distinguish between adenocarcinomas and squamous cell carcinomas in lung cancer patients (Paschoud *et al.*, 2007). Examination of Claudin-5 in 48 prostate cancer patients has reported that 35% of patients showed low expression of Claudin-5 in comparison with 65% that displayed a high level of expression. From those who were classified in the low-expression group, 88% had a Gleason score of 7 or even higher and 12% had a Gleason score of 6 points or lower, whereas those classified in the high-expression group 52% had a Gleason score of 7 or higher and 48% had a Gleason score of 6 points or lower. Therefore it can be concluded that Claudin-5 is associated with a Gleason score of 7 points or higher in prostate cancer patients (Seo *et al.*, 2010). In hepatocellular carcinoma, Claudin-5 has been reported to be down-regulated. Low levels of Claudin-5 and vasculobiliary invasion have been correlated with patients

displaying poor prognosis. Taking these results together, a possible role for Claudin-5 as a prognostic factor in hepatocellular carcinoma has been suggested (Sakaguchi *et al.*, 2008).

1.7 Aims of this study

The Claudin family are TJ proteins expressed in endothelial and epithelial cells. As already stated, they participate in the formation of tissue barriers between different tissue compartments by regulating the efflux of molecules through TJ complexes. At least 24 different Claudin members are known today, all of which are thought to vary in expression depending on location and cell type.

The role of Claudin proteins in carcinogenesis and progression to metastasis is an active area of investigation as a result of the frequent finding of altered Claudin expression in cancer. To date, the majority of studies on cancer have focused on Claudin-1, -3, -4, -7 , -10 and -16, but very little is known about Claudin-5. Therefore the aims of this thesis were to investigate the role of Claudin-5 in breast cancer by:

1. Determining the level of expression and distribution of Claudin-5 in human breast cancer and normal background tissues, using immunohistochemical staining and RT Q-PCR and analysing the levels of transcripts against clinical parameters such as grade of tumour, metastasis and clinical outcome of patients in order to investigate a possible link

between expression levels of Claudin-5 and aggressiveness in cells and patient outcome.

2. Investigating the *in vitro* effects of knockdown and forced expression of Claudin-5, in the MDA-MB-231 breast cancer cell line and in HECV human endothelial cells, on the growth, invasion, migration, adhesion, motility, tubule formation, transepithelial/transendothelial electrical resistance (TER) and electrical cell-substrate impedance sensing (ECIS).
3. Investigating *in vivo* the effects of over expression of Claudin-5 in growth of the human breast cancer cell line MDA-MB-231 and HECV cells.
4. Assessing the role of Claudin-5 on control of epithelial and endothelial motility involving the N-WASP and ROCK signalling cascade. This is a new avenue of research in determining the functions of Claudin-5 which in past studies is named as a "sealing" protein of TJ structure.

Chapter 2

General Materials and Methods

2.1 Standard solutions

2.1.1 Solutions for cell culture

All standard chemicals and reagents used in my work, unless otherwise specified, were obtained from Sigma (Dorset, UK).

0.05M EDTA

One gram of KCl (Fisons Scientific Equipment, Loughborough, UK), 5.72g of Na_2HPO_4, 1g of KH_2PO_4, 40g of NaCl and 1.4g EDTA (Duchefa Biochemie, Haarlem, The Netherlands) was dissolved in distilled water to make a final volume of 5L. We adjust the solution to pH 7.4 before it was autoclaved and stored for use.

Trypsin (25mg/ml)

Five hundred milligrams of trypsin was dissolved in 20ml 0.05M EDTA. The solution was mixed and filtered through a 0.2 μm minisart filter (Sartorious, Epson, UK), aliquoted in 250 μl samples and stored at -20°C until required. For use in routine cell culture one aliquot was diluted in a further 10ml of EDTA solution and used for cell detachment.

Penicillin (120mg/ml)

Six hundred milligrams crystapen injection benzylpenicillin sodium (Britannia Pharmaceuticals Limited, Surrey, UK) was dissolved into 5ml sterile injection waster (B.Braun, Germany).

Streptomycin Sulphate (250mg/ml)

Five grams of streptomycin sulphate was dissolved in 20ml sterile injection water, filtered thrugh a 0.2 μm minisart filter and stored at -20°C until required.

Balanced Saline Solution (BSS)

Seventy nine and a half grams of NaCl, 2.2g of KCl, 2.1g of KH_2PO_4 and 1.1 g of Na_2HPO_4 was dissolved in distilled water to make a final volume of 10L. We adjusted the solution to pH 7.2 before used.

2.1.2 Solutions for microbiological methods

Luria Bertani (LB) agar

Ten grams of tryptone (Duchefa Biochemie, Haarlem, The Netherlands), 5g of yeast extract (Duchefa Biochemie, Haarlem, The Netherlands), 10g of NaCl and 15g of agar was dissolved in distilled water up to a final volume of 1L, the pH adjusted to 7.0 and the solution was autoclaved. When required the solution was heated to liquid and cooled slightly before adding selective antibiotics (if required). The solution was then poured into $10cm^2$ petri dish plates (Bibby Sterilin Ltd., Staffs, UK), allowed to cool and harden, inverted and stored at 4°C.

LB broth

Ten grams of tryptone, 5g of yeast extract and 10 g NaCl was dissolved in distilled water up to a final volume of 1L and the pH adjusted to 7.0. It was autoclaved and allowed to cool before adding selective antibiotic (if required) and storing at room temperature.

2.1.3 Solutions for use in RNA and DNA molecular biology

DEPC treated water

Two hundred and fifty microlitres diethyl pyroncarbonate (DEPC) was added to 4750µl of distilled water. The solution was then autoclaved before use.

5X Tris, Boric acid, EDTA buffer (TBE)

A 5x stock solution comprising 545 g of Tris-Cl (Melford Laboratories Ltd., Suffolk, UK), 275g of Boric acid (Melford Laboratories Ltd., Suffolk, UK) and 46.5g of disodium EDTA (Duxhefa Biochemie, Haarlem, The Netherlands) were dissolved in distilled water and made up to a final volume of 10L. The solution was stored at room temperature and diluted to 1X concentrate prior to use in agarose gel electrophoresis.

Ethidum bromide

Ethidum bromide powder (100mg) was dissolved in 10ml of distilled water. The container was wrapped in aluminium foil to protect the solution from the light and stored safely before use.

2.1.4 Solutions for protein work

Lysis Buffer

Two millimolar $CaCl_2$, 0.5% of Triton X-100, 1mg/ml leupeptin, 1mg/ml aprotinin and 10 mM sodium orthovanadate was dissolved in distilled water and stored at 4^{0}C until it was required.

10% Ammonium Persulfate (APS)

One gram of ammonium persulfate was dissolved in 10ml of distilled water, and separated into 2.5ml aliquots and stored at 4°C until it was required.

10X Running buffer

A 10X stock solution (0.25M Tris, 1.92M glycine, 1%SDS, pH 8.3) was made by dissolving 303 g of Tris, 1.44Kg of glycine and 100g of SDS in 10L distilled water.

Transfer buffer

A 5 litre stock solution comprising 72g glycine, 15.15 g Tris and 1L Methanol (Fisher Scientific, Leicestershire, UK) were dissolved in distilled water up to the a final volume of 5L.

10X TBS

A 10x TBS stock solution comprising 121g Tris and 400.3g NaCl were dissolved in distilled water, made up to a final volume of 5L and adjusted to pH 7.4.

Ponceau S staining

As supplied (Sigma, Dorset, UK).

Amido black stain

Two and a half grams of amido black (Edward Gurr Ltd., London, UK) was dissolved in 50ml of Acetic acid (Fisher Scientific, Leicestershire, UK). 325 ml of distilled water was added and the solution was mixed.

Amido black destain

A hundred millilitres of Acetic acid and 250ml of ethanol were added to 650ml of distilled water.

2.1.5 Solutions for cell and tissue staining

DAB chromogen

The DAB (Diaminobenzidine) chromagen was prepared fresh by mixing the following reagents in order: 2 drops of wash buffer, 4 drops of DAB (Vector Laboratories Inc., Burlingame, USA) and 2 drops of H_2O_2 up to 5ml of distilled water. The container was wrapped in aluminium foil to protect the solution from the light.

ABC complex

The ABC complex was prepared using a kit (Vector Laboratories Inc., Burlingame, USA) by mixing the following reagents in order: 4 drops of reagent A were added to 20ml of wash buffer, followed by the addition of 4 drops of reagent B and mixed well. This was made up at least 30 minutes before being used.

2.2 Animals, cell lines and cell culture

All cell culture work was carried out in class II microflow cabinets. Pipettes, culture medium, and all other cell culture equipment was either purchased sterile or autoclaved prior to use. All cells were cultured in an incubator at 37°C in 5% carbon dioxide.

2.2.1 Cell lines, breast tissue and animals

The human breast cancer cells line MDA-MB-231 and the human endothelial cell line, HECV (ICLC Genova, Italy) were used in this study. The cells were routinely maintained in Dulbecco's Modified Eagle's medium supplemented with 10 % foetal calf serum (FCS), penicillin, and streptomycin (Sigma-Aldrich TD). Full details of four cell lines are provided in Table 2.1.

Claudin-5 expression was screened in a panel of other cell lines. Cell lines in this panel consisted of: MDA-MB-157, MDA-MB-463, BT-549, MCF-7, MDA-MB-436, ZR-751, MDA-MB-435S, BT-474, MDA-MB-231, BT-474KC, DU-145, PNT-19, PNT-2C2, PANC-1, MiaPaCa, Cor- L677, MCR5, RT-112, A-431, Ha-Cat ,HRT-18,HT-115, HECV and HUVEC.

All cell lines were obtained from ATCC, Rockville, Maryland, USA or ECACC, Salisbury, UK. The PNT1A and PNT2C2 cell lines were generous gifts from Professor Norman Maitland (University of York, England, UK).

A total of 133 breast samples were obtained from breast cancer patient (27 background normal breast tissue and 106 breast cancer tissue), with the consent of the patients and ethical committee. These tissues were collected immediately after mastectomies, and snap-frozen in liquid nitrogen. The pathologist (ADJ) verified normal background and cancer specimens, and it was confirmed that the background samples were free from tumour deposit.

The 4-6 week old CD-1 athymic nude mice used in the *in vivo* tumour development model were obtained from Charles Rivers Laboratories (Kent, England, UK) and maintained in filtertop cages under ethical conditions.

Cell line	Organism	Morpholo.	Ethnicity	Gender	Age	Source and Feature
MDA-MB-231	Homo sapiens	epithelial	Caucasian	female	51 years adult	**Organ:** mammary gland; breast **Disease:** adenocarcinoma **Derived from metastatic site:** pleural effusion
HECV	Homo sapiens	endothelial	Caucasian	female	newborn	**Organ:** umbilical vein **Tissue:** vascular endothelium **Disease:** normal

Table 2.1: Cell lines used in this study.

2.2.2 Preparation of growth medium

Cells were routinely cultured in Dulbecco's Modified Eagle's Medium (DMEM / Ham's F-12 with L-Glutamine (PAA Laboratories, Somerset, UK), supplemented with streptomycin (Streptomycin Sulphate salt, Sigma-Aldrich Co), penicillin (Benzylpenicillim, Britannia, Pharmaceutical, Ltd.) and 10% heat inactivated foetal calf serum (Invitrogen, Paisley, UK).

Transfected cell lines, containing the pEF6/ V5-His TOPO TA plasmid vector , were cultured for 10 days in selection medium containing 5μg/ml of Blasticidin S. and later were selection was completed were routinely cultured in a maintenance medium containing 0.5μg/ml of Blasticidin S.

2.2.3 Maintenance of cells

HECV and MDA-MB-231 cell lines were cultured in an incubator (Sanyo MDA15AC) and maintained in supplemented DMEM/Ham's F12 medium prepared as described above. Cells were grown to confluence in either 25 cm^3 or 75 cm^3 tissue cultured flasks loosely capped (Greiner Bio-One Ltd., Gloucestershire, UK) at 37°C in 5% carbon dioxide and 95% humidification. The flasks were left to reach confluency before commencement of experimental work.

All cell culture work was carried out following aseptic techniques inside a class II laminar flow cabinet and autoclaved instruments to keep conditions sterile.

2.2.4 Trypsinization of cells

Cell lines were grown until they reached approximately 80-90% confluence. Confluence was assessed by visually evaluating the coverage of cells over the

surface of the tissue culture flask using a light microscope. The culture medium was removed and the cells briefly rinsed at room temperature with 1-2 ml of trypsin Ethylenediaminetetraacetic acid (Sigma-Aldrich, Gillingham, Dorset, UK), which contains trypsin 0.01%(v/w) and EDTA 0.05% (v/w) in BSS buffer, for several minutes. The detached cell suspension was transferred to a 20 ml universal container (Greiner Bio-One Ltd., Gloucestershire, UK) and centrifuge at 1600 rpm for 8 minutes to pellet the cells. The supernatant was aspirated and the pellet was resuspended in 5 ml of cell culture medium.

The cells were then re-cultured into new tissue culture flasks, counted for immediate experimental work or stored by freezing in liquid nitrogen.

2.2.5 Cell counting

Cells were counted in a haemocytometer counting chamber using an inverted microscope (Reichert, Austria) at 10 x10 magnification for further *in vivo* and *in vitro* cellular functional assays. The dimensions of each 16 square area containing the cells to be counted, is 1mm x 1mmx 0.2 mm which allowed the number of cells per millilitre to be determined using the following equation:

Cell number/ml= (number of cells counted in 16 small squares ÷ 2) x (1×10^4)

2.2.6 Cell storage in liquid nitrogen

The cell lines were stored in liquid nitrogen after detachment from a large 75 cm^3 and pelleted in a centrifuge as described in section 2.2.4. The freezing medium was prepared by supplementing standard culture medium (as described above) with 10% Dimethylsulphoxide (DMSO) (Sigma-Aldrich, Gillingham, Dorset, UK).

Following resuspension, which was dependent on the number of samples to be frozen, 1ml of cells were transferred into 1.8 ml cryospreservation tubes (Nunc, Fisher Scientific, Leicestershire, UK). Tubes were wrapped loosely in 3 layers of tissue paper and stored overnight at -80°C in a deep freezer before storage in liquid nitrogen tanks for long term storage.

2.2.7 Recovery of cells from liquid nitrogen

Frozen cells were removed from liquid nitrogen and placed in a warm water bath at 37°C for 1-2 minutes to facilitate rapid thawing. After completely thawing the cell suspension was transferred to a universal container containing 10 ml of pre-warmed medium and allowed to revive for 10 min before being centrifuged at 1600 rpm for 8 minutes. The supernatant was aspirated, the pellet resuspended in 5ml of pre-warmed medium and placed into a fresh $25cm^3$ tissue culture flask and incubated at 37°C, 95% humidification and 5% CO_2. Following incubation, the flask was examined under a light microscope to ensure a sufficient number of healthy adherent cells.

2.3 Generation of mutant HECV and MDA-MB-231

2.3.1 Production of forced expression sequences

We designed primers using the Brecon Designer programme (Palo Alto, California, USA) which were synthesised by Invitrogen (Invitrogen, Inc., Paisley, UK) according to the mRNA sequence of Claudin-5, which is capable of amplifying the whole coding sequence (Table 2.2). Briefly, Claudin-5 was found to be highly

expressed in placenta tissue, subsequently cDNA from this tissue was used to generate the full length sequence of Claudin-5. These primers, together with placenta cDNA, were used in a PCR reaction following these parameters:

- Step 1: Initial denaturing period: 94 °C for 5 minutes.
- Step 2: Denaturing step: 94 °C for 15 seconds.
- Step 3: Annealing step: 55°C for 15 seconds, repeated over 36 cycles.
- Step 4: Extension step: 72°C for 30 seconds.
- Step 5: Final extension period: 72 °C for 7 minutes.

High fidelity long and accurate PCR was performed using DuraScript ™ RT-PCR kit (Sigma-Aldrich, Gillingham, Dorset, UK). The resultant gene products were excised from the gel and extracted using GelElute™ Gel extraction kit (Sigma-Aldrich, Dorset, UK). To confirm presence and correct size before being inserted into the plasmid vector the extracted band was electrophoretically run on a 2% agarose gel following the TOPO TA cloning procedure, as described in section 2.3.3.

2.3.2 Knockdown of gene transcripts using ribozyme transgene sequences

Hammerhead ribozymes are small self-cleaving RNAs, first discovered in viroids and satellite RNAs of plant viruses (Forster and Symons, 1987) that catalyze a specific phospodiester bond isomerization reaction in the course of rolling-circle replication. They have a catalytically active motif consisting of three base-paired helical stems (I, II, III) flanking a central core of 15 mostly invariant nucleotides (Haseloff and Gerlach, 1989). The conserved central bases are essential for the hammerhead ribozyme's catalytic activity.

The expression of Claudin-5 was targeted at mRNA level using Hammerhead ribozyme trangenes that specifically cleaved a GUC site (Table 2.3). The secondary mRNA structure of Claudin-5 was first generated by using Zuker's RNA mFold software (Zuker, 2003) (Figure 2.1). A suitable GUC ribozyme target site was then selected from within the secondary structure of Claudin-5. This allowed the Hammerhead catalytic region of the ribozyme to interact and accurately cleave the specific GUC sequence within the target mRNA transcript (Figure 2.2).

Ribozymes were synthesised using a Touchdown PCR procedure following these parameters:

- Step 1: Initial denaturing period: 95 °C for 5 minutes.
- Step 2: Denaturing step: 94 °C for 15 seconds.
- Step 3: Various annealing step: 60°C for 30 seconds, 58°C for 30 seconds, 56°C for 30 seconds, 54°C for 30 seconds, 52°C for 30 seconds, 50°C for 30 seconds and 48°C for 30 seconds.
- Step 4: Extension step: 72°C for 30 seconds.
- Step 5: Final extension period: 72 °C for 7 minutes.

The transgenes were electrophoretically run on a 2% agarose gel and cloned in a suitable vector which was followed by transformation and transfection.

Expression product	Primer name	Expression primer sequence (5'-3')	Predicted size (bp)
Claudin-5	CL5expR1	GACGTAGTTCTTCTTGTCGT	547
	CL5ExpF2	ATGGGGTCCGCAGCGTTGGAGATCCT	
β-actin	BACTF	ACTGAACCTGACCGTACA	580
	BACTR	GGACCTGACTGACTACCTCA	
Orientation checking	T7F	TAATACGACTCACTATAGG	

Table 2.2: Primers for amplifying Claudin-5 coding sequence.

Ribozyme target	Primer name	Ribozyme sequence (5' – 3')
Claudin-5	CL5Rib1F	ACTAGTCCGCAGCGTTGGAGATTTCGTCCTCACGGACT
	CL5Rib1R	CTGCAGACAGCACCAGGCCCAGCTGATGAGTCCGTGAG GA
	CL5Rib2F	CTGCAGCAGGTGGTCTGCGCCGTCACCTGATGAGTCCG TGAGGA
	CL5Rib2R	ACTAGTGACCGCCTTCCTGGACCACAACATTTCGTCCTC ACGGACT
Orientation checking	T7F	TAATACGACTCACTATAGG

Table 2.3: Primers used for ribozyme synthesis.

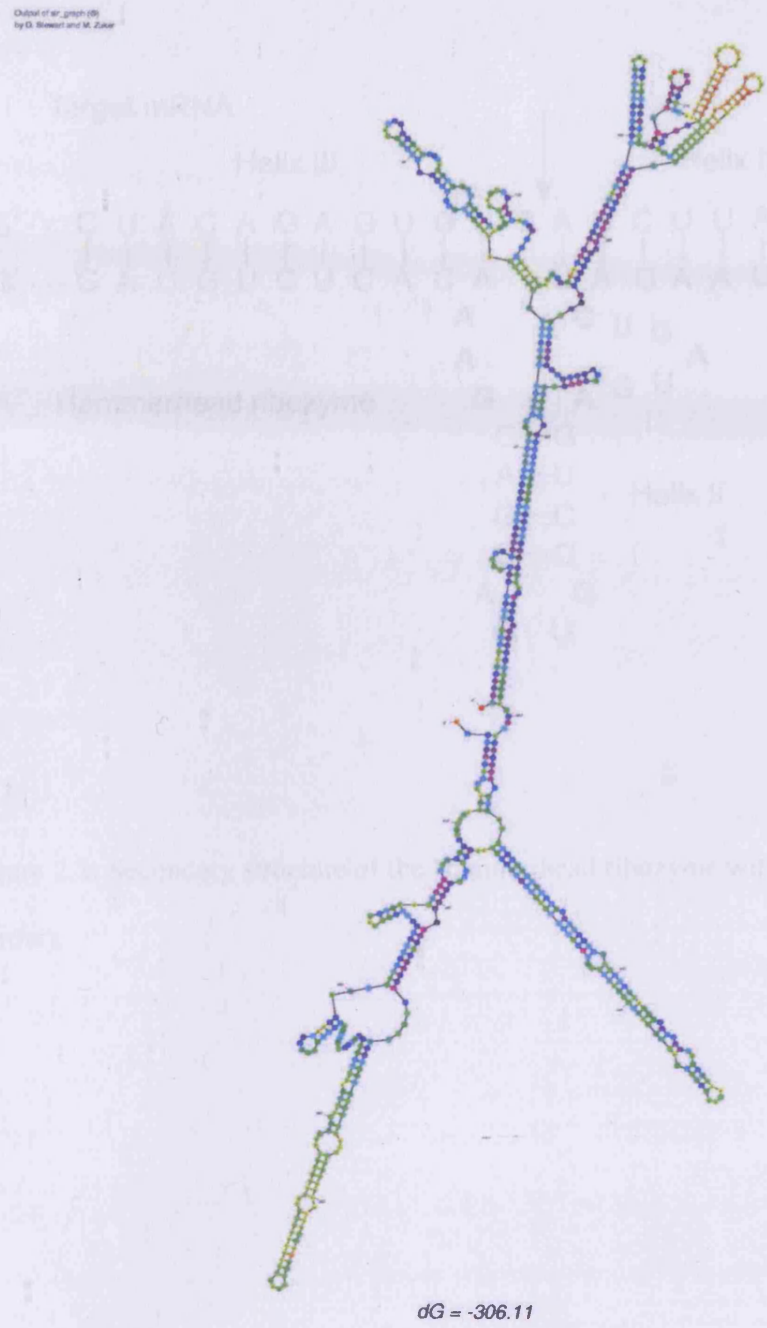

Figure 2.1: The secondary structure of human Claudin-5 mRNA.

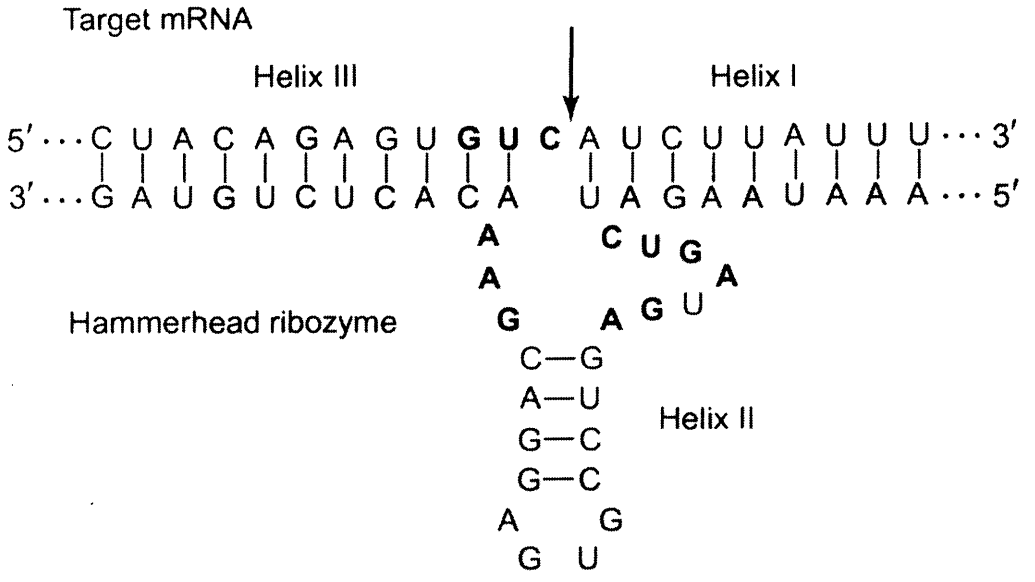

Figure 2.2: Secondary structure of the Hammerhead ribozyme with bound substrate (arrow).

2.3.3 TOPO cloning reaction

The pEF6/V5-His TOPO TA Expression system provides a highly efficient, 5 minute, one-step cloning strategy ("TOPO Cloning") for the direct insertion of Taq polymerase-amplified PCR products into a plasmid vector for high-level expression in mammalian cells. No ligase, post-PCR procedures, or PCR primers containing specific sequences are required. Once cloned, analyzed, and transfected into a mammalian host cell line, the PCR product can be constitutively expressed.

The plasmid vector pEF6/ V5-His TOPO TA plasmid vector (Invitrogen, Inc., Paisley, UK) was used in the current study in accordance with the protocol provided (Figure 2.3).

The TOPO cloning reaction was set up in a pre-labelled PCR tubes for each ribozyme or expression sequence used:

- PCR product (ribozyme or expression sequence): 4μl
- Salt solution: 1μl
- TOPO vector: 1μl

The reaction was mixed gently and then left for 5 minutes at room temperature. Following ligation, the cloning reaction was transformed immediately into *Escherichia coli* for successful efficiency in the transformation.

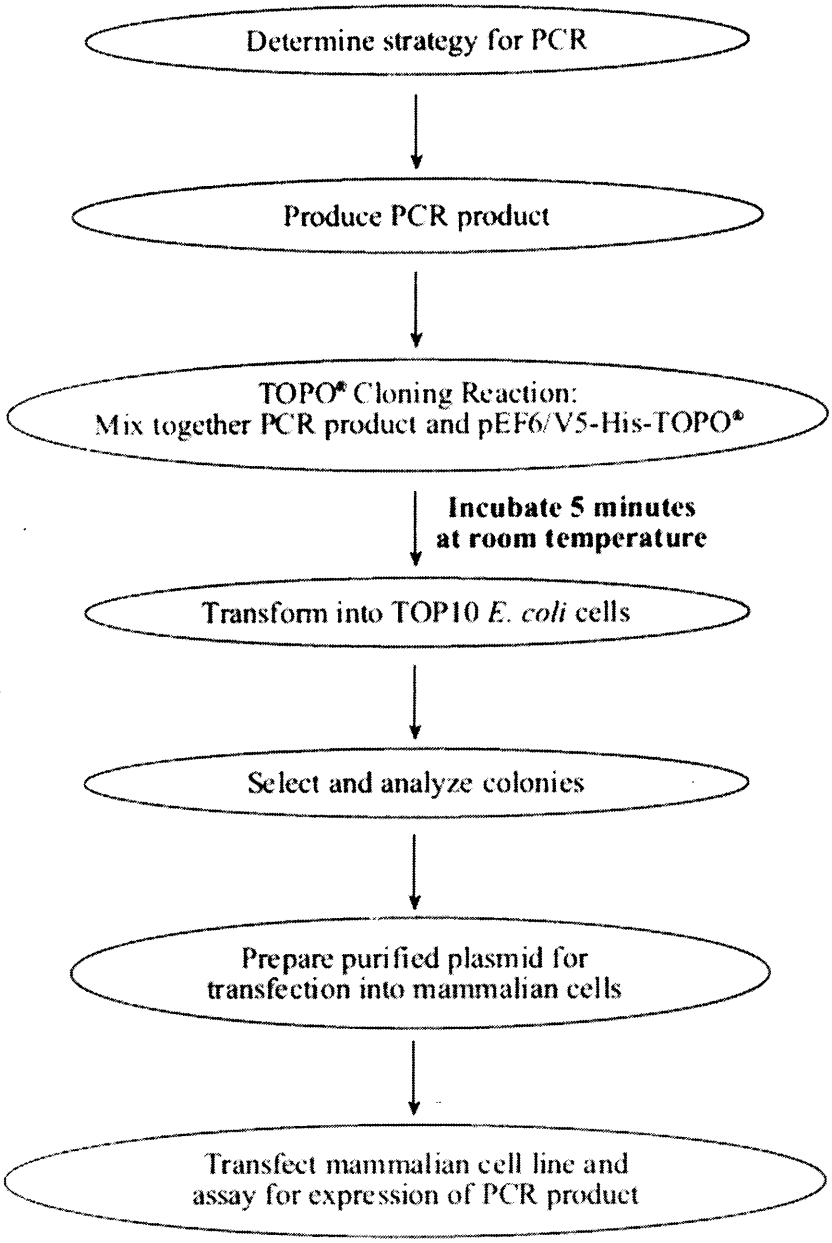

Figure 2.3: Flow chart of pEF6/ V5-His TOPO TA plasmid vector cloning procedure.

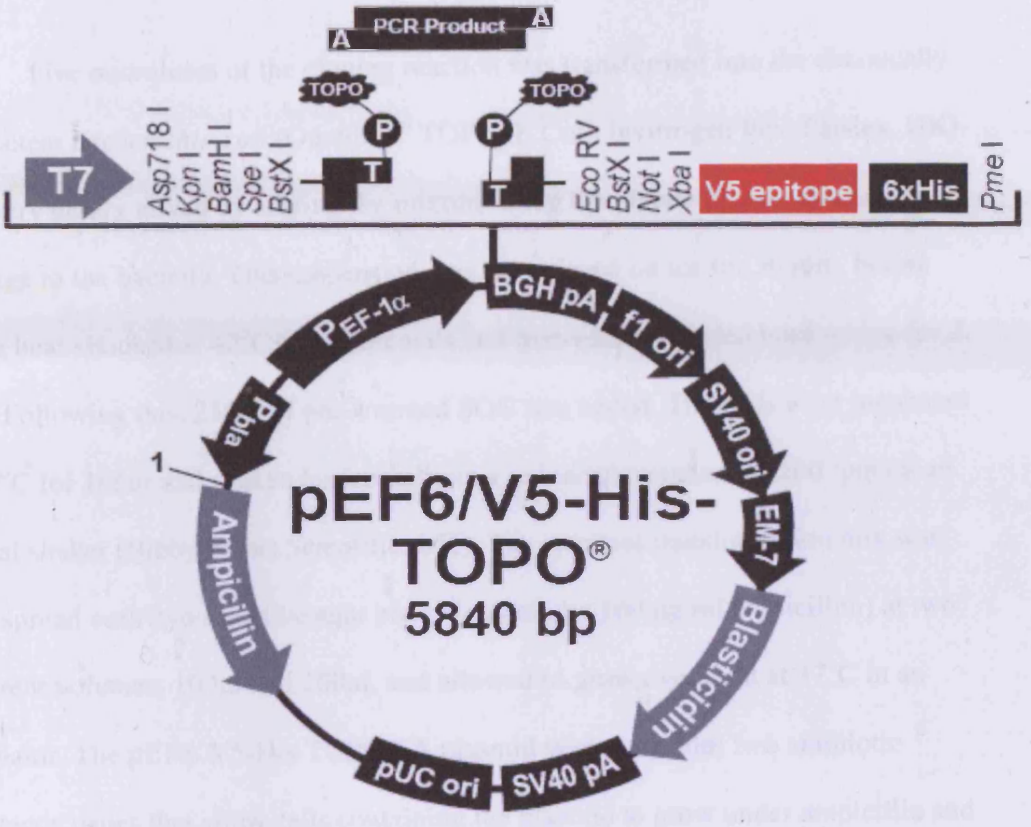

Figure 2.4: Schematic of pEF6/ V5-His TOPO TA plasmid vector plasmid (Figure duplicate from pEF6/V5-His TOPO TA Expression kit protocol)

2.3.4 Transformation of competent *Escherichia coli*

Five microlitres of the cloning reaction was transformed into the chemically competent *Escherichia coli* (OneShot^{tm} TOP10 E.Coli, Invitrogen Inc., Paisley, UK) and very gently mixed by stirring the mixture using the pipette tip, avoiding any damage to the bacteria. This suspension was then placed on ice for 30 min, before being heat-shocked at 42°C for 30 seconds and immediately placed back on ice for 2 min. Following this, 250µl of pre-warmed SOC was added. The cells were incubated at 37°C for 1hour and shaken horizontally in a universal container at 200 rpm on an orbital shaker (Bibby Stuart Scientific, UK). The resultant transformation mix was then spread onto two selective agar plates (containing 100 µg/ml ampicillim) at two different volumes, 100µl and 200µl, and allowed to grow overnight at 37°C in an incubator. The pEF6/ V5-His TOPO TA plasmid vector encodes two antibiotic resistance genes that allow cells containing the plasmid to grow under ampicillin and Blasticidin S (as shown in figure 2.4).

2.3.5 Selection and orientation analysis of positive colonies

Any colonies which grew on the selective plates should contain the pEF6/ V5-His TOPO TA plasmid vector, otherwise cells without the plasmid vector will not survive in the presence of the antibiotics. Analysis of the colonies is required to determine which of the colonies grown on the plate contains the ribozyme or expression sequence and have been inserted into the plasmid in the correct orientation to allow successful amplification of the sequences.

Screening involves PCR of 10 colonies randomly selected, using the forward primer specific to the plasmid (T7F), and the reverse primers to the ribozyme or expression sequence. Individual colonies were examined in order to test DNA presented by using a sterile pipette tip and touching the selective colony. Thus, it was placed into the PCR reaction mixture ready for specific amplification of the desired sequence. This will ensure that amplified products, at the expected size, are in the plasmid and inserted in the correct orientation. For each colony, two PCR reactions were carried out as follows (full primer sequences are given in table 2.3):

- Ribozyme orientation reaction 1:

  10μl – 2X REDTaq ReadyMix PCR Reaction mix

  9μl – PCR water

  0.5μl – T7F plasmid specific forward primer

  0.5μl – Ribozyme specific primer (CL5Rib1R)

- Ribozyme orientation reaction 2 :

  10μl – 2X REDTaq ReadyMix PCR Reaction mix

  9μl – PCR water

  0.5μl – T7F plasmid specific forward primer

  0.5μl – Ribozyme specific primer (CL5Rib2R)

Each reaction was subjected to the following conditions:

- Step 1: Initial denaturing period: 95 °C for 5 minutes.
- Step 2: Denaturing step: 94 °C for 30 seconds.

- Step 3: Annealing step: 55°C for 30 seconds.
- Step 4: Extension step: 72°C for 30 seconds.
- Step 5: Final extension period: 72 °C for 7 minutes.

Steps 2, 3 and 4 were repeated over 40 cycles.

The mixture was run on a 2% agarose gel. Thus, colonies showing the full sequence of Claudin-5 and the correct orientation of the insert were taken off the plate and used to inoculate 10 ml of ampicilin selective LB broth in universal containers and were horizontally shaken at 225 rpm overnight

2.3.6 Plasmid extraction, purification and quantification

Plasmid extraction was carried out using Sigma GenElute Plasmid MiniPrep Kit (Sigma-Aldrich, Dorset, UK), according to the provided protocol. Five millilitres of the LB broth previously inoculated with the correct colony and cultured overnight was centrifuged at 3000 rpm for 10 minutes to obtain a pellet of bacteria. The supernatant was discarded and the bacterial pellet resuspended in 200 µl of resuspension solution (containing RNAase A) and mixed through pipetting. To lyse the cells, 10 ml of cell lysis buffer was added and the solution was mixed gently inverting the container. Following 5 minutes incubation at room temperature, 350µl of the neutralisation solution was added and then centrifuged at 12.000 x g in a micro centrifuge. The cell lysate was filtered in a Mini Spin Column placed inside the collection tube allowing the plasmid to bind to the column and spun at 12000 x g for 30 seconds. The flow-through was discarded. Seven hundred and fifty microlitres of wash solution containing ethanol is added to the column before spinning at 12000 x g

for 30 seconds and the flow-through discarded. The column was again spun at 12000 x g for 30 seconds to remove any remaining flow- through before transferring the Mini Spin Column to a clean collection tube. Plasmid DNA was eluted through the addition of 100µl of elution solution and the column was spun at 12000 x g for 1 minute. The plasmid DNA was then run on a 0.8% gel to check both plasmid purity and size.

2.3.7 Transfection of mammalian cells using electroporation

Following plasmid purification and quantification, 2 µl of the extracted plasmid was used to transform the HECV and MDA-MB-231 cell lines.

Confluent HECV and MDA-MB-231 wild type cell lines were detached from the tissue culture flasks using trypsine/EDTA, pelleted and resuspended as previously described. One millilitre of cells were added to an electroporation cuvette (Eurgenetech, Soutampton, UK) together with the purified plasmid. The cuvette was loaded into the electroporator (Easyject, Flowgene, Surrey, UK), and a pulse of electricity (450 V) supplied. This will produce small perforations in the cell wall integrity allowing passage of the plasmid DNA across the membranes to be integrated in the cells. The mixture was immediately transferred into 10 ml of pre-warmed medium and place in an incubator under the usual incubation conditions.

2.3.8 Establishment of transformed Human Endothelial cell line HECV and the breast cancer cell line MDA-MB-231

The pEF6/ V5-His TOPO TA plasmid vector used in this study, encodes two antibiotic resistance genes: ampicillin and Blasticidin S.

The ampicillin resistance gene allows initial selection of prokaryotic bacterial cells containing the plasmid. Blasticidin S antibiotic inhibits protein synthesis in both prokaryotes and eukaryotes and is used to specifically select for mammalian cells containing the pEF6/ V5-His TOPO TA plasmid vector .The combination of both antibiotic resistance genes provides an accurate selection throughout the cloning process.

Following overnight incubation in supplemented DMEM medium, cells were move to an initial 10 days of intense selection through a selection medium containing 5μg/ml of Blasticidin S to kill all the cells that did not incorporate the plasmids and only remaining cells should all contain the plasmid. After this, cells were maintained in maintenance medium containing 0.5μg/ml of Blasticidin S (all media were described in section 2.2).

All cells were routinely tested to appraise the efficacy and stability of both the expression and the ribozyme transgene sequences using RT-PCR. Once the plasmid incorporation was assessed into the mammalian cell lines, the transfected cells were used in a series of *in vitro* studies to evaluate the forced expression and knockdown of the Claudin-5 gene.

2.4 Methods for detecting mRNA

2.4.1 Total RNA isolation

RNA is susceptible to degradation by RNAases, therefore special care has to be taken to minimise this during its isolation.

Cells were grown until reaching a confluent state (85-90% confluent), after the aspiration of culture medium 1ml of ABgene Total RNA Isolation Reagent (TRIR) kit (ABgene, Surrey, UK) was added to the cell monolayer. The resultant cell lysate was transferred through a pipette into a 1.8ml eppendorf tube (A laboratories, Hampshire, UK). The homogenate was stored for 5 minutes at 4 °C to allow complete dissociation of nucleoprotein complexes before adding 0.2ml of chloroform and energetically shaking the samples for 15 seconds, samples were centrifuged in a refrigerated centrifuge (Boeco, Wolf laboratories, York, UK) at 12000g (4 °C) for 15 minutes. The homogenate forms two phases: the organic (DNA and proteins) and aqueous phase (RNA). DNA and proteins are in the organic phase while RNA is in the aqueous. Carefully, the aqueous phase was removed and transferred to a pre-labelled eppendorf tube containing an equal volume of isopropanol, the samples were then stored at 4 °C for 10 minutes before centrifuging at 12000g (4 °C) for 10 minutes. RNA precipitation then forms a white pellet at the bottom of the eppendorf. The supernatant was discarded and the RNA pellet was washed twice with 1ml of 75% ethanol prepared using DEPC water (DEPC water is a histidine specific alkylating agent that inhibits the action of RNases which depend on histidines active sites for their activity. It is used to reduce the effects of any RNases that might be present) by vortexing and subsequent centrifugation at 7500g (4 °C) for 5 minutes. At the end of the procedure, as much ethanol as possible was removed before briefly drying the pellet in a Hybridiser drying oven (Wolf laboratories, York, UK) at 50 °C for 5-10 minutes (it is important not to let the RNA pellet dry completely as it will decrease its solubility). Finally, the RNA pellet was dissolved in 50-100µl of DEPC water before quantification.

2.4.2 RNA quantification

The concentration and purity of RNA was assessed by measuring with a UV1101 Biotech Photometer (WPA, Cambridge, UK), that has been set to detect ssRNA (μg/ μl) in a 1:10 dilution in DEPC water at A260nm wavelength. All samples were measured in a Starna glass cuvette (Optiglass limited, Essex, UK).

The RNA samples were either stored at -80 °C for further use or used immediately for reverse transcription (RT).

2.4.3 Reverse transcription-polymerase chain reaction (RT-PCR) of RNA

Following RNA isolation and quantification, RT-PCR was used to convert RNA into complementary DNA (cDNA) using DuraScript ™ RT-PCR kit (Sigma-Aldrich, Dorset, UK). According to the manufacturer's instructions, which are sketched below, a 20μl reaction mixture was added to an eppendorf:

- 0.5μg - total RNA template (volume depends on the concentration)
- PCR water (volume= 8μl- volume of the RNA template)
- 1μl - deoxynucleotide mix (500Mm of each dNTP)
- 1μl - anchored oligo $(dT)_{23}$

The tube was then mixed gently and centrifuged before placing the mix in a T-Cy Thermocycler (Creacon Technologies Ltd., The Netherlands) and heating at 25 °C for 5 minutes. This initial step helps to denature the secondary structure of the RNA allowing more effective reverse transcription. Tubes were then placed on ice before centrifuging and adding the following components to the samples:

- 6µl - PCR water
- 2µl -10X buffer for DuraScript ™ RT
- 1µl – RNase inhibitor
- 1µl – DuraScript reverse transcriptase

The resultant total volume in each eppendorf was 20µl. The samples were mixed, centrifuged and placed back in the thermal cycler to be heated at 42 °C for 30 minutes. The cDNA samples were diluted to 1:4 with PCR water and the success of the sample was confirmed using a conventional PCR probing for β-actin. The samples were stored at -20 °C until required.

2.4.4 Polymerase chain reaction (PCR)

PCR was carried out using REDTaq ReadyMix PCR Reaction mix (Sigma-Aldrich, Dorset, UK). A 20 µl reaction was prepared for each sample as follows:

- 10µl - REDTaq ReadyMix PCR Reaction mix
- 1µl – specific forward primer
- 1µl – specific reverse primer
- 5µl – PCR water
- 3µl –cDNA

Primers were designed using the Brecon Designer programme (Palo Alto, California, USA) and were synthesised by Invitrogen (Paisley, UK). All primers were diluted to a concentration of 10pM before being use for the PCR. The PCR reaction was set up in a 200µl PCR tube (ABgene, Surrey, UK), mixed and placed in a T-Cy thermocycler (company info) under the following conditions:

- Step 1: Initial denaturing period: 94 °C for 5 minutes.
- Step 2: Denaturing step: 94 °C for 30 seconds.
- Step 3: Annealing step: 55°C for 30 seconds.
- Step 4: Extension step: 72°C for 30 seconds.
- Step 5: Final extension period: 72 °C for 7 minutes.

Steps 2, 3 and 4 were repeated over 36 cycles.

PCR products were visualized on a 2% agarose gel through staining with ethidium bromide after electrophoresis. In all cases a negative control where PCR water replaced cDNA was included in the reaction.

2.4.5 Agarose gel DNA electrophoresis

The amplified DNA was separated according to size using 2% agarose gel electrophoresis.

Agarose gels were made by adding the required amount of agarose (Melford Chemicals, Suffolk, UK) to TBE solution. The mixture was then heated to a fully dissolve the agarose, poured into the electrophoresis cassette and a plastic comb was then inserted into the gel creating loading wells. Once the gel was set at room temperature for about 30-40 minutes, TBE running buffer was carefully poured into the electrophoresis tank. The PCR products were loaded into the wells, 8µl of a 1Kb ladder (Invitrogen, Paisley, UK) or 10µl of the sample. The samples were then electrophoretically separated using a power pack (Gibco BRL, Life Technologies Inc.) at a constant 95V for 30-50 minutes to allow sufficient separation of the samples.

2.4.6 DNA staining and detection

The PCR products were stained using ethidum bromide stain (10mg/ml) diluted in TBE buffer used in the run for 10 minutes on a rocking platform to ensure an even staining of the agarose gel. The gel was visualised under ultra violet light using a UV illuminator (UVitech, Cambridge, UK). If necessary, the gel can be returned to the stain for extra staining or to a container of distilled water to reduce the background staining.

2.4.7 Quantitative RT-PCR (Q-RT-PCR)

Q-RT-PCR is capable of detecting minuscule quantities of cDNA within a sample. The Amplifluor system was used to detect and quantify transcript copy number of Claudin-5 in tumour and background samples. The cDNA was generated as described above. Sixteen microlitre reactions were prepared for each sample as follows:

- Forward Z primer - 0.5 (1pmol/μl)
- Reverse primer - 0.5 (10pmol/μl)
- Q-PCR Master Mix - 8 μl
- Probe Ampiflour – 0.5 (10pmol/μl)
- PCR water – 2.5 μl
- cDNA - 4 μl

One of the primers used will have a Z-sequence (CACCGAGTCGTACACTTTGC) at 1:10 of the other primer and probe. The Amplifluor probe contains a region specific to the Z-sequence together with a hairpin

structure labelled with a fluorescent tag (FAM-490). The fluorescent tag whilst being in the hairpin does not produce any signal, however, the specificity of the 3' region of the Amplifluor probe to the Z-sequence causes the incorporation of the uniprimer (Table 2.4). As a result, following incorporations will cause the disruption of the hairpin structure and detectable signalling of the fluorescent tag within this structure.

The intensity of fluorescence within each sample compared to a range of standards of known transcript copy number allows the calculation of transcript copy number within each sample (Figure 2.5). Detection of GAPDH copy number within these samples was later used to allow further standardisation and normalisation of the samples.

Sample cDNA was amplified and quantified over a large number of shorter cycles using an iCycler^{IQ} thermal cycler and detection software (BioRad laboratories, Hammelhempstead, UK) (Figure 2.6) under the following conditions:

- Step 1: Initial denaturing period: 94 °C for 5 minutes.
- Step 2: Denaturing step: 94 °C for 10 seconds.
- Step 3: Annealing step: 55°C for 15 seconds.
- Step 4: Extension step: 72°C for 20 seconds.

Steps 2, 3 and 4 were repeated over 60 cycles.

The camera used in this system is set to detect signal during the annealing stage. Specific Q-PCR primers were verified using a positive control known to express Claudin-5 and a negative control, where PCR water replaced cDNA, was included to exclude any contamination in the reaction.

Gene of interest	Primer name	Primer sequence (5'– 3')
Claudin-5 (Q-PCR)	CL5Zr2	*ACTGAACCTGACCGTA*CACCGAGTCGTACACTTTGC
	CL5F2	TTCCTGGACCACAACATC
β-actin (Q-PCR)	BACTINZR	*ACTGAACCTGACCGTA*CGCTCGGTGAGGATCTTCA
	BACTINF1	GGACCTGACTGACTACCTCA
GAPDH (Q-PCR)	GAPDHZR	*ACTGAACCTGACCGTA*CAGAGATGATGACCCTTTTG
	GAPDHF1	CTGAGTACGTCGTGGAGTC

Table 2.4: Primers used for Q-PCR.

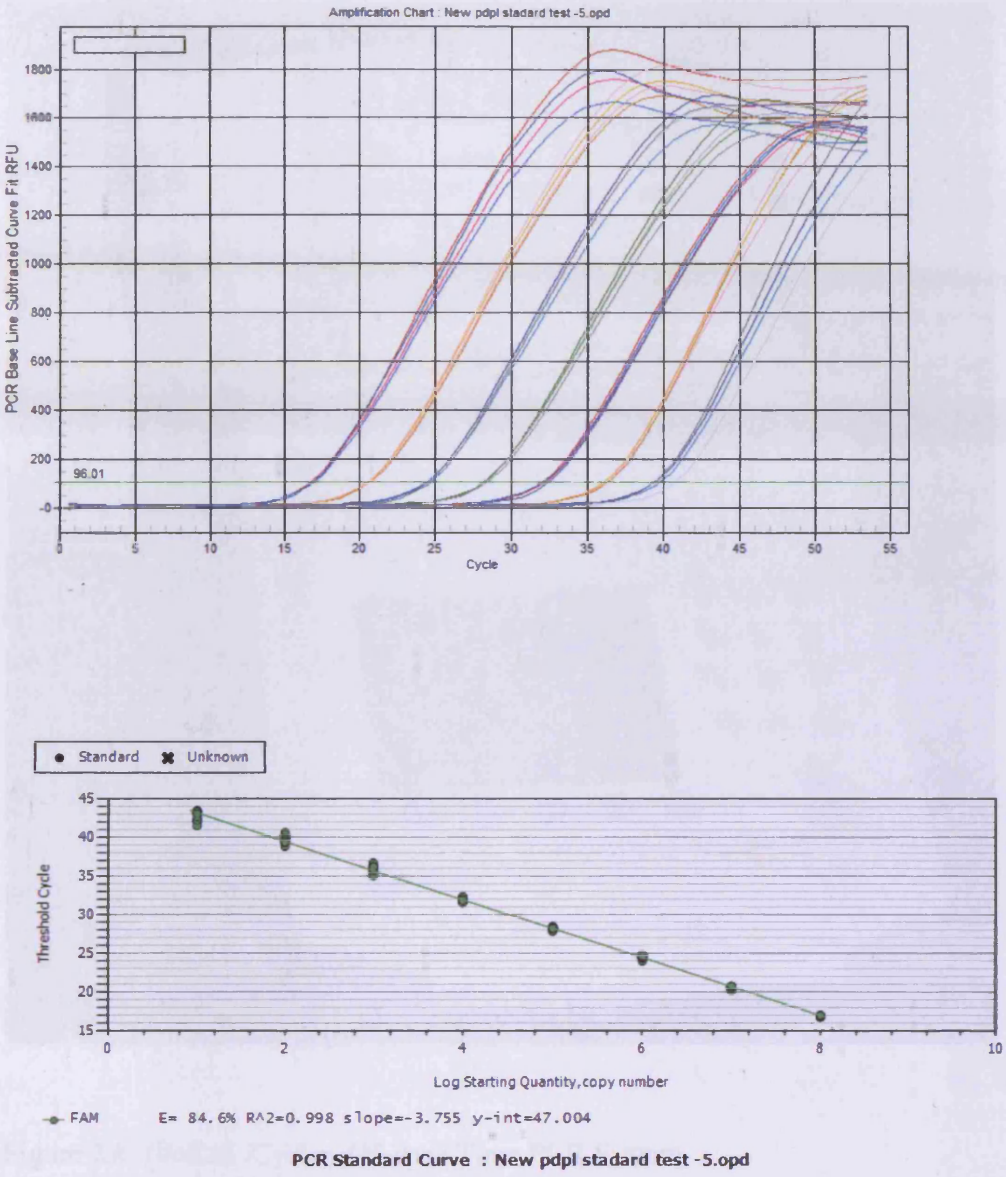

Figure 2.5: Q-PCR standard curve (on IQ5).

Figure 2.6: BioRad iCycler iQ5 Real Time PCR System.

2.5 Methods for detecting protein

2.5.1 SDS-polyacrylamide gel electrophoresis (SDS-PAGE) and Western blotting

2.5.1.1 Cell lysis and protein extraction

Upon reaching adequate confluency (90%), the cell monolayer was removed from the base of the cell culture flask using a disposable cell scraper. The detached cells and the medium were transferred to a universal container using a sterile transfer pipette and centrifuged for 5 minutes at 2000 rpm to pellet the cells at the bottom of the container. The supernatant was decanted and the pellet resuspended in 200-250µl of lysis buffer (see section 2.2.4), transferred to a 1.8ml eppendorf tube (A laboratories, Hampshire, UK) and placed on a Labinco rotating wheel for 1 hour (Wolf Laboratories, York , UK) in order to extract protein from the cell lysate. The lysis solution was then centrifuged at 13000 rpm for 15 minutes in a microcentrifuge to remove cellular debris and collect the protein. The supernatant was transferred to a clean eppendorf tube to wait quantification prior to use in Western blotting.

2.5.1.2 Protein quantification of cell lysates

Determination of protein concentration of cell lysates was based on a protocol provided by the supplier Bio- Rad DC, from whom the protein assay kit was purchased (Bio-Rad laboratories, Hammelhempstead, UK). Firstly, a serial dilution of bovine serum albumin (BSA) standard samples with known concentration of 10mg/ml (Sigma, Dorset, UK) were prepared in the same cell lysis buffer to give a working concentration range between 10mg/ml to 0.005mg/ml. Five microlitre of

either the sample or standard was pipetted into a 96 well plate before adding 25µl of 'working reagent A' followed by 200µl of reagent B. 'Working reagent A' was prepared by mixing each millilitre of reagent A with 20µl of reagent S. (final volume depends on the number of samples to quantify) (If the samples do not contain detergent this step can be skipped and reagent A is used as supplied). The mixture was left for 45 minutes allowing the colorimetric reaction to set. Absorbance of both samples and standards was read at 620nm using an ELx800 plate reading spectrophotometer (Bio-Tek, Wolf laboratories, York, UK). A standard protein curve was constructed for the bovine serum albumin standards and used to establish sample concentration. All protein concentrations were adjusted to the desired working concentrations of between 1 – 2mg/ml by diluting in cell lysis buffer followed by further dilutions in a 1:1(v/v) with 2X Lamelli sample buffer concentrate (Sigma-Aldrich, Dorset, UK). Samples were then boiled at 100°C for 5 minutes allowing denaturation of the samples before being stored at -20°C until required.

2.5.1.3 Preparation for immunoprecipitates

Cell lysate of the protein of interest was probed with Claudin-5 antibody (1:100 dilution) and placed on a Labinco rotating wheel for 2 hour (Wolf Laboratories, York, UK) allowing Claudin-5 antibody to bind to their targets. One hundred microlitres of conjugated A/G protein agarose beads (Santa-Cruz Biotechnologies Inc., CA, USA) were added to each sample to make the antibody-protein complex insoluble, followed by overnight incubation on the rotation wheel. The supernatant was discarded and the pellet was washed in 200µl of lysis buffer and resuspended in 200µl of 2X Lamelli sample buffer concentrate (Sigma-Aldrich,

Dorset, UK), then denatured for 5 minutes by boiling at 100 °C. Samples were then stored at -20 °C prior to use.

2.5.1.4 Loading samples

SDS-PAGE was undertaken using an OmniPAGE VS10 vertical electrophoresis system (OminPAGE, Wolf Laboratories, York, UK). Acrylamide gels were made up at a concentration appropriate to the molecule being analysed. They were prepared in a universal container and added between the two clean, dry glass plates and assembled on a casting stand. The amount of each ingredient required to make up to 15ml, sufficient for both the 8% gel (proteins in the range of 50KDa to 500KDa) and the 15% gel (proteins in the range of 3KDa to 100KDa) resolving gels is indicated below:

Component	8% Gel	15% Gel
Distilled water	6.9ml	3.4ml
30% acrylamide mix	4.0ml	7.5ml
1.5M Tris (pH 8.8)	3.8ml	3.8ml
10% SDS	0.15ml	0.15ml
10% ammonia persuphate	0.15ml	0.15ml
TEMED	0.009ml	0.006ml

Using a disposable plastic pipette, we applied the resolving gel between the glass plates and immediately covered the top with distilled water to ensure that the gel sets with a smooth surface. After approximately 30 minutes, we discarded the

distilled water and the stacking gel was added to the top of the resolving gel. A plastic comb was placed gently at the top of the stacking gel and the gel allowed to set. The components and quantities required to prepare 5ml of the stacking gel solution (enough for two gels) are shown below:

Component	
Distilled water	3.4ml
30% acrylamide mix	0.83ml
1.0M Tris (pH 8.8)	0.63ml
10% SDS	0.05ml
10% ammonia persuphate	0.05ml
TEMED	0.005ml

Once the stacking gel had set after approximately 30 minutes, the comb was carefully removed without tearing the edges of the wells. The loading cassette was placed into an electrophoresis tank filled up with 1X running buffer until the wells were completely covered.

Samples were loaded into the wells using a 50µl syringe (Hamilton) with a flat-tipped needle at equal volumes approximately 15µl. Control wells with 10µl of molecular weight marker SDSH2 (Sigma-Aldrich, Dorset, UK), were always used.

2.5.1.5 Running gel

The proteins were then separated according to molecular weight using electrophoresis at 125V, 40mA and 500W. Different lengths of time were used depending on the protein size and gel percentage.

2.5.1.6 Preparation of membrane and Western blotting

Following SDS-PAGE the protein samples were transferred onto a Hybond nitrocellulose membrane (Amersham Bioscience UK Ltd, Bucks, UK). Gels were taken out from the electrophoretic tank and separated from the glass plates after removing the stacking gel with a plastic edge. The nitrocellulose membrane and four sheets of filter paper were cut (7.5cm x 7.5cm) and immersed in 1X transfer buffer to ensure correct binding of the protein to the membrane for 20 minutes. The 'sandwich' of paper-nitrocellulose-gel-paper was set up for protein transfer from the gel to the membrane and placed in a SD10 SemiDry Maxi System blotting unit (Wolf Laboratories, York, UK). The surface of this sandwich was carefully smoothed out to remove the air bubbles which may interfere during the protein transfer. Electroblotting was performed at a constant current of 15V, 500mA, 8W for 40-45 minutes.

Once completed, membranes were removed and immersed in Poceau S. Stain (Sigma-Aldrich, Dorset, UK) for approximately one minute at room temperature followed by a wash in distilled water until protein bands were visible on the membrane. This allows us to verify that the proteins have been transferred to the membranes as well as indicate where the molecular marker is placed without

interfering with successive immunoprobing steps. Membranes were then stored at 4°C in 10% milk blocking solution (10% skimmed milk, 0.1% polyoxyethylene (20) sorbitan monolaurate (Tween 20) in TBS) until required.

2.5.1.7 Specific protein detection using antibody probing

Membranes were transferred into a clean 50ml falcon tube (Nunc, Fisher Scientific, Leicestershire, UK) and incubated in fresh 10% milk blocking solution for 30 minutes with agitation in a roller mixer (Stuart, Wolf Laboratories, York, UK). The blocking solution was then discarded and 5ml of specific primary antibody (1:500) made up in 3% milk solution (3% skimmed milk, 0.1% polyoxyethylene (20) sorbitan monolaurate (Tween 20) in TBS) was added to the falcon tube followed by 1 hour of incubation of the membranes with agitation (see Table 2.5). After the 1 hour of incubation, the primary antibody solution was removed and the membranes were washed 3 times for 10 minutes, each wash with 3% milk solution, to ensure complete removal of the primary antibody. The membranes were then incubated in 5ml of HRP conjugated secondary antibody (1:1000) solution made up in 3% milk solution with agitation for 1 hour (Table 2.5). The solution was discarded and membranes were washed 3 times in TTBS (TBS containing 0.1% tween 20), followed by a final 10 minute wash in TBS to remove any residual detergent.

2.5.1.8 Chemiluminescent detection of protein

The Supersignal West Pico Chemiluminescencent Substrate (Thermo Scientific, IL., USA) was used to detect the horseradish peroxidase (HRP) in the membranes. The two substrates were mixed in a 1:1 ratio with a final volume of

0.125ml/cm^2. Once the TBS was decanted, the membrane was placed in a clean falcon tube and covered for 5 minutes with the chemiluminescence working solution with agitation. Excess reagent was then removed and the membrane was placed on the tray that the UVITech imager (UVITech, Inc., Cambridge, UK) provides. The chemiluminiscence signal was captured and visualized in the computer connected to the imager. The membranes were exposed to several exposure times and images captured. The protein bands were then quantified by using UVIband software (UVITEC, Inc., Cambridge, UK).

Membranes were stained in Amido Black stain for 1 minute followed by immersion in destain until bands were clearly seen and a wash in distilled water. This provides a permanent record of the membrane for further comparison with the images captured with the imager.

2.5.2 Immunohistochemical staining for frozen sections (IHC) of breast sample tissues

Frozen sections of breast tumour and background tissue were cut at a thickness of 6 μm using a cryostat (Leica). The sections were mounted on super frost microscope slides (Fisher Scientific, Leicestershire, UK) air-dried and then fixed in a mixture of 50% acetone and 50% methanol. The sections were then placed in Optimax wash buffer (Menerium, Oxford, UK) for 5-10 min to rehydrate. Sections were incubated for 20 min in Horse serum albumin (Vector Labs., Peterborough, UK) blocking solution and probed with Claudin-5 antibody (1:100 dilution) for one hour, and without primary antibody as a negative control to verify the binding specificity. Primary antibodies were purchased from Santa-Cruz Biotechnologies Inc. (Santa-

Cruz, CA, USA). Following extensive washings, sections were incubated for 30min in the universal secondary biotinylated antibody (ABC Standard kit , Vector Laboratories, Peterborough, UK). Following extensive washings, the sections were incuabated in the dark for 5 min with the Diamino-benzine chromogen (Vector Laboratories, Peterborough, UK). Sections were then washed and counter stained in Gill's haematoxylin and dehydrated in ascending grades of methanol before clearing in xylene and mounting under a cover slip.

2.5.3 Immunofluorescent staining (IFC)

A 16-well chamber slide (Nunc, Fisher Scientific, Leicestershire, UK) was treated with 100 µl free serum medium for 1 hour. Medium was discarded and 20000 cells in 200 µl aliquots were seeded into each well and left in the incubator overnight to form a confluent monolayer. The medium was then aspirated and the cells fixed in absolute ethanol for 20 minutes at -20°C. Cells were rehydrated in BSS for 10 minutes and permeabilised in 0.1% Triton X-100 for 5 minutes followed by 3 washes in TBS. Blocking was performed using 10% Horse serum (Vector Labs., Peterborough, UK) in TBS for 40 minutes followed by a wash in TBS. The slides were probed with primary antibody for 1 hour 1:100 dilution made up in 3% Horse serum in TBS. Cells were washed 4 times in 3% Horse serum followed by 4 washes in TBS. Secondary antibody was prepared using 1:1000 dilution and cells were incubated for 1 hour in the dark according to the primary antibody used which was labelled with FITC or TRITC . Cells were washed in 3% Horse serum followed by 8 washes in TBS, mounted in FluorSave (Merck KGaA, Darmstadt, Germany) and stored in foil at -4°C until viewed using an Olympus BX51 Fluorescence microscope.

Antibody name	Host species	Antibody concentration	Suplier & catalogue number
Polyclonal Anti-rabbit (whole molecule) IgG Peroxidase conjugate	goat	1:1000	Sigma A-9169
Polyclonal Anti-mouse (whole molecule) IgG Peroxidase conjugate	Rabbit	1:1000	Sigma A-9044
Polyclonal Anti-goat (whole molecule) IgG Peroxidase conjugate	Rabbit	1:1000	Sigma A-5420
Monoclonal Anti-Claudin-5	mouse	1:500	Abnova H00007122-A01
Polyclonal Anti-Claudin-5	rabbit	1:100	Santa-Cruz Biotechnologies Inc. SC-28670
Monoclonal Anti-Actin	mouse	1:500	Santa-Cruz Biotechnologies Inc. SC-8432
Polyclonal Anti-N-WASP	goat	1:500	Santa-Cruz Biotechnologies Inc. SC-10122
Monoclonal Anti-ROCK 1	mouse	1:500	Santa-Cruz Biotechnologies Inc. SC-17794
Polyclonal Anti-rabbit IgG FICT	sheep	1:1000	Sigma F-7512

Table 2.5: Antibodies used during course of study.

2.6. Tumour cell function assays

2.6.1 *In vitro* tumour cell growth assay

The growth capacity of the cells used in this study was determined using an *in vitro* tumour growth assay. Cells were detached and counted (as described before in section 2.2.4 and 2.2.5). A number of 3,000 cells were seeded into a 96 well plate (Nunc, Fisher Scientific, Leicestershire, UK) in 200µl of normal medium. Four plates were seeded to obtain density readings after 4 hours (day 0), 1 day, 3 days and 4 days. Within each experiment four duplicates were set up. After appropriate incubation periods, cells were fixed in 4% formaldehyde in BSS for 5-10 minutes before staining for 10 minutes with 0.5% (w/v) crystal violet in distilled water. Following washings the crystal violet was then extracted from the cells using 10% acetic acid. Absorbance was determined at a wavelength of 540nm on a plate reading spectrophotometer (ELx800, Bio-Tek, Wolf laboratories, York, UK).

Using the following equation, cell growth was presented as percentage increase by comparing the absorbances of each incubation period:

Percentage increase = [(Day 3 or 5) – (Day 1)] / Day 1 X 100

2.6.2 *In vitro* tumour cell Matrigel invasion assay

The invasive capacity of the cells used in this study was assessed using an *in vitro* tumour cell Matrigel invasion assay. This assay measures the capacity of cells to penetrate and invade through a basement membrane artificially formed by using Matrigel (Matrigel^{TM}, BD Bioscience,Oxford, UK) and migrate through 8µm pore size, which is sufficiently large enough to allow cells to pass through.

Cell culture inserts (BD Falcom™ Cell Culture Inserts, BD Bioscience, Oxford, UK) were placed into a 24-well plate using forceps and coated in Matrigel. The working solution of Matrigel was prepared at a concentration of 0.5mg/ml in PCR water, adding 100µl to each insert and allowing to dry overnight. Once dried the inserts were rehydrated in 100µl sterile water for 1 hour. The water was then aspirated and cells were seeded in the inserts over the top of the artificial basement membrane at a density of 30,000 cells in 200µl per well. The plates were then incubates for 3 days at 37 °C with 5% CO_2.

After the incubation period, the Matrigel layer together with the non-invasive cells was cleaned from the inside of the insert with tissue paper. The cells which had migrated through the pores and invaded into the Matrigel were fixed in 4% formaldehyde (v/v) in BSS for 10 minutes before being stained in 0.5% crystal violet (w/v) in distilled water (Parish et al., 1992). The cells were then visualized under the microscope under X40 magnification, 5 random fields counted and duplicate inserts were set up for each test sample.

2.6.3 *In vitro* cell-matrix adhesion assay

The capacity of tumours cells to adhere to a basement membrane created artificially by using Matrigel (Matrigel™, BD Bioscience,Oxford, UK) was examined using an *in vitro* tumour cell Matrigel adhesion assay.

One hundred microlitres of free serum medium that contained 5µg of Matrigel was added in each well of a 96- well plate and dried at 55°C for 2 hours in an oven. The membrane was then rehydrated in 100µl of serum free medium for 30

minutes before the cells were seeded in the wells. Approximately 45,000 cells were seeded onto the Matrigel basement membrane in 200µl of normal medium and incubated at 37°C with 5% CO_2 for 40 minutes. After the incubation period, the medium was aspirated and the membrane washed 5 times with 150µl of BSS to remove the non-attached cells, then fixed in 4% formaldehyde (v/v) in BSS for 10 minutes before being stained in 0.5% crystal violet (w/v) in distilled water (Jiang et al., 1995a). The number of adherent cells were counted from 5 random fields per well and 5 duplicate wells per sample, under a microscope at X40 magnification.

2.6.4 *In vitro* tumour cell motility assay using Cytodex-2 beads

A number of $1X10^6$ cells from each cell line were incubated in universal containers with 20 ml of normal growth medium containing 1ml of Cytodex-2 beads (GE Healthcare, Cardiff, UK) for 2 hours. The medium was aspirated and the beads were washed twice in growth medium to remove non-adherent or dead cells. After the second wash the beads were resuspended in 5 ml of normal growth medium. Three hundred microlitres of this solution was then transferred into each well of a 24-well plate, 5 duplicate wells per sample, and incubated overnight. Following incubation, any cells that had migrated from the Cytodex-2 beads and adhered to the base of the wells were washed gently in BSS, fixed in 4% formaldehyde (v/v) in BSS for 10 minutes before being stained in 0.5% crystal violet (w/v) in distilled water (Jiang et al., 1995b). Five random fields were counted per well.

2.6.5 *In vitro* tumour cell migration (wound healing) assay

The migration of the cells across a wounded surface of a confluent monolayer was examined to assess the migratory properties of HECV and MDA-231-MB cell lines. Cells at a density of 40,000 cells per well were seeded in a 24 well plate and, upon reaching confluence, the medium was changed and the monolayer was scraped with a fine gauge needle to create a wound. A few drops of mineral oil were added to avoid evaporation of the medium. The plate was placed on a heated plate (Leica GmbH, Bristol, UK) to keep a constant temperature of 37°C. Cells were photographed after wounding and every 15 minutes during 1 hour with a CCD camera attached to a Leica DM IRB microscope (Leica GmbH, Bristol, UK) at X 20 magnification (Jiang et al., 1999a).

Cell migration was analysed using Image J software (free software) by measuring the distance between the two wounded fronts at 4 points per incubation; the arbitrary values obtained were converted into μm by multiplying each value by 1.6 as previously calibrated using a calibrated grid. The distance between the migrating fronts at each point time was determined by subtracting the distance between the two fronts at any of the specific times selected from that at the initial 0 minute starting point.

2.6.6 *In vitro* tubule formation

Matrigel endothelial cell tube formation assays were set up to assess any impact on angiogenic effect following treatment with different cell motility-related inhibitors (see Table 2.6). One hundred microlitres of free serum medium that

contained 250μg of Matrigel was seeded in each well of a 96- well plate and left to gel in an incubator for 30 minutes. Once the Matrigel was set, it was rehydrated in 100μl of serum free medium for 30 minutes before the cells were seeded in the wells. 40,000 HECV cells were seeded onto the Matrigel basement membrane in 100μl of normal medium and incubated at 37 °C with 5% CO_2 for 1 hour. After the incubation period, the medium was carefully aspirated and a second layer of Matrigel (250μg) was added on top following treatment of these cells. The membrane was then incubated at 37°C with 5% CO_2 for 30 minutes followed by addition of 100μl of normal medium (Sanders *et al.*, 2010). Cells were incubated overnight allowing tubules to form.

The number of tubules was counted under low magnification and images were captured from 5 random fields. Total tubule perimeter/field of these images was later quantified using ImageJ software

Inhibitor name	**Inhibitor concentration**	**Suplier & catalogue number**
N-WASP-Inhibitor Wiskostatin	50μM	Calbiochem (Gibbstown, USA) 681660-1MG
Rock Inhibitor Y-27632	50nM	Santa Cruz Biotechnologies Inc. sc-3536
Arp 2/3 Inhibitor CK-0944636	10 mM	Chemvid Inc. (San Diego, USA) 8012-5102

Table 2.6: Cell motility inhibitors used during course of study.

2.6.7 *In vivo* co-culture tumour growth and development model

Athymic nude mice (nu/nu) (Charles Rivers) were maintained in filter top units according to Home Office regulation. The mice were weighed and the size of the growing tumour measured using vernier callipers under sterile conditions every week. Those mice that developed tumours exceeding $1cm^3$ or suffered 25% weight loss during the experiment were terminated under Schedule 1 according to the UK Home Office and the UK Coordinating Committee on Cancer Research (UKCCCR) instructions. At the end of the experimental work, animals were weighed, terminated under Schedule 1 and tumours were removed if of sufficient size. Tumour volume was determined, at each point, using the following formula:

$$\text{Tumour volume} = 0.523 \times \text{width}^2 \times \text{length}$$

Each experimental group consisted of 5 mice and each mouse was injected with a mix of $2x10^6$ cancer cells in 100 µl in a 0.5 mg/ml Matrigel suspension in both flanks.

2.7 Functional assessment of Tight Junction

2.7.1 Measurement of transepithelial and transendothelial resistance in HECV and MDA-MB-231 cell lines (TER)

Cells were seeded into 0.4 µm transparent pore size inserts (Greiner bio-one, Stonehouse, UK) at a density of 50,000 cells in 200µl of ordinary medium within 24 well plates, grown to confluence, the medium removed and replace with fresh

Dulbecco's Modified Eagle's medium containing 15Mm Hepes, L-Glutamine (Lonza Laboratories, Verviers, Belgium). Medium alone was added to the base of the wells (control) or with 50ng/ml HGF (a kind gift from K. Matsumoto, Osaka University, Japan). The concentration of HGF (50 ng/ml) used for these experiments was selected based upon previous laboratory experience (Martin *et al.*, 2008b). Resistance across the layer of HECV and MDA-MB-231 cells was measured using an EVON volt-ohmmeter (EVON, World Precision Instruments, Aston, Herts, UK), equipped with static electrodes (WPI, FL, USA) (Martin *et al.*, 2004a). One electrode was placed in the upper and one in the lower chamber of the well and resistance measured at intervals from 0 to 240 minutes (Figure 2.7). At the end of each experiment the medium was removed, cells were stained with crystal violet and examined under the microscope to ensure that the cell layers had remained attached throughout the course of the experiment.

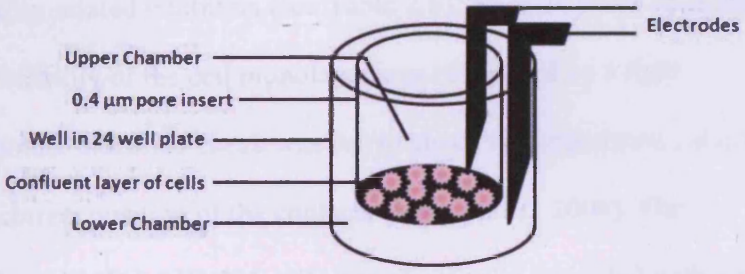

Figure 2.7: Measurement of TER using an EVON volt-ohmmeter.

2.7.2 ECIS (electric cell-substrate impedance sensing) for monitoring cell attachment and cell motility analysis in HECV and MDA-MB-231 cell lines

The 1600R model of the ECIS instrument (Applied Biophysics Inc, NJ, USA) was used for motility assay (wounding assay), wounding/cell modelling analysis in the study model. Cell modelling was carried out using the ECIS RbA modelling software, supplied by the manufacturer (Figure 2.8).

The 8W10 arrays (8 well format with 10 probes in each well) were used in the present study. The array surface was treated with 200µl of 10mM L-Cysteine solution for 20 minutes, which binds to the gold surface via its thiol group forming a monomolecular layer, followed by two washes in Dulbecco's Modified Eagle's medium with 15Mm Hepes, L-Glutamine (Lonza Laboratories, Verviers, Belgium). An electrode check was run to check the impedance value of the cell-free wells containing just fresh medium and to assess the integrity of the arrays. The arrays were seeded at a density of 40,000 cells in 400 µl of Dulbecco's Modified Eagle's medium with 15Mm Hepes, L-Glutamine to achieve confluent monolayers following treatment with motility-related inhibitors (see Table 2.6). After 24 hours in culture, the confluence and viability of the cell monolayer was confirmed by a light microscope, thus another electrode check was run to check the impedance value of the array to ensure correct position of the contacts (Keese *et al.*, 2004). The monolayer of HECV and MDA-MB-231 cells was electrically wounded with a 5V AC at 4,000Hz for 30 seconds (Figure 2.9). Impedance and resistance of the cell layer were immediately recorded every millisecond for a period of up to 5 hours.

Attachment and Migration were modelled using the ECIS RbA cell modelling software.

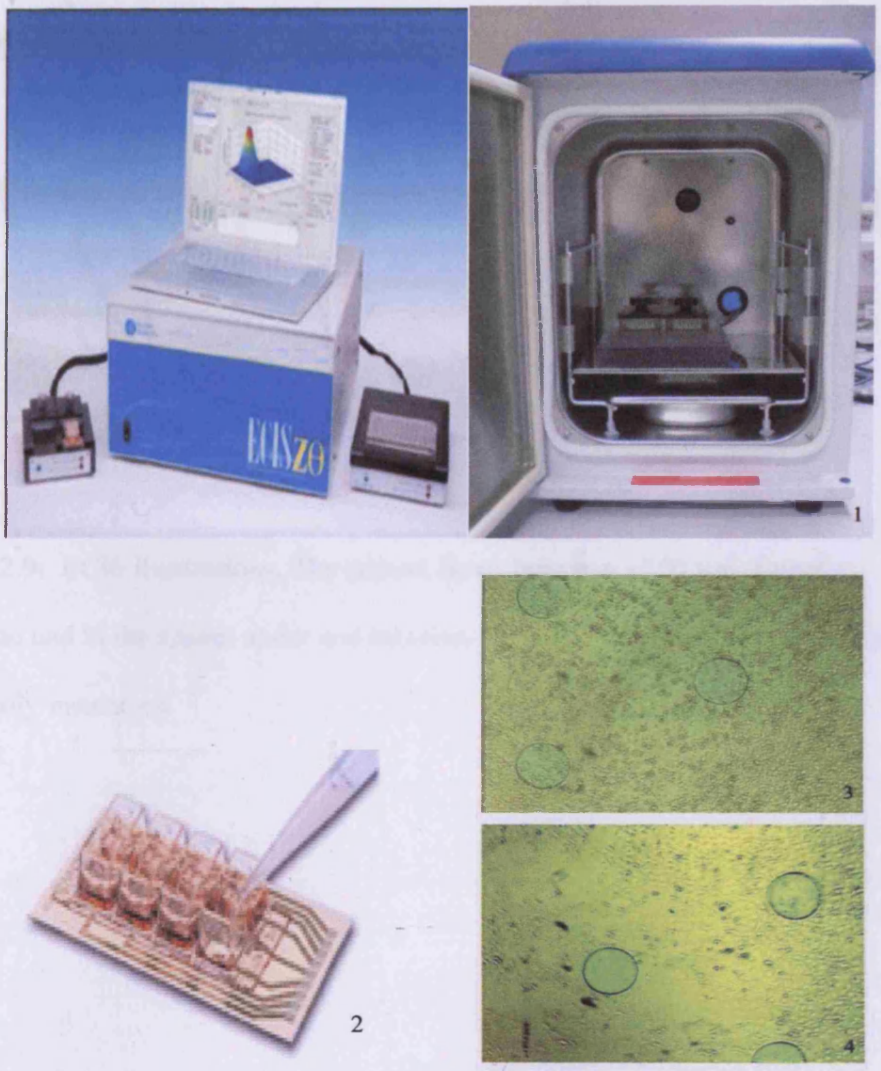

Figure 2.8: ECIS instrument (panel 1). The 8W10 array (panel 2). Micrographs taken from ECIS before (panel 3) and immediately after wounding (panel 4).

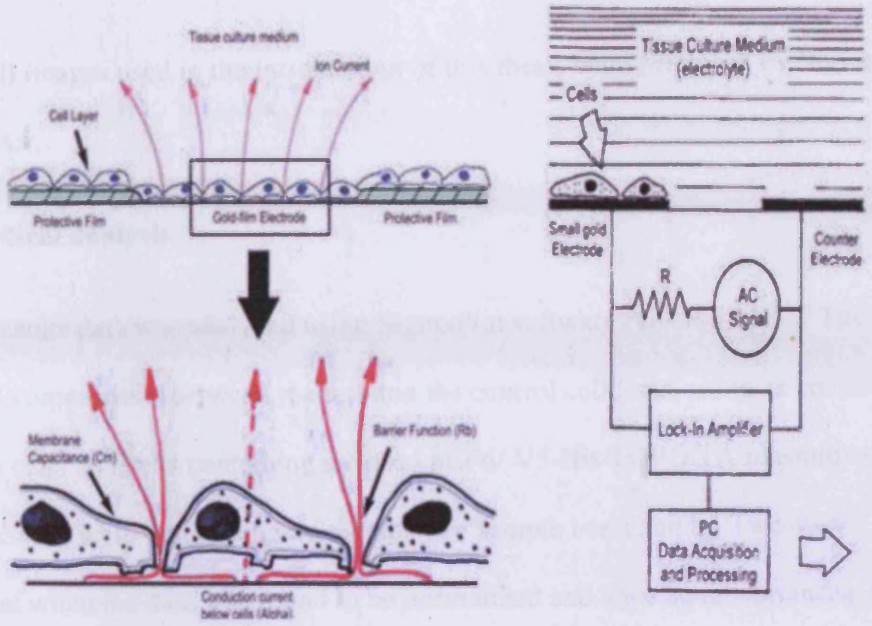

Figure 2.9: ECIS illustrations. The current flows between a 250 μm diameter electrode and in the spaces under and between the cells, as the cell membranes are essentially insulators.

2.8 Designed images

All images used in the introduction of this thesis were produced by Servier Medical Art.

2.9 Statistical analysis

Results data was analyzed using SigmaPlot software (version 11.0). The statistical comparisons between the test and the control cell lines, using as control wild type cells and cells containing a closed pEF6/ V5-His TOPO TA plasmid vector when possible, were made using a Students two sample t-test and by Two-way Anova test when the data was found to be normalized and have equal variances. In all cases 95% confidence intervals were used. All the graphs were created using Microsoft excel software.

Patient data was analyzed using both SigmaPlot and SPSS, etc.

Chapter 3

Expression of Claudin-5 in normal and cancer human breast tissues

3.1 Introduction

Tight Junctions (TJs) have been widely reported as being not only merely intercellular seals; they are also key structures in paracellular transport, gene transcription, cell signalling and cellular proliferation and differentiation. Therefore, in recent years they have become the focus of intense research. A substantial body of evidence for altered TJ structure in cancer development has been reported in the last several years.

Claudin proteins are seen as unusual proteins in the TJ structure as they are presented in a variety of tissues with different properties. The composition and distribution between the 24 members confers specific barrier properties to each cell. The impact that the loss of any of the Claudin proteins, or the up-regulation in several carcinomas, exerts on epithelial cells is only now beginning to be unmasked. Therefore, the study of the pattern of expression of Claudins in normal and human cancer tissues might be a useful tool for ascertaining clinical prognosis for the disease. To date, a number of studies have reported on the role of the Claudin-5 in cancer progression, however, there have been none in breast cancer.

This study aimed to determine, for the first time, the levels of expression and distribution of Claudin-5 in a cohort of 133 patients with breast cancer (106) and in normal background tissue (27), in order to investigate a possible link between levels of expression of Claudin-5 and patient outcome.

3.2 Material and method

3.2.1 Collection of breast tissues

A total of 133 breast samples were obtained from breast cancer patients (27 background normal breast tissue and 106 breast cancer tissue), with the consent of the patients and approved by the ethical committee. The pathologist (ADJ) verified normal background and cancer specimens, and it was confirmed that the background samples were free from tumour deposit.

3.2.2 RNA extraction and Q-PCR in tumour and normal breast tissue

RNA was isolated from both tumour and normal breast samples and used as templates for RT-PCR to convert RNA into complementary cDNA (see section 2.4.3 for method). The levels of Claudin-5 transcripts from cDNA were determined by Q-PCR using specific primers. Refer to section 2.4.7 for further details.

3.2.3 Immunohistochemistry staining of Claudin-5

Immunohistochemistry staining of Claudin-5 was carried out using a specific antibody for the protein, followed by secondary antibody, ABC complex and DAB. For detailed IHC procedure refer to section 2.5.2.

3.2.4 Statistical analysis

Comparison between different patients groups were made using two sample t-test where appropriate. In order to assess the long term survival rates of patients with high and low levels of Claudin-5, the overall survival data was used to plot Kaplan-Meier survival curves (SPSS version 14).

3.3 Results

3.3.1 Aberrant expression of Claudin-5 in human breast cancer

Levels of expression of Claudin-5 were examined at mRNA level using Q-PCR and normalised by GAPDH. Results revealed no significant difference between tumour and normal/background samples ($p=0.38$). However, in tissue sections, Claudin-5 was expressed at relatively high levels in tumour tissues, while in normal/background tissues levels were lower (Figure 3.1).

3.3.2 Immunohistochemical staining of Claudin-5

In this study immunohistochemical staining was used to assess the location, distribution and the degree of staining of Claudin-5 in tumour and normal/background samples. In normal mammary tissues, Claudin-5 appeared as strong staining in the endothelial cells, lining vessels, whereas epithelial cells stained weakly for Claudin-5. The staining for Claudin-5 within the tumour sections was however, significantly decreased in both endothelial and epithelial cells (Figure 3.2).

Moreover, the staining distribution within cells from normal/background sections was concordant with TJ location. No such distribution was observed in cells from tumour sections. Here, the staining was weak, diffuse and not located at the TJs.

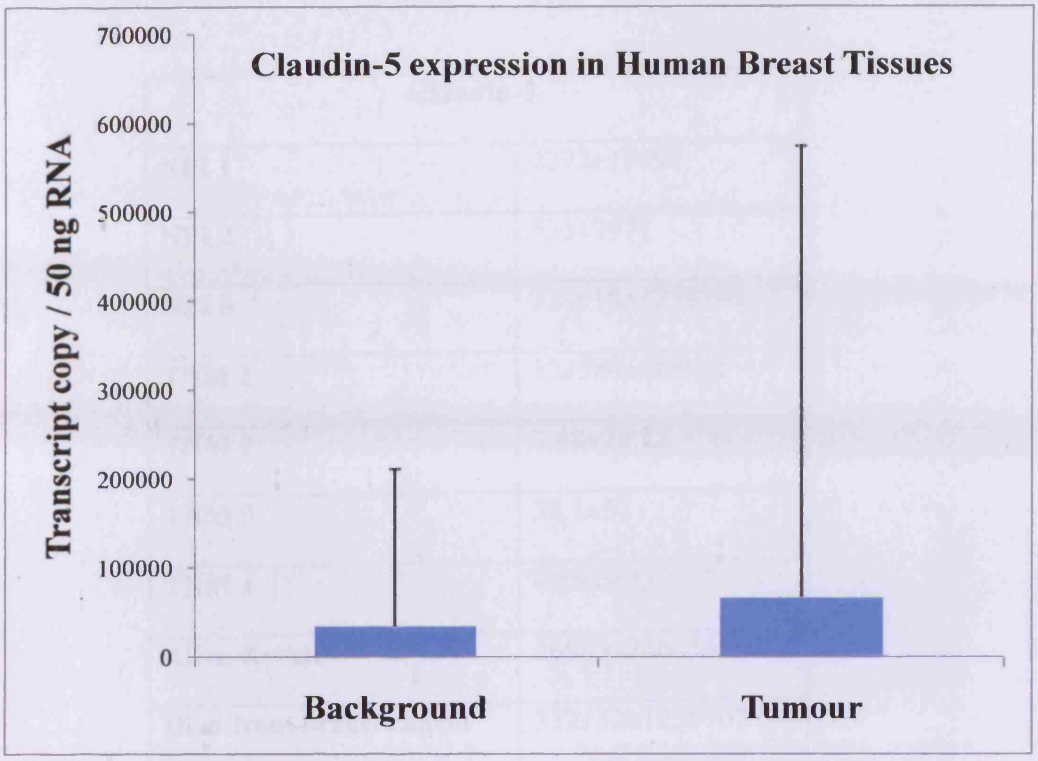

Figure 3.1: Comparison of levels of Claudin-5 in tumour samples compared with normal/background tissue (expressed as transcript copy number per 50 ng of RNA).

Claudin-5	
NPI 1	2293±15492
NPI 2	535±2977
NPI 3	324918±1258394
TNM 1	122580±689911
TNM 2	7.48±22.72
TNM 3	30.1±53
TNM 4	4.56±9.03
Alive & well	26983±226456
Died from breast cancer	332132±1256707

Table 3.1: Analysis of mRNA samples showing levels of Claudin-5 and tumour prognosis by NPI, nodal involvement (TNM) and patient outcome.

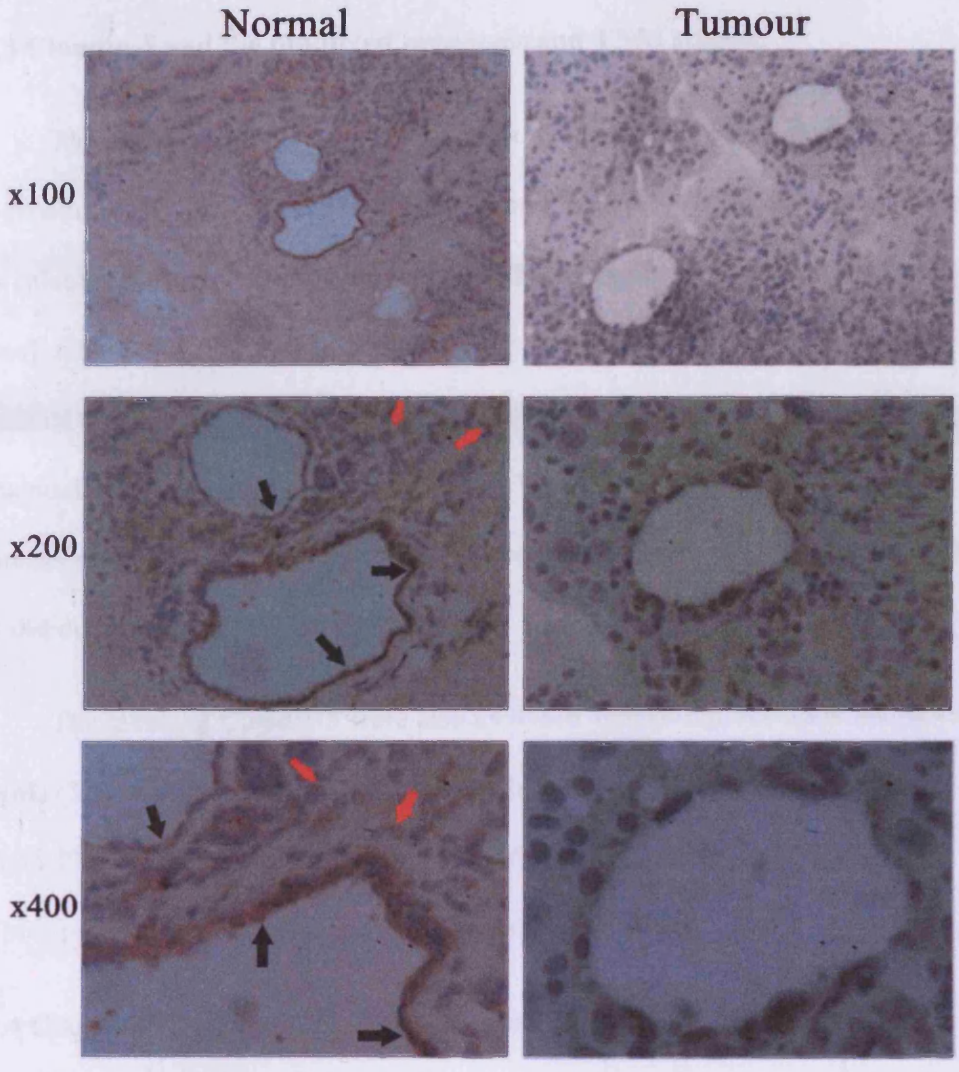

Figure 3.2: A comparison of expression of Claudin-5 protein levels in normal/background (left panel) tissue and tumour breast tissues (right panel) is shown in consecutively increasing magnification. Regions of Claudin-5 expression located at the TJ area in endothelial cells are indicated by black arrows. Red arrows indicate Claudin-5 expression in epithelial cells.

3.3.3 Claudin-5 and the predicted prognosis and TNM staging

The levels of the Claudin-5 transcripts were analysed using the Nottingham Prognostic Index (NPI), which indicates the predicted prognosis of the patients. NPI was calculated using the following equation [NPI= (0.2 X size) + grade + nodal status], where NPI< 3.4 is regarded as a good prognosis (NPI 1), NPI 3.4-5.4 as moderate (NPI 2) and NPI >5.4 as poor prognosis (NPI 3). Claudin-5 levels were sequentially increased with increasing NPI. There were higher levels of Claudin-5 expression seen in patients with poorer prognosis (Table 3.1) (Figure 3.3), although this did not reach significance (p=0.34).

The levels of Claudin-5 were also analysed against tumour-node-metastasis (TNM) (Table 3.1) (Figure 3.4). There were higher levels of Claudin-5 expression seen in TNM1 status when compared to TNM2 (p=0.19), TNM3 (p=0.19) and TNM4 (p=0.19), but significance was not reached.

3.3.4 Claudin-5 expression in different tumour grade

When comparing the levels of Claudin-5 against tumour grade (Table 3.1) (Figure 3.5), higher levels of expression were seen in grade 2 when compared with grade 1 tumours although this was not statistically different (p=0.85). However, grade 3 showed lower levels when compared to grade 1 although this did not reach significance (p=0.34).

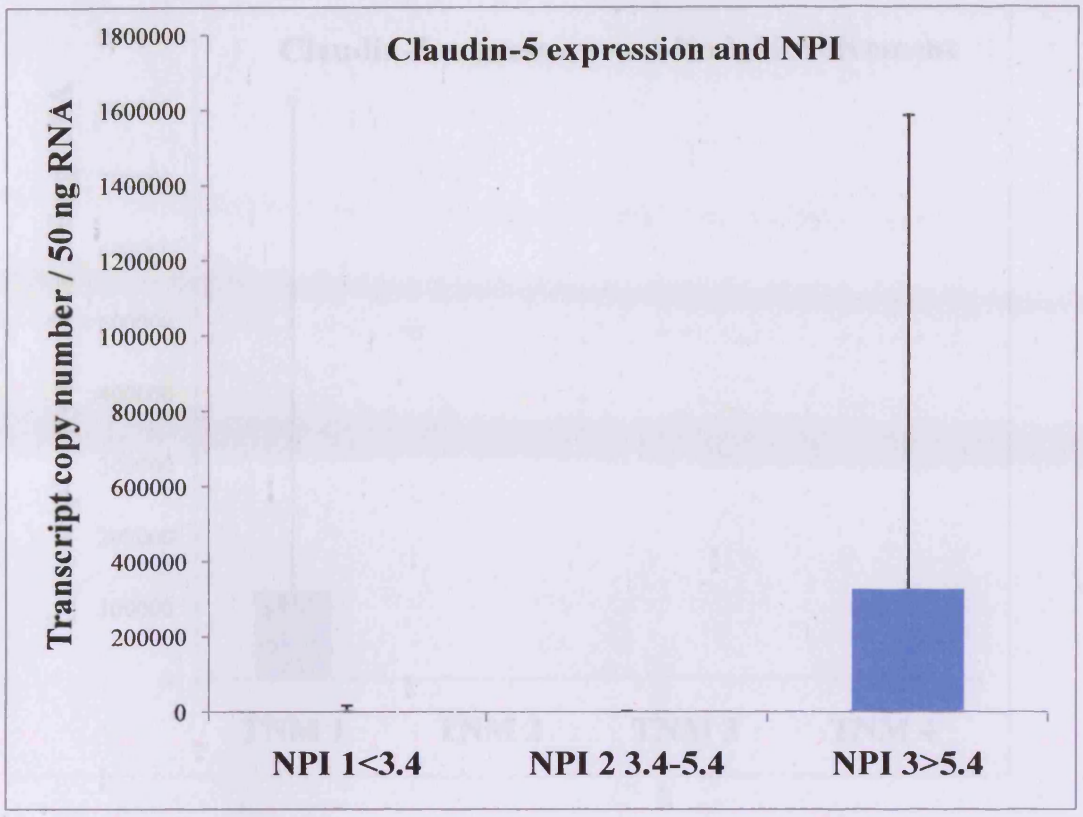

Figure 3.3: Levels of expression of Claudin-5 in relation to NPI status (expressed as transcript copy number per 50 ng of RNA).

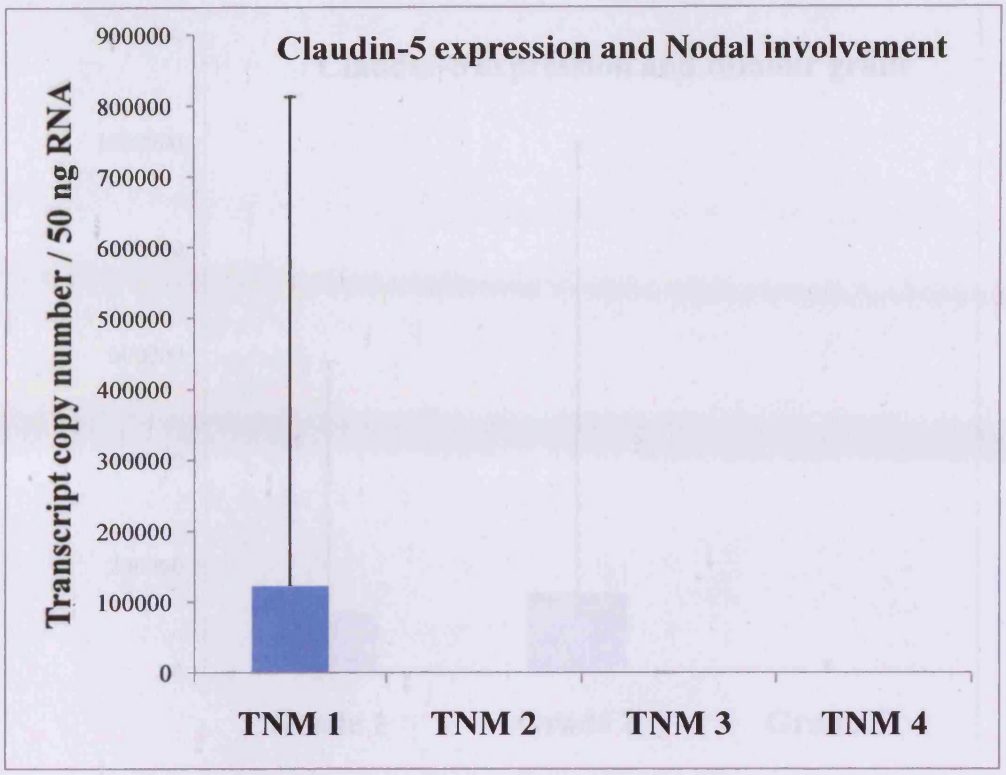

Figure 3.4: Levels of expression of Claudin-5 in relation to TNM status of tumours (expressed as transcript copy number per 50 ng of RNA).

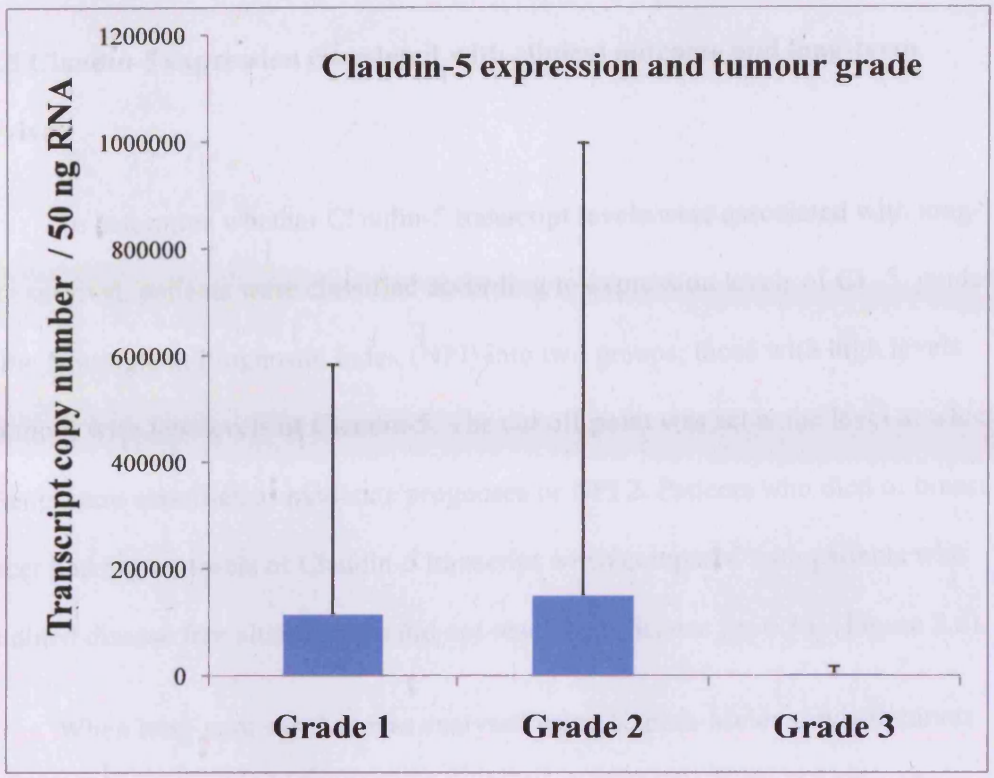

Figure 3.5: Levels of Claudin-5 in relation to tumour grade (expressed as transcript copy number per 50 ng of RNA).

3.3.5 Claudin-5 expression correlated with clinical outcome and long-term survival

To determine whether Claudin-5 transcript levels were associated with long-term survival, patients were classified according to expression levels of CL-5, guided by the Nottingham Prognostic Index (NPI) into two groups; those with high levels and those with low levels of Claudin-5. The cut off point was set at the level at which patients were classified as moderate prognoses or NPI 2. Patients who died of breast cancer had higher levels of Claudin-5 transcript when compared with patients who remained disease free although this did not reach significance (p=0.36) (Figure 3.6).

When long-term survival was analysed using Kaplan-Meier survival curves (Figure 3.7), patients with high levels of Claudin-5 transcript had a significantly shorter survival than patients with low levels of Claudin-5 (p=0.004); mean survival 129.780 moths (118.120-141.441 months, 95% CI) versus 66 months (41.520-90.480 months, 95% CI).

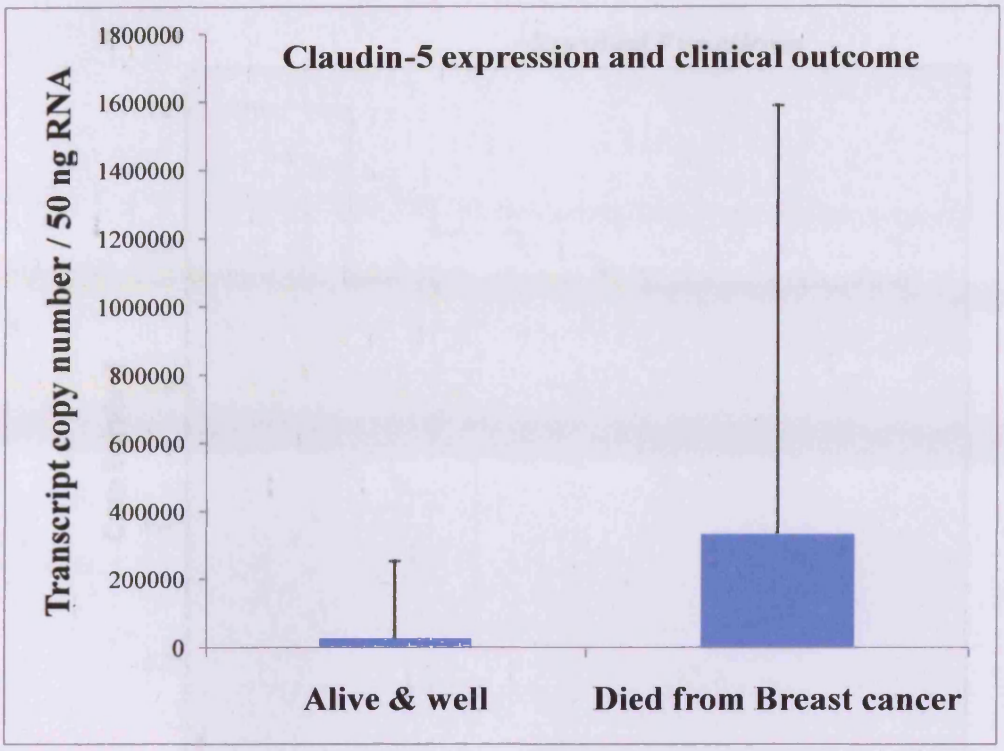

Figure 3.6: Levels of expression of Claudin-5 in relation to patient outcome (expressed as transcript copy number per 50 ng of RNA).

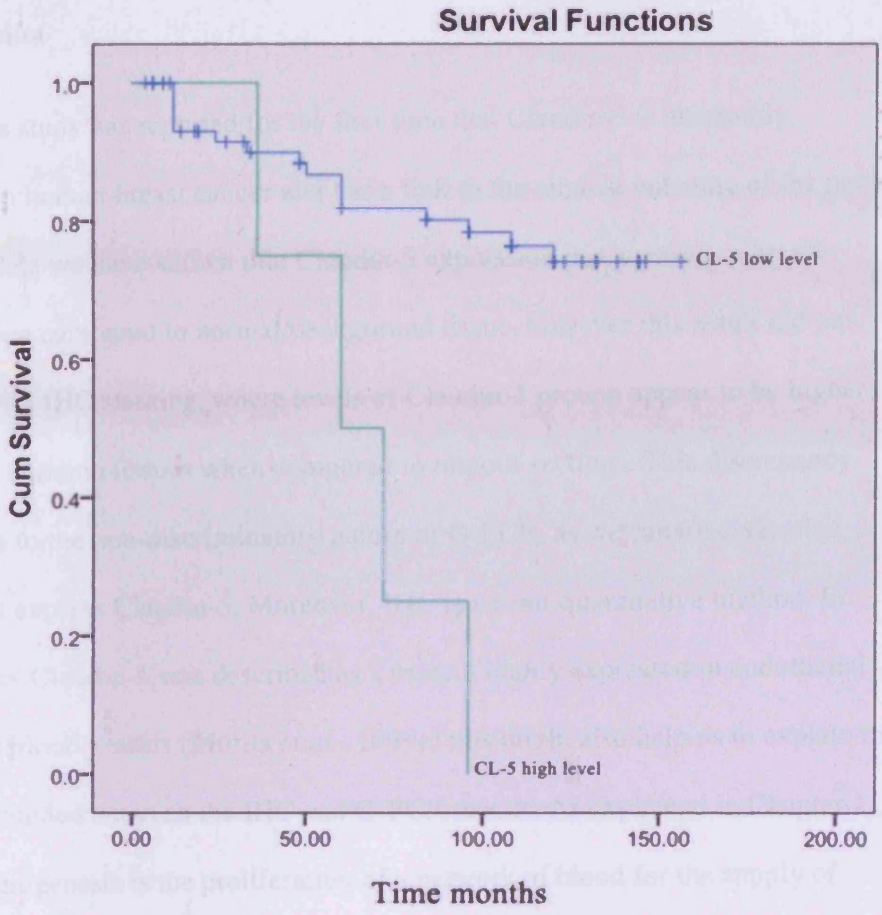

Figure 3.7: Kaplan-Meier survival curve in association of Claudin-5 expression (CL5/GAPDH ratio) for disease free survival (p=0.004) (Cut off 10,000).

3.4 Discussion

This study has reported for the first time that Claudin-5 is aberrantly expressed in human breast cancer and has a link to the clinical outcome of the patient. From this data we have shown that Claudin-5 expression is decreased in breast tumour tissue compared to normal/background tissue, however this result did not correlate with IHC staining, where levels of Claudin-5 protein appear to be higher in normal/background tissues when compared to tumour sections. This discrepancy may be due to the non-discriminatory nature of Q-PCR, as we cannot determine which cells express Claudin-5. Moreover, IHC is a semi-quantitative method. In early studies Claudin-5 was described as a protein highly expressed in endothelial cells of the blood vessels (Morita *et al.*, 1999c) this might also help us to explain the disparity founded between the IHC and Q-PCR results. As explained in Chapter 1, tumour angiogenesis is the proliferation of a network of blood for the supply of nutrients as well as oxygen and for removing waste products, therefore Claudin-5 theoretically should be highly expressed being a recognised member of the TJ structure in endothelial cells constituting these blood vessels. This, in itself, might reveal an angiogenic potential in assessing the aggressiveness of breast cancer.

For the clinical point of view, one of the most interesting observations from this study is the relationship between high levels of Claudin-5 and clinical outcome. Patients who died from breast cancer had higher levels of Claudin-5 compared with patients who remained disease-free. Furthermore, patients whose tumours expressed high levels of Claudin-5 had significantly shorter survival than those with low levels of expression of Claudin-5.

The Nottingham Prognostic Index (NPI), has been used as a prognostic indicator with its reliability being validated in several studies (Suen and Chow, 2006). Claudin-5 showed a high expression at NPI 3 when compared to NPI 1 and NPI 2 correlating these results with the poor prognosis seen when looking at clinical outcome for these patients as described above. Conversely, when Claudin-5 expression was compared with tumour grade and TNM status of tumours no trend was observed. Claudin-5 showed no obvious correlation as Claudin-5 was decreased in grade 3 when compared to grade 1 and grade 2. The same trend was observed when comparing levels with TNM classification, where Claudin-5 expressed high levels at TNM1, although none of these results reached significance.

In recent years, an increasing number of studies have revealed the differential expression of Claudins in human cancers (Oliveira and Morgado-Diaz, 2007). Although high levels of Claudin-5 have been reported in ovarian (Turunen *et al.*, 2009), prostate (Seo *et al.*) and lung cancers (Paschoud *et al.*, 2007) and low levels in hepatocellular carcinoma (Sakaguchi *et al.*, 2008), this is the first study to our knowledge to report levels of Claudin-5 in patients with breast cancer.

Collectively, these findings suggest that Claudin-5 is a potential prognostic factor in patients with breast cancer, as high levels of expression are clearly associated with indicators of poor prognosis as well as with high incidence of breast cancer-related death and shorter survival of patients. These results strongly indicate a prognostic value of Claudin-5 in breast cancer.

Chapter 4

Cloning and verification of Claudin-5 over-expression and knockdown

4.1 Introduction

The role of Claudins in carcinogenesis and progression to metastasis is an active area of research due largely to the discovery that Claudin expression is frequently altered in cancer. Although their functional role in cancer progression remains unclear, the differential expression of these proteins between tumour and normal cells, in addition to their membrane localisation, makes them prime candidates for cancer therapy (Kominsky, 2006; Tsukita *et al.*, 2008). The Claudin protein family was discovered in 1989 by Furuse *et al.*, (Tsukita, 1989). Since the initial discovery of the first claudin, at least 24 human Claudins have been identified. They are generally expressed in both epithelial and endothelial cells and thus are found throughout the body.

It has been shown that expression of Claudin-5 selectively decreased the permeability of the blood-brain barrier ions (Nitta *et al.*, 2003). A very limited number of studies have examined patterns of expression of Claudin-5 in human cancer, however, as already discussed in Chapter 1, levels of Claudin-5 expression appear to be altered in ovarian, lung, prostate and hepatocellular carcinomas.

Previous work in our research group initiated an investigation into the expression of Tight Junction (TJ) molecules in breast cancer. The original pilot study identified a number of target molecules that would allow for further investigation as having potential as breast cancer markers, prognostic indicators or possible therapeutic targets. One of these proteins of interest was Claudin-5.

The aim of this study is primarily to establish the role of Claudin-5 in endothelial cells during the defence of cancer invasion as well as its role in breast cancer cells.

4.2 Material and methods

4.2.1 Materials

Polyclonal rabbit anti-Claudin-5 antibody (SC-28670) was obtained from Santa-Cruz Biotechnologies Inc. (Santa-Cruz, CA, USA) and polyclonal mouse anti-Claudin-5 antibody (H00007122-A01) was obtained from Abnova (Abnova GmbH, Heidelberg, Germany). Secondary antibody for Immunofluorescence staining was labelled anti-rabbit IgG-FITC from Sigma (Sigma-Aldrich, Dorset, UK). Secondary antibody for Western blotting was labelled anti-mouse peroxidase conjugated (A-9044) from Sigma (Sigma-Aldrich, Dorset, UK). All primers used were manufactured and provided by Invitrogen (Invitrogen, Inc., Paisley, UK), all their sequences are located in table 2.2.

4.2.2 Cell lines

HECV and MDA-MB-231 cell lines were chosen to investigate the effects of forced expressed and knockdown of Claudin-5. They were cultured in DMEM-F12 medium as described in section 2.2.

4.2.3 Generation of Claudin-5 knockdown and forced expression MDA-MB-231 and HECV cells

Amplification of the Claudin-5 coding sequence was carried out using primers capable of amplifying the full length sequence of Claudin-5 (table 2.2) together with placental cDNA (previously shown to highly express Claudin-5) used as template.

Hammerhead ribozymes targeting Claudin-5, based on the secondary structure of Claudin-5 were used. For detailed procedures refer to section 2.3.

4.2.4 TOPO cloning of Claudin-5 coding sequence/transgenes into a pEF6/His TOPO plasmid vector

Claudin-5 coding sequence or transgene was cloned into pEF6/ V5-His TOPO TA plasmid vector, followed by transformation of constructed plasmid into *Escherichia coli.* The correct colonies were then amplified, and the plasmid extracted. For detailed procedures refer to section 2.3.

4.2.5 HECV and MDA-MB-231 cell transfection and generation of stable transfectants

Following plasmid verification, the plasmids were transfected into HECV and MDA-MB-231 cells and were placed in selection medium containing 5μg/ml Blasticidin S, following selection for up to 10 days. For detailed procedures refer to section 2.3.

4.2.6 Synthesis of complementary DNA and RT-PCR

RNA was isolated from the cells and RT-PCR was used to convert RNA into complementary cDNA as described in section 2.4. Conventional PCR was run to confirm the products which were visualized on a 2% agarose gels.

4.2.7 Protein extraction, SDS-PAGE and Western blotting analysis

Protein was extracted and quantified, followed SDS-PAGE as described in section 2.5. Proteins were transferred onto nitrocellulose membranes and probed with specific primary anti-Claudin-5 (full antibody data is given in table 2.5).

4.2.8 Immunofluorescent staining

Immunofluorescent staining of Claudin-5 in HECV and MDA-MB-231 cells was carried out using a specific antibody for the protein, followed by secondary-FITC antibody. For detailed IFC procedure refer to section 2.5.3.

4.3 Results

4.3.1 Screening of cell lines and tissues for Claudin-5 expression

The expression of Claudin-5 was examined in eleven breast cancer cell lines, including MDA-MB-157, MDA-MB-463, BT-549, MCF-7, MDA-MB-436, ZR-751, MDA-MB-435S, BT-474, MDA-MB-231 and BT-474KC. Relatively low levels of Claudin-5 were seen in most of these cells or Claudin-5 was absent. However, BT-549, MDA-MB-436 and MDA-MB-231 showed moderately high levels of Claudin-5 mRNA levels compared to the other breast cancer cell lines (Figure 4.1).

The expression of Claudin-5 was also screened in three prostate cell lines, DU-145, PNT-19 and PNT-2C2, revealing that Claudin-5 was expressed at relatively low levels in PNT-2C2 cells and completely absent in DU-145 and PNT-19. Pancreatic cell lines PANC-1, MiaPaCa and Cor- L677, the fibroblast cell line MCR5 (used as a control as fibroblasts do not have TJ), the bladder cancer cell line RT-112, the human epithelial carcinoma cell line A-431, the human keratinocyte cell line HaCaT and the two colorectal cell lines HRT-18 and HT-115 showed negative levels of Claudin-5 after screening.

In the endothelial cell lines HECV and HUVEC mRNA levels of Claudin-5 were seen as expected, as Claudin-5 has previously been reported to be highly expressed in the blood vessels in an early study (Morita *et al.*, 1999c). However, relatively low levels were seen in the HUVEC cell line when compared to HECV cells.

In all cell line samples, β-actin expression was also examined to confirm cDNA quality and to demonstrate normalised levels of cDNA within the separate cell lines.

This data demonstrated expression of Claudin-5 in several breast cancer cell lines, in the prostate cancer cell line PNT-2C2 and in endothelial cell lines HECV and HUVEC, providing us with information enabling us to choose a cell line with high levels of expression of Claudin-5. The MDA-MB-231 and HECV cell lines were among others selected to investigate the role of Claudin-5 in human endothelial and breast cancer cells and therefore they were established as *in vitro* cell models for this study.

Expression of Claudin-5 was also investigated in three different human tissues such as placenta, breast and colorectal tissue in order to choose cDNA templates for the amplification of Claudin-5 expression sequence for further analyses (Figure 4.2 A).

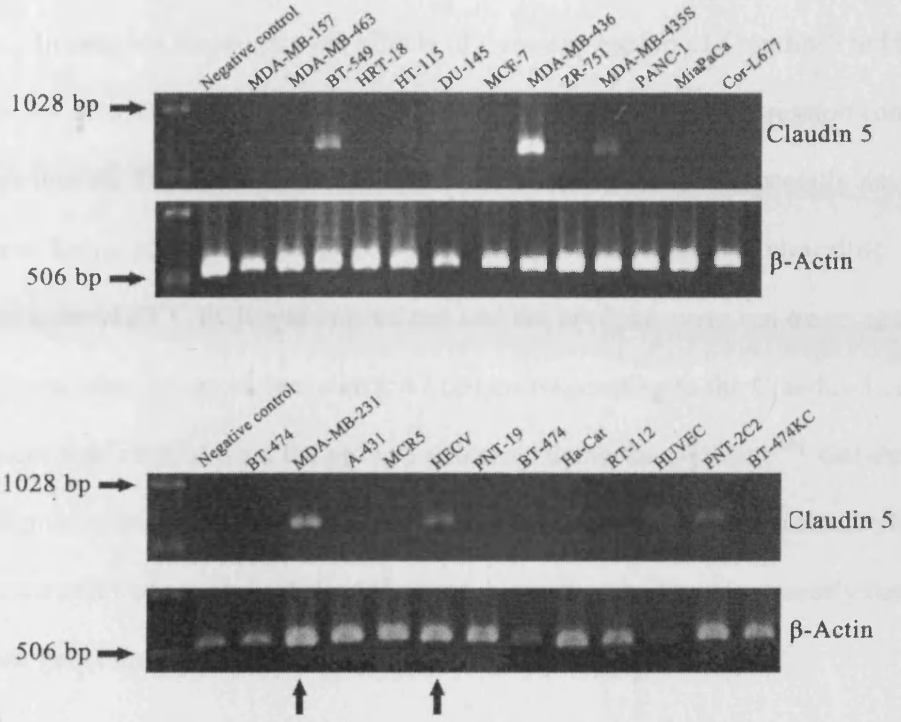

Figure 4.1: Screening of different cell lines for Claudin-5 mRNA levels using PCR . The arrows indicate the two cell lines chosen to be used in this study, the human breast cancer cell line MDA-MB-231 and the human endothelial cell line HECV.

4.3.2 Amplifying Claudin-5 expression sequence

In order to investigate the effects of over-expression of Claudin-5 in HECV and in the breast cancer MDA-MB-231 cell line, a mammalian expression construct was generated. The full length of Claudin-5 was amplified using specially designed primers. Using placenta tissue cDNA as a template and an optimal annealing temperature of 55°C PCR was carried out and the products were run on an agarose gel. The product of the correct size (547 bp) corresponding to the Claudin-5 coding sequence was excised from the gel and extracted using the GelElute™ Gel extraction kit (Sigma-Aldrich, Dorset, UK). In order to verify that the band was successfully extracted and truly contained the Claudin-5 sequence, it was subsequently run on a 2% agarose gel (Figure 4.2 B).

4.3.3 Cloning of expression sequence into plasmid vector

Once the Claudin-5 coding sequence was verified and prepared, it was cloned into a pEF6/ V5-His TOPO TA plasmid vector. Thus, the constructed plasmid was transform into *Escherichia coli* and the colonies were analysed to verify not only that they contained the Claudin-5 plasmid, but that the plasmids had incorporated the fragment in the correct orientation.

To achieve this, each of the selected colonies was tested in two separate PCR reactions: one using CL5expR1/ CL5expF2 to determine if the entire sequence of Claudin-5 had been inserted resulting in a 547bp product (sequences of primers table 2.2) and another independent PCR to the one above mentioned using T7F/ CL5expR1 to determine whether the insert was ligated in the correct orientation

(Figure 4.3 A). As T7F is located about 90bp upstream of the Claudin-5 insert, considering the insert is ligated in the correct orientation, the resulting product after using T7F coupled with CL5expR1primer should be approximately 637bp in length. Therefore, the colony displaying full sequence and correct orientation can be taken for amplifications as it contains the full Claudin-5 sequence in the correct orientation. The positive colonies were carefully picked and grown up in a large volume of LB medium and underwent plasmid extraction (Figure 4.3 B).

Plasmid extraction was carried out and, so as to determine plasmid integrity, the purified plasmid was run on an agarose gel as well as used as a template in a PCR using specific primers for Claudin-5 to ensure correct orientation (Figure 4.4). A posteriori, the plasmid was sent off to Geneservice Ltd. (Source Bioscience, Cambridge, UK) for sequencing in order to ultimately verify that the insert within the plasmid contained the correct Claudin-5 sequence. The results showed a positive match between the sequence cloned into plasmid vector, and the human Claudin-5 precursor sequence (Figure 4.5).

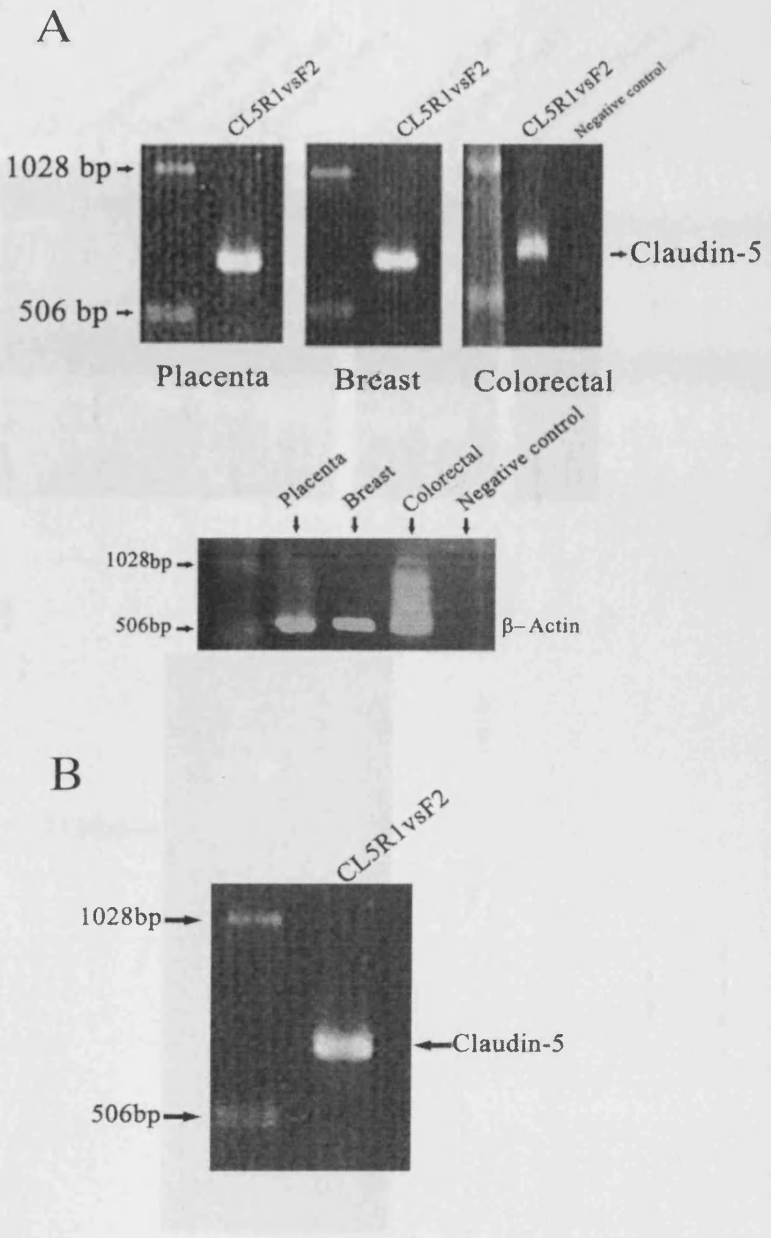

Figure 4.2: (A) PCR products visualised on an agarose gel from different human tissues of Claudin-5 coding sequence. The placenta tissue was selected as a template. The correct size of the product is 547bp as indicated with the arrow. (B) Agarose gel showing PCR product using the Claudin-5 coding sequence from previous gel above and used as a template with Claudin-5 specific primers R1vsF2.

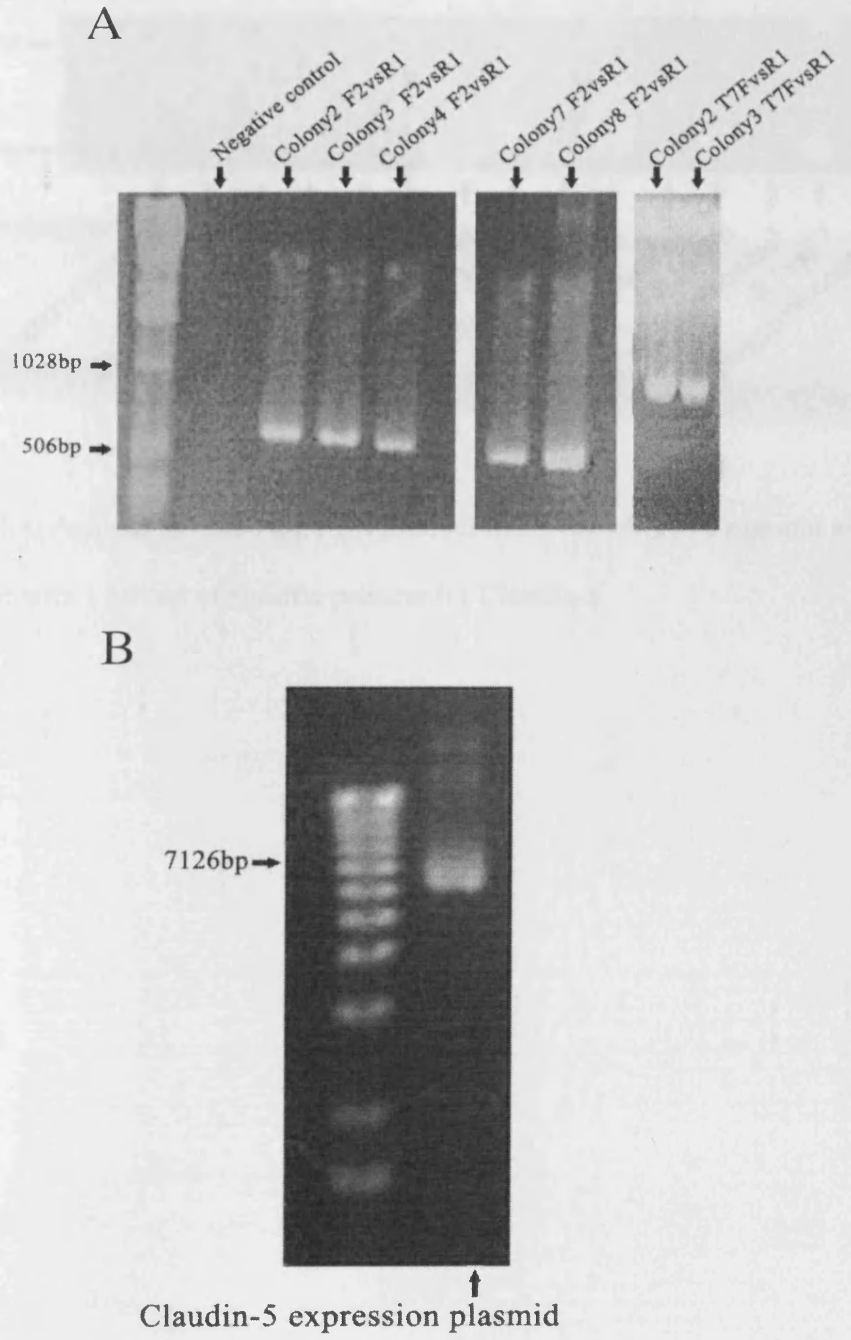

Figure 4.3: (A) Agarose gel showing PCR for *Escherichai coli* colony analysis to verify that they contained the Claudin-5 plasmid and in the correct orientation. (B) Agarose gel showing purified Claudin-5 plasmid.

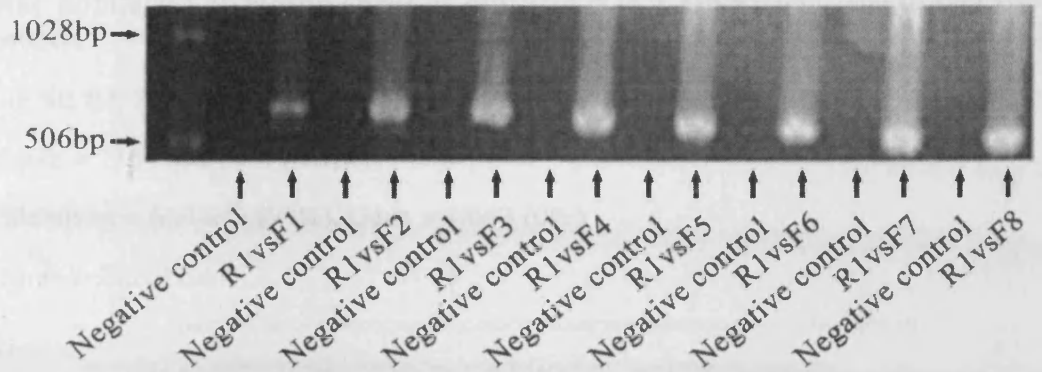

Figure 4.4: Agarose gel showing PCR product using the extracted plasmid as a template with a full set of specific primers for Claudin-5.

NM_001130861.1| **Homo sapiens claudin 5 (CLDN5)**, transcript variant 1, mRNA

GENE ID: 7122 CLDN5 | claudin 5 [Homo sapiens] (Over 10 PubMed links)

Score = 1164 bits (630), Expect = 0.0

Identities = 639/643 (99%), Gaps = 1/643 (0%)

Strand=Plus/Plus

```
Query 71   GAGATCCTGGGCCTGGTGCTGTGCCTGGTGGGCTGGGGGGGGTCTGATCCTGGCGTGCGGG 130

Sbjct 1101 GAGATCCTGGGCCTGGTGCTGTGCCTGGTGGGCTGGGGGGGGTCTGATCCTGGCGTGCGGG 1160

Query 131  CTGCCCATGTGGCAGGTGACCGCCTTCCTGGACCACAACATCGTGACGGCGCAGACCACC 190

Sbjct 1161 CTGCCCATGTGGCAGGTGACCGCCTTCCTGGACCACAACATCGTGACGGCGCAGACCACC 1220

Query 191  TGGAAGGGGCTGTGGATGTCGTGCGTGGTGCAGAGCACCGGGCACATGCAGTGCAAAGTG 250

Sbjct 1221 TGGAAGGGGCTGTGGATGTCGTGCGTGGTGCAGAGCACCGGGCACATGCAGTGCAAAGTG 1280

Query 251  TACGACTCGGTGCTGGCTCTGAGCACCGAGGTGCAGGCGGCGCGGGCGCTCACCGTGAGC 310

Sbjct 1281 TACGACTCGGTGCTGGCTCTGAGCACCGAGGTGCAGGCGGCGCGGGCGCTCACCGTGAGC 1340

Query 311  GCCGTGCTGCTGGCGTTCGTTGCGCTCTTCGTGACCCTGGCGGGCGCGCAGTGCACCACC 370

Sbjct 1341 GCCGTGCTGCTGGCGTTCGTTGCGCTCTTCGTGACCCTGGCGGGCGCGCAGTGCACCACC 1400

Query 371  TGCGTGGCCCCCGGGCCCGGCCAAGGCGCGTGTGGCCCTCACGGGAGGCGTGCTCTACCTG 430

Sbjct 1401 TGCGTGGCCCCCGGGCCCGGCCAAGGCGCGTGTGGCCCTCACGGGAGGCGTGCTCTACCTG 1460

Query 431  CTCTGCGGGCTGCTGGCGCTCGTGCCACTCTGCTGGTTCGCCAACATTGTCGTCCGCGAG 490

Sbjct 1461 TTTTGCGGGCTGCTGGCGCTCGTGCCACTCTGCTGGTTCGCCAACATTGTCGTCCGCGAG 1520

Query 491  TTTTACGACCCGTCTGTGCCCGTGTCGCAGAAGTACGAGCTGGGCGCAGCGCTGTACATC 550

Sbjct 1521 TTTTACGACCCGTCTGTGCCCGTGTCGCAGAAGTACGAGCTGGGCGCAGCGCTGTACATC 1580

Query 551  GGCTGGGCGGCCACCGCGCTGCTCATGGTAGGCGGCTGCCTCTTGTGCTGCGGCGCCTGG 610

Sbjct 1581 GGCTGGGCGGCCACCGCGCTGCTCATGGTAGGCGGCTGCCTCTTGTGCTGCGGCGCCTGG 1640

Query 611  GTCTGCACCGGCCGTCCCGACCTCAGCTTCCCCGTGAAGTACTCAGCGCCGCGGCGGCCC 670

Sbjct 1641 GTCTGCACCGGCCGTCCCGACCTCAGCTTCCCCGTGAAGTACTCAGCGCCGCGGCGGCCC 1700

Query 671  ACGGCCACCGGCGACTACGACAAGAAGAACTACGTCA-AGGGC 712

Sbjct 1701 ACGGCCACCGGCGACTACGACAAGAAGAACTACGTCTGAGGGC 1743
```

Figure 4.5: Figure confirming that extracted plasmid shows a positive match for Claudin-5 when sequence compared to the BLAST database.

4.3.4 Generation of Claudin-5 ribozyme transgenes

In order to silence the expression of Claudin-5 in HECV and in the breast cancer MDA-MB-231 cell line, ribozyme transgenes of Claudin-5 were generated and cloned into a pEF6/ V5-His TOPO TA plasmid vector and subsequently transfected into mammalian cells. This would allow for comparison between the effects of knocking down, and forced expression of Claudin-5 in the above mentioned cell lines.

Based on the secondary structure of Claudin-5, which was generated using Zuker's RNA mFold program, an appropriate targeting site for the ribozyme was first designed. Ribozymes were generated using touchdown PCR and followed by cloning into a pEF6/ V5-His TOPO TA plasmid vector (Figure 4.6 A). In order to verify the correct orientation of the ribozyme transgene, specific primers to the ribozyme transgene were paired with T7F respectively. Each colony was tested with two independent PCRs, once to confirm the presence of the transgene using specific primers for Claudin-5 ribozyme CL5Rib1R/ CL5Rib1F and CL5Rib2R/ CL5Rib2F resulting in a 100bp products, and another to confirm orientation. For this purpose, T7F primer was coupled with CL5Rib1R and CL5Rib2R respectively. If the transgene is correctly orientated, a PCR product should be seen at approximately 200bp as the ribozyme sequence is around 100bp and T7F promoter starts at approximately 90bp before insert (Figure 4.6 B).

Positive colonies were selected for further amplification and subsequent plasmid extraction. The plasmids were then verified using DNA electrophoresis in order to verify successful plasmid extraction (Figure 4.7 A). In addition to this,

conventional PCR was carried out using specific primers for Claudin-5 ribozyme CL5Rib1R/CL5Rib1F and CL5Rib2R/ CL5Rib2F in order to demonstrate the presence of the ribozyme (Figure 4.7 B).

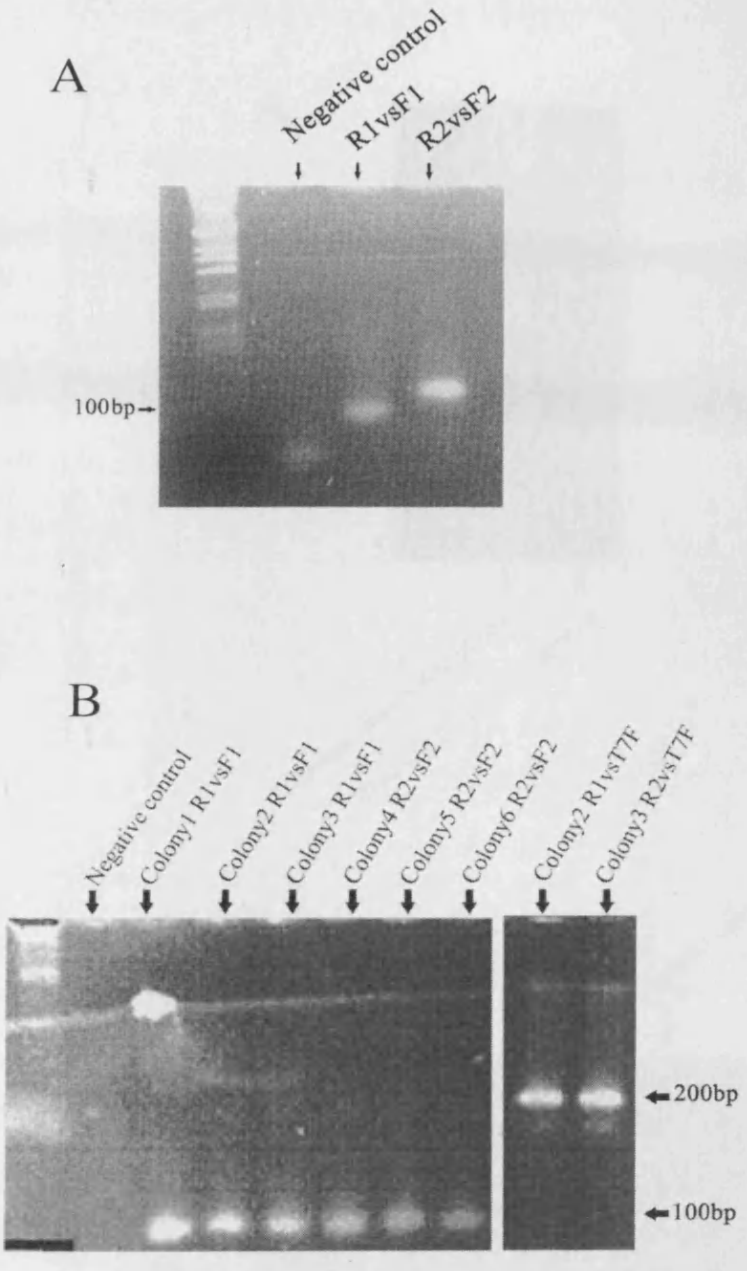

Figure 4.6: (A) Ribozymes synthesis using touchdown PCR. (B) Agarose gel showing PCR for *Escherichai coli* colony analysis to verify insertion and correct orientation of the transgene.

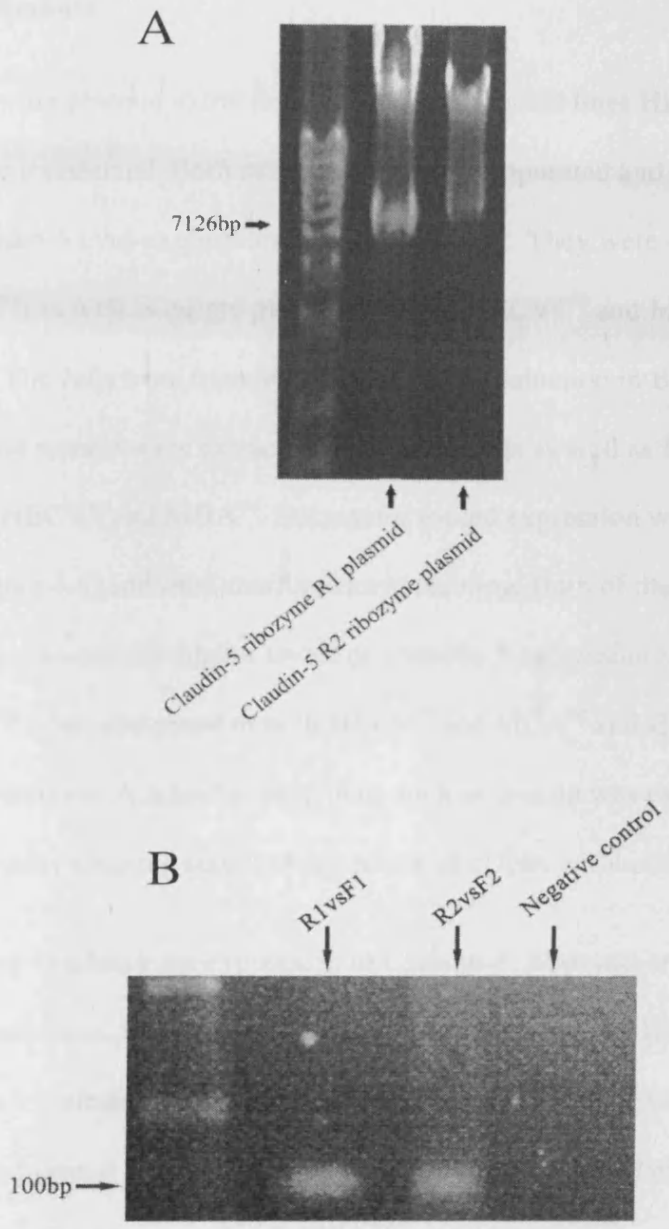

Figure 4.7: (A) Plasmids were extracted and verified with DNA electrophoresis. (B) Agarose gel showing PCR products using specific primers for Claudin-5 ribozyme. and the extracted plasmids as a template in order to demonstrate the presence of the ribozyme.

4.3.5 Transfection of HECV and MDA-MB-231 cells and verification of the stable transfectants

Following plasmid extraction, the mammalian cell lines HECV and MDA-MB-231 were transfected. Both cell lines were electroporated and thus transfected with the Claudin-5 over-expression plasmid construct. They were named $HECV^{Cl5exp}$ and MDA^{Cl5exp}, as well as empty plasmid control, $HECV^{pef6}$ and MDA^{pef6} respectively. The cells were transfected followed by selection in Blasticidin S for 10 days; RNA and protein were extracted from these cells as well as from wild type cell lines, named $HECV^{wt}$ and MDA^{wt}. Successful forced expression was confirmed using RT-PCR (Figure 4.8) and immunofluorescent staining. Both of these methods demonstrated considerably higher levels of Claudin-5 expression in both $HECV^{Cl5exp}$ and MDA^{Cl5exp} when compared to both $HECV^{wt}$ and MDA^{wt} and $HECV^{pef6}$ and MDA^{pef6} respectively. A housekeeping gene such as β-actin was used in the PCR as internal control by showing standardized levels of cDNA within the samples.

In order to silence the expression of Claudin-5, ribozyme transgenes were used in both cell lines. Similarly to Claudin-5 over-expression, HECV and MDA-MB-231 were transfected with two different Claudin-5 targeting ribozymes, together with an empty plasmid control. Using RT-PCR, expression of Claudin-5 mRNA was absent in the case of ribozyme 2 ($HECV^{CL5rib2}$ and $MDA^{CL5rib2}$) compared to the controls ($HECV^{wt}$/MDA^{wt} and $HECV^{pef\ 6}$/MDA^{pef6}). Ribozyme 1 was unsuccessful in knockdown of Claudin-5 expression (Figure 4.8). A similar reduction in Claudin-5 protein level was seen in $HECV^{CL5rib2}$ (Figure 4.10) and $MDA^{CL5rib2}$ (Figure 4.11) when carrying out double Immunofluorescence staining of HECV and MDA-MB-

231 cells using anti-Claudin-5 (FITC) and Phalloidin (TRITC) in order to visualise possible changes in the distribution of the actin filaments. Differences in cell morphology was observed in $HECV^{CL5rib2}$ and $MDA^{CL5rib2}$ cells compared to the controls, where cell shape changed from flat, well-attached cells with a well defined cytoskeleton seen in $HECV^{wt}/MDA^{wt}$ cells to round cells displaying a perinuclear staining of actin following Claudin-5 knockdown. In both $HECV^{Cl5exp}$ and MDA^{Cl5exp}, immunofluorescence staining revealed a reduction in actin filaments as well as elongated and starred cell morphology in MDA^{Cl5exp}.

A similar reduction of Claudin-5 protein level was demonstrated in both $HECV^{CL5rib2}$ and $MDA^{CL5rib2}$ cells, whereas an enhanced level of protein was seen in $HECV^{Cl5exp}$ and MDA^{Cl5exp} compared to the $HECV^{wt}$ and MDA^{wt} controls, when carrying out Western blotting analysis (Figure 4.9).

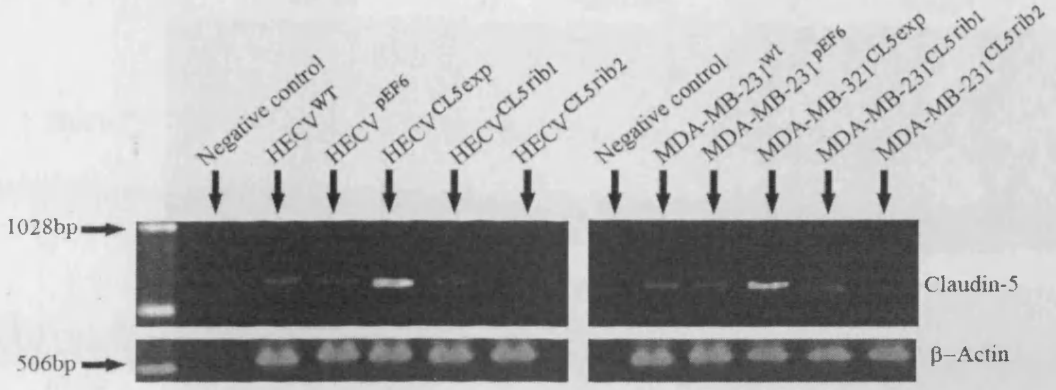

Figure 4.8: Agarose gel verifying over-expression and knockdown of Claudin-5 in mammalian transfected cells using specific primers for Claudin-5. RT-PCR demonstrates successful over-expression and silencing of Claudin-5 in ribozyme 2 for HECV and MDA-MB-231 cell lines compared to the controls.

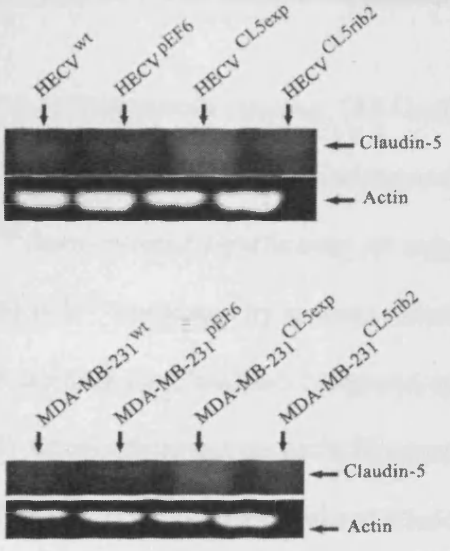

Figure 4.9: Western blotting analysis demonstrating enhanced level of Claudin-5 protein in HECV^{Cl5exp} and MDA^{Cl5exp} compared to the HECV^{wt} and MDA^{wt} controls. Decreased levels of Claudin-5 protein were observed in HECV^{CL5rib2} and MDA^{CL5rib2} when compared to the controls.

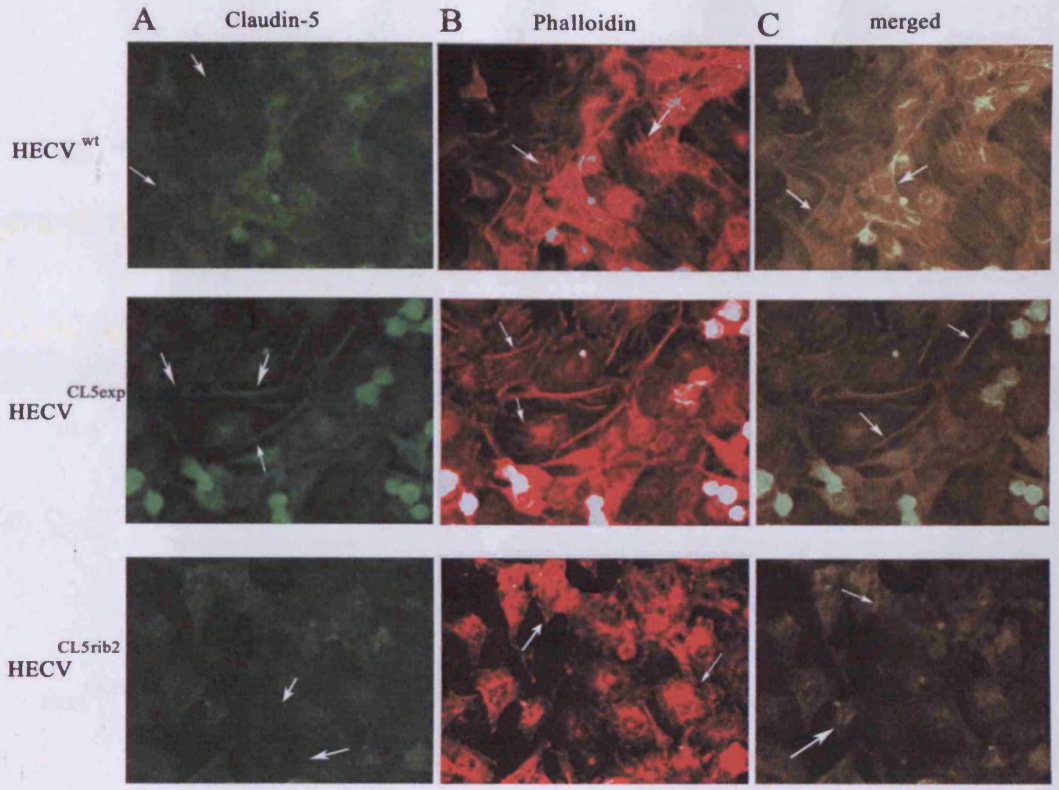

Figure 4.10: Double Immunofluorescence staining. (A) Confirming over-expression and knockdown in HECV cells of Claudin-5 levels using anti-Claudin-5 (FITC) Left hand column. HECV^{Cl5exp} demonstrated significantly stronger staining when compared to the control HECV^{wt} (indicated by arrows) whereas, HECV^{CL5rib2} cells showed considerably less staining for Claudin-5 compared to the control HECV^{wt} (indicated by arrows). (B) Arrows demonstrate actin filament staining pattern as detected by Phalloidin (TRITC). (C) Co-localization of Claudin-5 and actin filaments.

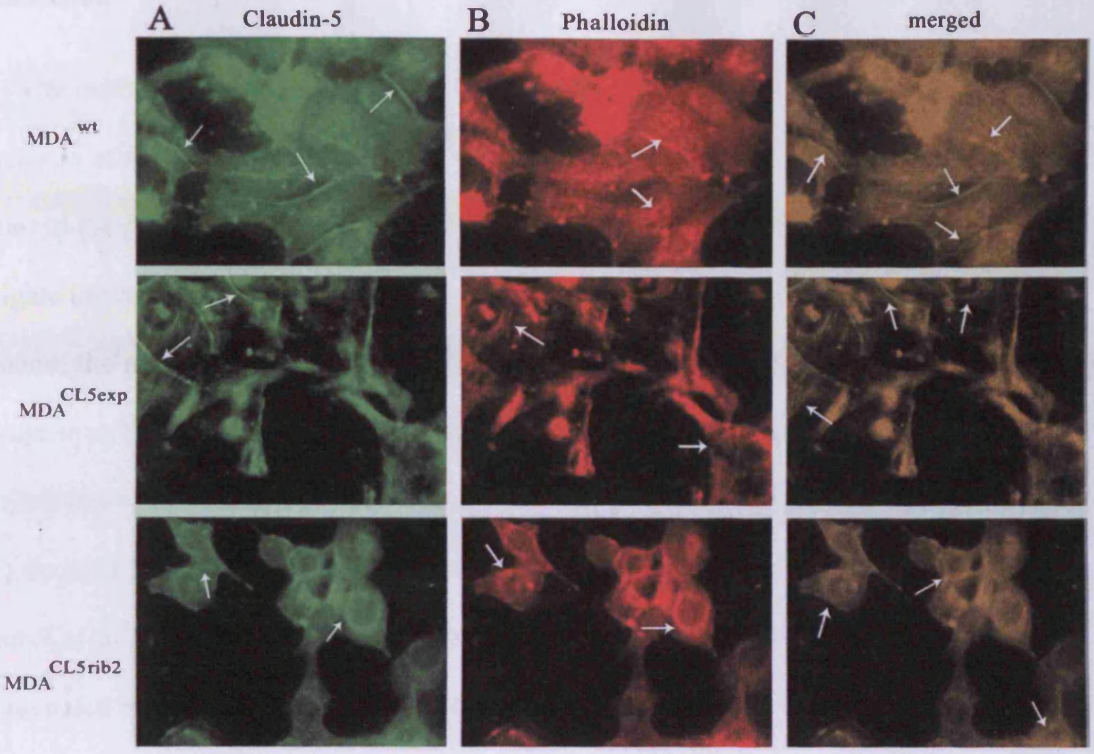

Figure 4.11: Double Immunofluorescence staining. (A) Verification of Claudin-5 over-expression and knockdown in MDA-MB-231 cell using anti-Claudin-5 (FITC) Left hand column. Claudin-5 expression was considerably stronger in the MDA^{Cl5exp} compared to the control MDA^{wt} (indicated by arrows) whereas; Claudin-5 staining in $MDA^{CL5rib2}$ cells was much less compared to the control MDA^{wt} (indicated by arrows). (B) Arrows demonstrate actin filament staining pattern as detected by Phalloidin (TRITC). (C) Co-localization of Claudin-5 and actin filaments.

4.4 Discussion

The initial screening undertaken in this chapter revealed levels of expression of Claudin-5 in three of the eleven breast cancer cell lines examined, in endothelial cells and in the prostate cell line PNT-2C2. As the aim of this current study was to investigate the role of Claudin-5 in endothelial and breast cancer cells by altering its expression, the prostate cell line was discarded. Claudin-5 has been reported to be expressed in epithelial cell lines of the stomach, liver, pancreas (Rahner *et al.*, 2001), colon (Amasheh *et al.*, 2005) as well as in the brain and lung (Morita *et al.*, 1999c).To our knowledge, no previous study has investigated the biological role of Claudin-5 in any of the two cell lines selected. However, an early study from Morita *et al.*, revealed high levels of expression of Claudin-5 in endothelial cells of the blood vessels (Morita *et al.*, 1999c) and Martin *et al.*, reported the regulation of Claudin-5 in MDA-MD-231 when cells were treated with HGF (Martin *et al.*, 2004a).

The screening process provided data for the determination of which cells to use for this study. In order to investigate the role of Claudin-5 in endothelial cells and in breast cancer cells, we altered Claudin-5 expression in HECV and MDA-MB-231 cells as they were seen to express high levels of Claudin-5. We constructed a mammalian expression vector containing the entire Claudin-5 coding region. Claudin-5 over-expression was verified at both the mRNA and protein level using PCR and immunofluorescent staining. In addition, we used hammerhead ribozymes to silence the expression of Claudin-5 after transcription in both cell lines. Claudin-5 was successfully down-regulated by the use of ribozyme transgenes *in vitro* as proved at both the mRNA and protein level. This would aid to confirm that the effect

of over-expressing Claudin-5 in HECV and MDA-MB-231 is due to its alteration and not to other external factors that could have had an effect on the natural behaviour of the cells.

These genetic manipulations will allow us to create established *in vitro* models providing us with information about the unknown biological role of Claudin-5 in endothelial and breast cancer cell lines.The impact of Claudin-5 manipulation on the function of cells were subsequently investigated using these cell models and are presented in the following chapters.

Chapter 5

Effect of Claudin-5 expression on the aggressive nature of the MDA-MB-231 human breast cancer cell line

5.1 Introduction

The link between alterations in Tight Junctions (TJs) and epithelial tumour development has been confirmed in early studies (Swift *et al.*, 1983). The epithelium constitutes one of the primary physical barriers that protect the organism against infectious agents in the environment. Most cancers, including breast cancer, originate from epithelial tissues. Cancer cells are characterised by abnormal and uncontrolled growth as well as presenting disorders in cell communication. Additional underlying changes include changes in cell-cell and cell-substrate adhesion, a fundamental step allowing cancer cells to spread and ultimately metastasise. Consequently, the polarity of the cells and the paracellular transport is altered. Claudins are proteins in the TJ structure and the mixture and interaction of these proteins together with differences in expression patterns of the 24 members that comprise the family, place them in the front line of cancer research. The primary role of Claudins is in the regulation of paracellular selectivity through pores formed by the proteins themselves (Tsukita and Furuse, 2000). However, new roles for Claudins as proteins involved in regulating cell phenotype and growth control are starting to emerge (Findley and Koval, 2009). This new data opens the door to a new concept of what role Claudins might have, changing the perception that they are more than simple sealing proteins.

The present study used a well characterized breast cancer cell line, MDA-MB-231, and following forced expression and knockdown of Claudin-5, cellular biological functions were investigated in response to Hepatocyte Growth Factor (HGF) in order to establish the functional role of Claudin-5 and a possible link with motility-related proteins in this particular breast cancer cell line.

5.2 Materials and methods

5.2.1 Cell line

The breast cancer cell line MDA-MB-231 was used in this study to investigate the effect of Claudin-5; the sublines created were MDA^{Cl5exp} (forced expression) and $MDA^{CL5rib2}$ (knockdown). Experiments also included MDA^{wt} and MDA^{pef6} as controls. Cells were continuously maintained in DMEM-F12 media as described in section 2.2.

5.2.2 *In vitro* tumour cell growth assay

The cells were seeded into four 96 well plates and incubated for a broad range of hours as described in section 2.6.1. Absorbance was measured in order to determine cell number.

5.2.3 *In vitro* tumour cell Matrigel adhesion assay

The cells were seeded into a 96 well plate containing a layer of Matrigel as described in section 2.6.3. The number of cells that had adhered to the artificial basement membrane was counted.

5.2.4 *In vitro* co-culture Matrigel tumour cell invasion assay

The cells were seeded into inserts previously coated with Matrigel as described in section 2.6.2. The number of cells which had migrated through the layer of endothelial cells was counted.

5.2.5 *In vitro* tumour cell motility assay using Cytodex-2 beads and the effect of HGF

The cells were incubated with Cytodex-2 beads as described in section 2.6.4. The number of cells that were carried by the beads and moved from the beads to the base of the well was counted. The same protocol was followed when cells were treated with HGF.

5.2.6 *In vitro* tumour cell migration (wound healing) assay

The migration of the cells across a wounded surface of a confluent monolayer formed by the same cell line was examined as described in section 2.6.5.

5.2.7 Transepithelial resistance and the effect of HGF

The cells were seeded into transparent inserts and the resistance across the layer was measured as described in section 2.7.1. The same protocol was followed when cells were treated with HGF.

5.2.8 ECIS

The cells were seeded into electrical arrays allowing the cells to adhere to the gold electrodes within the array as described in section 2.7.2 causing a change in resistance followed by electrical wounding of the formed monolayer. The same protocol was followed when cells were treated with HGF and motility-related inhibitors.

5.2.9 Analysis of protein levels of N-WASP and ROCK 1 using western blotting. Claudin-5 co-immunoprecipitation with N-WASP and ROCK 1

Western Blotting was used to demonstrate levels of expression of N-WASP and ROCK 1 as described in section 2.5. Claudin-5 co-immunoprecipitation was carried out using cell lysate of MDA^{wt} and MDA^{Cl5exp} and probed with antibodies against N-WASP and ROCK1 as described in section 2.5.1.6. N-WASP and ROCK1 co-immunoprecipitation was carried out as described above and probed with antibodies against Claudin-5.

5.2.10 *In vivo* tumour growth and development

The impact of Claudin-5 on tumour growth was assessed in an *in vivo* system as described in section 2.6.8., where a broad number of factors may influence the effects of over-expression of Claudin-5 in this particular development model.

5.3 Results

5.3.1 Effect of altering Claudin-5 expression on MDA-MB-231 breast cancer cell growth

The MDA-MB-231 sublines MDA^{Cl5exp} and $MDA^{CL5rib2}$ alongside MDA^{wt} and MDA^{pef6} were examined following 1, 3 and 4 day incubation periods using an *in vitro* cell growth assay. No significant difference in the *in vitro* growth rate of the MDA^{wt} and MDA^{pef6} cells compared to MDA^{Cl5exp} or $MDA^{CL5rib2}$ were found following the three different incubation periods (Figure 5.1). However, the growth

rate of MDA^{Cl5exp} at day 1, 3 and 4 was found to be increased when compared to the controls MDA^{wt} and MDA^{pef6}; day 1 MDA^{wt} (24.95%±10.58), MDA^{pef6} (27.49%±12.76) and MDA^{Cl5exp} (35.30%±12.7), (p=0.20 and p=0.35 respectively); day 3 MDA^{wt} (370.45%±44.54), MDA^{pef6} (378.10%±110.41) and MDA^{Cl5exp} (411.61%±64.10), (p=0.27 and p=0.57 respectively); day 4 MDA^{wt} (664.02%±94.57), MDA^{pef6} (645.21%±144.60) and MDA^{Cl5exp} (685.04%±123.85), (p=0.87 and p=0.65 respectively). The opposite effect was observed in the incubation period day 3 and day 4 of $MDA^{CL5rib2}$ where the cell growth was decreased when compared to the controls; day 3 MDA^{wt} (370.45%±44.54), MDA^{pef6} (378.10%±110.41) and $MDA^{CL5rib2}$ (340.40%±83.52), (p=0.49 and p=0.55 respectively); day 4 MDA^{wt} (664.02%±94.57), MDA^{pef6} (645.21%±144.60) and $MDA^{CL5rib2}$ (594.99%±121.60), (p=0.34 and p=0.56 respectively).

5.3.2 Effect of Claudin-5 on MDA-MB-231 breast cancer cell adhesion

The ability of MDA^{Cl5exp} and $MDA^{CL5rib2}$ cells to adhere to matrix was assessed in an *in vitro* Matrigel adhesion assay (Figure 5.2). There was a significant difference between the adherence of $MDA^{CL5rib2}$ and MDA^{wt} and MDA^{pef6} with $MDA^{CL5rib2}$ cells being less adherent to matrix (MDA^{wt} 87.59±8.94, MDA^{pef6} 80.03±11.66 and $MDA^{CL5rib2}$ 38.36±5.35, ($p<0.001$ for both controls). In the case of MDA^{Cl5exp}, the opposite effect was seen, however differences did not reach statistical significance when compared to the controls (MDA^{wt} (87.59±8.94), MDA^{pef6} (80.03±11.66) and MDA^{Cl5exp} (96.56±21.85), (p=0.079 and p=0.062 respectively).

5.3.3 Effect of Claudin-5 on MDA-MB-231 breast cancer cell invasiveness

The invasive potential of the transfected cells MDA^{Cl5exp} and $MDA^{CL5rib2}$ was examined using an *in vitro* Matrigel invasion assay (Figure 5.3). Both cell lines were found to have no significant differences when compared to the controls MDA^{wt} and MDA^{pef6}. However, a non significant marginal reduction in the invasive capacity of $MDA^{CL5rib2}$ was seen (MDA^{wt} (17±1.58), MDA^{pef6} (16.4±2.30) and $MDA^{CL5rib2}$ (15.8 ±1.48, ($p=0.25$ and $p=0.63$ respectively).

5.3.4 Effect of Claudin-5 on MDA-MB-231 breast cancer cell motility and the effect of HGF

Transfected and control cells, either untreated or treated with HGF, were evaluated for their motility using a Cytodex-2 bead motility assay to explore the possibility of Claudin-5 involvement in motility. MDA^{Cl5exp} cells did not show significant differences when compared to the controls (MDA^{wt} (4.28±1.24), MDA^{pef6} (3.8±1.25) and MDA^{Cl5exp} (3.83±1.37), ($p=0.238$ and $p=0.930$ respectively). In contrast, $MDA^{CL5rib2}$ cells demonstrated a significant reduction in cell motility compared to the controls (MDA^{wt} (4.28±1.24), MDA^{pef6} (3.8±1.25) and $MDA^{CL5rib2}$ (3.08±0.84), ($p<0.001$ and $p=0.027$ respectively). (Figure 5.4 A)

The cells were additionally evaluated after treatment with HGF. This motogen increased cell motility in MDA^{Cl5exp} and control cells, MDA^{wt} and MDA^{pef6}, when compared to untreated cells (MDA^{wt}+HGF (6.44±1.78), MDA^{pef6}+HGF (5.27±0.98) and MDA^{Cl5exp}+HGF (6±1.08), $p<0.001$ for both controls). In the case of $MDA^{CL5rib2}$, although a slight increase in the number of motile cells was observed,

the data was not found to be significant ($MDA^{CL5rib2}$+HGF (3.65±1.84), p=0.18) (Figure 5.4 B).

5.3.5 Effect of Claudin-5 on MDA-MB-231 breast cancer cell migration

The effect of Claudin-5 over-expression and knockdown on cell migration was assessed using a migration (wound healing) assay. MDA^{Cl5exp} showed an increased cellular migration compared to the controls 60 minutes after wounding (MDA^{wt} (10.84±8.5), MDA^{pef6} (18.08±16.62) and MDA^{Cl5exp} (39.64±24.81). A decreased cell migration was seen in $MDA^{CL5rib2}$ after 60 minutes when compared to controls (MDA^{wt} (10.84±8.5), MDA^{pef6} (18.08±16.62) and $MDA^{Cl5rib2}$ (2.66±2.82). Although the differences in motility are not statistically significant when comparing to the controls, the trend appears to be evident (Figure 5.5).

5.3.6 Effect of Claudin-5 on MDA-MB-231 breast cancer cell Transepithelial resistance (TER) and their response to HGF

Transepithelial resistance was measured to assess the effect of over-expressing or knocking-down Claudin-5 on TJ functionality in MDA-MB-231 breast cancer cells. MDA^{Cl5exp} showed increased TER over a period of 4 hours in comparison with the control MDA^{wt} (change in TER after 30 minutes MDA^{wt} (-211±1) vs. MDA^{Cl5exp} (-204±2); 60 minutes MDA^{wt} (-233.66±0.57) vs. MDA^{Cl5exp} (-215.66±2.3); 2 hours MDA^{wt} (-244.66±2.88) vs. MDA^{Cl5exp} (-244.66.33±0.57); 4 hours MDA^{wt} (-279.66±1.52) vs. MDA^{Cl5exp} (-267±1.73), p<0.01). Changes in TER were more evident in $MDA^{CL5rib2}$ when compare to the control (change in TER after 30 minutes MDA^{wt} (-211±1) vs. $MDA^{CL5rib2}$ (-141±16.77); 60 minutes MDA^{wt} (-

244.66±2.88) vs. $MDA^{CL5rib2}$ (-156.6±1.52); 2 hours MDA^{wt} (-279.66±1.52) vs. $MDA^{CL5rib2}$ (-168.66±2); 4 hours MDA^{wt} (-279.66±1.52) vs. $MDA^{CL5rib2}$ (-184.66±5.85), $p<0.001$) (Figure 5.6).

Treatment of cells with HGF (50ng/ml) resulted in a significant reduction of the transepithelial resistance in transfected and in control cells when compare to untreated cells over a period of 4 hours (change in TER after 30 minutes MDA^{wt}+HGF (-270±1.5), MDA^{Cl5exp}+HGF (-243±1.6), $MDA^{CL5rib2}$+HGF (-169±3.2); 60 minutes MDA^{wt}+HGF (-286±1.1), MDA^{Cl5exp}+HGF (-263.67±1.7), $MDA^{CL5rib2}$+HGF (-182.33±2.64); 2 hours MDA^{wt}+HGF (-299±2.08), MDA^{Cl5exp}+HGF (-279±2.3), $MDA^{CL5rib2}$+HGF (-202±2.08); 4 hours MDA^{wt}+HGF (-340±1.1), MDA^{Cl5exp}+HGF (-299.67±1.15), $MDA^{CL5rib2}$+HGF (-238.67±1), $p<0.05$) (Figure 5.7).

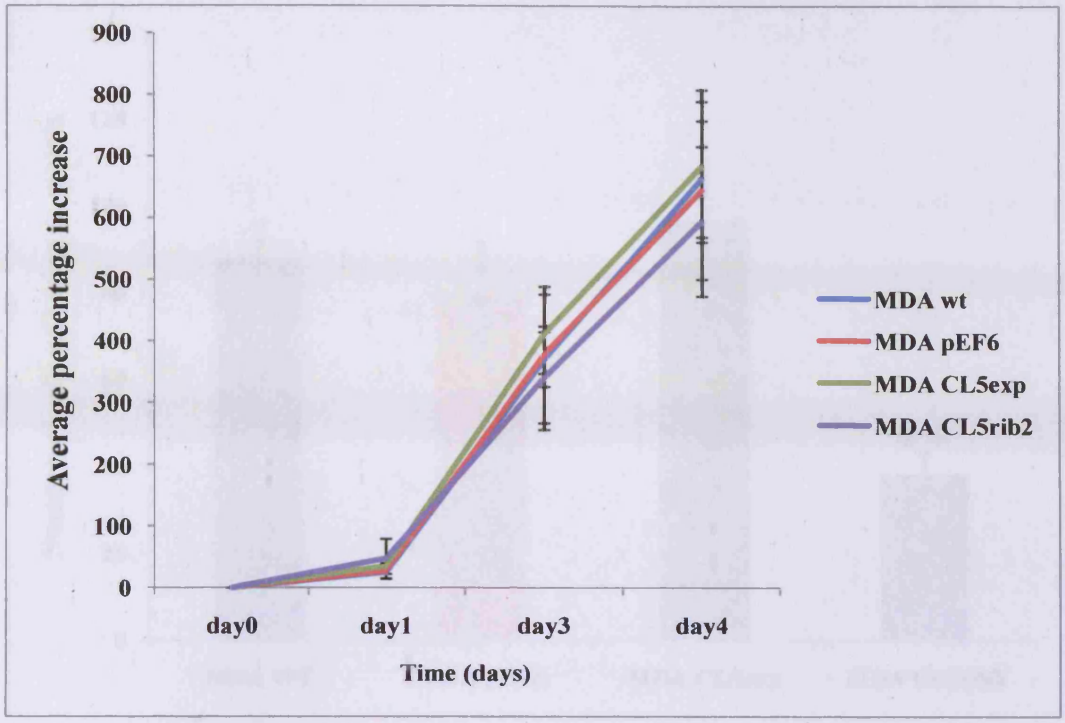

Figure 5.1: Effect of Claudin-5 on *in vitro* cell growth of MDA-MB-231 cells using an *in vitro* cell growth assay. The cell growth of MDA^{Cl5exp} and $MDA^{CL5rib2}$ did not show any significant difference when compared to MDA^{wt} and MDA^{pef6} (mean ±SD, n=3).

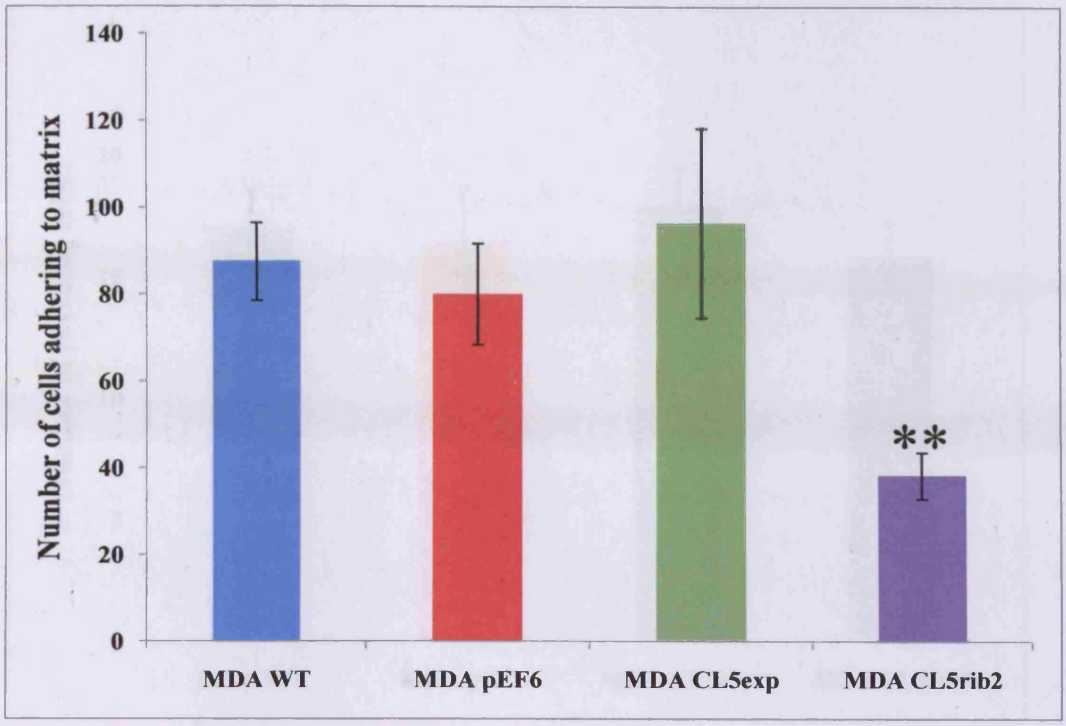

Figure 5.2: Effect of Claudin-5 on *in vitro* cell adhesion of MDA-MB-231 cells using the *in vitro* Matrigel adhesion assay. The data presented is representative is the mean of at least 3 independent repeats and the error bars represent the standard error of the mean. The adhesive capacity of $MDA^{CL5rib2}$ was significantly decreased in comparison with the controls MDA^{wt} and MDA^{pef6} (** represents $p<0.001$ compared to both controls).

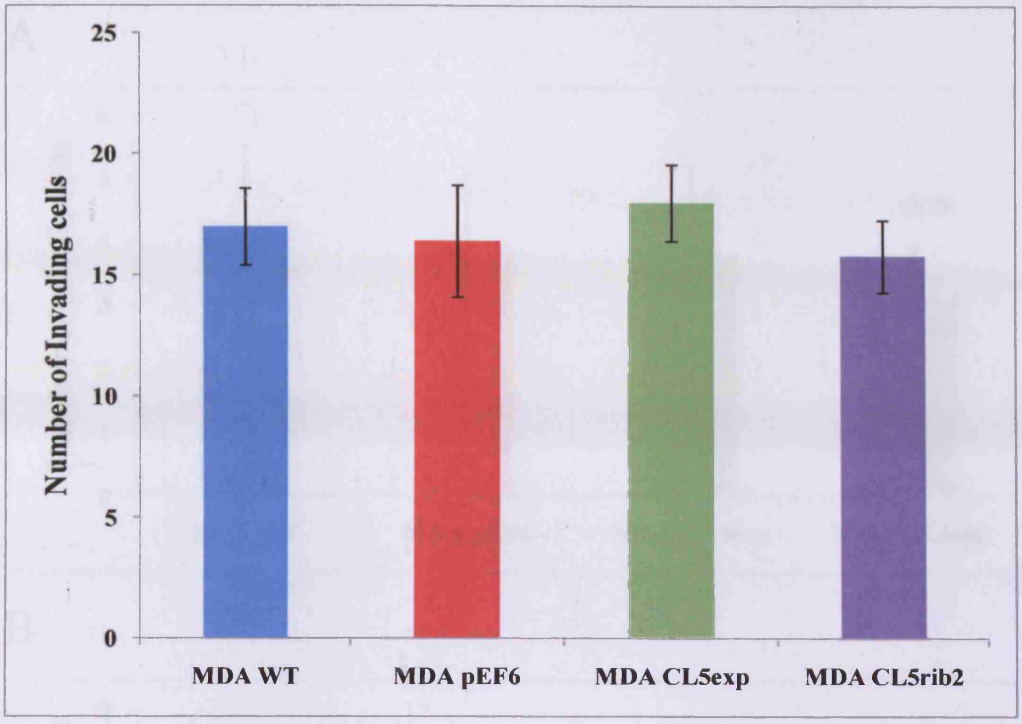

Figure 5.3: Effect of Claudin-5 on cell invasiveness of MDA-MB-231 cells using the *in vitro* Matrigel invasion assay. The data presented is representative is the mean of at least 3 independent repeats and the error bars represent the standard error of the mean. The invasive capacity of MDA^{Cl5exp} and $MDA^{CL5rib2}$ did not show any significant difference when compared to MDA^{wt} and MDA^{pef6}.

A

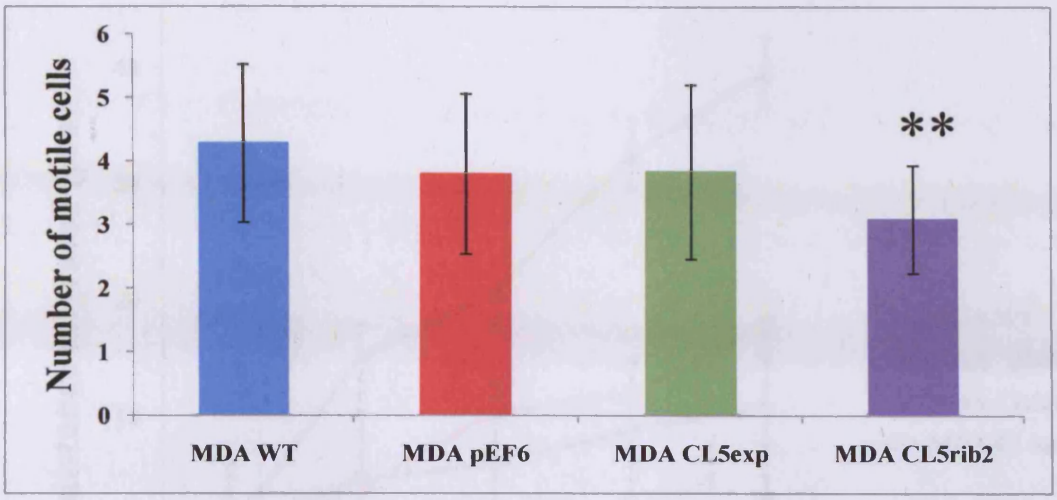

B

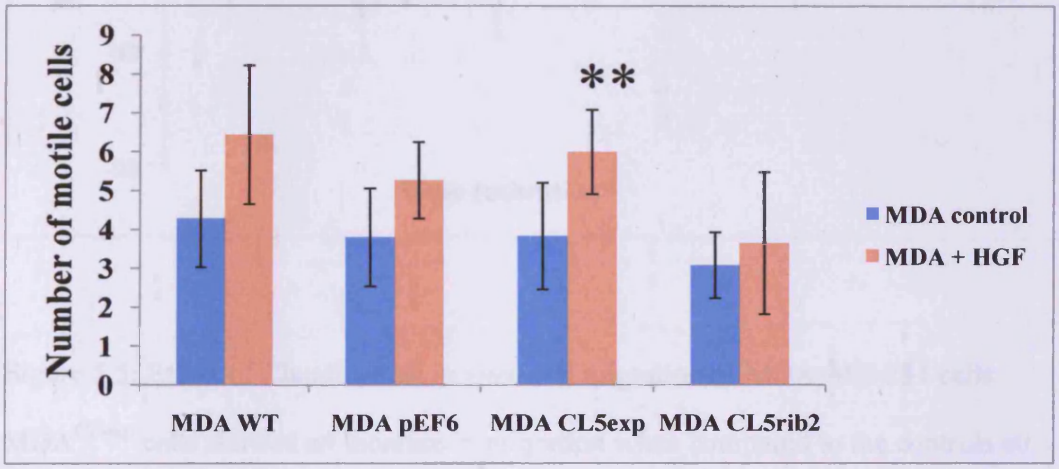

Figure 5.4: (A) Effect of Claudin-5 on *in vitro* cell motility of MDA-MB-231 cells. The motility of $MDA^{CL5rib2}$ was significantly reduced in comparison to the controls ($p<0.001$ and $p=0.027$ respectively). (B) Effect on motility after treatment with HGF. Transfected and control cells showed an increase in motility, however only the controls and MDA^{Cl5exp} results were significant ($p<0.001$). The data presented is representative is the mean of at least 3 independent repeats and the error bars represent the standard error of the mean.

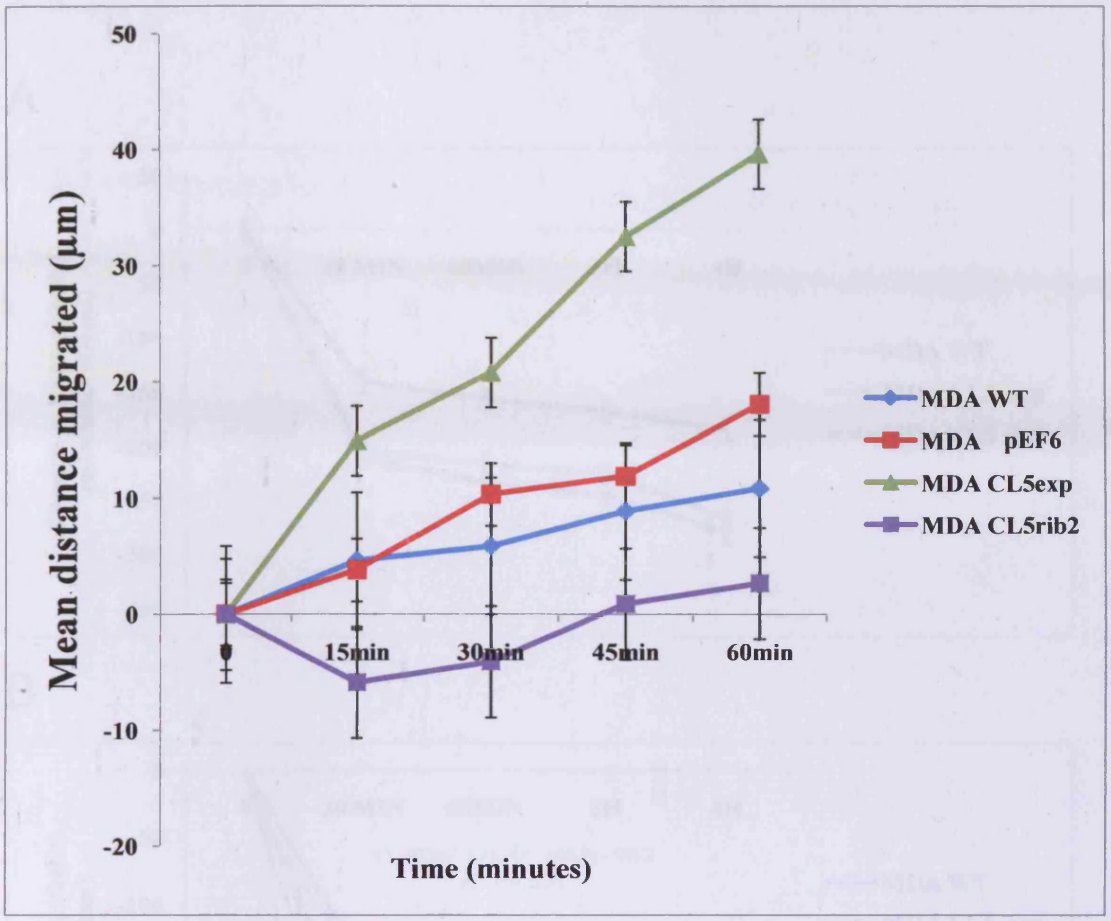

Figure 5.5: Effect of Claudin-5 on *in vitro* cell migration of MDA-MB-231 cells. MDA^{Cl5exp} cells showed an increase in migration when compared to the controls 60 minutes after wounding. The migration of $MDA^{CL5rib2}$ was reduced in comparison to the controls at 60 minutes. However, no significant differences were found (mean ±SD, n=3).

A

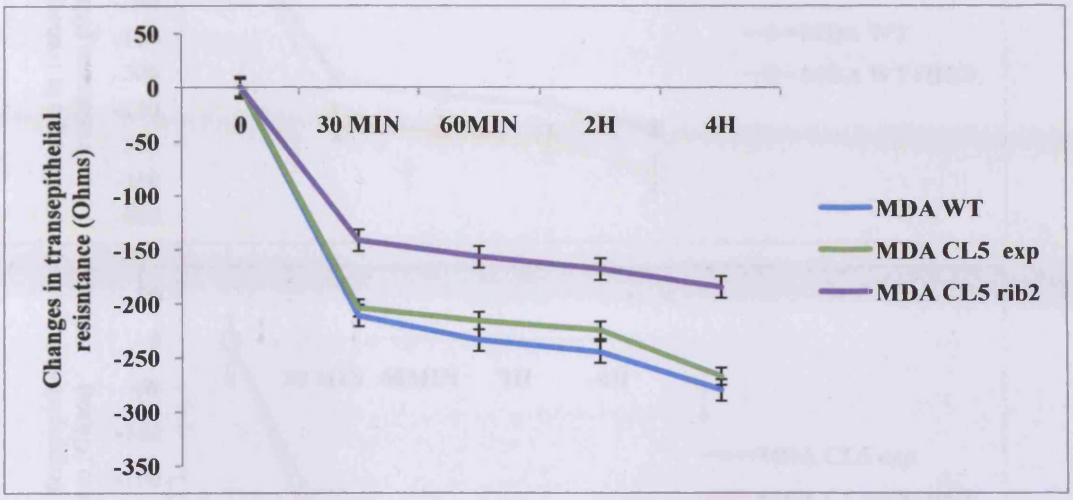

B

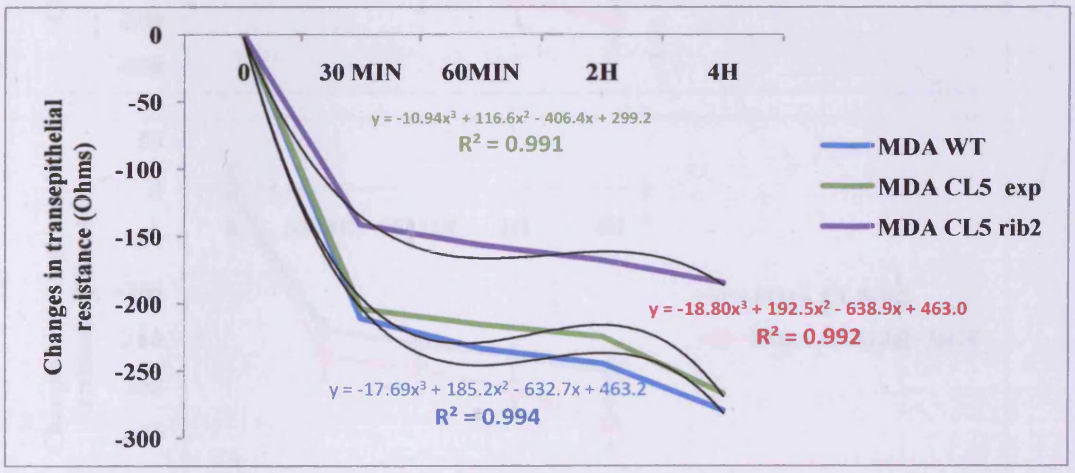

Figure 5.6: (A) Effect of Claudin-5 on transepithelial resistance of MDA-MB-231 cells. Significant changes were seen in MDA^{Cl5exp} and $MDA^{CL5rib2}$ over a period of 4 hours when compared to the control ($p<0.01$ and $p<0.001$ respectively). (B) A polynomial model was used to visualize the trend of the presented data. R^2 indicates that the regression line clearly fits the data (mean ±SD, n=3).

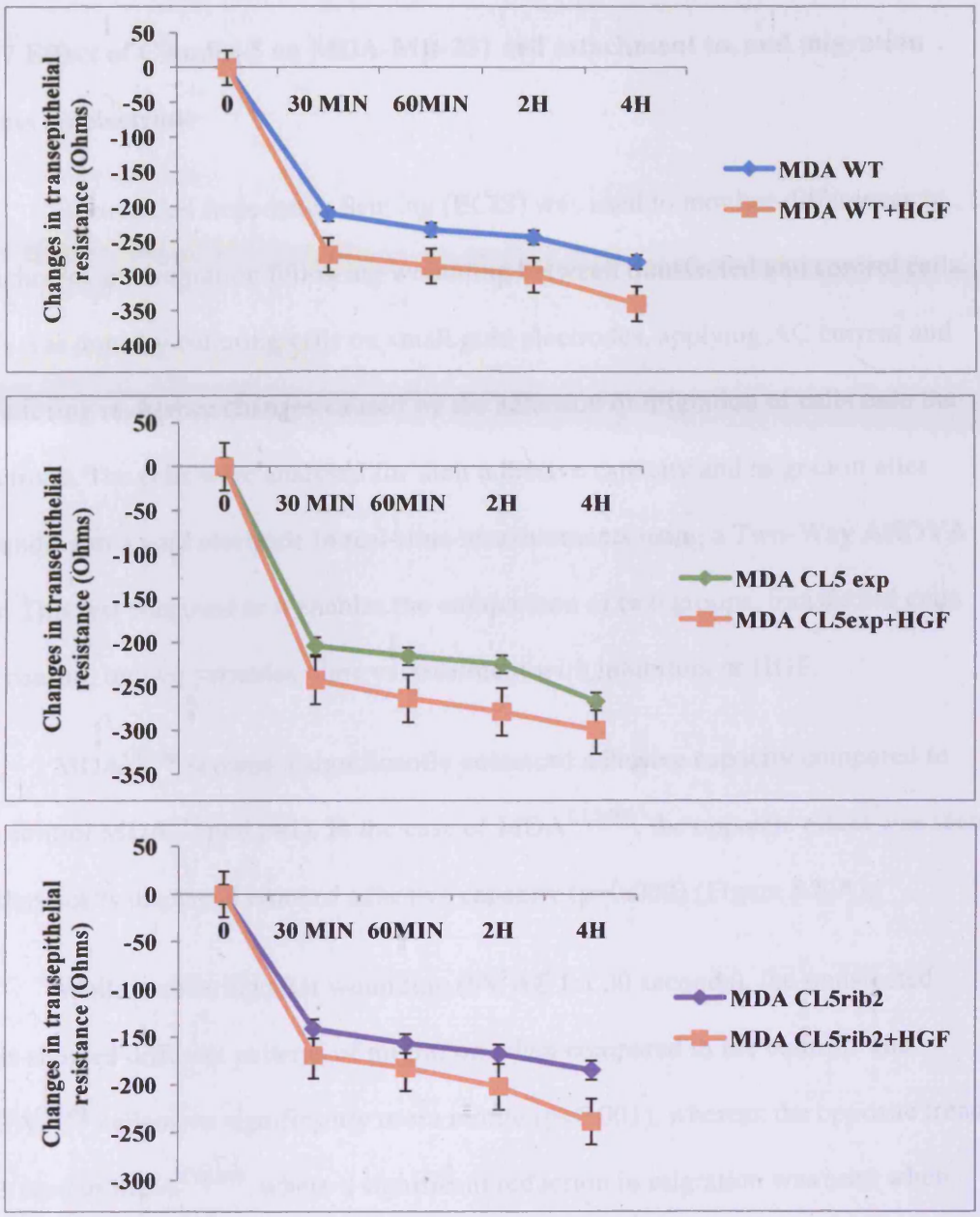

Figure 5.7: Effect of Claudin-5 on transepithelial resistance of MDA-MB-231 cells after treatment with HGF. Significant changes were seen on transfected and control cells over a period of 4 hours when compared to the untreated cells ($p<0.05$) (mean ±SD, n=3).

5.3.7 Effect of Claudin-5 on MDA-MB-231 cell attachment to, and migration across an electrode

Electric Cell Impedance Sensing (ECIS) was used to monitor differences in attachment and migration following wounding between transfected and control cells. This was done by culturing cells on small gold electrodes, applying AC current and monitoring resistance changes caused by the adhesion or migration of cells onto the electrode. The cells were analysed for their adhesive capacity and migration after wounding to a gold electrode in real-time measurements using a Two-Way ANOVA test. This test was used as it enables the comparison of two groups, transfected cells vs. control, on two variables, time vs. treatment with inhibitors or HGF.

MDA^{Cl5exp} showed a significantly enhanced adhesive capacity compared to the control MDA^{wt} ($p=0.041$). In the case of $MDA^{CL5rib2}$, the opposite effect was seen, as these cells displayed reduced adhesive capacity ($p=0.002$) (Figure 5.8 A).

While recovering after wounding (5V AC for 30 seconds), the transfected cells showed different patterns of migration when compared to the control. The MDA^{Cl5exp} cells were significantly more motile ($p<0.001$), whereas the opposite trend was seen in $MDA^{CL5rib2}$, where a significant reduction in migration was seen when compared to MDA^{WT} $p<0.001$) (Figure 5.8 B).

A

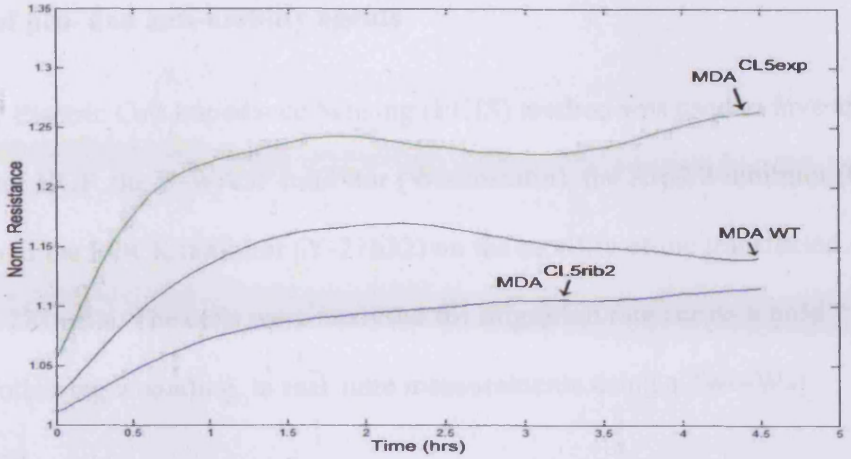

B

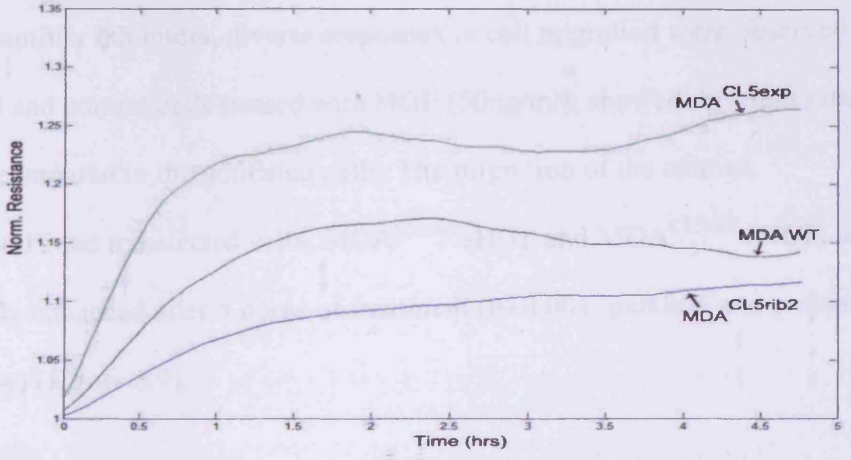

Figure 5.8: (A) Effect of Claudin-5 on the adhesion of MDA-MB-231 cells using ECIS. Significant differences were seen in transfected cells when compared to the control. MDA^{Cl5exp} showed a significantly enhanced adhesive capacity ($p=0.041$), however in $MDA^{CL5rib2}$ cells adhesion was significantly decreased ($p=0.002$). (B) Significant differences were seen after wounding, MDA^{Cl5exp} displayed increased migration, whereas the opposite effect was seen in $MDA^{CL5rib2}$ ($p<0.001$, $n=3$).

5.3.8 Effect of Claudin-5 on MDA-MB-231 cell migration over an electrode and the effect of pro- and anti-motility agents

The Electric Cell Impedance Sensing (ECIS) method was used to investigate the impact of HGF, the N-WASP inhibitor (Wiskostatin), the Arp2/3 inhibitor (CK-0944636) and the ROCK inhibitor (Y-27632) on the motility of the transfected MDA-MB-231 cells. The cells were analysed for migration rate across a gold electrode following wounding, in real-time measurements using a Two-Way ANOVA test.

Following electrical wounding (5V AC for 30 seconds) and treatment with HGF and motility inhibitors, diverse responses in cell migration were observed. The transfected and control cells treated with HGF (50ng/ml), showed different rates of migration compared to the untreated cells. The migration of the control, MDA^{wt}+HGF, and transfected cells, MDA^{Cl5exp}+HGF and $MDA^{CL5rib2}$+HGF, was significantly enhanced after 5 hours of treatment ($p<0.001$, $p<0.001$ and $p=0.003$ respectively) (Figure 5.9).

When cells were treated with the N-WASP inhibitor (50μM), the migration rate of MDA^{wt}+N-WASP, MDA^{Cl5exp}+ N-WASP and $MDA^{CL5rib2}$+ N-WASP was markedly reduced after 5 hours of treatment when compared to untreated cells ($p<0.001$, $p=0.006$ and $p=0.018$ respectively) (Figure 5.10).

Treatment of cells with the Arp2/3 inhibitor (10nM) adversely affected the motility of the MDA^{wt}+Arp2/3 and the transfected cells, MDA^{Cl5exp}+ Arp2/3, when compared to untreated cells after wounding ($p<0.001$ respectively). Surprisingly,

$MDA^{CL5rib2}$+ Arp2/3 did not show a significant reduction in migration after treatment ($p=0.06$) (Figure 5.11).

The ROCK inhibitor (50nM) was capable of altering the motility of MDA^{wt}+ROCK when compared to the untreated cells ($p<0.001$). However, no significant differences were found in the transfected cells, MDA^{Cl5exp}+ ROCK MDA^{Cl5exp}+ ROCK, when compared to the untreated cells ($p=0.403$ and $p=0.072$ respectively) (Figure 5.12).

All the results are summarized in Table 5.1.

5.3.9 Effect of Claudin-5 on protein levels of N-WASP and ROCK1 and their interaction

MDA^{wt}, MDA^{Cl5exp} and $MDA^{CL5rib2}$ Western blotting demonstrated very low levels of the N-WASP at protein level. Protein levels of ROCK 1 revealed similar high levels in the transfected and control cells (Figure 5.13 A).

Immunoprecipitation of Claudin-5 followed by immunoblotting with N-WASP and ROCK 1 showed a protein-protein interaction between Claudin-5 and these motility-related proteins in MDA^{wt} and MDA^{Cl5exp} (Figure 5.13 B). In keeping with this, immunoprecipitation with either N-WASP (Figure 5.13 C) or ROCK1 (Figure 5.13 D) followed by immunoblotting with Claudin-5 produced consistent results.

5.3.10 Effect of Claudin-5 on MDA-MB-231 breast cancer cell tumour growth *in vivo*

The growth and capability of developing tumours of MDA^{Cl5exp} in an *in vivo* model was examined and compared to the control MDA^{pef6} cells after subcutaneous injection into the athymic nude mouse model. Over the period of 33 days, no significant difference was observed between the two groups, the control (injected with MDA^{pef6}) and those injected with MDA^{Cl5exp} ($p=0.291$) (Figure 5.14).

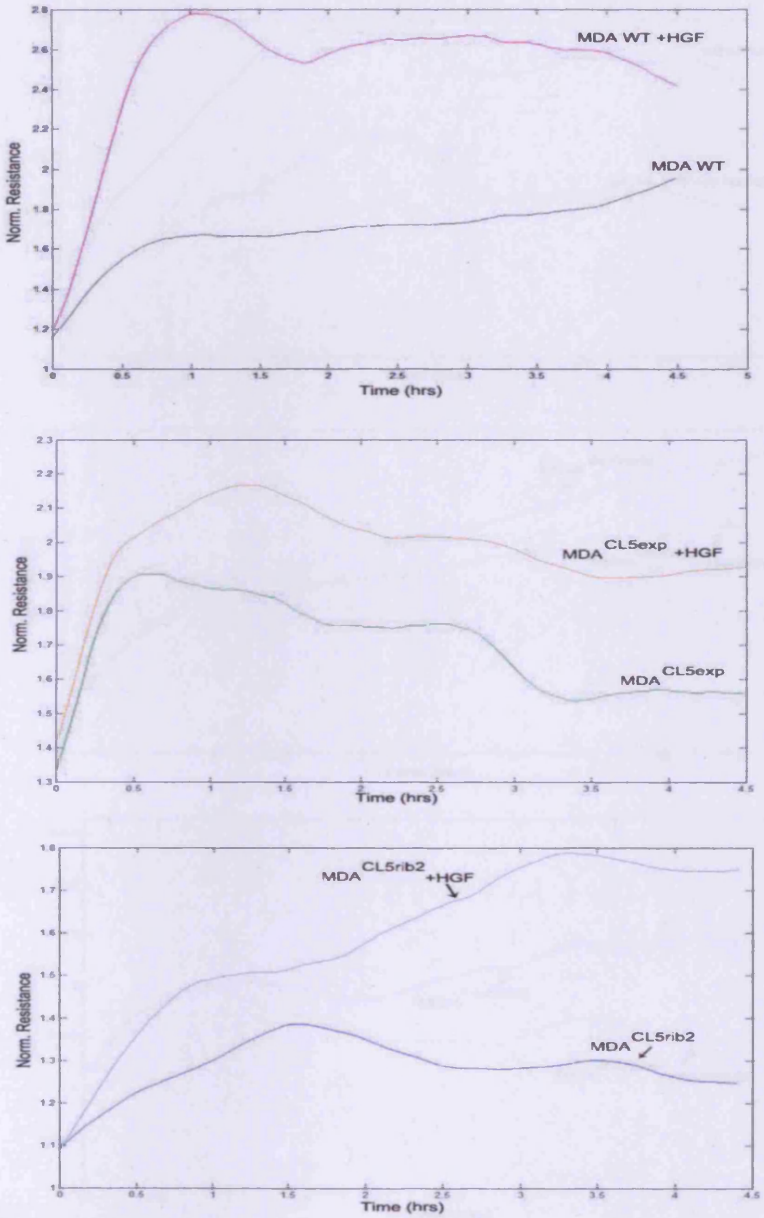

Figure 5.9: Effect of Claudin-5 on MDA-MB-231 cell migration following treatment with HGF using ECIS. Migration was significantly increased in MDA^{wt}+HGF, MDA^{Cl5exp}+HGF and $MDA^{CL5rib2}$+HGF when compared to untreated cells ($p<0.001$, $p<0.001$ and $p=0.003$ respectively, $n=3$).

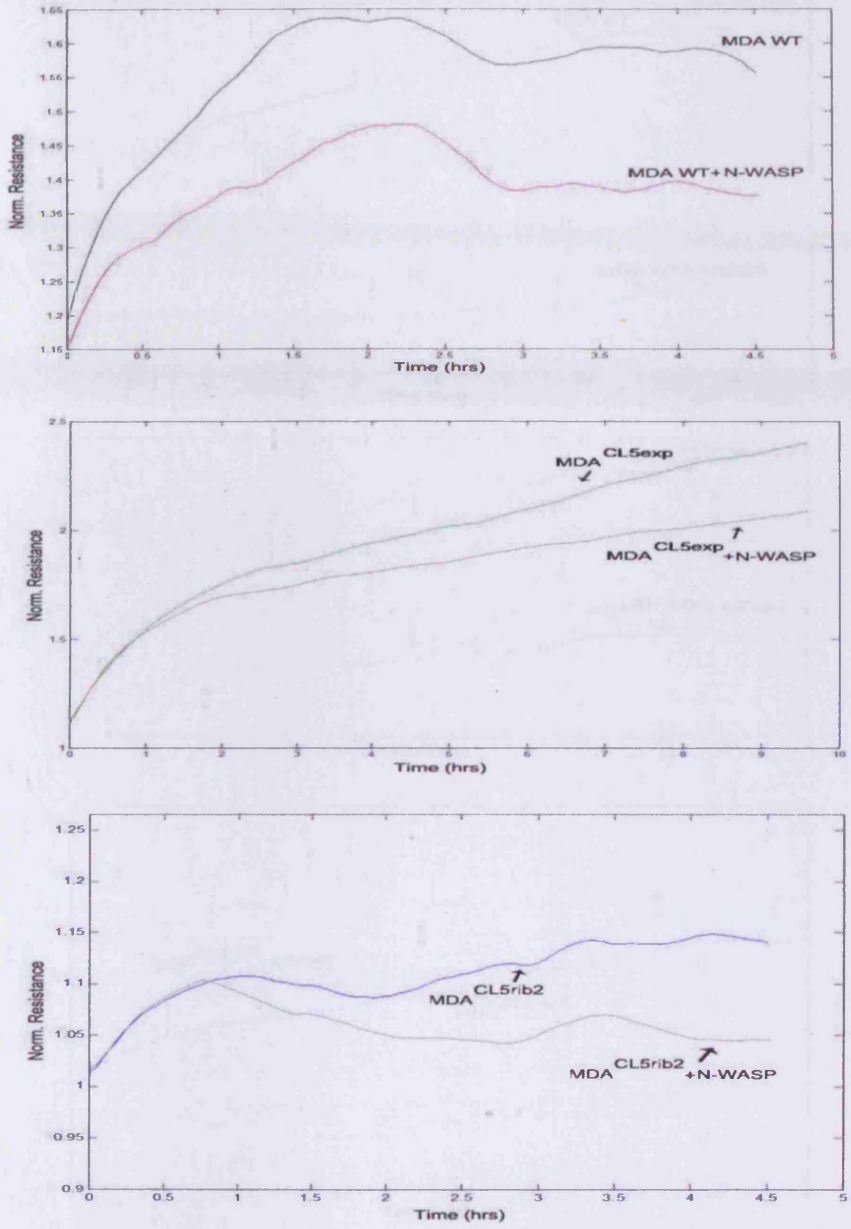

Figure 5.10: Effect of Claudin-5 on MDA-MB-231 cell migration following treatment with N-WASP inhibitor using ECIS. Migration was significantly decreased in MDA^{wt}+ N-WASP inhibitor, MDA^{Cl5exp}+ N-WASP inhibitor and $MDA^{CL5rib2}$+ N-WASP inhibitor when compared to untreated cells ($p<0.001$, $p=0.006$ and $p=0.018$ respectively, $n=3$).

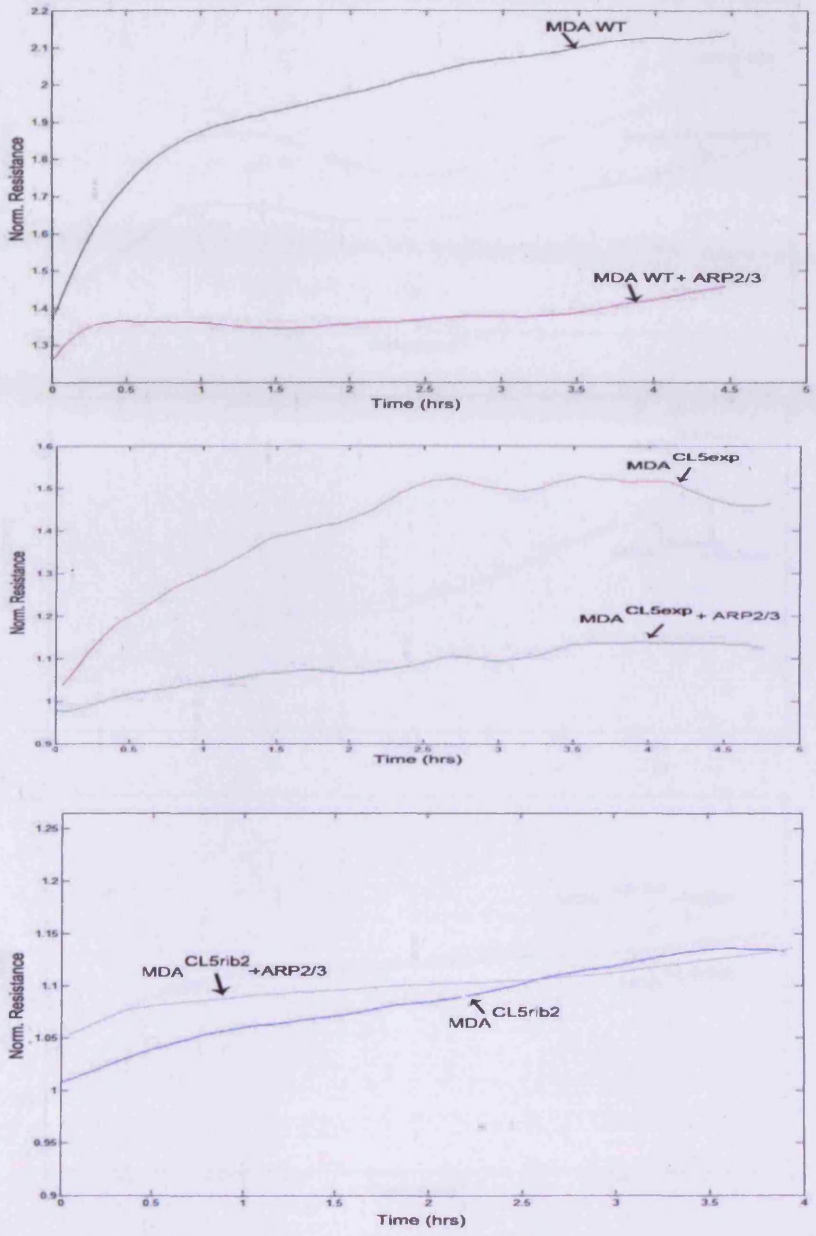

Figure 5.11: Effect of Claudin-5 on MDA-MB-231 cell migration following treatment with Arp2/3 inhibitor using ECIS. Migration was significantly decreased in MDA^{wt}+Arp2/3 inhibitor and MDA^{Cl5exp}+Arp2/3 inhibitor ($p<0.001$ respectively). $MDA^{CL5rib2}$+Arp2/3 inhibitor did not show significant differences when compared to untreated cells ($p=0.06$, $n=3$).

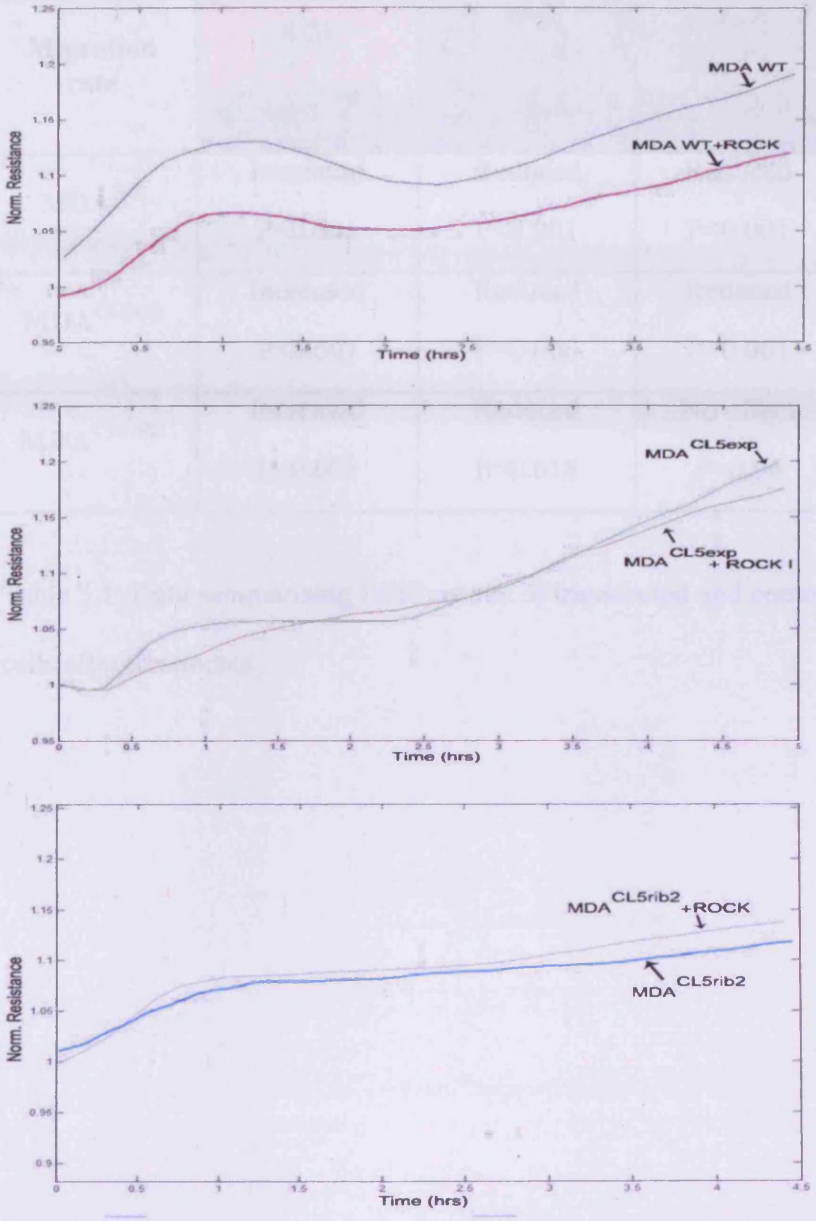

Figure 5.12: Effect of Claudin-5 on MDA-MB-231 cell migration following treatment with ROCK inhibitor using ECIS. Migration was significantly decreased in MDA^{wt}+ ROCK inhibitor ($p<0.001$). MDA^{Cl5exp}+ ROCK inhibitor and $MDA^{CL5rib2}$+ ROCK inhibitor did not show significant differences when compared to untreated cells ($p=0.403$ and $p=0.072$ respectively, $n=3$).

Migration rate	HGF	N-WASP inhibitor	Arp2/3 inhibitor	ROCK inhibitor
	vs. untreated	vs. untreated	vs. untreated	vs. untreated
MDA^{WT}	Increased P<0.001	Reduced P<0.001	Reduced P<0.001	Reduced P<0.001
MDA^{CL5exp}	Increased P<0.001	Reduced P=0.006	Reduced P<0.001	No effect P=0.403
$MDA^{CL5rib2}$	Increased P=0.003	Reduced P=0.018	No effect P=0.06	No effect P=0.072

Table 5.1: Data summarising ECIS results of transfected and control MDA-MB-231 cells after treatments.

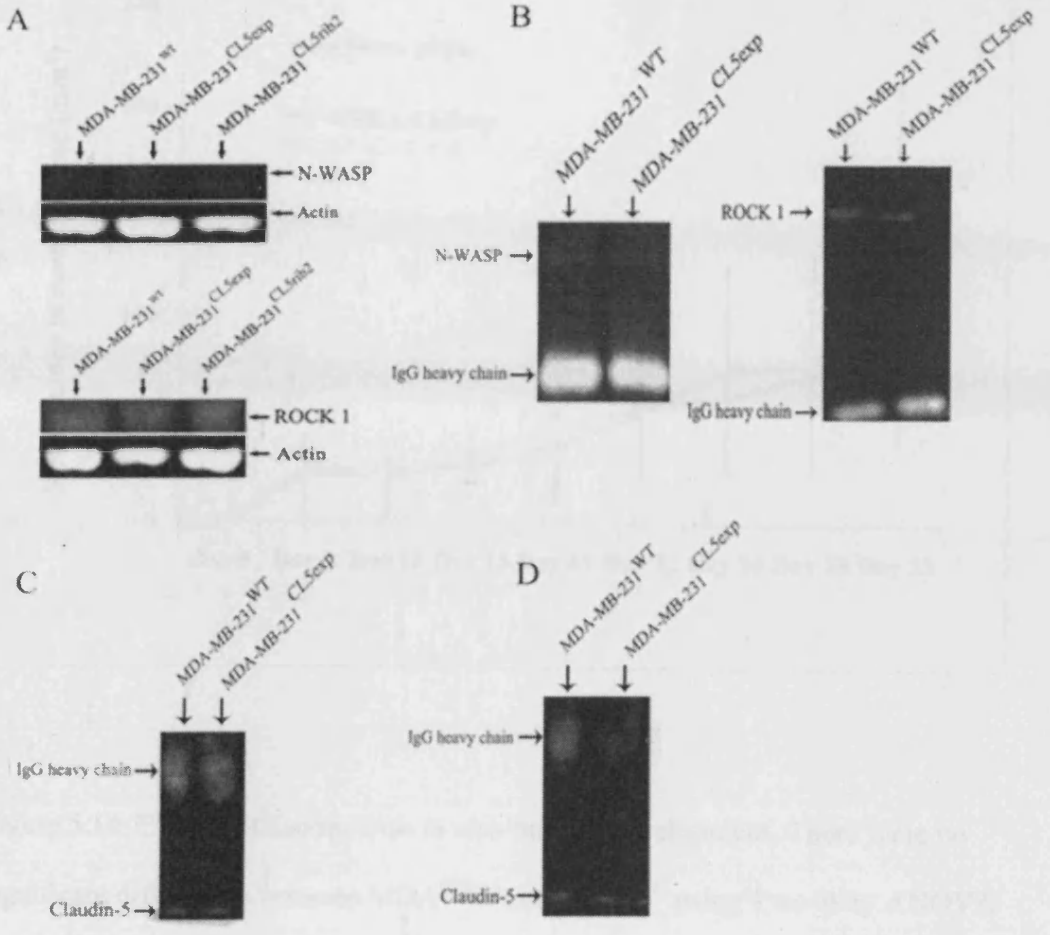

Figure 5.13: (A) Expression of N-WASP and ROCK 1 in transfected and control cells. (B) Co-immunoprecipitation of Claudin-5 with N-WASP and ROCK 1. (C) Co-immunoprecipitation of N-WASP with Claudin-5. (D) Co-immunoprecipitation of ROCK 1 with Claudin-5.

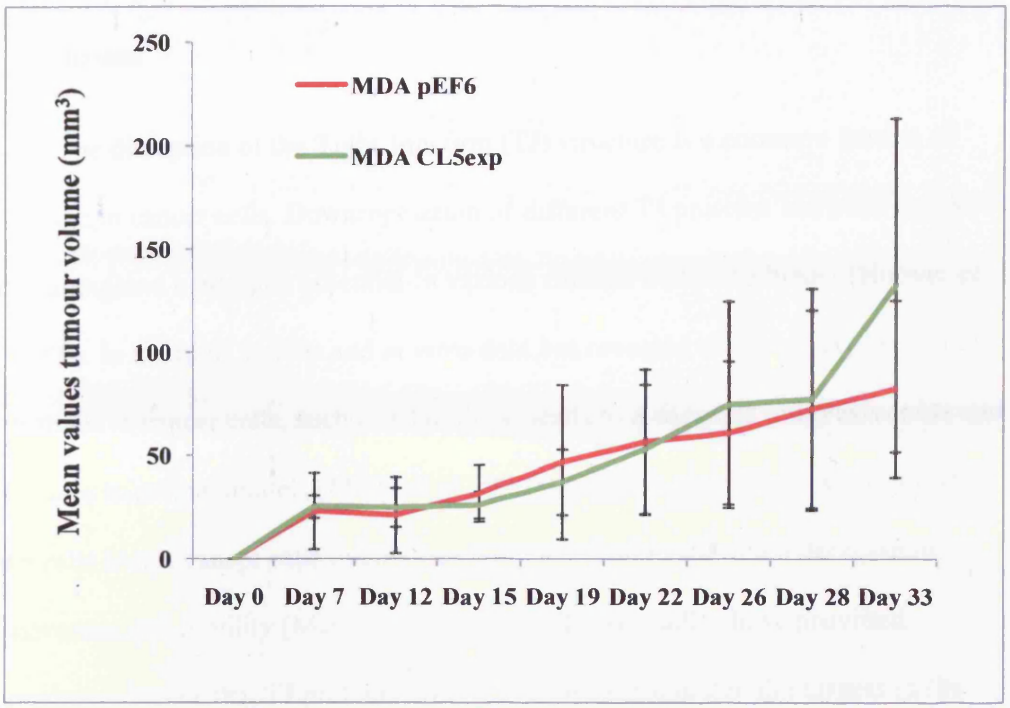

Figure 5.14: Effect of Claudin-5 on *in vivo* tumour development. There were no significant differences between MDA^{Cl5exp} and MDA^{pef6} using Two-Way ANOVA test ($p=0.29$), indicating that Claudin-5 has no direct effect on tumour development.

5.4 Discussion

The disruption of the Tight Junction (TJ) structure is a common feature of many human cancer cells. Downregulation of different TJ proteins has been linked with staging and metastatic potential in various cancers including breast (Hoover *et al.*, 1998). In addition, *in vivo* and *in vitro* data has revealed that over-expression of TJ proteins in cancer cells, such as Claudin-4, leads to a decrease in invasiveness and metastases in animal models (Michl *et al.*, 2003). Similar conclusions were found when cells breast cancer cells overexpressing Claudin-16, showed a decrease in invasiveness and motility (Martin *et al.*, 2008a). These studies have provided promising evidence that TJ proteins might serve as useful molecular targets in the prognosis of cancer. In this study, we used cells transfected with Claudin-5 expression sequence and ribozyme transgenes to assess the impact of reducing the expression of our protein of interest as well as enhancing it in order to evaluate changes in the aggressive nature of MDA-MB-231 cells. The other purpose of the study was to establish a possible link between Claudin-5 and motility of the cells. This was done as the initial results suggested that Claudin-5 might play a role in cell motility, not just functioning as a simple sealing protein in the TJ structure.

Initially, we questioned the role of Claudin-5 when transepithelial electric resistance (TER) was measured. Transepithelial electric resistance (TER) is the easiest and most sensitive measure of barrier strength. $MDA^{CL5rib2}$ showed the highest resistance, whereas the resistance of MDA^{Cl5exp} and the control were lower and followed the same trend, although MDA^{Cl5exp} was significantly higher than control cells. These preliminary results revealed that Claudin-5 was not playing a real

role in keeping the cell barrier tight. In fact, the compensation of the lack of Claudin-5 could be balanced with one of the other 23 members of the Claudin family which might alter the barrier strength, therefore explaining why the knockdown cells displayed higher transepithelial resistance. The same explanation could be applied to forced-expression and the very similar trends that it shared with the control cells.

The involvement of Claudin-5 in cell growth was tested, although there appeared not to be an involvement of Claudin-5 in cell growth. Cell adhesion to extracellular matrix is fundamental in the organization of the epithelium as a continuous layer but also in the regulation of many cellular processes such as motility (Chlenski *et al.*, 1999). $MDA^{CL5rib2}$ demonstrated a decrease in adhesion whereas MDA^{Cl5exp} appeared to increase adhesion when compared to the control cells, although these results did not reach significance. Integrins are described as being the "eyes" of cancer cells in identifying their surrounding extracellular matrix (ECM), and they participate in the maintenance of positional stability in normal epithelia; in breast cancer however, different studies have linked integrins with metastasis (Felding-Habermann *et al.*, 2001). The question therefore arises as to whether the absence of Claudin-5 in a cell alters levels of integrins and other adhesion-related proteins, thus changing the adhesion of the cancer cell when compared to the control. The results obtained when the ability to adhere to a gold electrode trough ECIS technology was measured in real time agreed with the *in vitro* function assay. Once again, Claudin-5 knockdown appears to have the lowest adherence (as in the Matrigel experiments) to the gold electrode. The invasiveness of the cells through the ECM did not show any relevant differences between cells over-expressing or

knocking-down levels of Claudin-5. This result agrees with the data obtained in the *in vivo* experiments, where the MDA^{Cl5exp} cells were analysed for their ability to grow and develop in nude mice. Over a period of one month, no differences were found between the two groups of animals, the control (injected with MDA^{pef6}) and those injected with MDA^{Cl5exp}.

Taking these results together, we began to speculate whether Claudin-5 might be involved in cell motility. We performed a further set of experiments to assess the level of involvement of Claudin-5 in breast cancer motility. As breast cancer cells acquire a motile phenotype, this is translated into changes in highly dynamic structures like actin filaments and cytoplasmic microtubular complex (Insall and Jones, 2006). We decided to investigate the effects on motility of over-expression or knockdown of Claudin-5. To achieve this, an *in vitro* motility assay and a traditional wound healing assay was carried out, both revealing that $MDA^{CL5rib2}$ showed a reduction in motility. Moreover, ECIS was used in order to measure in real time how fast cells migrate after wounding. Similar results were obtained; $MDA^{CL5rib2}$ was indeed slower when compared to the control. However, MDA^{Cl5exp} cells were the fastest in each of the assays mentioned above and their capability to adhere to the electrode was increased, agreeing with the preliminary results obtained when the *in vitro* adhesion assay was performed.

Until now, we have shown that knockdown of Claudin-5 expression in a breast cancer cell line resulted in a less adhesive and less motile cell phenotype when compared to controls. The opposite was seen when Claudin-5 expression was forced, resulting in a more adhesive and more motile phenotype but with no differences in

invasiveness *in vivo* and *in vitro*. We might tentatively conclude from this that Claudin-5 might be a motility regulator, or at least have a role in the motility of these human breast cancer cells.

The Metastasis and Angiogenesis Research Group has carried out a significant body of work on the role and effect of HGF in epithelial cancer cells. HGF is a powerful motogen able to promote proliferation, invasion, and migration of epithelial cells by binding to its tyrosine kinase receptor c-met (Jiang *et al.*, 2005) as well as modulating expression and function of TJ molecules in human breast cancer cell lines and decreasing trans-epithelial resistance (Martin *et al.*, 2004a). Cells displaying enhanced or suppressed expression of Claudin-5 respond in keeping with the well established effect after treatment with HGF, showing reduced epithelial resistance and increased motility. ECIS experiments corroborated these results.

To address the possibility that Claudin-5 might play a role in regulating cell motility, different motility-regulators were studied in order to search for any possible links between Claudin-5 and a range of motility-related proteins. Cell motility was analysed using ECIS after being treated with different motility inhibitors. In particular the N-WASP inhibitor (Wiskostatin), the Arp2/3 inhibitor (CK-0944636) and the ROCK inhibitor (Y-27632) responded in an unexpected way in our transfected cells. Neuronal Wiskott - Aldrich syndrome protein, N-WASP, is ubiquitously expressed in mammalian tissues and it is responsible for connecting several signalling pathways to the initiation of actin assembly via the Arp2/3 complex. N-WASP has been reported to exist in a self-folded auto-inhibited conformation. When activated, conformational changes occur facilitating the

interaction with the Arp2/3 complex and subsequent nucleation. In other words, the Arp2/3 complex acts as a pattern for the elongation of the actin microfilaments (Dovas and Cox, 2010). The Rho-associated serine-threonine protein kinase, ROCK, is ubiquitously expressed in mammalian tissues and it is directly linked, after activation, with numerous processes related to actin-myosin, such as actin cytoskeletal reorganisation and the formation of focal adhesions. It also has an important role in cell migration by promoting the contraction of the cell body and is required for tail retraction in cancer cells (Lane *et al.*, 2008). The transfected and control cells were treated with the N-WASP inhibitor, responsible for stabilising the auto-inhibited conformation of the N-WASP protein (Guerriero and Weisz, 2007), and their rate of speed was measured using ECIS after wounding. Results showed an inhibition in their motility, however, this inhibition was marginally reduced in knockdown cells. The Arp2/3 inhibitor, responsible for blocking the active conformation of the complex (Nolen *et al.*, 2009), was able to inhibit cell motility in the control cells and in cells over-expressing Claudin-5. However, to our surprise, Arp2/3 was no longer able to inhibit motility in the knockdown cells. The effect of the ROCK inhibitor (Y-27632) was also studied in our cells. The inhibitor specificity is, however, questioned as *in vitro* studies revealed that it not only exerts an inhibitory effect on ROCK proteins but on other kinases also (Grise *et al.*, 2009). Nevertheless, the control cells responded to its inhibition showing a lower rate of migration; conversely both transfected cells did not respond to its inhibitory effects. Thus far we have shown that the absence of Claudin-5 clearly caused an alteration in cell motility as the Arp2/3 and ROCK inhibitors were no longer inhibiting cell motility in $MDA^{CL5rib2}$. Additionally, in the case of $MDA^{CL5rib2}$ cells treated with N-

WASP inhibitor, we observed some inhibition, but at a considerably reduced manner compared to N-WASP inhibitor in control and MDA^{Cl5exp} cells.

The next question to be addressed following the ECIS results, was to investigate any possible protein-protein interaction between Claudin-5 and N-WASP or Claudin-5 and ROCK 1 as well as whether any direct effect was occurring at the protein level of these molecules in the control and transfected cells. Co-immunoprecipitation with Claudin-5, followed by immunoblotting with either N-WASP or ROCK 1 demonstrated an interaction between Claduin-5 and N-WASP as well as with ROCK 1. To confirm these interactions, a co-immunoprecipitation with either N-WASP or ROCK 1 followed by immunoblotting with Claudin-5 was carried out confirming the interactions between these protein pairs. Previously, studies have already linked TJ with N-WASP and the Arp2/3 complex. The intestinal epithelial cells, T84, when treated with N-WASP inhibitor showed an inhibition in the formation of TJ (Ivanov *et al.*, 2005). A more recent study using Sertoli cells linked the inhibition of N-WASP, and therefore the inhibition of Arp2/3, in the nucleation process with barrier disruption in the blood-testis barrier causing a failure of spermatic transit (Lie *et al.*, 2010). N-WASP protein in MDA-MB-231 cells has been reported to be expressed at a very low level (Martin *et al.*, 2008b). The results obtained in the current study agree. The levels of ROCK 1 did not show any real differences among transfected and control cells, this possibly could be due to the high level of this protein found in MDA-MB-231 wild type cells as already reported (Lane *et al.*, 2008).

This study suggests that Claudin-5 might be involved in cancer cell motility; in particular, it appears to be involved in the signal pathway of N-WASP and ROCK. However, understanding cell motility requires detailed knowledge not only of the signalling networks, but also about their dynamics. Unfortunately, some of the signalling pathways are only just starting to be analysed and we clearly still have a great deal to learn about cell motility, particular in cancer cells. This possible new role of Claudin-5 in breast cancer cell motility opens the door to future studies in which Claudin-5 and therefore TJ might switch from static structures to very dynamic ones, and offers an exciting glimpse into how modulation of transmembrane TJ proteins could be targeted in cancer metastasis.

Chapter 6

Effect of Claudin-5 expression on HECV human endothelial cells

6.1 Introduction

Epithelial and endothelial cell monolayers form barriers that seal the intercellular space between neighbouring cells and transform the layer of individual cells into an effective permeability barrier. Tight Junctions (TJs) are highly regulated areas of adhesion between epithelial and endothelial cells. A key step in metastasis is the interaction and penetration of the vascular endothelium by dissociated cancer cells. Tumour cells have to invade the surrounding tissues, reach the endothelial barrier and penetrate the barrier to escape and enter the bloodstream. Therefore, TJ, as the first barrier that cancer cells must overcome in order to metastasise, have emerged as an essential structure in the prevention of cancer metastasis.

Claudins are members of the network of proteins that constitute the TJ structure. The primary role of Claudins is in the regulation of paracellular selectively to small ions through the pores that they themselves are capable of forming (Tsukita and Furuse, 2000). However, recent results have challenged the idea that Claudins function only as sealing proteins. Claudins have now been shown to be involved in cellular growth and in epithelial-mesenchymal transition (EMT) (Ohkubo and Ozawa, 2004). These results suggest that Claudins play multiple roles beyond acting as a "doorman" in the paracellular barrier opening a new avenue of research.

The present study used the HECV endothelial cell line and, following forced expression and knockdown of Claudin-5, examined the cellular biological functions in response to Hepatocyte Growth Factor (HGF) in order to clarify the role of

Claudin-5 and to investigate a possible link with motility-related proteins in endothelial cells.

6.2 Materials and methods

6.2.1 Cell line

The HECV endothelial cell line was used in this study to investigate the effect of Claudin-5 in transfected cell lines $HECV^{Cl5exp}$ and $HECV^{CL5rib2}$, including $HECV^{wt}$ and $HECV^{pef6}$. Cells were continuously maintained in DMEM-F12 media as described in section 2.2.

6.2.2 *In vitro* cell growth assay

The cells were seeded into four 96 well plates and incubated for a broad range of hours as described in section 2.6.1. Absorbance was measured in order to determine cell number.

6.2.3 *In vitro* cell Matrigel adhesion assay

The cells were seeded into a 96 well plate containing a layer of Matrigel as described in section 2.6.3. The number of cells adhered to the artificial basement membrane was counted.

6.2.4 *In vitro* tubule formation assay and the effect of pro- and anti-motility agents

The cells were seeded into a 96 well plate containing a layer of Matrigel. After incubation another layer of Matrigel was added on top as described in section

2.6.7. The tubule perimeter was measured. The same protocol was followed when cells were treated with HGF and motility-related inhibitors.

6.2.5 *In vitro* cell motility assay using Cytodex-2 beads and the effect of HGF

The cells were incubated with Cytodex-2 beads as described in section 2.6.4. The number of cells that were carried by the beads and moved from the beads to the base of the well was counted. The same protocol was followed when cells were treated with HGF.

6.2.6 *In vitro* cell migration (wound healing) assay

The migration of HECV cells across a wounded surface of a confluent monolayer formed by the same cell line was examined as described in section 2.6.5.

6.2.7 Transendothelial resistance and the effect of HGF

The cells were seeded into transparent inserts and the resistance across the layer was measured as described in section 2.7.1. The same protocol was followed when cells were treated with HGF.

6.2.8 ECIS

The cells were seeded into electrical arrays allowing the cells to adhere to the gold electrodes within the array as described in section 2.7.2 causing a change in resistance followed by electrical wounding of the formed monolayer. The same protocol was followed when cells were treated with HGF and motility-related inhibitors.

6.2.9 Analysis of protein levels of N-WASP and ROCK 1 using Western blotting. Claudin-5 co-immunoprecipitation for N-WASP and ROCK 1

Western Blotting was used to see levels of expression of N-WASP and ROCK 1 as described in section 2.5. Claudin-5 co-immunoprecipitation was carried out using cell lysates of $HECV^{wt}$ and $HECV^{Cl5exp}$ and probed with antibodies against N-WASP and ROCK 1 as described in section 2.5.1.6. N-WASP and ROCK 1 co-immunoprecipitation was carried out as described above and probed with antibodies against Claudin-5.

6.2.9 *In vivo* tumour growth and development

The impact of Claudin-5 on tumour growth was assessed in an *in vivo* system as described in section 2.6.8., where a broad number of factors may influence the effects of over-expression of Claudin-5 in this particular development model. In this model, breast cancer cells were co-injected with endothelial cells that had a different Claudin-5 expression profile, in order to assess the contribution of claudin-5 in endothelial cell to the growth of breast tumours.

6.3 Results

6.3.1 Effect of altering Claudin-5 expression on HECV cell growth

The effect of suppressing and over-expressing Claudin-5 expression on the growth of the HECV endothelial cell line was examined following 1,3 and 4 day incubation periods using an *in vitro* cell growth assay (Figure 6.1). No significant

differences in cell growth rate between $HECV^{wt}$, $HECV^{pef6}$ and $HECV^{Cl5exp}$ or $HECV^{CL5rib2}$ were seen in any of the incubation periods. However, the growth rate of $HECV^{Cl5exp}$ was reduced in each of the measurements when compared to $HECV^{wt}$ and $HECV^{pef6}$; day 1 $HECV^{wt}$ (52%±38.15), $HECV^{pef6}$ (57.01%±8.96) and $HECV^{Cl5exp}$ (26.65%±21.30), (p=0.29 and p=0.069 respectively); day 3 $HECV^{wt}$ (497.19%±68.86), $HECV^{pef6}$ (487.41%±31.35) and $HECV^{Cl5exp}$ (459.90%±84.77), (p=0.52 and p=0.06 respectively); day 4 $HECV^{wt}$ (705.85%±96.32), $HECV^{pef6}$(735.95%±57.84) and $HECV^{Cl5exp}$ (702.72%±142.90), (p=0.97 and p=0.69 respectively). The opposite effect was observed in the incubation period day 3 and day 4 of $HECV^{CL5rib2}$ where the cell growth was increased when compared to the controls; day 3 $HECV^{wt}$ (497.19%±68.86), $HECV^{pef6}$ (487.41%±31.35) and $HECV^{CL5rib2}$ (567.52%±36.55), (p=0.12 and p=0.44 respectively); day 4 $HECV^{wt}$ (705.85%±96.32), $HECV^{pef6}$ (735.95%±57.84) and $HECV^{CL5rib2}$ (736.62.72%±36.92), (p=0.68 and p=0.98 respectively).

6.3.2 Effect of Claudin-5 on HECV cell adhesion

The adhesive capacity of $HECV^{Cl5exp}$ and $HECV^{CL5rib2}$ cells to adhere to matrix was analysed in an *in vitro* Matrigel adhesion assay (Figure 6.2). There was a significant difference between the adherence of $HECV^{Cl5exp}$ and $HECV^{wt}$ and $HECV^{pef6}$ with $HECV^{Cl5exp}$ cells being less adherent to matrix ($HECV^{wt}$ (87.68±7.09), $HECV^{pef6}$(80.2±15.99) and $HECV^{Cl5exp}$ (19.66±3.33), ($p<0.001$ for both controls). In the case of $HECV^{CL5rib2}$, no significant differences were found when compared to the controls ($HECV^{wt}$ (87.68±7.09), $HECV^{pef6}$ (80.2±15.99) and $HECV^{CL5rib2}$ (88.94±13.50), (p=0.743 and p=0.087 respectively).

6.3.3 Effect of Claudin-5 on HECV cell tubule formation

The angiogenic potential of the untreated cells $HECV^{wt}$, $HECV^{pef6}$ $HECV^{Cl5exp}$ and $HECV^{CL5rib2}$ alongside cells treated with the pro-motility and angiogenic factor HGF and motility inhibitors (against N-WASP, ROCK and Arp 2/3) and a combination of both agents was assessed using an *in vitro* Matrigel tubule formation assay. Untreated HECV cells formed tubule structures (Figure 6.3); however significant differences were found in the transfected cells when compared with controls. $HECV^{Cl5exp}$ demonstrated a significant decrease in tubules when compared to $HECV^{wt}$ and $HECV^{pef6}$ ($HECV^{wt}$ (4050.03±220.67), $HECV^{pef6}$ (4102.978±585.82) and $HECV^{Cl5exp}$ (654±686.13), ($p<0.001$for both controls). The opposite effect was observed in $HECV^{CL5rib2}$ where a significant increase in tubules was seen when compared to $HECV^{wt}$ and $HECV^{pef6}$ ($HECV^{wt}$ (4050.03±220.67), $HECV^{pef6}$ (4102.978±585.82) and $HECV^{CL5rib2}$ (5749.93±873.24), $p<0.001$ for both controls).

Treatment with HGF (50ng/ml) positively affected the capability of these cell lines to form tubules (Figure 6.4). Following quantification of tubule perimeter, a significant increase in tubules was observed in comparison to untreated control. Control cells displayed a significant increase in tubules when compared to untreated cells, $HECV^{wt}$+HGF ($HECV^{wt}$ (3911.60±457.09) and $HECV^{wt}$+HGF (6252.46±373.39), $HECV^{pef6}$+HGF ($HECV^{pef6}$ (4224.74±375.06) and $HECV^{pef6}$+HGF (5616.23±990.80) ($p<0.001$ for both controls). $HECV^{Cl5exp}$ demonstrated a significant increase in tubules when compared to $HECV^{Cl5exp}$+HGF ($HECV^{Cl5exp}$ (344±751.07) and $HECV^{Cl5exp}$+HGF (664.26±240.58), ($p<0.005$). A

similar response to HGF was observed in $HECV^{CL5rib2}$, where significant differences were found when compared to $HECV^{CL5rib2}$+HGF ($HECV^{CL5rib2}$ (5690.70±383.33) and $HECV^{CL5rib2}$+HGF (7556±244.09), ($p<0.001$).

Following treatment with motility inhibitors, diverse responses were observed in these cells. When cells were treated with the N-WASP inhibitor (50μM) (Figure 6.5), control cells displayed a significant decrease in tubules when compared to untreated cells, $HECV^{wt}$+N-WASP ($HECV^{wt}$ (3911.60±457.09) and $HECV^{wt}$+N-WASP (3034.54±197.42), $HECV^{pef6}$+N-WASP ($HECV^{pef6}$ (4224.74±375.06) and $HECV^{pef6}$+N-WASP (3140.45±69.58) ($p<0.001$ for both controls). $HECV^{Cl5exp}$ had significantly decreased levels of tubule formation compared with untreated cells ($HECV^{Cl5exp}$ (344.93±383.33) and $HECV^{Cl5exp}$+N-WASP (155.03±69.58), $p=0.045$). However, although $HECV^{CL5rib2}$ demonstrated a reduced number of tubules compared to untreated cells, the data was not statistically significantly different ($HECV^{CL5rib}$ (5690.70±383.32) and $HECV^{CL5rib}$+N-WASP (5347.18±307.06), $p=0.052$). Treatment of these cells with Arp2/3 inhibitor (10nM) adversely affected the capability to form tubule structures in the control cells, $HECV^{wt}$+ Arp2/3 ($HECV^{wt}$ (3911.60±457.09) and $HECV^{wt}$+ Arp2/3 (3108.92±212.12), $HECV^{pef6}$+ Arp2/3 ($HECV^{pef6}$ (4224.74±375.06) and $HECV^{pef6}$+ Arp2/3 (3222.42±193.95) ($p<0.001$ for both controls), and transfected cells $HECV^{Cl5exp}$ and $HECV^{CL5rib}$ (Figure 6.6). However, from the transfected cells only $HECV^{Cl5exp}$ displayed significant differences when compared to untreated cells ($HECV^{Cl5exp}$ (344.93±251.07) and $HECV^{Cl5exp}$+Arp2/3 (95.112±51.41), $p<0.001$). Conversely, $HECV^{CL5rib}$ did not show significant differences when compared to treated cells ($HECV^{CL5rib}$ (5690.70±383.32) and $HECV^{CL5rib}$+Arp2/3 (5396.65±288.53), $p=0.084$). ROCK

inhibitor (50nM) was also capable of altering the ability of these cells to form tubules (Figure 6.7). Similar to the effect of the above mentioned inhibitors, control cells and $HECV^{Cl5exp}$ had significantly decreased tubule formation when compared with untreated cells, $HECV^{wt}$+ ROCK ($HECV^{wt}$ (3911.60±457.09) and $HECV^{wt}$+ ROCK (2754.10±394.93), $HECV^{pef6}$+ ROCK ($HECV^{pef6}$ (4224.74±375.06) and $HECV^{pef6}$+ ROCK (3134.94.42±142.27) ($p<0.001$ for both controls), $HECV^{Cl5exp}$ (344.93±251.07) and $HECV^{Cl5exp}$+ROCK (126.62±82.93), $p<0.05$). In the case of $HECV^{CL5rib2}$ however, although there was a slight reduction in the number of tubules formed, the data was not found to be significant ($HECV^{CL5rib}$ (5690.70±383.32) and $HECV^{CL5rib}$+ROCK (5412.67±289.08), $p=0.133$).

Having established the impact of the motility inhibitors and HGF on these cell lines, we examined the combination of these agents with HGF. Cells treated with a combination of HGF/N-WASP inhibitor showed differences in the number of tubules formed. The control cells treated with HGF/N-WASP inhibitor revealed a decrease in the number of tubules formed when compared with untreated and HGF treated cells ($HECV^{wt}$ (3911.60±457.09), $HECV^{wt}$+HGF (6252.46±323.35) and $HECV^{wt}$+HGF/N-WASP (3909.50±329.10), ($HECV^{wt}$ vs. $HECV^{wt}$+HGF/N-WASP $p=0.68$, and $HECV^{wt}$+HGF vs. $HECV^{wt}$+HGF/N-WASP $p<0.001$); ($HECV^{pef6}$(4224.74±375.06), $HECV^{pef6}$+HGF (5612.23±410.80) and $HECV^{pef6}$+HGF/N-WASP (3839.36±247.41), ($HECV^{pef6}$ vs. $HECV^{pef6}$+HGF/N-WASP $p=0.02$, and $HECV^{pef6}$+HGF vs. $HECV^{pef6}$+HGF/N-WASP $p<0.001$). $HECV^{Cl5exp}$ cells treated with HGF/N-WASP inhibitor also revealed a decrease in the number of tubules formed compared with untreated and HGF treated cells ($HECV^{Cl5exp}$ (344.93±251.07), $HECV^{Cl5exp}$+HGF (664.26±240.58) and

$HECV^{Cl5exp}$+HGF/N-WASP (247.10±93.03), ($HECV^{Cl5exp}$ vs. $HECV^{Cl5exp}$+HGF/N-WASP p=0.28, and $HECV^{Cl5exp}$+HGF vs. $HECV^{Cl5exp}$+HGF/N-WASP p<0.001). $HECV^{CL5rib}$ cells treated with HGF/N-WASP inhibitor showed a small reduction in the number of tubules formed compared with HGF treated cells, however no significant differences were seen. Significant differences were found when comparing untreated $HECV^{CL5rib}$ with $HECV^{CL5rib}$ +HGF/N-WASP ($HECV^{CL5rib}$ (5690.703±383.32), $HECV^{CL5rib}$ +HGF (7556.08±244.09) and $HECV^{CL5rib}$ +HGF/N-WASP (7282.16±312.05), ($HECV^{CL5rib}$ vs. $HECV^{CL5rib}$ +HGF/N-WASP p<0.001, and $HECV^{CL5rib}$ +HGF vs. $HECV^{CL5rib}$ +HGF/N-WASP p=0.054). Control cells, $HECV^{wt}$ and $HECV^{pef6}$, show similar behaviour when treated with HGF+N-WASP. In both cell lines a significant decrease in the number of tubules formed was seen (p<0.001) (Figure 6.8).

Treatment of HECV with a combination of HGF/Arp2/3 inhibitor again revealed differences in the number of tubules formed in the transfected and control cells. The control cells treated with HGF/Arp2/3 inhibitor revealed a decrease in the number of tubules formed when compared untreated and HGF treated cells($HECV^{wt}$ (3911.60±457.09), $HECV^{wt}$+HGF (6252.46±323.35) and $HECV^{wt}$+HGF/Arp2/3 (3387.59±174.18), ($HECV^{wt}$ vs. $HECV^{wt}$+HGF/ Arp2/3 p=0.005, and $HECV^{wt}$+HGF vs. $HECV^{wt}$+HGF/ Arp2/3 p<0.001); ($HECV^{pef6}$ (4224.74±375.06), $HECV^{pef6}$+HGF (5612.23±410.80) and $HECV^{pef6}$+HGF/ Arp2/3 (3589.01±278.02), ($HECV^{pef6}$ vs. $HECV^{pef6}$+HGF/ Arp2/3 p<0.001, and $HECV^{pef6}$+HGF vs. $HECV^{pef6}$+HGF/ Arp2/3 p<0.001).

$HECV^{Cl5exp}$ cells treated with HGF/Arp2/3 inhibitor displayed a decrease in the number of tubules formed compared with untreated and HGF treated cells ($HECV^{Cl5exp}$ (344.93±251.07), $HECV^{Cl5exp}$+HGF (664.26±240.58) and $HECV^{Cl5exp}$+HGF/Arp2/3 (164.03±33.49), ($HECV^{Cl5exp}$ vs. $HECV^{Cl5exp}$+HGF/Arp2/3 $p=0.04$, and $HECV^{Cl5exp}$+HGF vs. $HECV^{Cl5exp}$+HGF/Arp2/3 $p<0.001$). $HECV^{CL5rib}$ cells treated with HGF/Arp2/3 inhibitor showed a small reduction in the number of tubules formed compared with HGF treated cells, however, no significant differences were seen. Nevertheless, significant differences were found when comparing untreated $HECV^{CL5rib}$ with $HECV^{CL5rib}$ +HGF/Arp2/3 ($HECV^{CL5rib}$ (5690.703±383.32), $HECV^{CL5rib}$ +HGF (7556.08±244.09) and $HECV^{CL5rib}$ +HGF/Arp2/3 (7344.40±307.32), ($HECV^{CL5rib}$ vs. $HECV^{CL5rib}$ +HGF/Arp2/3 inhibitor $p<0.001$, and $HECV^{CL5rib}$ +HGF vs. $HECV^{CL5rib}$ +HGF/Arp2/3 $p=0.12$). Control cells ($HECV^{wt}$ and $HECV^{pef6}$) exhibited similar behaviour when treated with HGF+Arp2/3. In both cell lines, a significant decrease in the number of tubules formed was seen ($p<0.001$) (Figure 6.9).

The impact of combining HGF/ROCK inhibitor was examined in the transfected as well as control cells. The control cells treated with HGF/ROCK inhibitor revealed a decrease in the number of tubules formed when compared untreated and HGF treated cells ($HECV^{wt}$ (3911.60±457.09), $HECV^{wt}$+HGF (6252.46±323.35) and $HECV^{wt}$+HGF/ROCK (3505.72±256.78), ($HECV^{wt}$ vs. $HECV^{wt}$+HGF/ ROCK $p=0.03$, and $HECV^{wt}$+HGF vs. $HECV^{wt}$+HGF/ ROCK $p<0.001$); ($HECV^{pef6}$ (4224.74±375.06), $HECV^{pef6}$+HGF (5612.23±410.80) and $HECV^{pef6}$+HGF/ ROCK (3287.79±73.06), ($HECV^{pef6}$ vs. $HECV^{pef6}$+HGF/ ROCK $p<0.001$, and $HECV^{pef6}$+HGF vs. $HECV^{pef6}$+HGF/ ROCK $p<0.001$). $HECV^{Cl5exp}$

cells treated with HGF/ROCK inhibitor data displayed a decrease in the number of tubules formed compared with untreated and HGF treated cells ($HECV^{Cl5exp}$ (344.93±251.07), $HECV^{Cl5exp}$+HGF (664.26±240.58) and $HECV^{Cl5exp}$+HGF/ROCK (218.24±60.21), ($HECV^{Cl5exp}$ vs. $HECV^{Cl5exp}$+HGF/ROCK $p=0.16$, and $HECV^{Cl5exp}$+HGF vs. $HECV^{Cl5exp}$+HGF/ROCK $p<0.001$). $HECV^{CL5rib}$ cells treated with HGF/ROCK inhibitor showed a small increase in the number of tubules formed compared with HGF treated cells, however, no significant differences were seen. Nevertheless, significant differences were found when comparing untreated $HECV^{CL5rib}$ with $HECV^{CL5rib}$ +HGF/ROCK ($HECV^{CL5rib}$ (5690.703±383.32), $HECV^{CL5rib}$ +HGF (7556.08±244.09) and $HECV^{CL5rib}$ +HGF/ROCK (7621.91±266.025), ($HECV^{CL5rib}$ vs. $HECV^{CL5rib}$ +HGF/ROCK $p<0.001$, and $HECV^{CL5rib}$ +HGF vs. $HECV^{CL5rib}$ +HGF/ROCK $p=0.59$). Control cells, $HECV^{wt}$ and $HECV^{pef6}$, revealed similar behaviour when treated with HGF+ROCK inhibitor. In both cell lines a significant decrease in the number of tubules formed was seen ($p<0.001$) (Figure 6.10).

All the results are summarized in Table 6.1.

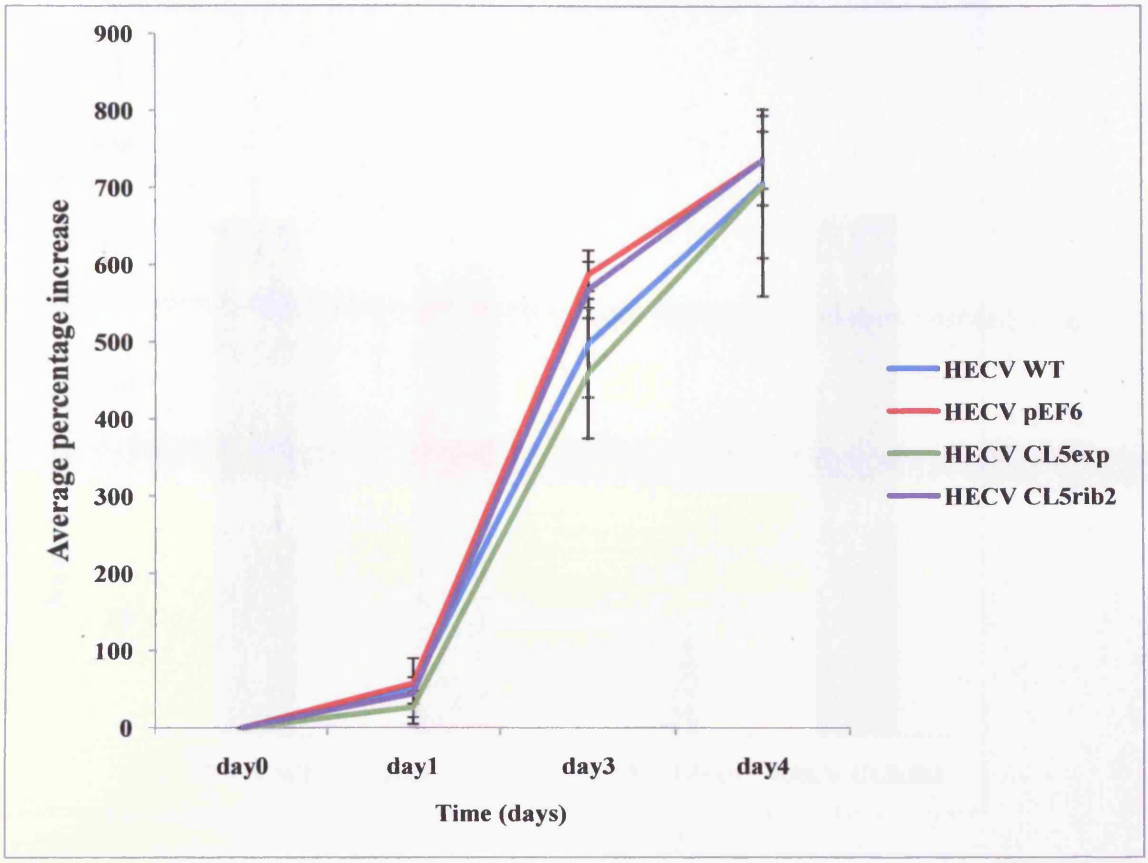

Figure 6.1: Effect of Claudin-5 on *in vitro* cell growth of HECV cells using the *in vitro* cell growth assay. The cell growth of $HECV^{Cl5exp}$ and $HECV^{CL5rib2}$ did not show any significant difference when compared to $HECV^{wt}$ and $HECV^{pef6}$ (mean ±SD, n=3).

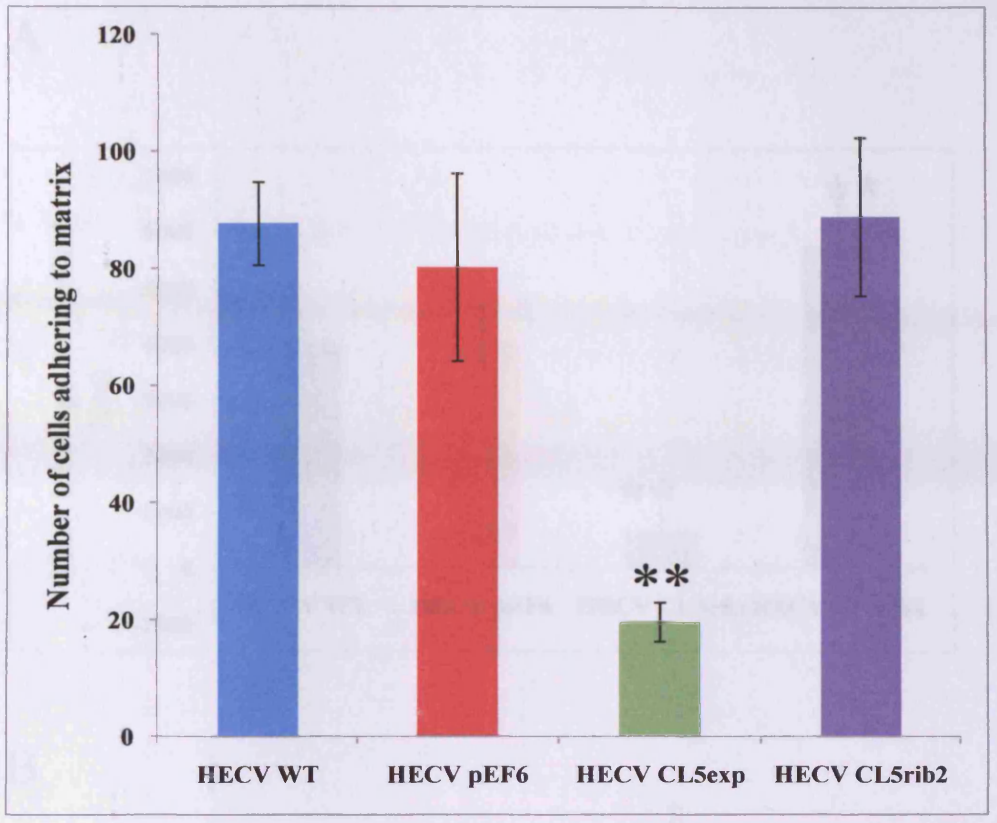

Figure 6.2: Effect of Claudin-5 on *in vitro* cell adhesion of HECV cells using the *in vitro* Matrigel adhesion assay. The data presented is representative is the mean of at least 3 independent repeats and the error bars represent the standard error of the mean. The adhesive capacity of $HECV^{Cl5exp}$ was significantly decreased in comparison with the controls $HECV^{wt}$ and $HECV^{pef6}$ (** represents $p<0.001$ for both controls).

A

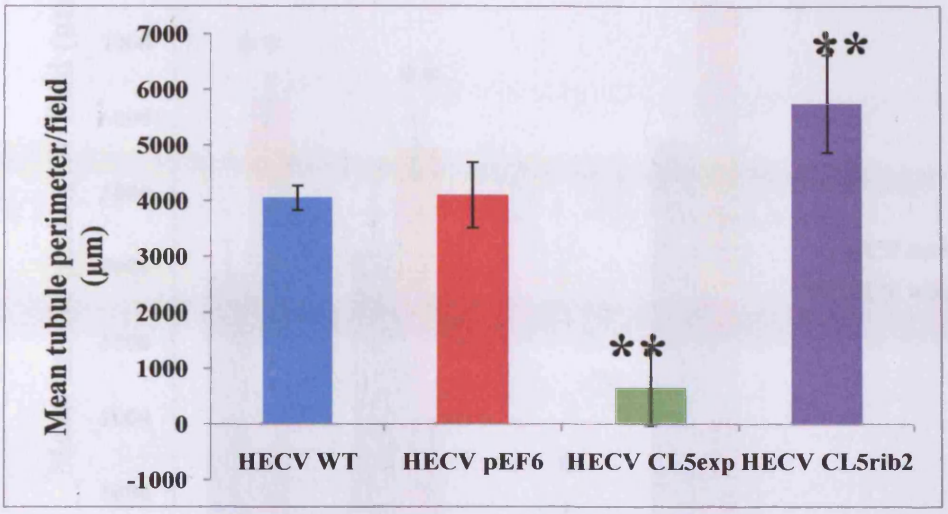

B

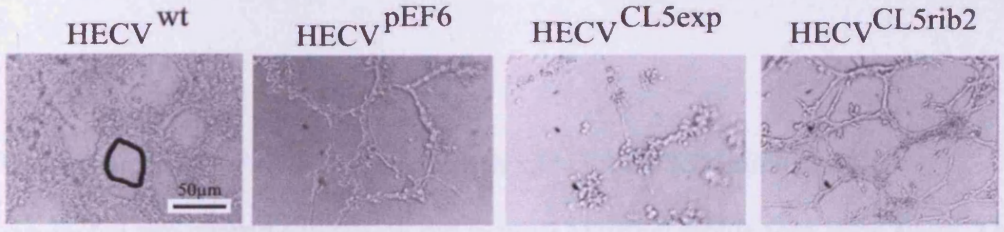

Figure 6.3: (A) Effect of Claudin-5 on *in vitro* tubule formation of HECV cells using the *in vitro* Matrigel tubule formation assay. The data presented is representative is the mean of at least 3 independent repeats and the error bars represent the standard error of the mean. The ability to form tubules of $HECV^{Cl5exp}$ was significantly decreased in comparison with the controls $HECV^{wt}$ and $HECV^{pef6}$ (** represents $p<0.001$ for both controls). In contrast, the capacity of $HECV^{CL5rib2}$ to form tubules was significantly increased when compared to the controls $HECV^{wt}$ and $HECV^{pef6}$ (**$p<0.001$ for both controls). (B) Representative pictures of tubule formation in HECV cells.

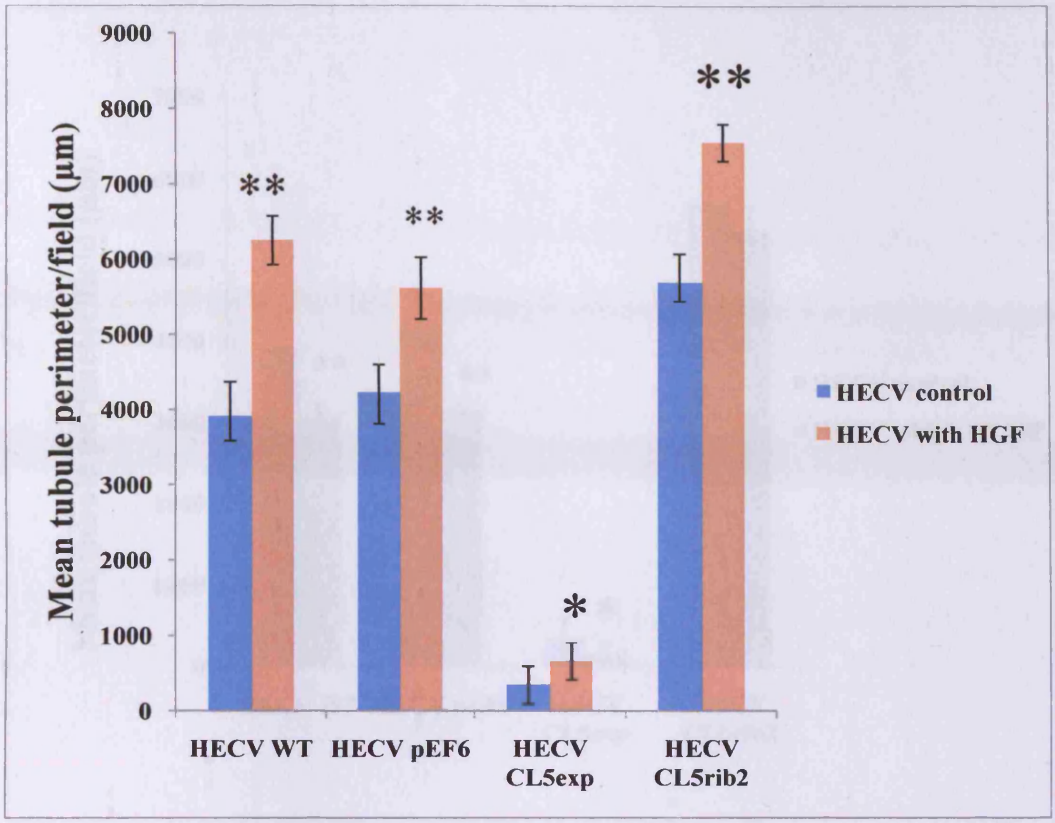

Figure 6.4: Effect of HGF treatment on *in vitro* tubule formation of HECV transfected and control cells using the *in vitro* Matrigel tubule formation assay. The data presented is representative is the mean of at least 3 independent repeats and the error bars represent the standard error of the mean. The ability of $HECV^{Cl5exp}$ and $HECV^{CL5rib2}$ to form tubules after treatment with HGF was significantly increased in comparison with the untreated cells (*represents $p<0.05$ and ** $p<0.001$).

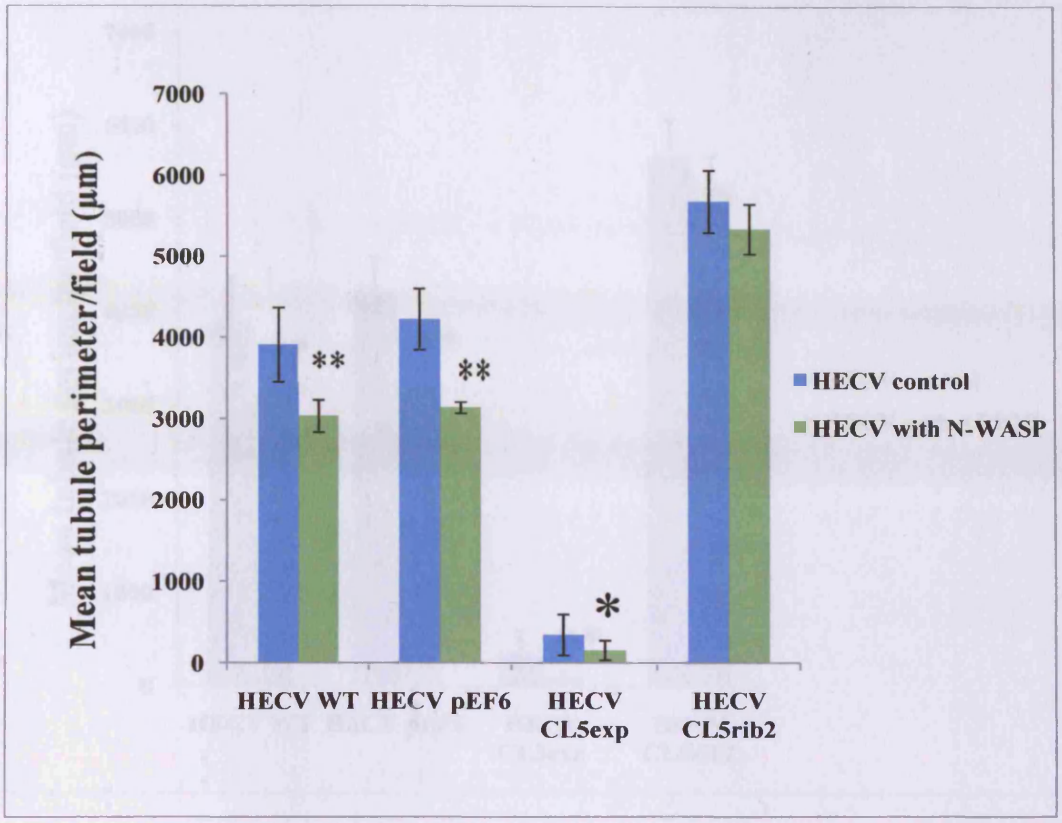

Figure 6.5: Effect of N-WASP inhibitor on *in vitro* tubule formation of HECV transfected and control cells using the *in vitro* Matrigel tubule formation assay. The data presented is representative is the mean of at least 3 independent repeats and the error bars represent the standard error of the mean. The ability of $HECV^{Cl5exp}$ and $HECV^{CL5rib2}$ to form tubules after treatment with N-WASP inhibitor was reduced in comparison with the untreated cells, however, only $HECV^{Cl5exp}$ shows significant differences (*represents $p<0.05$).

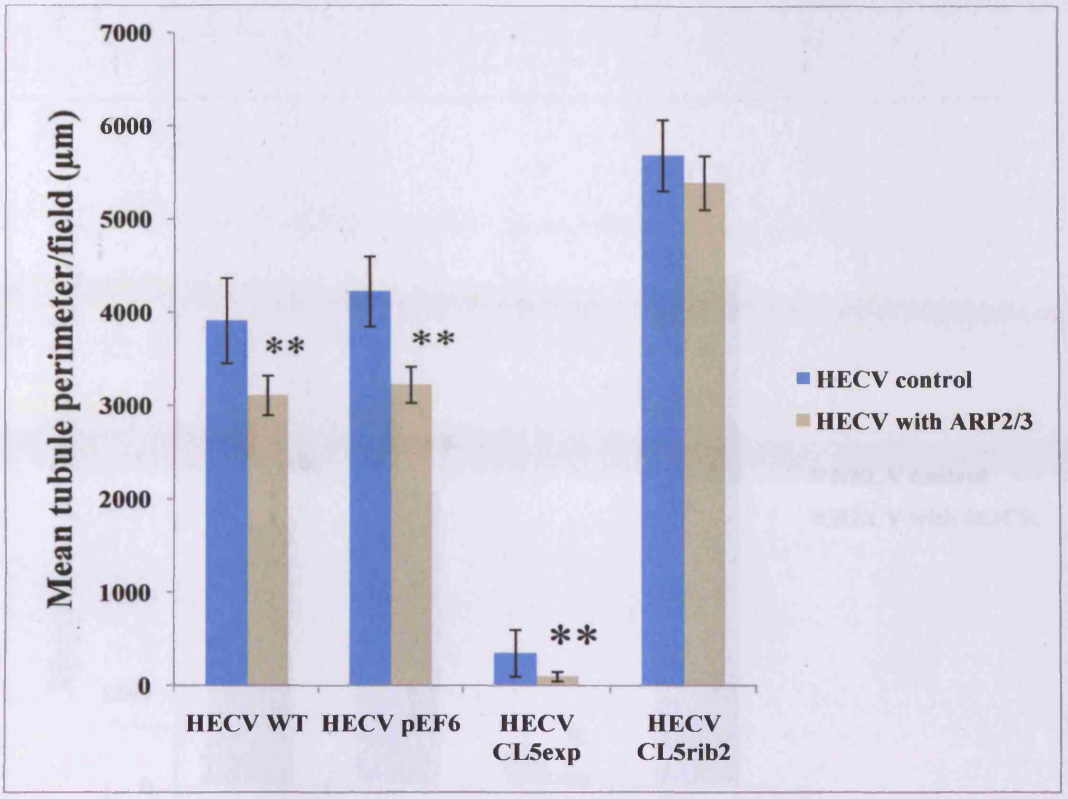

Figure 6.6: Effect of Arp2/3 inhibitor on *in vitro* tubule formation of HECV transfected and control cells using the *in vitro* Matrigel tubule formation assay. The data presented is representative is the mean of at least 3 independent repeats and the error bars represent the standard error of the mean. The ability of $HECV^{Cl5exp}$ and $HECV^{CL5rib2}$ to form tubules after treatment with Arp2/3 inhibitor was reduced in comparison with the untreated cells, however, only $HECV^{Cl5exp}$ shows significant differences (*represents $p<0.001$).

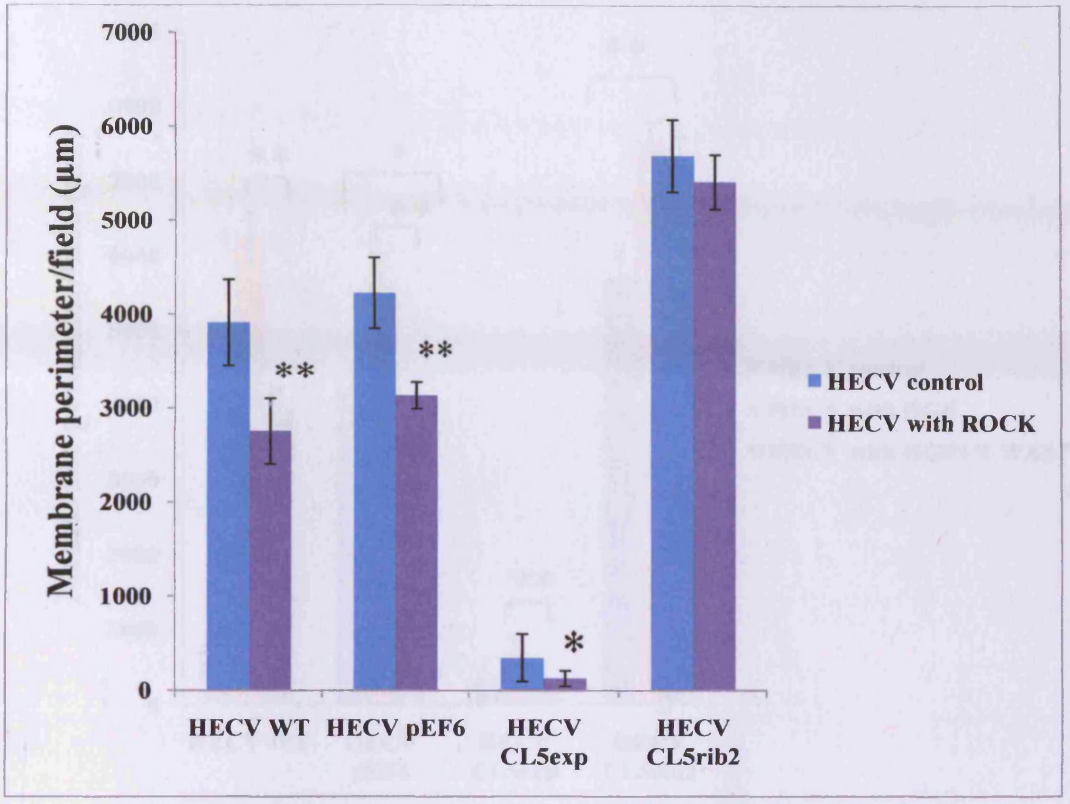

Figure 6.7: Effect of ROCK inhibitor on *in vitro* tubule formation of HECV transfected and control cells using the *in vitro* Matrigel tubule formation assay. The data presented is representative is the mean of at least 3 independent repeats and the error bars represent the standard error of the mean. The capability of $HECV^{Cl5exp}$ and $HECV^{CL5rib2}$ to form tubules after treatment with ROCK inhibitor was reduced in comparison with the untreated cells, however, only $HECV^{Cl5exp}$ shows significant differences (*represents $p<0.05$).

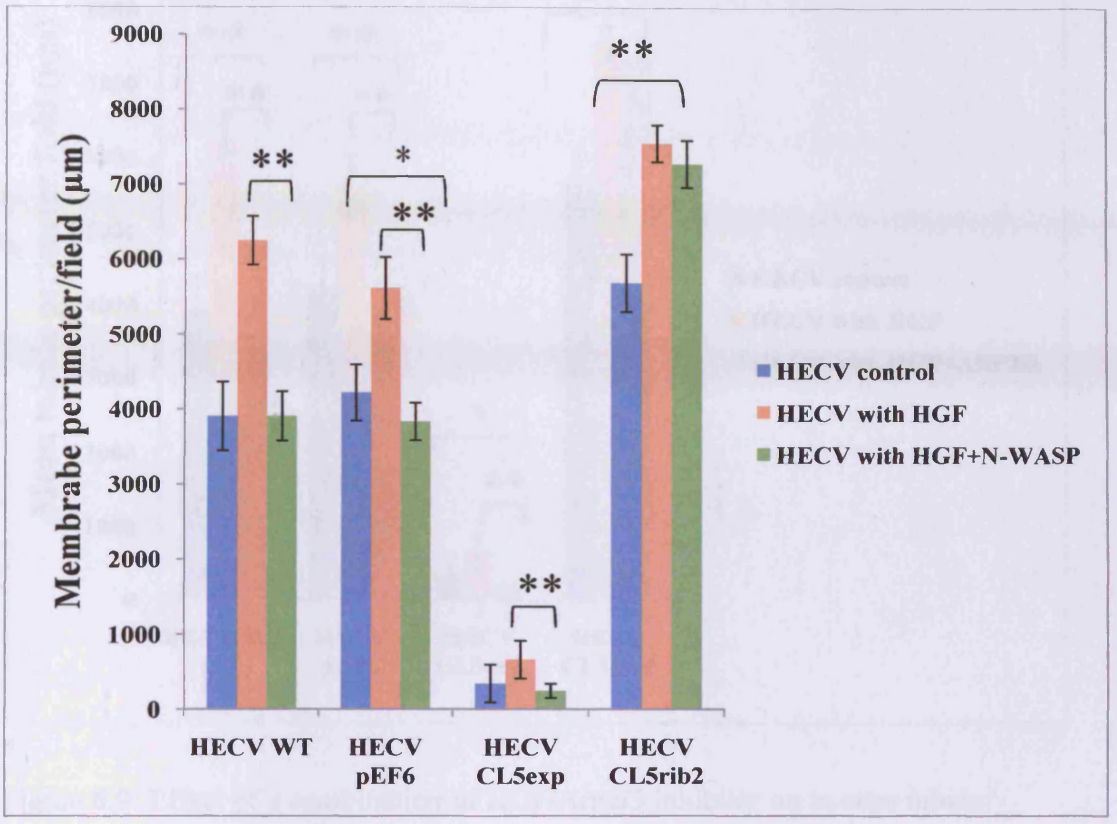

Figure 6.8: Effect of a combination of HGF/N-WASP inhibitor on *in vitro* tubule formation of HECV transfected and control cells using the *in vitro* Matrigel tubule formation assay. The data presented is representative is the mean of at least 3 independent repeats and the error bars represent the standard error of the mean. $HECV^{Cl5exp}$+HGF/N-WASP data revealed a significant decrease in the number of tubules formed compared to HGF treated cells, however no significant differences were found compared to untreated cells ($HECV^{Cl5exp}$ vs. $HECV^{Cl5exp}$+HGF/N-WASP $p=0.28$, and $HECV^{Cl5exp}$+HGF vs. $HECV^{Cl5exp}$+HGF/N-WASP $p<0.001$). No significant differences were found between $HECV^{CL5rib2}$+HGF and $HECV^{CL5rib2}$+HGF/N-WASP $p=0.054$. Untreated $HECV^{CL5rib2}$ showed significantly less tubules compared to $HECV^{CL5rib2}$+HGF/N-WASP $p<0.001$.

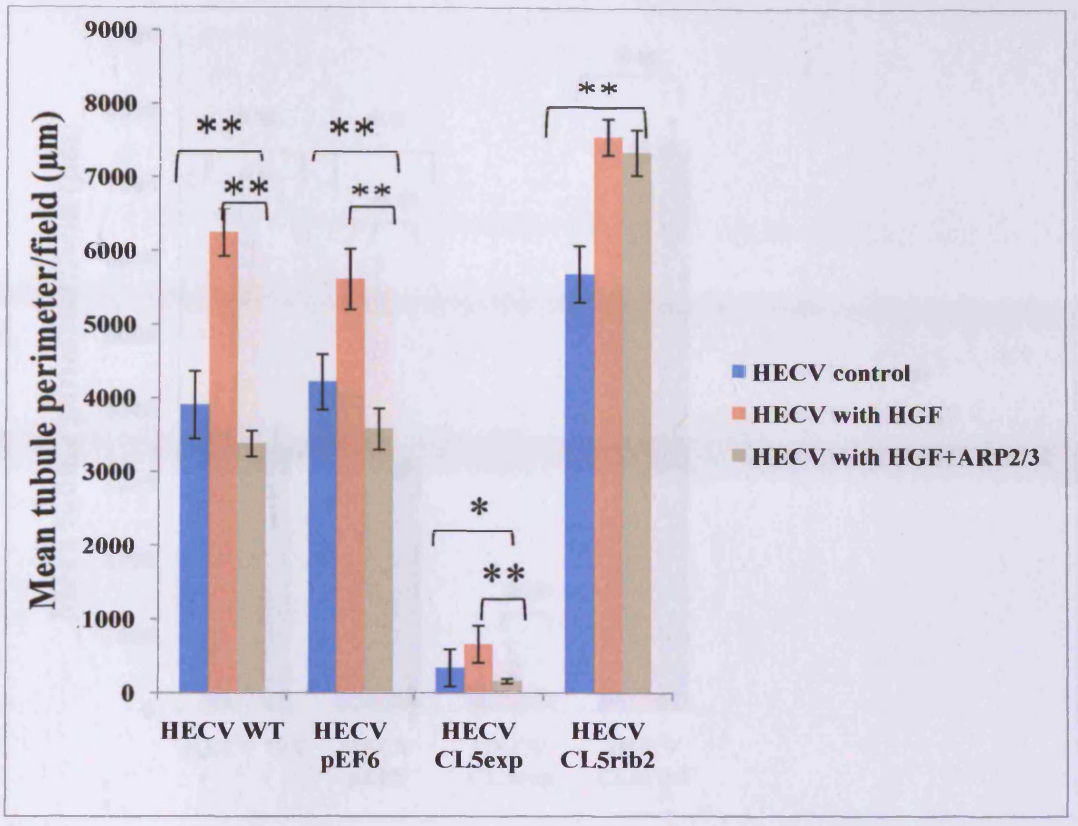

Figure 6.9: Effect of a combination of HGF/Arp2/3 inhibitor on *in vitro* tubule formation of HECV transfected and control cells using the *in vitro* Matrigel tubule formation assay. The data presented is representative is the mean of at least 3 independent repeats and the error bars represent the standard error of the mean. $HECV^{Cl5exp}$+HGF/Arp2/3 data revealed a significant decrease in the number of tubules formed compared with untreated and HGF treated cells ($HECV^{Cl5exp}$ vs. $HECV^{Cl5exp}$+HGF/Arp2/3 $p=0.04$, and $HECV^{Cl5exp}$+HGF vs. $HECV^{Cl5exp}$+HGF/Arp2/3 $p<0.001$). No significant differences where found between $HECV^{CL5rib2}$+HGF and $HECV^{CL5rib2}$+HGF/Arp2/3 $p=0.12$ Untreated $HECV^{CL5rib2}$ formed significantly less tubules compared to $HECV^{CL5rib2}$+HGF/Arp2/3 $p<0.001$.

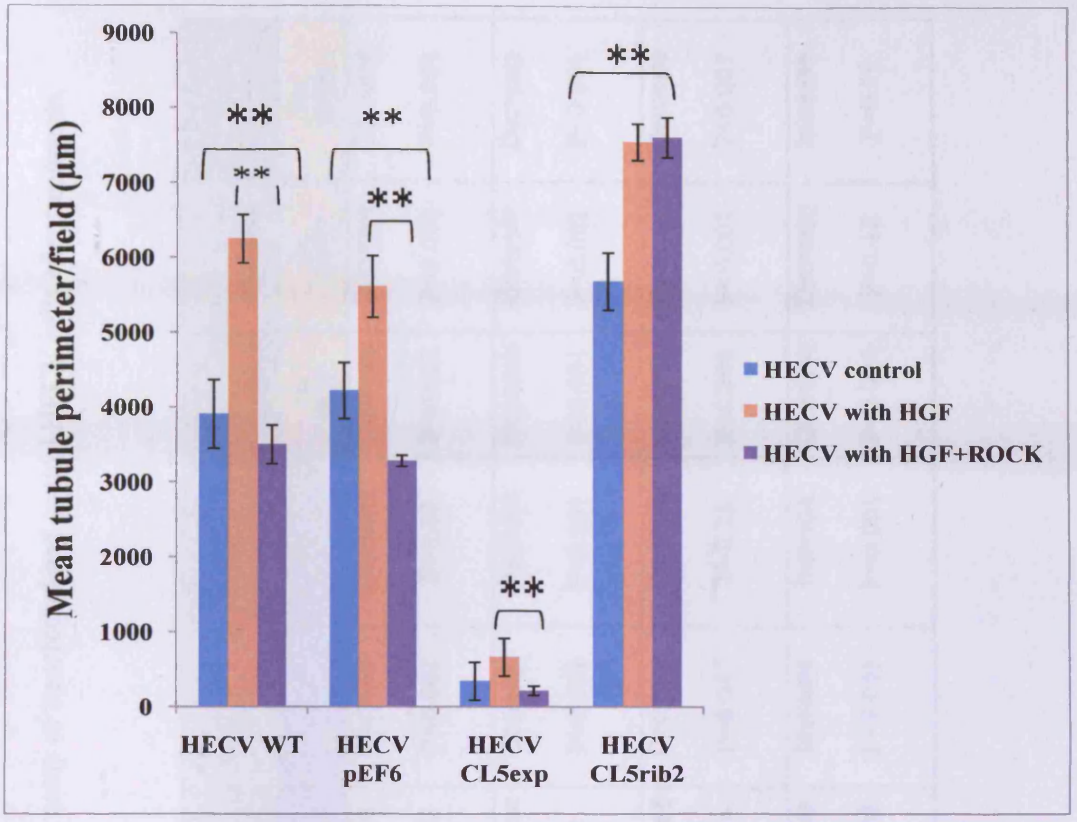

Figure 6.10: Effect of a combination of HGF/ROCK inhibitor on *in vitro* tubule formation of HECV transfected and control cells using the *in vitro* Matrigel tubule formation assay. The data presented is representative is the mean of at least 3 independent repeats and the error bars represent the standard error of the mean. $HECV^{Cl5exp}$+HGF/ROCK data revealed a significant decrease in the number of tubules formed compared with HGF treated cells, however no significant differences were observed in untreated cells ($HECV^{Cl5exp}$ vs. $HECV^{Cl5exp}$+HGF/ROCK $p=0.16$, and $HECV^{Cl5exp}$+HGF vs. $HECV^{Cl5exp}$+ROCK $p<0.001$). No significant differences were found between $HECV^{CL5rib2}$+HGF and $HECV^{CL5rib2}$+HGF/ROCK $p=0.59$. Untreated $HECV^{CL5rib2}$ formed significantly less tubules compared to $HECV^{CL5rib2}$+HGF/ROCK $p<0.001$.

Table 6.1: Data summarising the results of tubule formation assay of transfected and control HECV cells after treatments.

Mean tubule perimeter/field (μm)	HGF	N-WASP inhibitor	Arp2/3 inhibitor	ROCK inhibitor	HGF/N-WASP inhibitor	HGF/Arp2/3 inhibitor	HGF/ROCK inhibitor	HGF/N-WASP inhibitor	HGF/Arp2/3 inhibitor	HGF/ROCK inhibitor
	vs. untreated	vs. untreated	vs. untreated	vs. untreated	vs. untreated	vs. untreated	vs. untreated	vs. HGF	vs. HGF	vs. HGF
$HECV^{wt}$	Increase P<0.001	Decrease P<0.001	Decrease P<0.001	Decrease P<0.001	Decrease P=0.68	Decrease P<0.001	Decrease P=0.03	Decrease P<0.001	Decrease P<0.001	Decrease P<0.001
$HECV^{pef}$	Increase P<0.001	Decrease P<0.001	Decrease P<0.001	Decrease P<0.001	Decrease P=0.02	Decrease P<0.001	Decrease P<0.001	Decrease P<0.001	Decrease P<0.001	Decrease P<0.001
$HECV^{Cl5exp}$	Increase P=0.015	Decrease P=0.045	Decrease P<0.001	Decrease P=0.045	Decrease P=0.28	Decrease P=0.047	Decrease P=0.16	Decrease P<0.001	Decrease P<0.001	Decrease P<0.001
$HECV^{CL5rib2}$	Increase P<0.001	Decrease P=0.052	Decrease P=0.084	Decrease P=0.133	Increase P<0.001	Increase P<0.001	Increase P<0.001	Decrease P=0.054	Decrease P=0.12	Increase P=0.59

6.3.4 Effect of Claudin-5 on HECV cell motility and the effect of HGF

A Cytodex-2 bead motility assay was used to examine a possible role of Claudin-5 in cell motility. Transfected and control cells, either untreated or treated with HGF, were evaluated. $HECV^{Cl5exp}$ cells did not show significant differences when compare to the controls ($HECV^{wt}$ (7.44±2.63), $HECV^{pef6}$ (6.5±3.34) and $HECV^{Cl5exp}$ (6.82±2.77), (p=0.43 and p=0.74 respectively). In contrast, $HECV^{CL5rib2}$ cells demonstrated significantly increased cell motility compared to the controls ($HECV^{wt}$ (7.44±2.63), $HECV^{pef6}$ (6.5±3.34) and $HECV^{CL5rib2}$ (18.7±3.49), $p<0.001$ for both controls) (Figure 6.11 A).

The cells were additionally evaluated after treatment with HGF. This pro-motility agent increases cell motility in $HECV^{Cl5exp}$ and control cells, $HECV^{wt}$ and $HECV^{pef6}$, when compared to untreated cells ($HECV^{wt}$+HGF (18.26±5.62), $HECV^{pef6}$+HGF (22.31±6.60) and $HECV^{Cl5exp}$+HGF (18.18±4.75), $p<0.001$). However, in the case of $HECV^{CL5rib2}$, although a slight increase in the number of motile cells was observed, the data was not found to be significant ($HECV^{CL5rib2}$+HGF (19.44±4.93), p=0.64) (Figure 6.11 B).

6.3.5 Effect of Claudin-5 on HECV cell migration

The effect of Claudin-5 on cellular migration was examined using an *in vitro* cellular migration assay. $HECV^{CL5rib2}$ showed a significantly increased cellular migration when compared to the controls 60 minutes after wounding ($HECV^{wt}$ (13.51±14.80), $HECV^{pef6}$ (22.57±1.34) and $HECV^{CL5rib2}$ (56.75±21.38), $p<0.05$ for both controls). A decreased cell migration was seen in $HECV^{Cl5exp}$ after 60 minutes

when compared to controls ($HECV^{wt}$ (13.51±14.80), $HECV^{pef6}$ (22.57±1.34) and $HECV^{Cl5exp}$ (7.02±1.42), p=0.49 and p<0.05respectively). Although the effect is only statistically significant when comparing to $HECV^{pef6}$, the trend remains marked (Figure 6.12).

6.3.6 Effect of Claudin-5 on HECV Transendothelial resistance and their response to HGF

Transendothelial resistance (TER) was used to assess the effect of over-expressing or knocking-down of Claudin-5 on Tight Junction functionality in HECV cells. $HECV^{Cl5exp}$ showed increased TER over a period of 4 hours in comparison with the control $HECV^{wt}$ (change in TER after 30 minutes $HECV^{wt}$ (-98.66±1.3) vs. $HECV^{Cl5exp}$ (-65.66±1.6); 60 minutes $HECV^{wt}$ (-142.66±0.77) vs. $HECV^{Cl5exp}$ (-128.33±4.3); 2 hours $HECV^{wt}$ (-167.66±2.18) vs. $HECV^{Cl5exp}$ (-156. 33±2.8); 4 hours $HECV^{wt}$ (-194.33±2.42) vs. $HECV^{Cl5exp}$ (-175±2.15), p<0.01). Changes in TER were more evident in $HECV^{CL5rib2}$ when compare to the control (change in TER after 30 minutes $HECV^{wt}$ (-98.66±1.3) vs. $HECV^{CL5rib2}$ (-69.66±6.77); 60 minutes $HECV^{wt}$ (-142.66±0.77) vs. $HECV^{CL5rib2}$ (-118 ±3.2); 2 hours $HECV^{wt}$ (-167.66±2.18) vs. $HECV^{CL5rib2}$ (-124.33±1.81); 4 hours $HECV^{wt}$ (-194.33±2.42) vs. $HECV^{CL5rib2}$ (-89.33±2.1), p<0.001) (Figure 6.13).

Treatment of cells with HGF (50ng/ml) resulted in a significant reduction of TER in transfected and control cells when compared to untreated cells over a period of 4 hours (change in TER after 30 minutes $HECV^{wt}$+HGF (-125±1.2), $HECV^{Cl5exp}$+HGF (-109.66±2.3), $HECV^{CL5rib2}$+HGF (-95±1.6); 60 minutes $HECV^{wt}$+HGF (-160.66±4.24), $HECV^{Cl5exp}$+HGF (-190±1.64), $HECV^{CL5rib2}$+HGF (-

160±1.89); 2 hours $HECV^{wt}$+HGF (-199.66±1.7), $HECV^{Cl5exp}$+HGF (-210±4.3), $HECV^{CL5rib2}$+HGF (-189±5.6); 4 hours $HECV^{wt}$+HGF (-245.66±1.3), $HECV^{Cl5exp}$+HGF (-240±2.4), $HECV^{CL5rib2}$+HGF (-180.66±2. 8), $p<0.001$) (Figure 6.14).

A

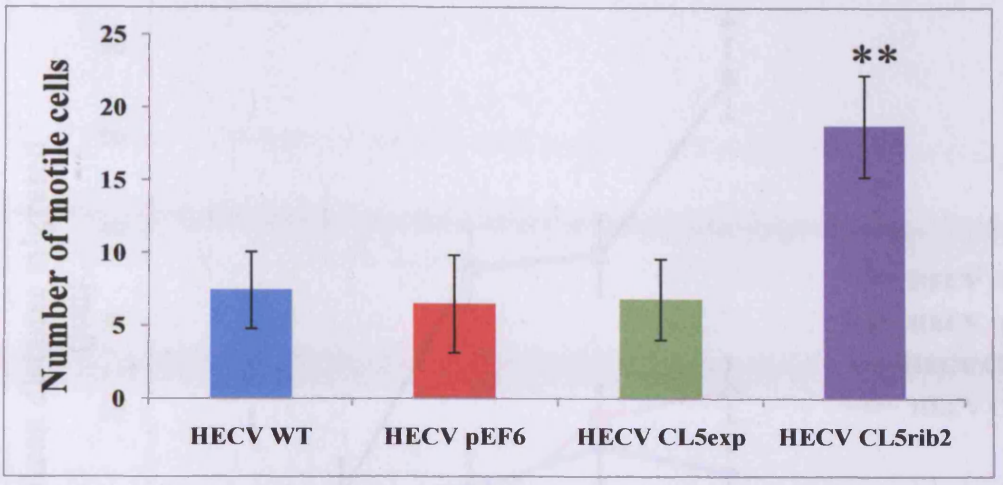

B

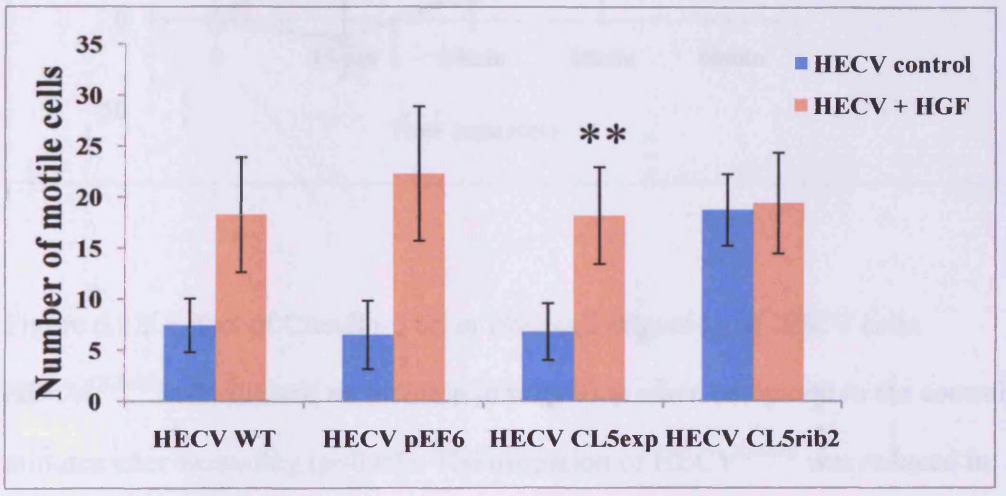

Figure 6.11: (A) Effect of Claudin-5 on *in vitro* cell motility of HECV cells. The motility of $HECV^{CL5rib2}$ was significantly increased in comparison to the controls ($p<0.001$ for both controls). (B) Effect on motility after treatment with HGF. Transfected and control cells showed an increase in motility, however, only the controls and $HECV^{Cl5exp}$ results were significant ($p<0.001$). The data presented is representative is the mean of at least 3 independent repeats and the error bars represent the standard error of the mean.

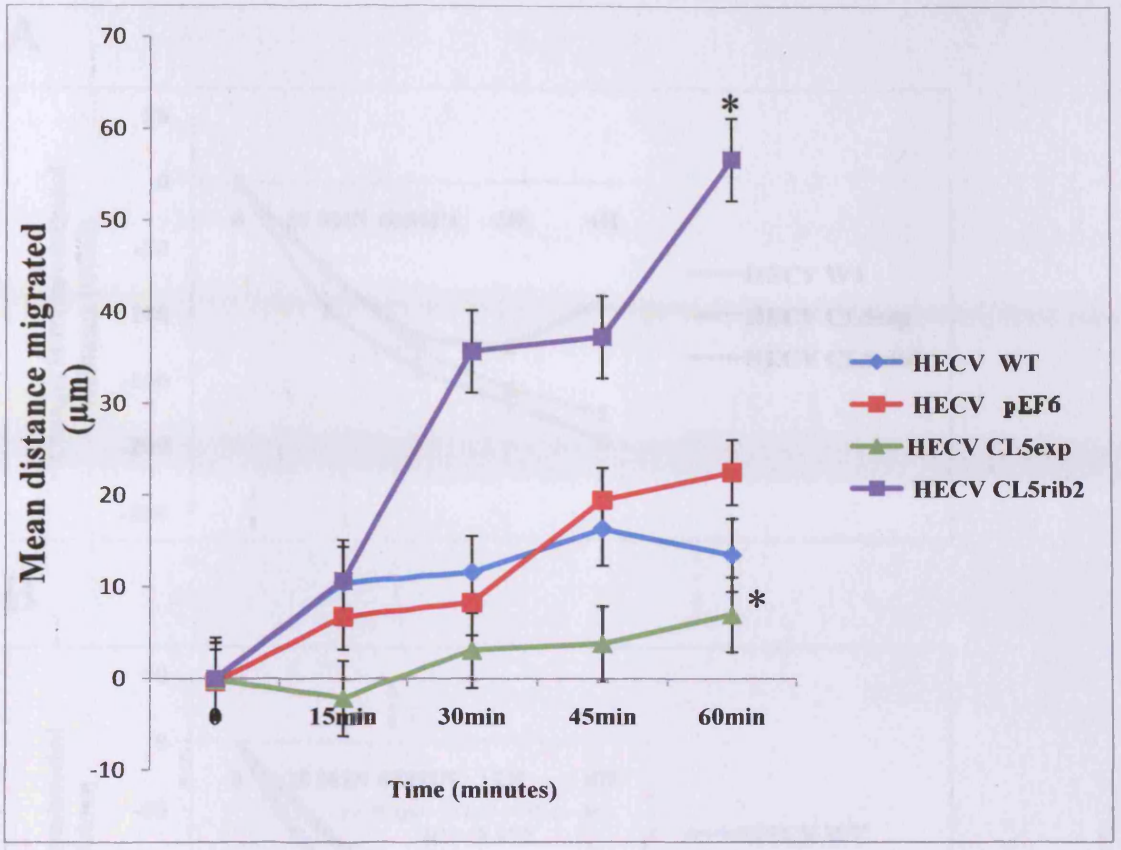

Figure 6.12: Effect of Claudin-5 on *in vitro* cell migration of HECV cells. $HECV^{CL5rib2}$cells showed an increase in migration when compared to the controls 60 minutes after wounding ($p<0.05$). The migration of $HECV^{Cl5exp}$ was reduced in comparison to the controls at 60 minutes. However, only significant differences were found when compared to $HECV^{pef6}$ ($p<0.05$) (mean ±SD, n=3).

A

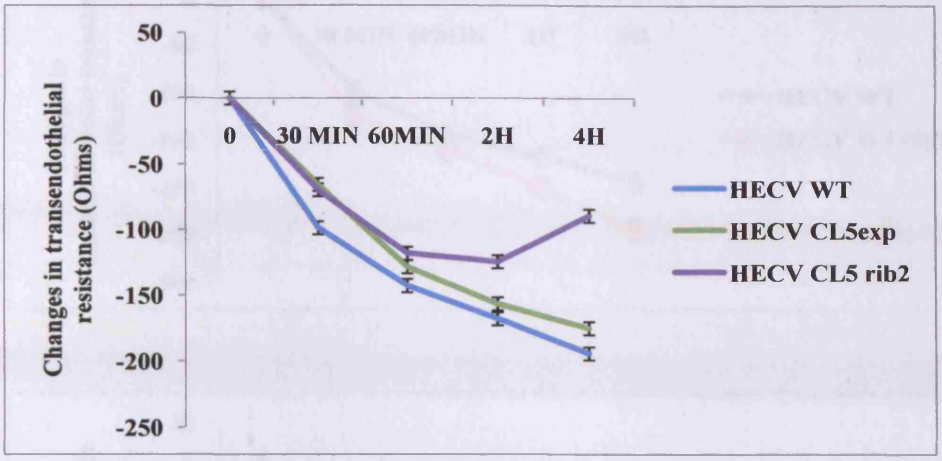

B

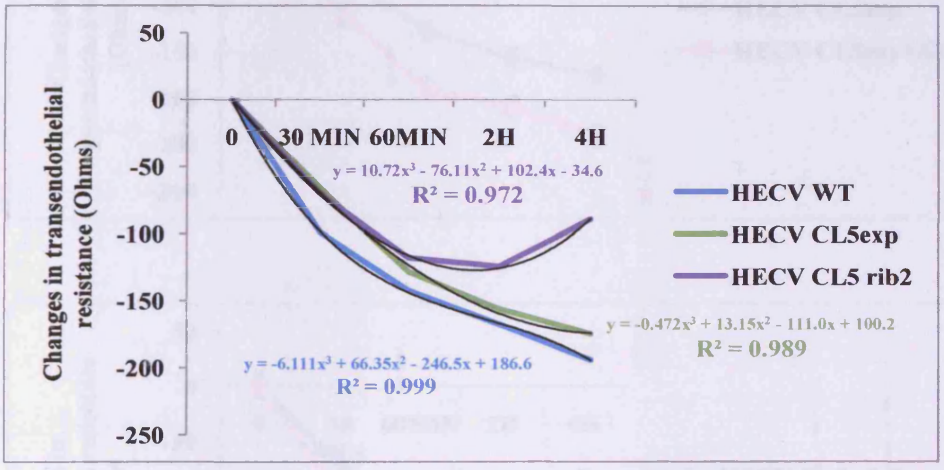

Figure 6.13: (A) Effect of Claudin-5 on transendothelial resistance on HECV cells. Significant changes were seen on HECV^{Cl5exp} and HECV^{CL5rib2} over a period of 4 hours when compared to the control ($p<0.01$ and $p<0.001$ respectivley). (B) A polynomial model was used to visualise the trend of the presented data. R^2 indicates that the regression line clearly fits the data (mean ±SD, n=3).

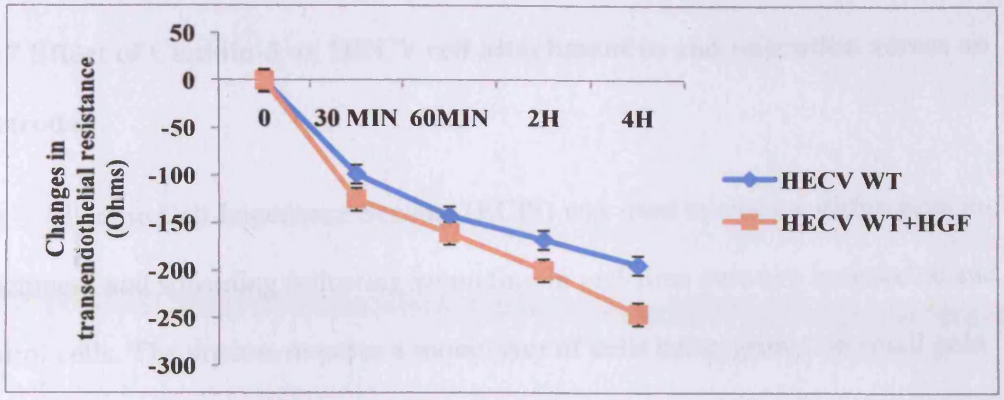

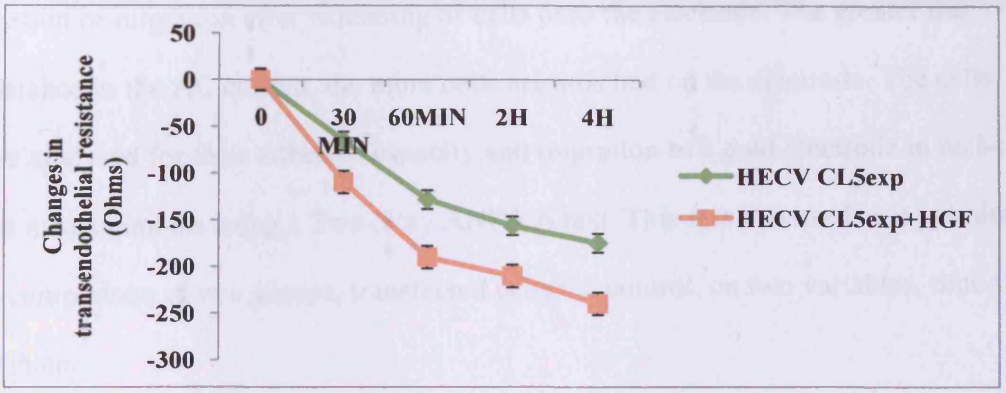

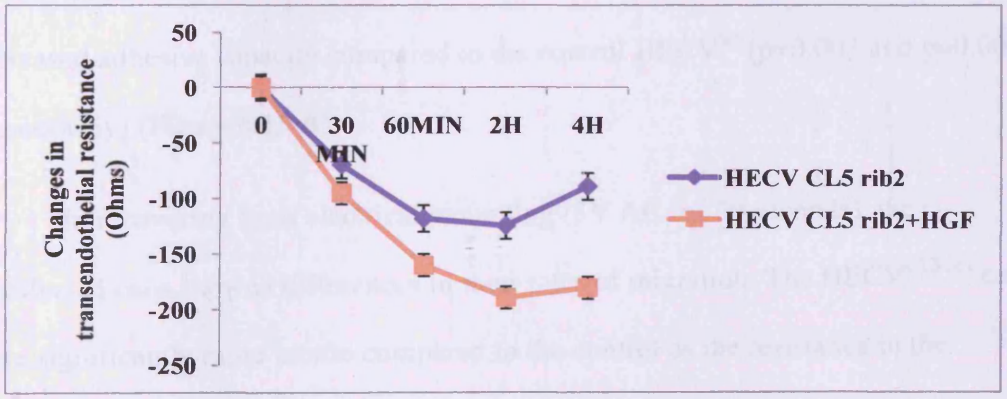

Figure 6.14: Effect of Claudin-5 on transendothelial resistance on HECV cells after treatment with HGF. Significant changes were seen in transfected and control cells over a period of 4 hours when compared to the untreated cells ($p<0.001$) (mean ±SD, n=3).

6.3.7 Effect of Claudin-5 on HECV cell attachment to and migration across an electrode

Electric Cell Impedance Sensing (ECIS) was used to analyse differences in attachment and spreading following wounding in real-time between transfected and control cells. The process requires a monolayer of cells being grown on small gold electrodes, applying AC current and monitoring resistance changes caused by the adhesion or migration after wounding of cells onto the electrode. The greater the resistance to the AC current, the more cells are attached on the electrode. The cells were analysed for their adhesive capacity and migration to a gold electrode in real-time measurements using a Two-Way ANOVA test. This test was used as it permits the comparison of two groups, transfected cells vs. control, on two variables, time vs. treatment.

The $HECV^{Cl5exp}$ and $HECV^{CL5rib2}$ cells demonstrated a significantly decreased adhesive capacity compared to the control $HECV^{wt}$ ($p=0.003$ and $p=0.002$ respectively) (Figure 6.15 A).

In recovering from electrical wounding (5V AC for 30 seconds), the transfected cells showed differences in their rates of migration. The $HECV^{CL5rib2}$ cells were significantly more motile compared to the control as the resistance in the electrode increased as the cells begin to spread over the electrode ($p=0.047$). However, the $HECV^{Cl5exp}$ cells showed a markedly reduced migration ($p<0.001$) (Figure 6.15 B).

A

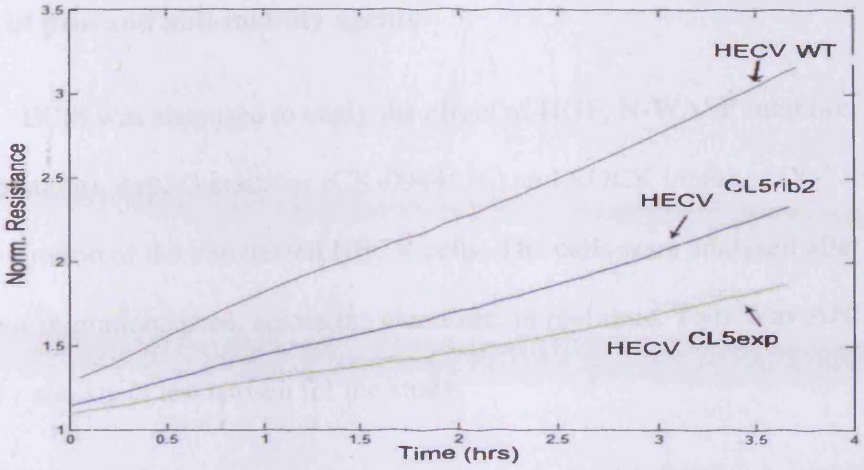

B

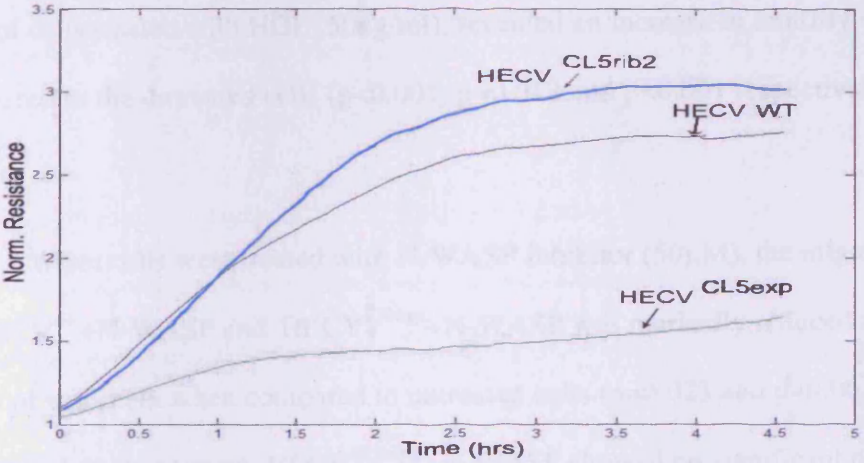

Figure 6.15: (A) Effect of Claudin-5 on the cell adhesion of HECV cells using ECIS. Significant differences were seen in transfected cells when compared to the control. $HECV^{Cl5exp}$ and $HECV^{CL5rib2}$showed a significantly reduced adhesive capacity ($p=0.003$ and $p=0.002$ respectively). (B) Significant differences were revealed after wounding. $HECV^{CL5rib2}$ showed significant increased migration ($p=0.04$) whereas $HECV^{Cl5exp}$ showed a decreased migration rate ($p<0.001$).The data presented is representative of at least 3 independent repeats.

6.3.8 Effect of Claudin-5 on HECV cell migration over an electrode and the effect of pro- and anti-motility agents

ECIS was also used to study the effect of HGF, N-WASP inhibitor (Wiskostatin), Arp2/3 inhibitor (CK-0944636) and ROCK inhibitor (Y-27632) on cell migration of the transfected HECV cells. The cells were analysed after wounding for their migration speed, across the electrode, in real time. Two-Way ANOVA test was the statistical test chosen for the study.

Following electrical wounding and treatment with HGF and motility inhibitors differences in cell capability to migrate were seen. The transfected and control cells treated with HGF (50ng/ml), revealed an increase in motility when compared to the untreated cells ($p<0.001$, $p=0.012$ and $p<0.001$ respectively) (Figure 6.16).

When cells were treated with N-WASP inhibitor (50μM), the migration speed of $HECV^{wt}$ +N-WASP and $HECV^{Cl5exp}$+N-WASP was markedly reduced after 5 hours of treatment when compared to untreated cells ($p=0.023$ and $p=0.001$ respectively). In contrast, $HECV^{CL5rib2}$+N-WASP showed no significant differences when compared to the untreated cells ($p=0.173$) (Figure 6.17).

Arp2/3 inhibitor (10nM) adversely inhibited the migration of $HECV^{wt}$ + Arp2/3 and $HECV^{Cl5exp}$+ Arp2/3, when compared to untreated cells after wounding ($p<0.001$for both cell lines). Surprisingly, the migration of $HECV^{CL5rib2}$+ Arp2/3 was no longer inhibited, in contrast, it was enhanced when compared to untreated cells ($p=0.015$) (Figure 6.18).

Treatment of cells with ROCK inhibitor reduced their migration of $HECV^{wt}$ + ROCK and $HECV^{Cl5exp}$+ ROCK, when compared to untreated cells after wounding ($p=0.013$ and $p<0.001$). However, in $HECV^{CL5rib2}$+ ROCK the migration of the cells was reduced although significant differences were not seen when compared to the untreated cells ($p=0.087$) (Figure 6.19).

All the results are summarized in Table 6.2.

6.3.9 Effect of Claudin-5 on protein level of N-WASP and ROCK1 and their interaction

$HECV^{wt}$, $HECV^{Cl5exp}$ and $HECV^{CL5rib2}$ Western blotting showed very low levels of N-WASP at protein levels. Protein levels of ROCK 1 revealed similar high levels in the transfected and control cells (Figure 6.20 A).

Immunoprecipitation of Claudin-5 followed by immunoblotting with N-WASP and ROCK showed a protein-protein interaction between Claudin-5 and these motility-related proteins in $HECV^{wt}$ and $HECV^{Cl5exp}$ (Figure 6.20 B). To further confirm this, immunoprecipitation results with either N-WASP (Figure 6.20 C) or ROCK 1 (Figure 6.20 D) followed by immunoblotting with Claudin-5 confirmed the interaction of the proteins.

6.3.10 Effect of Claudin-5 on HECV cell tumour growth *in vivo*

To assess the impact of altering Claudin-5 expression in HECV cells on tumour development *in vivo*, $HECV^{Cl5exp}$ cells co-injected alongside with MDA^{pef6}, were compared to $HECV^{pef6}$ co-injected with MDA^{pef6}. Tumour development over 33 days was monitored. $HECV^{Cl5exp}$ did not seem to alter tumour development in this

model and no significant differences were seen between control MDA^{pef6} and $HECV^{pef6}$ tumours and MDA^{pef6} and $HECV^{Cl5exp}$ tumour ($p = 0.25$) (Figure 6.21).

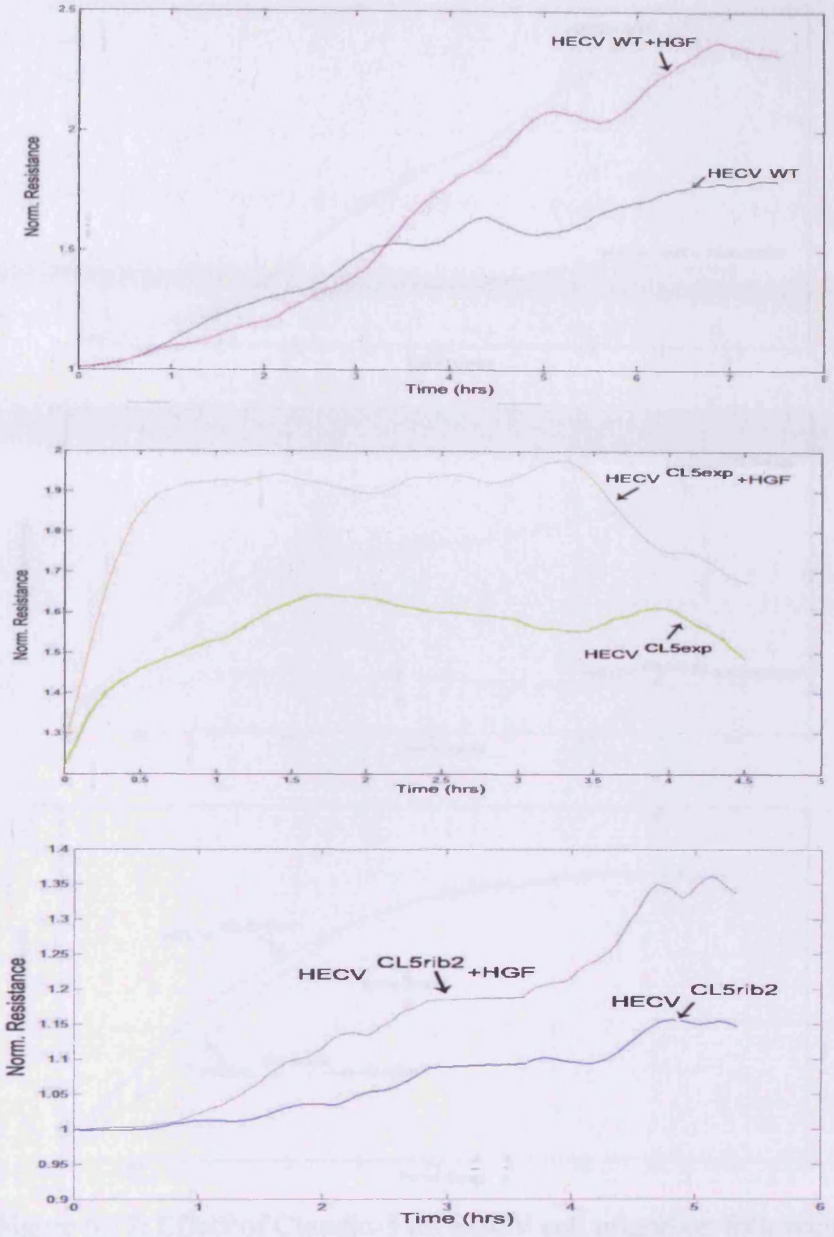

Figure 6.16: Effect of Claudin-5 on HECV cell migration following treatment with HGF using ECIS. Migration was significantly increased in $HECV^{wt}$+HGF, $HECV^{Cl5exp}$+HGF and $HECV^{CL5rib2}$+HGF when compared to untreated cells ($p<0.001$, $p=0.012$ and $p<0.001$ respectively). The data presented is representative of at least 3 independent repeats.

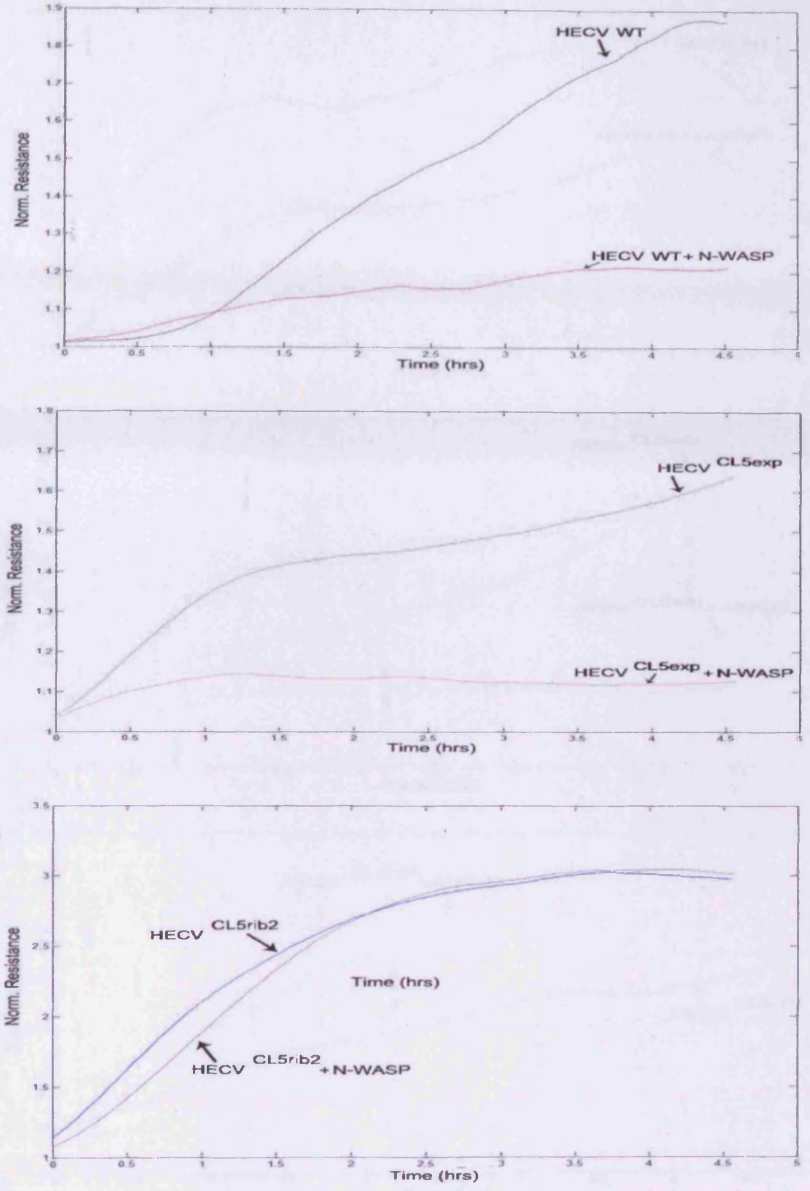

Figure 6.17: Effect of Claudin-5 on HECV cell migration following treatment with N-WASP inhibitor using ECIS. Migration was significantly decreased in $HECV^{wt}$+ N-WASP inhibitor and $HECV^{Cl5exp}$+ N-WASP inhibitor when compared to untreated cells (p=0.023 and p=0.001). $HECV^{CL5rib2}$+ N-WASP inhibitor did not show any difference in cell migration (p=0.173). The data presented is representative of at least 3 independent repeats.

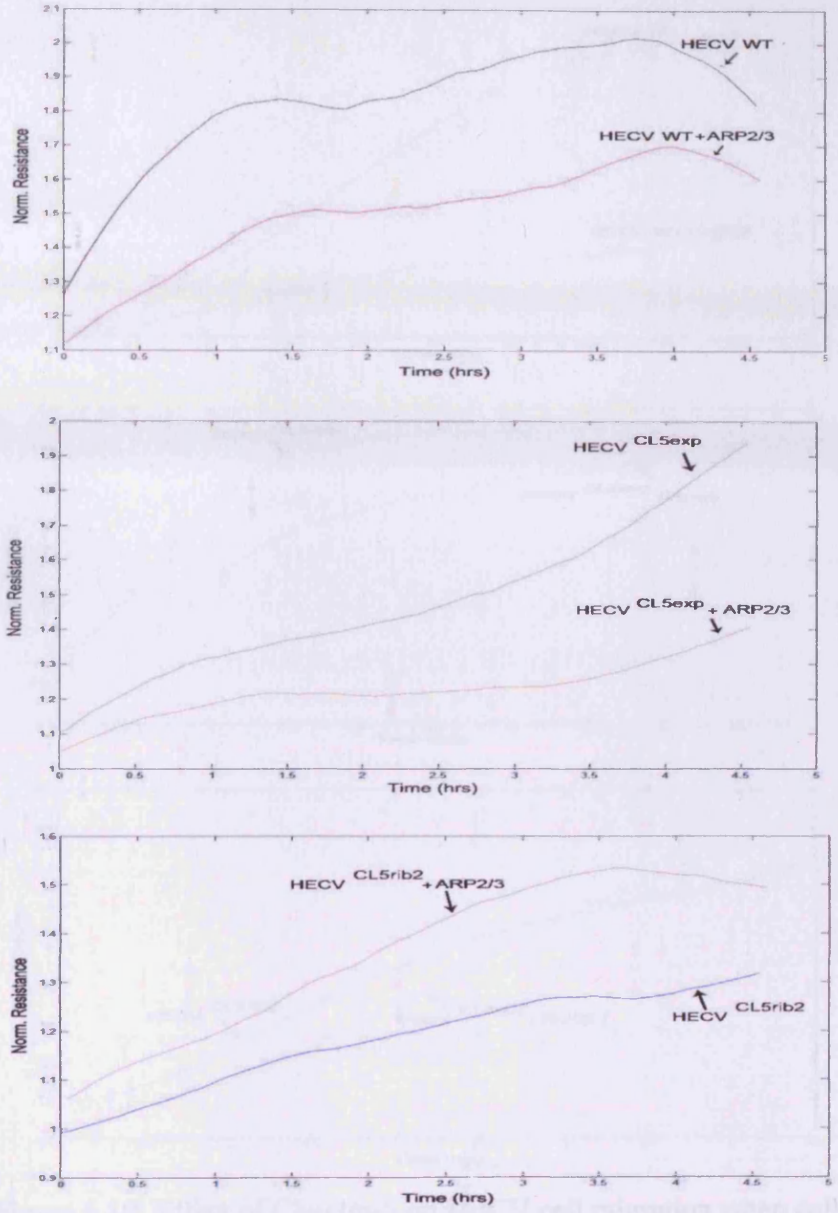

Figure 6.18: Effect of Claudin-5 on HECV cell migration following treatment with Arp2/3 inhibitor using ECIS. Migration was significantly decreased in $HECV^{wt}$+Arp2/3 inhibitor and $HECV^{Cl5exp}$+Arp2/3 inhibitor ($p<0.001$ vs. respective untreated controls). $HECV^{CL5rib2}$+Arp2/3 inhibitor showed an increase in migration when compared to untreated cells ($p=0.015$).The data presented is representative of at least 3 independent repeats.

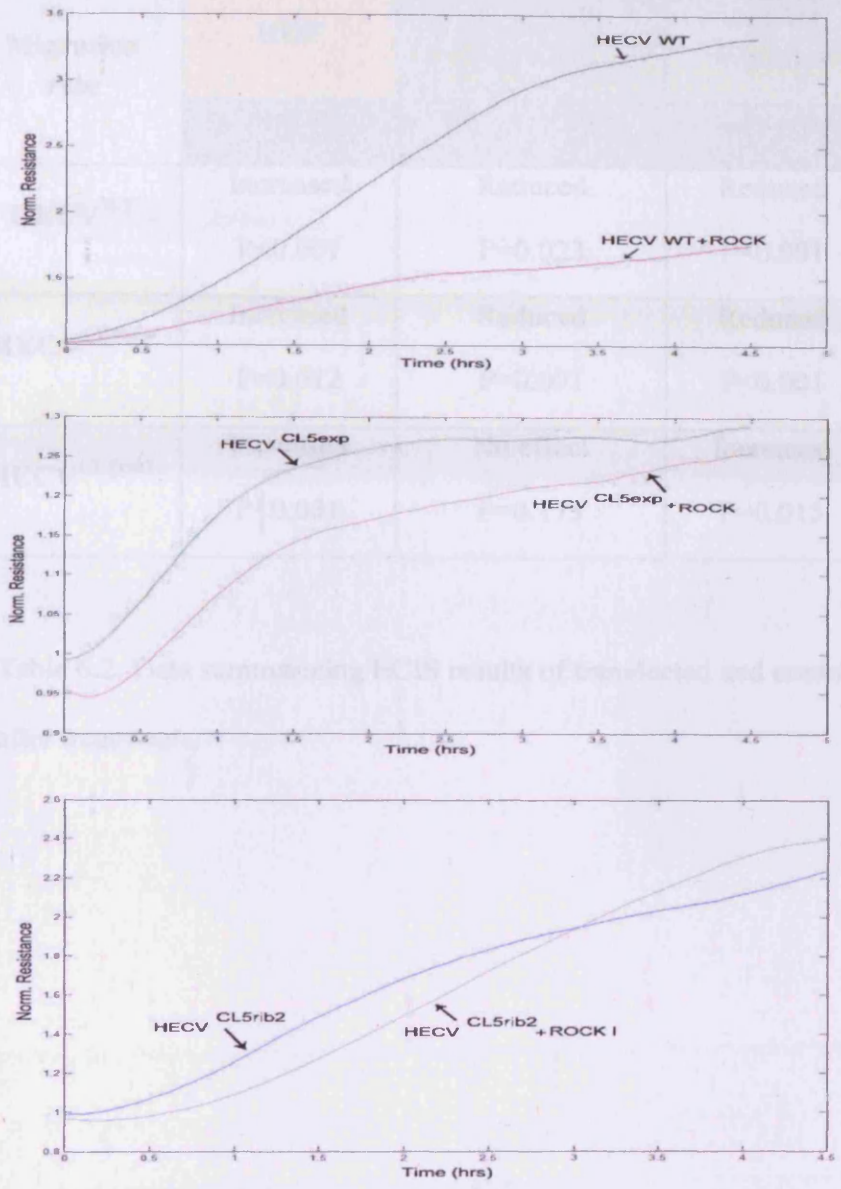

Figure 6.19: Effect of Claudin-5 on HECV cell migration when cells were treated with ROCK inhibitor using ECIS. Migration was significantly decreased in $HECV^{wt}$+ ROCK inhibitor and $HECV^{Cl5exp}$+ ROCK inhibitor ($p=0.013$ and $p<0.001$ vs. respective untreated controls). $HECV^{CL5rib2}$+ ROCK inhibitor showed a decrease in migration when compared to untreated cells ($p=0.087$). The data presented is representative of at least 3 independent repeats.

Migration rate	HGF	N-WASP inhibitor	Arp2/3 inhibitor	ROCK inhibitor
	vs. untreated	vs. untreated	vs. untreated	vs. untreated
$HECV^{WT}$	Increased P<0.001	Reduced P=0.023	Reduced P<0.001	Reduced P=0.013
$HECV^{CL5exp}$	Increased P=0.012	Reduced P=0.001	Reduced P<0.001	Reduced P<0.001
$HECV^{CL5rib2}$	Increased P<0.001	No effect P=0.173	Increased P=0.015	No effect P=0.087

Table 6.2: Data summarizing ECIS results of transfected and control HECV cells after treatments.

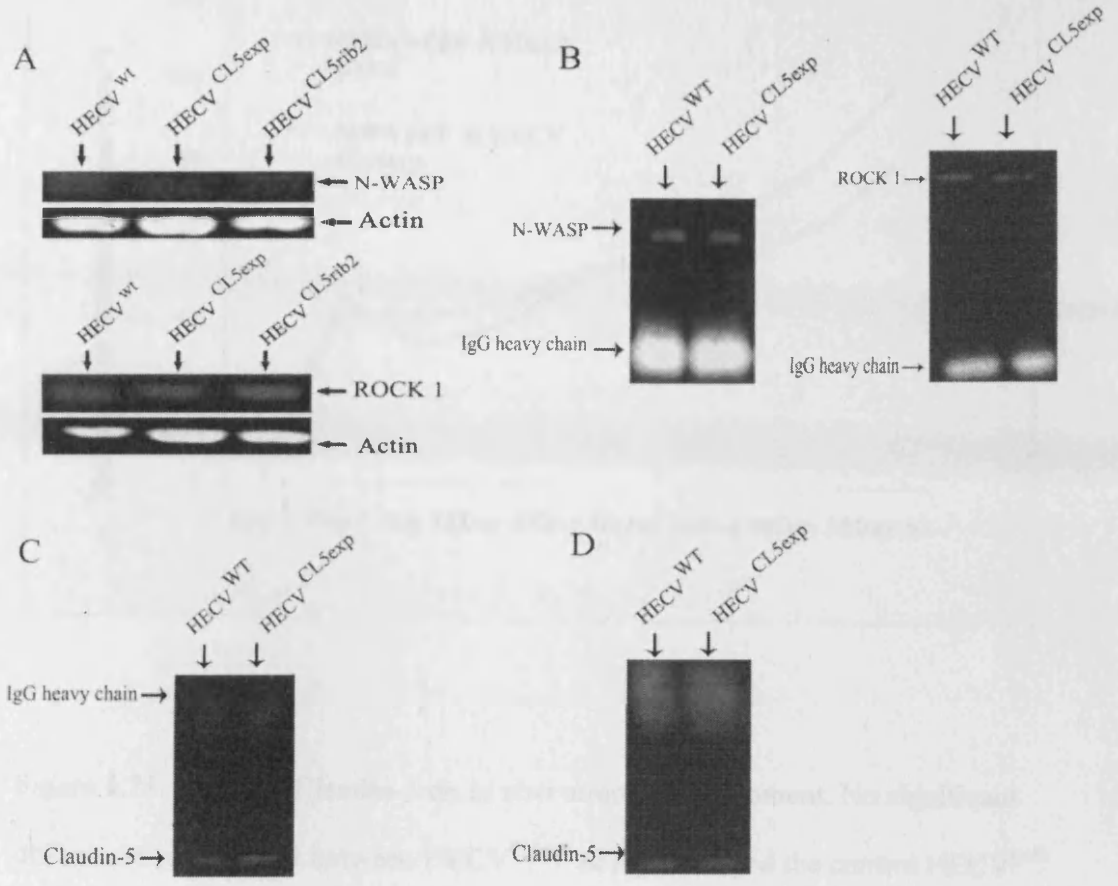

Figure 6.20: (A) Expression of N-WASP and ROCK 1 in transfected and control cells. (B) Co-immunoprecipitation of Claudin-5 with N-WASP and ROCK 1. (C) Co-immunoprecipitation of N-WASP with Claudin-5. (D) Co-immunoprecipitation of ROCK 1 with Claudin-5.

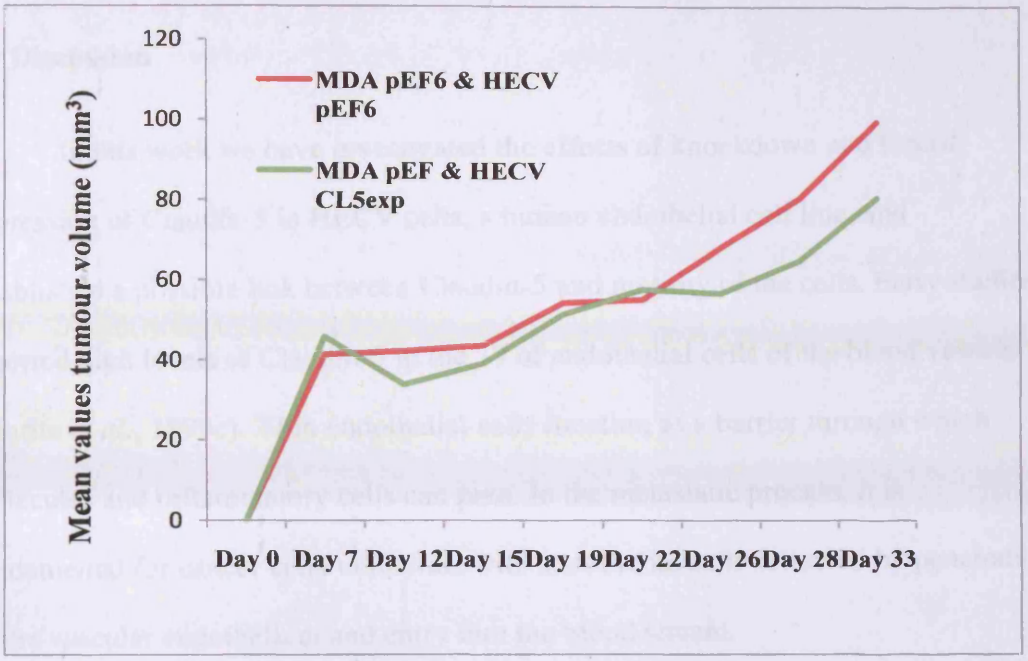

Figure 6.21: Effect of Claudin-5 on *in vivo* tumour development. No significant differences were found between $HECV^{Cl5exp}$ & MDA^{pef6} and the control $HECV^{pef6}$ &MDA^{pef6} using Two-Way ANOVA test (p=0.25).

6.4 Discussion

In this work we have investigated the effects of knockdown and forced expression of Claudin-5 in HECV cells, a human endothelial cell line, and established a possible link between Claudin-5 and motility of the cells. Early studies reported high levels of Claudin-5 in the TJ of endothelial cells of the blood vessels (Morita *et al.*, 1999c). TJ in endothelial cells function as a barrier through which molecules and inflammatory cells can pass. In the metastatic process, it is fundamental for cancer cells to interact with endothelial cells followed by penetration of the vascular endothelium and entry into the blood stream.

The results obtained from measuring Transendothelial electric resistance (TER), the easiest and most sensitive method to assess the resistance formed by the cellular sheets, revealed that $HECV^{CL5rib2}$ cells showed the highest resistance, whereas the resistance of $HECV^{Cl5exp}$ and the control were lower, although $HECV^{Cl5exp}$ cells displayed a significantly higher resistance than the control cells. These preliminary results were an indication of a possible new role of Claudin-5 as it appears not to be involved in keeping the cell barrier tight. One possible explanation might be that the absence of Claudin-5 could be balanced by one of the other 23 members of the Claudin family which might alter the overall barrier strength. A similar explanation could be applied for the forced expression cells and their similar trend shared with the control cells. Thus, interactions and feedback loops between Claudin family members, dependent on expression within a tissue, might be key in regulating TJ stability.

The involvement of Claudin-5 in cell growth was assessed; however, results showed that Claudin-5 had no role in the growth of endothelial cells. Cell adhesion to the extracellular matrix is fundamental for living tissue since there are many activities in mammalian cells *in vivo*, such as mitosis, morphogenesis, cell orientation and cell motility which depend on it (Mitchison and Cramer, 1996). Adhesion is of critical importance for endothelial cells in the context of angiogenesis and wound healing. $HECV^{Cl5exp}$ cells demonstrated a decrease in cell adhesion whereas no significant differences were observed between $HECV^{CL5rib2}$ and control cells. As explained in section 5.4, integrins, among other adhesive molecules, have been proved to be essential in cell adhesion of epithelial and endothelial cells as they give the cell critical signals about the nature of its surroundings (Short *et al.*, 1998). The question therefore arises as to whether the over-expression of Claudin-5 might alter levels of integrins and other adhesion-related proteins, thus, changing the normal adhesive feature of the endothelial cell. To complement these results, the ability of the cells to adhere to a gold electrode through ECIS technology was measured in real time. The results agreed with the *in vitro* cell Matrigel adhesion assay used. Once again, forced expression of Claudin-5 resulted in cells displaying the lowest adherence, as in the Matrigel experiments.

Considering the results from TER experiments, which revealed that the absence of Claudin-5 increases the barrier strength therefore excluding Claudin-5 from a sealing protein role, we studied a possible link between Claudin-5 and cell motility. To achieve this, a set of experiments were carried out in order to assess the grade of involvement of Claudin-5 in cell motility. The *in vitro* cell motility assay alongside a traditional wound healing assay was performed. The results revealed a

significant increase in motility in the knockdown cells when compared to the control cells. In agreement with this, ECIS was used in order to measure motility in real time after the monolayer of cells was wounded. The same results were obtained, i.e. $HECV^{CL5rib2}$ cells appeared to be faster than the control cells. In the case of $HECV^{Cl5exp}$ however, the effect of forced expression of Claudin-5 seems to be opposite and reduced the migration capacity of the cells after wounding, as shown in both the wound healing assay and ECIS, revealing a significant reduction when compared to the control.

Until now, we have shown that knocking down the expression of Claudin-5 in endothelial cells resulted in a more motile cell phenotype, although no differences in adhesion were seen when compared to the control. The opposite was observed when Claudin-5 expression was forced, resulting in less adhesive and less motile cells. Taking all these results together, we can conclude that Claudin-5 might be involved in motility or indeed, be a motility regulator itself.

It has been demonstrated that endothelial cells rapidly form capillary-like or tubule structures *in vitro* when seeded within a sandwich of reconstituted extracellular matrix (ECM) such as Matrigel. The formation of tubules is a process that involves several steps including cell adhesion, cell migration, alignment and protease secretion among others (Arnaoutova *et al.*, 2009). Because the formation of these tubules is quantifiable, we used this assay to assess a possible impact on angiogenic effect when the levels of expression of Claudin-5 are altered in the cells. This provides another technique to assess a possible effect of Claudin-5 in the motile nature of endothelial cells. The results showed that the capacity of $HECV^{CL5rib2}$ cells

to form tubules was significantly increased when compared to the controls, agreeing with results obtained when motility was assessed, whereas for $HECV^{Cl5exp}$ was significantly decreased.

As explained in section 5.4., HGF is routinely used in our laboratories, mostly as a positive control, it is a very powerful angiogenic and motility factor as well as a factor that regulates Tight Tunctions (Jiang *et al.*, 2005). Cells displaying enhanced and reduced expression levels of Claudin-5 respond positively to the effects of HGF. The transfected and control cells showed a reduction in endothelial resistance, an increase in cell motility and an increase in the number of tubules formed. ECIS experiments corroborated these results.

Based on the results obtained in Chapter 5, where MDA-MB-231 cells were treated with a number of motility-regulators in order to search for any possible links between Claudin-5 and a range of motility-related proteins, we treated the cells transfected with Claudin-5 expression sequence and ribozyme transgenes with N-WASP inhibitor, Arp2/3 inhibitor and ROCK inhibitor (see details in section 5.6) to assess the impact on the cell motility using ECIS and the *in vitro* tubule formation assay. The ECIS results revealed that forced expression and control cells respond as expected to all the inhibitors, showing a decrease in the motility. However, the knockdown cells did not follow the same inhibition trend. In fact, the three inhibitors were no longer able to inhibit the motility of the cells where Claudin-5 was absent, suggesting a possible link between Claudin-5 and the signal pathway of N-WASP and ROCK. Other studies have already shown the effect of N-WASP inhibitor in endothelial cells, where the addition of the inhibitor led to almost complete

disappearance of podosomes, which are actin structures responsible amongst others for cell motility (Osiak *et al.*, 2005). Another study has reported that the addition of ROCK inhibitor in endothelial cells prevented transendothelial migration of lung carcinoma cells and changes in the TJ structure in the blood brain-barrier preventing metastasis (Li *et al.*, 2006).

Surprisingly, when Arp2/3 inhibitor was added to the knockdown cells, an increase in motility was observed. An explanation for this unexpected observation could be the complex regulation of F-actin formation and degradation. Actin polymerisation is regulated by a signal transduction pathway that shows many intrinsic positive as well as negative feedback loops. Examples are the positive feedback between PI3K and Rac (Dawes and Edelstein-Keshet, 2007; Weiner *et al.*, 2007) and the negative feedback between Rho and Cdc42 (Dawes and Edelstein-Keshet, 2007). All these molecules are well characterised members of the RhoGTPase family and are key regulators of cytoskeletal dynamics in cells, including those of endothelial origin. A theoretical study has also addressed the activity of Arp2/3 and showed that it operates with an auto-catalytic like mechanism. The activation of Arp2/3 will amplify the level of PI (4,5) P2, a phospholipid component enriched at the plasma membrane where it is a substrate for a number of important signalling proteins, at the leading edge of the cell which again will increase the activity of Arp2/3 (Dawes and Edelstein-Keshet, 2007).

When tubule formation was tested following treatment with the inhibitors, both forced expression and control cells were seen to have a significant reduction in tubule structures formed compared to the untreated cells. However, although

knockdown cells resulted in a decrease in tubule structures formed; differences were no longer significant. These results are linked to the motile nature of endothelial cells, and reveal a possible new role for Claudin-5 related to the N-WASP and ROCK signal pathways. Additional experiments were carried out to study the effect of a combination of HGF and each individual inhibitor. The addition of a combination of HGF/N-WASP inhibitor, HGF/Arp2/3 inhibitor and HGF/ROCK inhibitor significantly negated the effect of HGF in the forced-expression and control cells, however, in the knockdown cells the differences between HGF treatment alone and a mixture of HGF and the inhibitors were not significant. These results agree with our suggestion of a new role for Claudin-5, linked to the N-WASP and ROCK signalling pathways, as the absence of Claudin-5 resulted in cells that did not respond to the inhibitors, and the HGF effect is no longer negated by the inhibitors when combined.

At this point of the study, the next two questions to be addressed were, could there be possible protein-protein interaction between Claudin-5 and N-WASP or Claudin-5 and ROCK, and were there any direct effects that might occur at the protein level of these molecules when the level of expression of Claudin-5 is altered. Co-immunoprecipitation with Claudin-5 followed by immunoblotting with either N-WASP or ROCK 1 demonstrated an interaction between Claduin-5 and N-WASP as well as with ROCK 1. To confirm these interactions, a co-immunoprecipitation with either N-WASP or ROCK 1 followed by immunoblotting with Claudin-5 was carried out confirming the interactions between these protein pairs. The protein level of N-WASP appeared to be very low in the transfected and control cells. In agreement with these results, very low transcript levels of N-WASP in some cells was previously reported. It has been suggested that very high or very low levels of N-

WASP can have the same effect (Martin *et al.*, 2008b). N-WASP and ROCK 1 protein expression did not show any real differences among transfected and control cells in non co-precipitated samples. Together this suggests that Claudin-5 might interact with N-WASP and ROCK 1 in some manner but does not appear to have any direct effect on their expression in HECV cells.

In vivo experiments did not reveal any significant differences in tumour development when HECV cells with forced expression of Claudin-5 were co-injected alongside control MDA-MB-231 breast cancer cells. Unfortunately, at the time of the *in vivo* study the Claudin-5 knockdown cells were unavailable and could not be included, however it would be interesting to see what effect suppressing Claudin-5 in endothelial cells could have on tumour development in this *in vivo* model.

Cell motility is orchestrated by a variety of complicated signal pathways, with most of them just starting to be unravelled. However, understanding cell motility not only requires knowledge of the signal pathways regulating actin polymerization, but also how the components involved in cell motility work together as a dynamic and integrated system. In this study we have investigated the role of Claudin-5 in endothelial cells. Our results have revealed that Claudin-5 is not just a sealing protein in charge of the passage of small ions; in fact, Claudin-5 appears to be involved in cell motility. This proposed new role for Claudin-5 should instigate an interesting avenue for further research into cell motility.

Chapter 7

General discussion

7.1 Breast cancer and metastasis

Breast cancer is the most common cancer diagnosed in women, with over one million of new cases reported each year worldwide. It is widely recognised that the high incidence of breast cancer in the more affluent world areas is due to the presence of screening programs that help to detect early stages of invasive cancers. Every year about half a million new cased of breast cancer are reported in Europe, with 45.000 new cases in the UK.

Breast cancer is characterized by having unusually long latency. It is capable of spreading to a variety of secondary sites that include vital organs such as bone, liver and lungs. The chances of survival from metastatic breast cancer are less than 5%. Therefore, the major focus of research in breast cancer is the prevention and treatment of metastasis. A key factor that determines the metastatic nature of cancer cells is their motility. A defining characteristic of cancer cells is the acquirement of a motile phenotype due to changes in their cytoskeletal architecture. A great deal of evidences exists suggesting that Tight Junctions represent a critical barrier which the motile cancer cells must overcome in order to penetrate and initiate the metastatic cascade. Nevertheless, different studies have shown dysregulation in TJ structure of several cancers including breast. Until the early nineties, TJ were mainly seen as structure with an exclusive task of sealing the gap between two cells, however, recent studies have shown how TJ are involved in the regulation of cell proliferation, gene transcription and cellular differentiation. Among other components of the TJ structure, Claudin family appear to regulate the paracellular barrier of the cells to small ions. However, the role of Claudin proteins in carcinogenesis and progression

to metastasis needs to be unmasked. Therefore, it is not surprising that the role of Claudins has become an active area of research as a result of altered levels of expression observed in different cancers including breast.

7.2 Aims of this thesis

The first aim of this thesis was to examine the role of Claudin-5 in human breast cancer by examining the level of expression and distribution in breast tumour and normal breast tissues and analysing the levels of transcripts against clinical parameters in order to investigate a possible connection between Claudin-5 and the clinical outcome of patients.

This thesis was also aimed to examine the effect of knockdown and forced expression of Claudin-5 in the MDA-MB-231 aggressive breast cancer cell line and in the HECV human endothelial cell line as well as to assess the effect of Claudin-5 forced expression on *in vivo* development of mammary tumours. We also aimed to examine whether the invasive nature of the breast cancer cells, their adherence to matrix, the integrity of the paracellular barrier, their possible role in cell growth and their motility might be compromised in the absence of Claudin-5 as well as when Claudin-5 is overexpressed in the cancer cell. Similarly, we studied the effect of altering Claudin-5 expression in human endothelial cells and the effect caused on their adherence, in the paracellular barrier, in growth, in motility and in their capability to form tubules of the endothelial cells. Finally, the effect on cell motility

after inhibition of N-WASP, ROCK and Arp2/3 complex was assessed in both cell lines.

7.3 Main conclusions from results / significance of this thesis

7.3.1 Claudin-5 and human breast cancer

This thesis has shown for first time that Claudin-5 is aberrantly expressed in human breast cancer and has a link to the clinical outcome of the patient. Patients who died from breast cancer had higher levels of Claudin-5 compared with patients who remained disease-free. Furthermore, patients whose tumours expressed high levels of Claudin-5 had significantly shorter survival than those with low levels of expression of Claudin-5. Thus, it can be seen from this work carried out on human breast tissue samples that Claudin-5 may be a useful prognostic tool in the assessment of patient outcome in breast cancer.

7.3.2 Claudin-5 in MDA-MB-231 breast cancer cells

The results of the TER experiments carried out on MDA-MB-231 breast cancer cells revealed interesting differences between control, over expression and knock down cells. This showed that the role of Claudin-5 was not primarily in keeping the cell barrier tight. In fact, the lack of Claudin-5 might be compensated by one of the other 23 members of the Claudin family.

The results obtained from the *in vitro* tumour cell (Matrigel) adhesion assays agreed with the results from the ECIS attachment experiments; where knockdown

cells were significantly less adhesive than the control cells. However, in real time measurements using ECIS, the forced expression of Claudin-5 gave the cells a significantly enhanced adhesive capacity agreeing with the trend (although not reaching significance) seen in the *in vitro* adhesion assays. Further to this, alteration of Claudin-5 levels of expression did not affect the invasive nature of the MDA-MB-231 breast cancer cells. Our results also showed that alteration of Claudin-5 levels appeared to have no effect on the growth of MDA-MB-231 cells *in vitro* or on tumour growth *in vivo.*

7.3.3 Claudin-5 in HECV human endothelial cells

The measurement of TER in HECV human endothelial cells produced similar results to those demonstrated in MDA-MB-231 breast cancer cells; with differences shown between control, over-expression and knockdown cells. These observations speculate that the absence of Claudin-5 might be balanced by another member of the Claudin family; as previous studies have reported differential expression of Claudin family members in different tissues.

The result of this thesis shows that alteration of Claudin-5 levels in HECV cells was not capable of promoting cell growth *in vitro.*

Manipulation of HECV cells by forced expression of Claudin-5 caused these cells to significantly decrease their adhesive properties both in *in vitro* adhesion assay experiments and using ECIS technology. Interestingly, real time measurements using ECIS revealed significant reduction in adherence in the knockdown cells when compared to the controls which was not seen in the *in vitro* adhesion assays.

The natural ability of endothelial cells to rapidly form capillary-like structures was altered when Claudin-5 was over-expressed, showing a significant decrease in the number of tubules formed. However, the effect was reversed in the absence of Claudin-5 displaying a significantly larger number of tubules formed when compared to the controls. These results clearly indicate that Claudin-5 plays an important role in angiogenesis.

Additionally, the *in vivo* experiments were carried out in order to identify whether forced expression of Claudin-5 in HECV cells, when co-injected with MDA-MB-231 breast cancer cells resulted in any changes in tumour development. No significant differences were found in this experiment. Unfortunately, there were some problems in growing the knockdown cells and hence we were unable to assess the effect of Claudin-5 knockdown on *in vivo* tumour cell development.

7.3.4 Claudin-5 and its role in cell motility

One hallmark of breast cancer cells is their ability to acquire a motile phenotype. The results of a panel of motility assays in MDA-MB-231 revealed that knockdown of Claudin-5 resulted in a significant decrease in cell motility as shown by ECIS and cytodex-2 bead motility assays. The same trend was seen in the wounding assay but did not reach a level of significance. The opposite effect was seen in cells over-expressing Claudin-5, however, only ECIS results reached significance.

Three different cell motility signalling pathways were investigated in relation to altered levels of Claudin-5, namely HGF, N-WASP and ROCK. Results disclosed

that both transfected cells, as well as controls responded in the same way to the addition of HGF. That is, all cells showed reduced TER and increased motility in response to HGF, indicating that Claudin-5 is not linked to the HGF motility signalling pathway.

Control cells treated with either N-WASP inhibitor (Wiskostatin), ROCK inhibitor (Y27632) or Arp2/3 inhibitor (CK-0944636) displayed a decrease in cell motility as shown by ECIS. The transfected cells responded in different ways. Treatment with N-WASP inhibitor caused a highly significant decrease in cell motility in forced expression cells and a less significant effect in the knockdown cells. The Arp2/3 inhibitor showed a similar effect to the N-WASP inhibitor on motility with a highly significant decrease in motility in forced expression cells but no significant change in motility in knockdown cells. These findings are of interest because the Arp2/3 complex acts downstream of N-WASP and this study shows that when Claudin-5 is decreased in the cells the Arp2/3 inhibitor was no longer able to inhibit motility, agreeing with the trend seen when cells were treated with the N-WASP inhibitor, as the knockdown cells showed a reduced response to the inhibitor. ROCK inhibitor did not change the motility of either type of transfected cells indicating a possible connection between the level of expression of Claudin-5 in the cells and the ROCK signalling pathway.

This study is the first to reveal a link between Claudin-5 and cell motility in breast cancer cells. This possible link was also demonstrated when interactions between Claudin-5 and N-WASP, and Claudin-5 and ROCK were investigated in

breast cancer cells by co-immunoprecipitation of Claudin-5 as well as N-WASP and ROCK.

The same panel of experiments was used to analyse the effect of altering levels of expression of Claudin-5 on motility of HECV human endothelial cells. The opposite results were observed in these cells compared with the breast cancer cells. A significant increase in cell motility was seen in all assays including ECIS when Claudin-5 was knocked down. These results agree with the findings of the tubule formation assays as the formation of tubules is a process that involves cell migration.

As with MDA-MB-231 breast cancer cells, the addition of the powerful motogen HGF to the HECV cells increased cell motility, tubule formation and decreased TER across all cell types. These results also indicate that the HGF pathway is not connected to Claudin-5.

The HECV cells were examined after treatment with the same inhibitors used for the MDA-MB-231 breast cancer cells. When cells were treated with N-WASP inhibitor a decrease in cell motility was observed in control and forced expression cells, however, no effect was seen in the cells displaying a reduction in Claudin-5 levels. These results are in agreement with those from the tubule formation assays where addition of N-WASP inhibitor decreased the ability of both transfected cells to form tubules although only reaching significance in the forced expression cells. These results clearly indicate a link between the N-WASP pathway and Claudin-5 as when Claudin-5 levels are reduced the inhibitor's effect was marginal.

When cells were treated with the Arp2/3 inhibitor similar results were obtained as when the N-WASP inhibitor was used. This is not surprising as Arp2/3 complex is seen downstream of N-WASP.

Although ROCK is involved in a different cell motility pathway, the cells responded to the ROCK inhibitor in a parallel way to N-WASP and Arp2/3 complex inhibitors; again showing that the knockdown of Claudin-5 in these cells masked their response to these inhibitors.

Furthermore, with the use of the combination of HGF with each of the inhibitors during tubule formation assays, we saw a negation in the effect of HGF in both control and forced-expression cells. However, the reduction of Claudin-5 levels in HECV cells restored the effects of HGF as the inhibitors were less effective on these cells.

This study is the first to reveal a link between Claudin-5 and cell motility in endothelial cells (Figure 7.1). This possible link was further demonstrated when interactions between Claudin-5 and N-WASP, and Claudin-5 and ROCK 1 were investigated in HECV human endothelial cells by co-immunoprecipitation of Claudin-5 as well as N-WASP and ROCK 1.

This study has revealed the different effects of altering Claudin-5 expression in two different cell types, the human breast cancer cell line MDA-MB-231 and the human endothelial cell line HECV. This study portrays a very new and interesting role for Claudin-5 in cell motility. It is clear from the data presented in my thesis that expression of Claudin-5 in different cell types have different impact on cells

functions: namely Claudin-5 forced expression increases the aggressiveness of breast cancer, but reduces the angiogenic effect on endothelial cells. These two observations have contrasting impact on cancer progression. It is clear that the clinical data of the present study totally support the conclusion from the cellular data on breast cancer cells. Although the angiogenic impacts observed with endothelial cells contradict those seen with breast cancer and breast cancer cells, the following possibilities exist and should be explored in future: 1.Claudin-5 expression in the body. Claudin-5 has been indicated to be mainly expressed in endothelial cells in the central nervous system. It is therefore plausible that the relatively low levels in endothelial cells in mammary gland may only have a minor effect on breast cancer; 2. The level of expression in endothelial cells in breast cancer. In the present study, we have not been able to specifically compare the levels of Claudin-5 in endothelial cells from normal mammary tissues and breast cancer tissues, an important topic to following in future studies. It is possible that Claudin-5 in these two types of tissues (normal vs tumour) do not vary. Together, I believe that the angiogenic effect observed with Claudin-5 may be an important biological observation and its link to disease progression in cancer, particularly in breast cancer, is an exciting topic for future research.

Although Claudin-5 is expressed naturally in both cell lines the effect of altering its expression is different. These results are not contradictory as cancer cells are not normal and do not behave in the same way as normal, healthy cells explaining why the same molecule has different effects when its levels are altered. However, in both parallel studies this thesis proves a link between Claudin-5 and

motility. Many questions still need to be answered but this study has shed light on a possible role for Claudin-5 in the metastasis and progression of human breast cancer.

Figure 7.1: Cell motility pathways. The complexity of cell motility is illustrated. The question marks indicate the missing gap between Caludin-5 and N-WASP, and Claudin-5 and ROCK signalling pathway (Figure modified from Ingenuity Systems, Inc.).

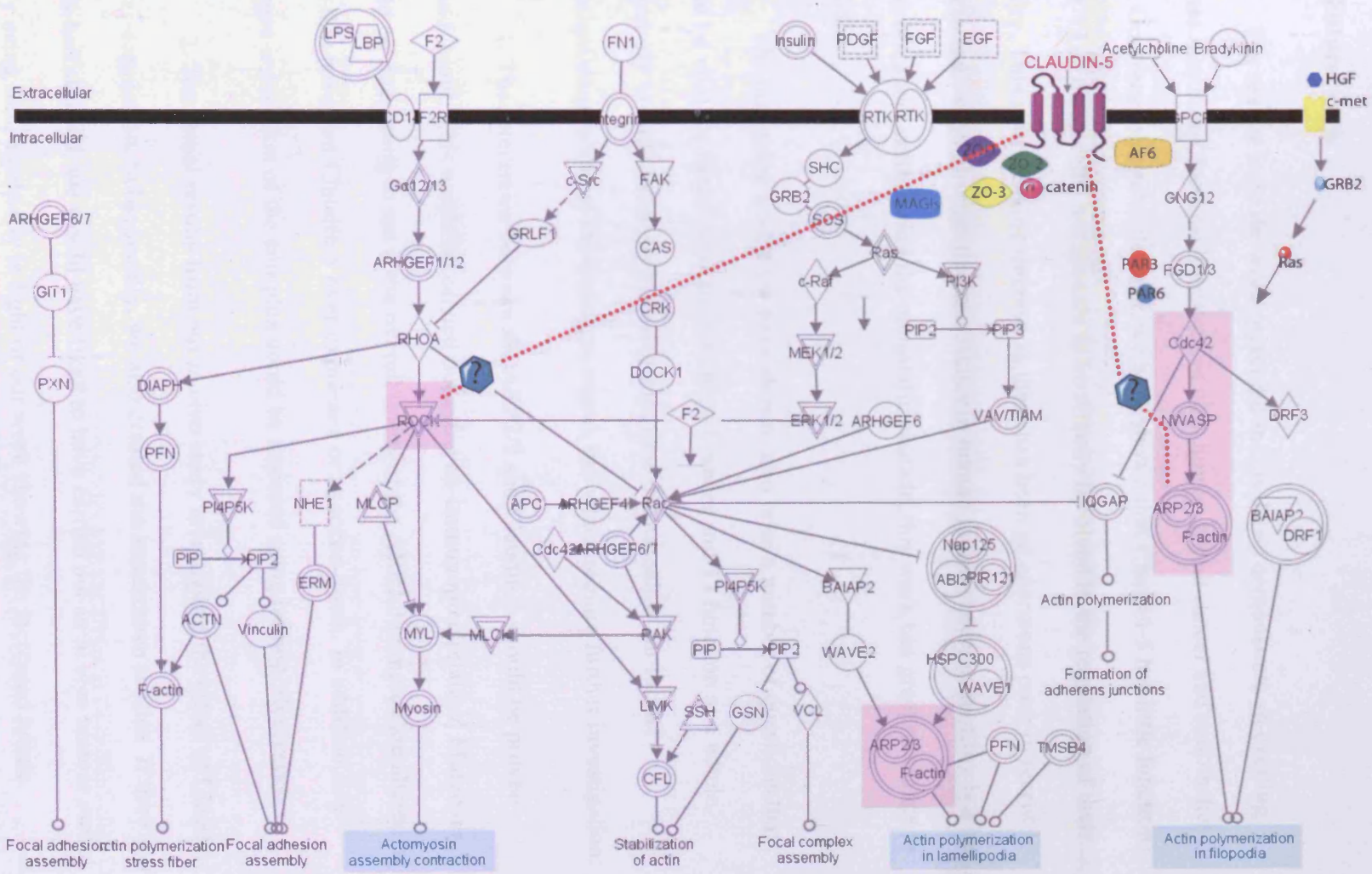

7.4 Future work

The results from the work presented in this thesis demonstrate an exciting glimpse into how Claudin-5 functions in both human breast cancer and endothelial cells. Contrary to popular thought, we have shown that Claudin-5 has little function in the TJ of these cells, but appears to be directly involved in the regulation of their motility. This is of extreme interest, as there has been an enormous push in recent years to find ways of inhibiting metastasis in human breast cancer as motility is a key aspect of cancer cells during the metastatic cascade, this work has great relevance in this field.

The intriguing results we have shown, also raise a number of questions that would be vital for future work on both breast cancer and TJ function as a whole, particularly in endothelial cells. Obviously, time did not allow for further investigation of some of the questions raised, but which require further investigation:

1. The interaction between the ARP2/3 and Claudin-5 should be proved beyond doubt. This would be carried out using co-immunoprecipitation. Moreover, it would be interesting to see if the overall levels of the ARP2/3 complex are altered in cells that have had Claudin-5 over-expressed or knocked-down. In addition, any changes in location of the complex could be assessed using immunofluorescence.

2. The initial results from our *in vivo* study investigated the effect of Claudin-5 over-expression. Subsequently, we also created the knockdown subline. If time and funds had allowed, we would have liked to have carried out an *in vivo* tumour model study using this, especially in light of our work showing the increased tubule

formation obtained from the Claudin-5 knockdown cells. This shows that Claudin-5 has the potential to be a target in anti-angiogenesis therapy, and would provide an avenue of research that would constitute another thesis in itself.

3. From our work, we have shown that Claudin-5 is involved in the signalling pathway related to the N-WASP family for motility and cytoskeletal rearrangements. We did not have sufficient time to investigate this fully; the pathway is complex, with many members. Future work should look at which other members Claudin-5 could have possible interactions with, how it prevents the effect of the N-WASP, Arp2/3 and ROCK inhibitors. Moreover, this is also true for the motility pathway regulated in part by the GEFs, and in our study, the effect that Claudin-5 has on ROCK function. There appears to be some link between both these motility regulators, as shown in Figure 7.1. The question marks indicate our gap in current knowledge, and certainly beg for further research.

4. Both N-WASP and ROCK are activated by GTPase. We would have liked to investigate how this might be turned off by Claudin-5; is the physical interaction between the molecules enough to prevent activation? Or does Claudin-5 have some other effect on these proteins? The phosphorylation status of ROCK and N-WASP in cells with/without Claudin-5 could be assessed.

5. We know from our research shown here, that Claudin-5 did not interrupt the signalling pathway for motility as initiated using HGF. It would be interesting to see if there is a similar response if we used other growth factors, e.g. VEGF, FGF, IGF, EGF, PDGF and other angiogenic factors.

6. Although not shown in this thesis, we also discovered that Claudin-5 directly precipitates with β-catenin. Although we did not have time in the current study to investigate this more thoroughly, it suggests that Claudin-5 might also be involved in the construction of adherens junctions, in addition to being present in TJ (as expected). It might be that there is a dynamic interaction between the Adherens and Tight junctions, as more evidence has shed light on the proteins that although once thought to be specific to a particular junction type, have now been shown to be found in both (Martin TA, personal communication).

The work presented in this thesis has revealed a hitherto unknown role for Claudin-5 in both breast cancer and endothelial cells and has opened an avenue for future work that could be of great interest to the field.

Chapter 8

References

- Ahrens, T., Pertz, O., Haussinger, D., Fauser, C., Schulthess, T., and Engel, J. (2002). Analysis of heterophilic and homophilic interactions of cadherins using the c-Jun/c-Fos dimerization domains. J Biol Chem *277*, 19455-19460.
- Aijaz, S., D'Atri, F., Citi, S., Balda, M. S., and Matter, K. (2005). Binding of GEF-H1 to the tight junction-associated adaptor cingulin results in inhibition of Rho signaling and G1/S phase transition. Dev Cell *8*, 777-786.
- Akhtari, M., Mansuri, J., Newman, K. A., Guise, T. M., and Seth, P. (2008). Biology of breast cancer bone metastasis. Cancer Biol Ther *7*, 3-9.
- Alexandre, M. D., Lu, Q., and Chen, Y. H. (2005). Overexpression of claudin-7 decreases the paracellular Cl- conductance and increases the paracellular Na+ conductance in LLC-PK1 cells. J Cell Sci *118*, 2683-2693.
- Amasheh, S., Milatz, S., Krug, S. M., Markov, A. G., Gunzel, D., Amasheh, M., and Fromm, M. (2009). Tight junction proteins as channel formers and barrier builders. Ann N Y Acad Sci *1165*, 211-219.
- Amasheh, S., Schmidt, T., Mahn, M., Florian, P., Mankertz, J., Tavalali, S., Gitter, A. H., Schulzke, J. D., and Fromm, M. (2005). Contribution of claudin-5 to barrier properties in tight junctions of epithelial cells. Cell Tissue Res *321*, 89-96.
- Anderson, J. M., and Van Itallie, C. M. (1995). Tight junctions and the molecular basis for regulation of paracellular permeability. Am J Physiol *269*, G467-475.
- Angelow, S., Ahlstrom, R., and Yu, A. S. (2008). Biology of claudins. Am J Physiol Renal Physiol *295*, F867-876.

- Angelow, S., El-Husseini, R., Kanzawa, S. A., and Yu, A. S. (2007). Renal localization and function of the tight junction protein, claudin-19. Am J Physiol Renal Physiol *293*, F166-177.
- Arnaoutova, I., George, J., Kleinman, H. K., and Benton, G. (2009). The endothelial cell tube formation assay on basement membrane turns 20: state of the science and the art. Angiogenesis *12*, 267-274.
- Bazzoni, G. (2003). The JAM family of junctional adhesion molecules. Curr Opin Cell Biol *15*, 525-530.
- Ben-Yosef, T., Belyantseva, I. A., Saunders, T. L., Hughes, E. D., Kawamoto, K., Van Itallie, C. M., Beyer, L. A., Halsey, K., Gardner, D. J., Wilcox, E. R., *et al.* (2003). Claudin 14 knockout mice, a model for autosomal recessive deafness DFNB29, are deaf due to cochlear hair cell degeneration. Hum Mol Genet *12*, 2049-2061.
- Berndt, H., and Titze, U. (1969). TNM clinical stage classification of breast cancer. Int J Cancer *4*, 837-844.
- Blasig, I. E., Winkler, L., Lassowski, B., Mueller, S. L., Zuleger, N., Krause, E., Krause, G., Gast, K., Kolbe, M., and Piontek, J. (2006). On the self-association potential of transmembrane tight junction proteins. Cell Mol Life Sci *63*, 505-514.
- Boireau, S., Buchert, M., Samuel, M. S., Pannequin, J., Ryan, J. L., Choquet, A., Chapuis, H., Rebillard, X., Avances, C., Ernst, M., *et al.* (2007). DNA-methylation-dependent alterations of claudin-4 expression in human bladder carcinoma. Carcinogenesis *28*, 246-258.

- Borka, K., Kaliszky, P., Szabo, E., Lotz, G., Kupcsulik, P., Schaff, Z., and Kiss, A. (2007). Claudin expression in pancreatic endocrine tumors as compared with ductal adenocarcinomas. Virchows Arch *450*, 549-557.
- Burek, M., Arias-Loza, P. A., Roewer, N., and Forster, C. Y. (2010). Claudin-5 as a novel estrogen target in vascular endothelium. Arterioscler Thromb Vasc Biol
- Burek, M., and Forster, C. Y. (2009). Cloning and characterization of the murine claudin-5 promoter. Mol Cell Endocrinol *298*, 19-24.
- Busch, C., Hanssen, T. A., Wagener, C., and B, O. B. (2002). Down-regulation of CEACAM1 in human prostate cancer: correlation with loss of cell polarity, increased proliferation rate, and Gleason grade 3 to 4 transition. Hum Pathol *33*, 290-298.
- Carrozzino, F., Pugnale, P., Feraille, E., and Montesano, R. (2009). Inhibition of basal p38 or JNK activity enhances epithelial barrier function through differential modulation of claudin expression. Am J Physiol Cell Physiol *297*, C775-787.
- Carrozzino, F., Soulie, P., Huber, D., Mensi, N., Orci, L., Cano, A., Feraille, E., and Montesano, R. (2005). Inducible expression of Snail selectively increases paracellular ion permeability and differentially modulates tight junction proteins. Am J Physiol Cell Physiol *289*, C1002-1014.
- Carty, N. J., Foggitt, A., Hamilton, C. R., Royle, G. T., and Taylor, I. (1995). Patterns of clinical metastasis in breast cancer: an analysis of 100 patients. Eur J Surg Oncol *21*, 607-608.

- Cereijido, M., Contreras, R. G., Shoshani, L., Flores-Benitez, D., and Larre, I. (2008). Tight junction and polarity interaction in the transporting epithelial phenotype. Biochim Biophys Acta *1778*, 770-793.
- Charoenphandhu, N., Wongdee, K., Tudpor, K., Pandaranandaka, J., and Krishnamra, N. (2007). Chronic metabolic acidosis upregulated claudin mRNA expression in the duodenal enterocytes of female rats. Life Sci *80*, 1729-1737.
- Chen, Z., Zandonatti, M., Jakubowski, D., and Fox, H. S. (1998). Brain capillary endothelial cells express MBEC1, a protein that is related to the Clostridium perfringens enterotoxin receptors. Lab Invest *78*, 353-363.
- Chlenski, A., Ketels, K. V., Korovaitseva, G. I., Talamonti, M. S., Oyasu, R., and Scarpelli, D. G. (2000). Organization and expression of the human zo-2 gene (tjp-2) in normal and neoplastic tissues. Biochim Biophys Acta *1493*, 319-324.
- Chlenski, A., Ketels, K. V., Tsao, M. S., Talamonti, M. S., Anderson, M. R., Oyasu, R., and Scarpelli, D. G. (1999). Tight junction protein ZO-2 is differentially expressed in normal pancreatic ducts compared to human pancreatic adenocarcinoma. Int J Cancer *82*, 137-144.
- Citi, S., Paschoud, S., Pulimeno, P., Timolati, F., De Robertis, F., Jond, L., and Guillemot, L. (2009). The tight junction protein cingulin regulates gene expression and RhoA signaling. Ann N Y Acad Sci *1165*, 88-98.
- Claude, P. (1978). Morphological factors influencing transepithelial permeability: a model for the resistance of the zonula occludens. J Membr Biol *39*, 219-232.

- Colegio, O. R., Van Itallie, C., Rahner, C., and Anderson, J. M. (2003). Claudin extracellular domains determine paracellular charge selectivity and resistance but not tight junction fibril architecture. Am J Physiol Cell Physiol *284*, C1346-1354.
- Cory, G. O., and Ridley, A. J. (2002). Cell motility: braking WAVEs. Nature *418*, 732-733.
- D'Souza, T., Agarwal, R., and Morin, P. J. (2005). Phosphorylation of claudin-3 at threonine 192 by cAMP-dependent protein kinase regulates tight junction barrier function in ovarian cancer cells. J Biol Chem *280*, 26233-26240.
- Daniels, D. L., Cohen, A. R., Anderson, J. M., and Brunger, A. T. (1998). Crystal structure of the hCASK PDZ domain reveals the structural basis of class II PDZ domain target recognition. Nat Struct Biol *5*, 317-325.
- Daugherty, B. L., Ward, C., Smith, T., Ritzenthaler, J. D., and Koval, M. (2007). Regulation of heterotypic claudin compatibility. J Biol Chem *282*, 30005-30013.
- Dawes, A. T., and Edelstein-Keshet, L. (2007). Phosphoinositides and Rho proteins spatially regulate actin polymerization to initiate and maintain directed movement in a one-dimensional model of a motile cell. Biophys J *92*, 744-768.
- Diamond, J. R., Finlayson, C. A., and Borges, V. F. (2009). Hepatic complications of breast cancer. Lancet Oncol *10*, 615-621.
- Dickman, K. G., Hempson, S. J., Anderson, J., Lippe, S., Zhao, L., Burakoff, R., and Shaw, R. D. (2000). Rotavirus alters paracellular permeability and

energy metabolism in Caco-2 cells. Am J Physiol Gastrointest Liver Physiol *279*, G757-766.

- Dovas, A., and Cox, D. (2010). Regulation of WASp by phosphorylation: Activation or other functions? Commun Integr Biol

- Du, D., Xu, F., Yu, L., Zhang, C., Lu, X., Yuan, H., Huang, Q., Zhang, F., Bao, H., Jia, L., *et al.* (2010). The Tight Junction Protein, Occludin, Regulates the Directional Migration of Epithelial Cells. Dev Cell *18*, 52-63.
- Escaffit, F., Boudreau, F., and Beaulieu, J. F. (2005). Differential expression of claudin-2 along the human intestine: Implication of GATA-4 in the maintenance of claudin-2 in differentiating cells. J Cell Physiol *203*, 15-26.
- Fedwick, J. P., Lapointe, T. K., Meddings, J. B., Sherman, P. M., and Buret, A. G. (2005). Helicobacter pylori activates myosin light-chain kinase to disrupt claudin-4 and claudin-5 and increase epithelial permeability. Infect Immun *73*, 7844-7852.
- Felding-Habermann, B., O'Toole, T. E., Smith, J. W., Fransvea, E., Ruggeri, Z. M., Ginsberg, M. H., Hughes, P. E., Pampori, N., Shattil, S. J., Saven, A., and Mueller, B. M. (2001). Integrin activation controls metastasis in human breast cancer. Proc Natl Acad Sci U S A *98*, 1853-1858.
- Findley, M. K., and Koval, M. (2009). Regulation and roles for claudin-family tight junction proteins. IUBMB Life *61*, 431-437.
- Fink, C., Weigel, R., Hembes, T., Lauke-Wettwer, H., Kliesch, S., Bergmann, M., and Brehm, R. H. (2006). Altered expression of ZO-1 and ZO-2 in Sertoli

cells and loss of blood-testis barrier integrity in testicular carcinoma in situ. Neoplasia *8*, 1019-1027.

- Fontijn, R. D., Volger, O. L., Fledderus, J. O., Reijerkerk, A., de Vries, H. E., and Horrevoets, A. J. (2008). SOX-18 controls endothelial-specific claudin-5 gene expression and barrier function. Am J Physiol Heart Circ Physiol *294*, H891-900.
- Forster, A. C., and Symons, R. H. (1987). Self-cleavage of plus and minus RNAs of a virusoid and a structural model for the active sites. Cell *49*, 211-220.
- Fujibe, M., Chiba, H., Kojima, T., Soma, T., Wada, T., Yamashita, T., and Sawada, N. (2004). Thr203 of claudin-1, a putative phosphorylation site for MAP kinase, is required to promote the barrier function of tight junctions. Exp Cell Res *295*, 36-47.
- Fujita, H., Chiba, H., Yokozaki, H., Sakai, N., Sugimoto, K., Wada, T., Kojima, T., Yamashita, T., and Sawada, N. (2006). Differential expression and subcellular localization of claudin-7, -8, -12, -13, and -15 along the mouse intestine. J Histochem Cytochem *54*, 933-944.
- Fujita, K., Katahira, J., Horiguchi, Y., Sonoda, N., Furuse, M., and Tsukita, S. (2000). Clostridium perfringens enterotoxin binds to the second extracellular loop of claudin-3, a tight junction integral membrane protein. FEBS Lett *476*, 258-261.
- Furuse, M., Hata, M., Furuse, K., Yoshida, Y., Haratake, A., Sugitani, Y., Noda, T., Kubo, A., and Tsukita, S. (2002). Claudin-based tight junctions are

crucial for the mammalian epidermal barrier: a lesson from claudin-1-deficient mice. J Cell Biol *156*, 1099-1111.

- Furuse, M., Hirase, T., Itoh, M., Nagafuchi, A., Yonemura, S., and Tsukita, S. (1993). Occludin: a novel integral membrane protein localizing at tight junctions. J Cell Biol *123*, 1777-1788.
- Furuse, M., Itoh, M., Hirase, T., Nagafuchi, A., Yonemura, S., and Tsukita, S. (1994). Direct association of occludin with ZO-1 and its possible involvement in the localization of occludin at tight junctions. J Cell Biol *127*, 1617-1626.
- Furuse, M., Sasaki, H., and Tsukita, S. (1999). Manner of interaction of heterogeneous claudin species within and between tight junction strands. J Cell Biol *147*, 891-903.
- Furuse, M., and Tsukita, S. (2006). Claudins in occluding junctions of humans and flies. Trends Cell Biol *16*, 181-188.
- Gerhard, D. S., Wagner, L., Feingold, E. A., Shenmen, C. M., Grouse, L. H., Schuler, G., Klein, S. L., Old, S., Rasooly, R., Good, P., *et al.* (2004). The status, quality, and expansion of the NIH full-length cDNA project: the Mammalian Gene Collection (MGC). Genome Res *14*, 2121-2127.
- Glaunsinger, B. A., Weiss, R. S., Lee, S. S., and Javier, R. (2001). Link of the unique oncogenic properties of adenovirus type 9 E4-ORF1 to a select interaction with the candidate tumor suppressor protein ZO-2. EMBO J *20*, 5578-5586.
- Gospodarowicz, M. K., Miller, D., Groome, P. A., Greene, F. L., Logan, P. A., and Sobin, L. H. (2004). The process for continuous improvement of the TNM classification. Cancer *100*, 1-5.

- Gow, A., Davies, C., Southwood, C. M., Frolenkov, G., Chrustowski, M., Ng, L., Yamauchi, D., Marcus, D. C., and Kachar, B. (2004). Deafness in Claudin 11-null mice reveals the critical contribution of basal cell tight junctions to stria vascularis function. J Neurosci *24*, 7051-7062.
- Gow, A., Southwood, C. M., Li, J. S., Pariali, M., Riordan, G. P., Brodie, S. E., Danias, J., Bronstein, J. M., Kachar, B., and Lazzarini, R. A. (1999). CNS myelin and sertoli cell tight junction strands are absent in Osp/claudin-11 null mice. Cell *99*, 649-659.
- Grise, F., Bidaud, A., and Moreau, V. (2009). Rho GTPases in hepatocellular carcinoma. Biochim Biophys Acta *1795*, 137-151.
- Guerriero, C. J., and Weisz, O. A. (2007). N-WASP inhibitor wiskostatin nonselectively perturbs membrane transport by decreasing cellular ATP levels. Am J Physiol Cell Physiol *292*, C1562-1566.
- Guillemot, L., Paschoud, S., Pulimeno, P., Foglia, A., and Citi, S. (2008). The cytoplasmic plaque of tight junctions: a scaffolding and signalling center. Biochim Biophys Acta *1778*, 601-613.
- Guttman, J. A., and Finlay, B. B. (2009). Tight junctions as targets of infectious agents. Biochim Biophys Acta *1788*, 832-841.
- Hadj-Rabia, S., Baala, L., Vabres, P., Hamel-Teillac, D., Jacquemin, E., Fabre, M., Lyonnet, S., De Prost, Y., Munnich, A., Hadchouel, M., and Smahi, A. (2004). Claudin-1 gene mutations in neonatal sclerosing cholangitis associated with ichthyosis: a tight junction disease. Gastroenterology *127*, 1386-1390.

- Hall, A. (1998). Rho GTPases and the actin cytoskeleton. Science *279*, 509-514.
- Haorah, J., Heilman, D., Knipe, B., Chrastil, J., Leibhart, J., Ghorpade, A., Miller, D. W., and Persidsky, Y. (2005). Ethanol-induced activation of myosin light chain kinase leads to dysfunction of tight junctions and blood-brain barrier compromise. Alcohol Clin Exp Res *29*, 999-1009.
- Haseloff, J., and Gerlach, W. L. (1989). Sequences required for self-catalysed cleavage of the satellite RNA of tobacco ringspot virus. Gene *82*, 43-52.
- Hoevel, T., Macek, R., Mundigl, O., Swisshelm, K., and Kubbies, M. (2002). Expression and targeting of the tight junction protein CLDN1 in CLDN1-negative human breast tumor cells. J Cell Physiol *191*, 60-68.
- Hoover, K. B., Liao, S. Y., and Bryant, P. J. (1998). Loss of the tight junction MAGUK ZO-1 in breast cancer: relationship to glandular differentiation and loss of heterozygosity. Am J Pathol *153*, 1767-1773.
- Huerta, M., Munoz, R., Tapia, R., Soto-Reyes, E., Ramirez, L., Recillas-Targa, F., Gonzalez-Mariscal, L., and Lopez-Bayghen, E. (2007). Cyclin D1 is transcriptionally down-regulated by ZO-2 via an E box and the transcription factor c-Myc. Mol Biol Cell *18*, 4826-4836.
- Ikenouchi, J., Furuse, M., Furuse, K., Sasaki, H., and Tsukita, S. (2005). Tricellulin constitutes a novel barrier at tricellular contacts of epithelial cells. J Cell Biol *171*, 939-945.
- Ikenouchi, J., Matsuda, M., Furuse, M., and Tsukita, S. (2003). Regulation of tight junctions during the epithelium-mesenchyme transition: direct

repression of the gene expression of claudins/occludin by Snail. J Cell Sci *116*, 1959-1967.

- Insall, R. H., and Jones, G. E. (2006). Moving matters: signals and mechanisms in directed cell migration. Nat Cell Biol *8*, 776-779.
- Ishizaki, T., Chiba, H., Kojima, T., Fujibe, M., Soma, T., Miyajima, H., Nagasawa, K., Wada, I., and Sawada, N. (2003). Cyclic AMP induces phosphorylation of claudin-5 immunoprecipitates and expression of claudin-5 gene in blood-brain-barrier endothelial cells via protein kinase A-dependent and -independent pathways. Exp Cell Res *290*, 275-288.
- Ivanov, A. I., Hunt, D., Utech, M., Nusrat, A., and Parkos, C. A. (2005). Differential roles for actin polymerization and a myosin II motor in assembly of the epithelial apical junctional complex. Mol Biol Cell *16*, 2636-2650.
- Jiang, W. G., Bryce, R. P., Horrobin, D. F., and Mansel, R. E. (1998). Regulation of tight junction permeability and occludin expression by polyunsaturated fatty acids. Biochem Biophys Res Commun *244*, 414-420.
- Jiang, W. G., Hiscox, S., Hallett, M. B., Scott, C., Horrobin, D. F., and Puntis, M. C. (1995a). Inhibition of hepatocyte growth factor-induced motility and in vitro invasion of human colon cancer cells by gamma-linolenic acid. Br J Cancer *71*, 744-752.
- Jiang, W. G., Hiscox, S., Singhrao, S. K., Nakamura, T., Puntis, M. C., and Hallett, M. B. (1995b). Inhibition of HGF/SF-induced membrane ruffling and cell motility by transient elevation of cytosolic free Ca2+. Exp Cell Res *220*, 424-433.

- Jiang, W. G., Hiscox, S. E., Parr, C., Martin, T. A., Matsumoto, K., Nakamura, T., and Mansel, R. E. (1999a). Antagonistic effect of NK4, a novel hepatocyte growth factor variant, on in vitro angiogenesis of human vascular endothelial cells. Clin Cancer Res *5*, 3695-3703.
- Jiang, W. G., Martin, T. A., Matsumoto, K., Nakamura, T., and Mansel, R. E. (1999b). Hepatocyte growth factor/scatter factor decreases the expression of occludin and transendothelial resistance (TER) and increases paracellular permeability in human vascular endothelial cells. J Cell Physiol *181*, 319-329.
- Jiang, W. G., Martin, T. A., Parr, C., Davies, G., Matsumoto, K., and Nakamura, T. (2005). Hepatocyte growth factor, its receptor, and their potential value in cancer therapies. Crit Rev Oncol Hematol *53*, 35-69.
- Jonsson, A. S., and Palmblad, J. E. (2001). Effects of ethanol on NF-kappaB activation, production of myeloid growth factors, and adhesive events in human endothelial cells. J Infect Dis *184*, 761-769.
- Kakutani, H., Kondoh, M., Saeki, R., Fujii, M., Watanabe, Y., Mizuguchi, H., and Yagi, K. (2010). Claudin-4-targeting of diphtheria toxin fragment A using a C-terminal fragment of Clostridium perfringens enterotoxin. Eur J Pharm Biopharm.
- Katsuno, T., Umeda, K., Matsui, T., Hata, M., Tamura, A., Itoh, M., Takeuchi, K., Fujimori, T., Nabeshima, Y., Noda, T., and Tsukita, S. (2008). Deficiency of zonula occludens-1 causes embryonic lethal phenotype associated with defected yolk sac angiogenesis and apoptosis of embryonic cells. Mol Biol Cell *19*, 2465-2475.

- Keese, C. R., Wegener, J., Walker, S. R., and Giaever, I. (2004). Electrical wound-healing assay for cells in vitro. Proc Natl Acad Sci U S A *101*, 1554-1559.
- Keiper, T., Al-Fakhri, N., Chavakis, E., Athanasopoulos, A. N., Isermann, B., Herzog, S., Saffrich, R., Hersemeyer, K., Bohle, R. M., Haendeler, J., *et al.* (2005). The role of junctional adhesion molecule-C (JAM-C) in oxidized LDL-mediated leukocyte recruitment. FASEB J *19*, 2078-2080.
- Kimura, Y., Shiozaki, H., Hirao, M., Maeno, Y., Doki, Y., Inoue, M., Monden, T., Ando-Akatsuka, Y., Furuse, M., Tsukita, S., and Monden, M. (1997). Expression of occludin, tight-junction-associated protein, in human digestive tract. Am J Pathol *151*, 45-54.
- Kinugasa, T., Huo, Q., Higashi, D., Shibaguchi, H., Kuroki, M., Tanaka, T., Futami, K., Yamashita, Y., Hachimine, K., Maekawa, S., *et al.* (2007). Selective up-regulation of claudin-1 and claudin-2 in colorectal cancer. Anticancer Res *27*, 3729-3734.
- Kitajiri, S. I., Furuse, M., Morita, K., Saishin-Kiuchi, Y., Kido, H., Ito, J., and Tsukita, S. (2004). Expression patterns of claudins, tight junction adhesion molecules, in the inner ear. Hear Res *187*, 25-34.
- Kleeff, J., Shi, X., Bode, H. P., Hoover, K., Shrikhande, S., Bryant, P. J., Korc, M., Buchler, M. W., and Friess, H. (2001). Altered expression and localization of the tight junction protein ZO-1 in primary and metastatic pancreatic cancer. Pancreas *23*, 259-265.

- Kolonel, L. N., Altshuler, D., and Henderson, B. E. (2004). The multiethnic cohort study: exploring genes, lifestyle and cancer risk. Nat Rev Cancer *4*, 519-527.
- Kominsky, S. L. (2006). Claudins: emerging targets for cancer therapy. Expert Rev Mol Med *8*, 1-11.
- Kominsky, S. L., Argani, P., Korz, D., Evron, E., Raman, V., Garrett, E., Rein, A., Sauter, G., Kallioniemi, O. P., and Sukumar, S. (2003). Loss of the tight junction protein claudin-7 correlates with histological grade in both ductal carcinoma in situ and invasive ductal carcinoma of the breast. Oncogene *22*, 2021-2033.
- Kominsky, S. L., Vali, M., Korz, D., Gabig, T. G., Weitzman, S. A., Argani, P., and Sukumar, S. (2004). Clostridium perfringens enterotoxin elicits rapid and specific cytolysis of breast carcinoma cells mediated through tight junction proteins claudin 3 and 4. Am J Pathol *164*, 1627-1633.
- Kondoh, M., and Yagi, K. (2007). Tight junction modulators: promising candidates for drug delivery. Curr Med Chem *14*, 2482-2488.
- Konrad, M., Schaller, A., Seelow, D., Pandey, A. V., Waldegger, S., Lesslauer, A., Vitzthum, H., Suzuki, Y., Luk, J. M., Becker, C., *et al.* (2006). Mutations in the tight-junction gene claudin 19 (CLDN19) are associated with renal magnesium wasting, renal failure, and severe ocular involvement. Am J Hum Genet *79*, 949-957.
- Kramer, F., White, K., Kubbies, M., Swisshelm, K., and Weber, B. H. (2000). Genomic organization of claudin-1 and its assessment in hereditary and sporadic breast cancer. Hum Genet *107*, 249-256.

- Krause, G., Winkler, L., Mueller, S. L., Haseloff, R. F., Piontek, J., and Blasig, I. E. (2008). Structure and function of claudins. Biochim Biophys Acta *1778*, 631-645.
- Lane, J., Martin, T. A., Watkins, G., Mansel, R. E., and Jiang, W. G. (2008). The expression and prognostic value of ROCK I and ROCK II and their role in human breast cancer. Int J Oncol *33*, 585-593.
- Li, B., Zhao, W. D., Tan, Z. M., Fang, W. G., Zhu, L., and Chen, Y. H. (2006). Involvement of Rho/ROCK signalling in small cell lung cancer migration through human brain microvascular endothelial cells. FEBS Lett *580*, 4252-4260.
- Lie, P. P., Chan, A. Y., Mruk, D. D., Lee, W. M., and Cheng, C. Y. (2010). Restricted Arp3 expression in the testis prevents blood-testis barrier disruption during junction restructuring at spermatogenesis. Proc Natl Acad Sci U S A.
- Lipschutz, J. H., Li, S., Arisco, A., and Balkovetz, D. F. (2005). Extracellular signal-regulated kinases 1/2 control claudin-2 expression in Madin-Darby canine kidney strain I and II cells. J Biol Chem *280*, 3780-3788.
- Litkouhi, B., Kwong, J., Lo, C. M., Smedley, J. G., 3rd, McClane, B. A., Aponte, M., Gao, Z., Sarno, J. L., Hinners, J., Welch, W. R., *et al.* (2007). Claudin-4 overexpression in epithelial ovarian cancer is associated with hypomethylation and is a potential target for modulation of tight junction barrier function using a C-terminal fragment of Clostridium perfringens enterotoxin. Neoplasia *9*, 304-314.

- Liu, Y., Sun, W., Zhang, K., Zheng, H., Ma, Y., Lin, D., Zhang, X., Feng, L., Lei, W., Zhang, Z., *et al.* (2007). Identification of genes differentially expressed in human primary lung squamous cell carcinoma. Lung Cancer *56*, 307-317.
- Lu, X., and Kang, Y. (2007). Organotropism of breast cancer metastasis. J Mammary Gland Biol Neoplasia *12*, 153-162.
- Martin, T. A., Das, T., Mansel, R. E., and Jiang, W. G. (2006). Synergistic regulation of endothelial tight junctions by antioxidant (Se) and polyunsaturated lipid (GLA) via Claudin-5 modulation. J Cell Biochem *98*, 1308-1319.
- Martin, T. A., Das, T., Mansel, R. E., and Jiang, W. G. (2007). Enhanced tight junction function in human breast cancer cells by antioxidant, selenium and polyunsaturated lipid. J Cell Biochem *101*, 155-166.
- Martin, T. A., Harrison, G. M., Watkins, G., and Jiang, W. G. (2008a). Claudin-16 reduces the aggressive behavior of human breast cancer cells. J Cell Biochem *105*, 41-52.
- Martin, T. A., and Jiang, W. G. (2009). Loss of tight junction barrier function and its role in cancer metastasis. Biochim Biophys Acta *1788*, 872-891.
- Martin, T. A., Mansel, R. E., and Jiang, W. G. (2002). Antagonistic effect of NK4 on HGF/SF induced changes in the transendothelial resistance (TER) and paracellular permeability of human vascular endothelial cells. J Cell Physiol *192*, 268-275.
- Martin, T. A., Pereira, G., Watkins, G., Mansel, R. E., and Jiang, W. G. (2008b). N-WASP is a putative tumour suppressor in breast cancer cells, in

vitro and in vivo, and is associated with clinical outcome in patients with breast cancer. Clin Exp Metastasis *25*, 97-108.

- Martin, T. A., Watkins, G., Mansel, R. E., and Jiang, W. G. (2004a). Hepatocyte growth factor disrupts tight junctions in human breast cancer cells. Cell Biol Int *28*, 361-371.
- Martin, T. A., Watkins, G., Mansel, R. E., and Jiang, W. G. (2004b). Loss of tight junction plaque molecules in breast cancer tissues is associated with a poor prognosis in patients with breast cancer. Eur J Cancer *40*, 2717-2725.
- Matter, K., and Balda, M. S. (2007). Epithelial tight junctions, gene expression and nucleo-junctional interplay. J Cell Sci *120*, 1505-1511.
- McPherson, K., Steel, C. M., and Dixon, J. M. (2000). ABC of breast diseases. Breast cancer-epidemiology, risk factors, and genetics. BMJ *321*, 624-628.
- McSherry, E. A., McGee, S. F., Jirstrom, K., Doyle, E. M., Brennan, D. J., Landberg, G., Dervan, P. A., Hopkins, A. M., and Gallagher, W. M. (2009). JAM-A expression positively correlates with poor prognosis in breast cancer patients. Int J Cancer *125*, 1343-1351.
- Michl, P., Barth, C., Buchholz, M., Lerch, M. M., Rolke, M., Holzmann, K. H., Menke, A., Fensterer, H., Giehl, K., Lohr, M., *et al.* (2003). Claudin-4 expression decreases invasiveness and metastatic potential of pancreatic cancer. Cancer Res *63*, 6265-6271.
- Mitchison, T. J., and Cramer, L. P. (1996). Actin-based cell motility and cell locomotion. Cell *84*, 371-379.

- Mitic, L. L., and Anderson, J. M. (1998). Molecular architecture of tight junctions. Annu Rev Physiol *60*, 121-142.
- Miyamoto, T., Morita, K., Takemoto, D., Takeuchi, K., Kitano, Y., Miyakawa, T., Nakayama, K., Okamura, Y., Sasaki, H., Miyachi, Y., *et al.* (2005). Tight junctions in Schwann cells of peripheral myelinated axons: a lesson from claudin-19-deficient mice. J Cell Biol *169*, 527-538.
- Montgomery, E., Mamelak, A. J., Gibson, M., Maitra, A., Sheikh, S., Amr, S. S., Yang, S., Brock, M., Forastiere, A., Zhang, S., *et al.* (2006). Overexpression of claudin proteins in esophageal adenocarcinoma and its precursor lesions. Appl Immunohistochem Mol Morphol *14*, 24-30.
- Morita, K., Furuse, M., Fujimoto, K., and Tsukita, S. (1999a). Claudin multigene family encoding four-transmembrane domain protein components of tight junction strands. Proc Natl Acad Sci U S A *96*, 511-516.
- Morita, K., Sasaki, H., Fujimoto, K., Furuse, M., and Tsukita, S. (1999b). Claudin-11/OSP-based tight junctions of myelin sheaths in brain and Sertoli cells in testis. J Cell Biol *145*, 579-588.
- Morita, K., Sasaki, H., Furuse, M., and Tsukita, S. (1999c). Endothelial claudin: claudin-5/TMVCF constitutes tight junction strands in endothelial cells. J Cell Biol *147*, 185-194.
- Morohashi, S., Kusumi, T., Sato, F., Odagiri, H., Chiba, H., Yoshihara, S., Hakamada, K., Sasaki, M., and Kijima, H. (2007). Decreased expression of claudin-1 correlates with recurrence status in breast cancer. Int J Mol Med *20*, 139-143.

- Muller, D., Kausalya, P. J., Meij, I. C., and Hunziker, W. (2006). Familial hypomagnesemia with hypercalciuria and nephrocalcinosis: blocking endocytosis restores surface expression of a novel Claudin-16 mutant that lacks the entire C-terminal cytosolic tail. Hum Mol Genet *15*, 1049-1058.
- Muresan, Z., Paul, D. L., and Goodenough, D. A. (2000). Occludin 1B, a variant of the tight junction protein occludin. Mol Biol Cell *11*, 627-634.
- Naik, M. U., Naik, T. U., Suckow, A. T., Duncan, M. K., and Naik, U. P. (2008). Attenuation of junctional adhesion molecule-A is a contributing factor for breast cancer cell invasion. Cancer Res *68*, 2194-2203.
- Navarro, C., Nola, S., Audebert, S., Santoni, M. J., Arsanto, J. P., Ginestier, C., Marchetto, S., Jacquemier, J., Isnardon, D., Le Bivic, A., *et al.* (2005). Junctional recruitment of mammalian Scribble relies on E-cadherin engagement. Oncogene *24*, 4330-4339.
- Niimi, T., Nagashima, K., Ward, J. M., Minoo, P., Zimonjic, D. B., Popescu, N. C., and Kimura, S. (2001). claudin-18, a novel downstream target gene for the T/EBP/NKX2.1 homeodomain transcription factor, encodes lung- and stomach-specific isoforms through alternative splicing. Mol Cell Biol *21*, 7380-7390.
- Nishimura, Y., Itoh, K., Yoshioka, K., Tokuda, K., and Himeno, M. (2003). Overexpression of ROCK in human breast cancer cells: evidence that ROCK activity mediates intracellular membrane traffic of lysosomes. Pathol Oncol Res *9*, 83-95.

- Nitta, T., Hata, M., Gotoh, S., Seo, Y., Sasaki, H., Hashimoto, N., Furuse, M., and Tsukita, S. (2003). Size-selective loosening of the blood-brain barrier in claudin-5-deficient mice. J Cell Biol *161*, 653-660.
- Nolan, M. E., Aranda, V., Lee, S., Lakshmi, B., Basu, S., Allred, D. C., and Muthuswamy, S. K. (2008). The polarity protein Par6 induces cell proliferation and is overexpressed in breast cancer. Cancer Res *68*, 8201-8209.
- Nolen, B. J., Tomasevic, N., Russell, A., Pierce, D. W., Jia, Z., McCormick, C. D., Hartman, J., Sakowicz, R., and Pollard, T. D. (2009). Characterization of two classes of small molecule inhibitors of Arp2/3 complex. Nature *460*, 1031-1034.
- Nunes, F. D., Lopez, L. N., Lin, H. W., Davies, C., Azevedo, R. B., Gow, A., and Kachar, B. (2006). Distinct subdomain organization and molecular composition of a tight junction with adherens junction features. J Cell Sci *119*, 4819-4827.
- Ohkubo, T., and Ozawa, M. (2004). The transcription factor Snail downregulates the tight junction components independently of E-cadherin downregulation. J Cell Sci *117*, 1675-1685.
- Oliveira, S. S., and Morgado-Diaz, J. A. (2007). Claudins: multifunctional players in epithelial tight junctions and their role in cancer. Cell Mol Life Sci *64*, 17-28.
- Osanai, M., Murata, M., Chiba, H., Kojima, T., and Sawada, N. (2007a). Epigenetic silencing of claudin-6 promotes anchorage-independent growth of breast carcinoma cells. Cancer Sci *98*, 1557-1562.

- Osanai, M., Murata, M., Nishikiori, N., Chiba, H., Kojima, T., and Sawada, N. (2006). Epigenetic silencing of occludin promotes tumorigenic and metastatic properties of cancer cells via modulations of unique sets of apoptosis-associated genes. Cancer Res *66*, 9125-9133.
- Osanai, M., Murata, M., Nishikiori, N., Chiba, H., Kojima, T., and Sawada, N. (2007b). Occludin-mediated premature senescence is a fail-safe mechanism against tumorigenesis in breast carcinoma cells. Cancer Sci *98*, 1027-1034.
- Oshima, T., Blaschuk, O., Gour, B., Symonds, M., Elrod, J. W., Sasaki, M., Jackson, T. H., and Alexander, J. S. (2003). Tight junction peptide antagonists enhance neutrophil trans-endothelial chemotaxis. Life Sci *73*, 1729-1740.
- Osiak, A. E., Zenner, G., and Linder, S. (2005). Subconfluent endothelial cells form podosomes downstream of cytokine and RhoGTPase signaling. Exp Cell Res *307*, 342-353.
- Parish, C. R., Jakobsen, K. B., and Coombe, D. R. (1992). A basement-membrane permeability assay which correlates with the metastatic potential of tumour cells. Int J Cancer *52*, 378-383.
- Parkin, D. M., Bray, F., Ferlay, J., and Pisani, P. (2005) Global cancer statistics, 2002.
- Paschoud, S., Bongiovanni, M., Pache, J. C., and Citi, S. (2007). Claudin-1 and claudin-5 expression patterns differentiate lung squamous cell carcinomas from adenocarcinomas. Mod Pathol *20*, 947-954.
- Peter, Y., Comellas, A., Levantini, E., Ingenito, E. P., and Shapiro, S. D. (2009). Epidermal growth factor receptor and claudin-2 participate in A549

permeability and remodeling: implications for non-small cell lung cancer tumor colonization. Mol Carcinog *48*, 488-497.

- Piontek, J., Winkler, L., Wolburg, H., Muller, S. L., Zuleger, N., Piehl, C., Wiesner, B., Krause, G., and Blasig, I. E. (2008). Formation of tight junction: determinants of homophilic interaction between classic claudins. FASEB J *22*, 146-158.
- Polette, M., Gilles, C., Nawrocki-Raby, B., Lohi, J., Hunziker, W., Foidart, J. M., and Birembaut, P. (2005). Membrane-type 1 matrix metalloproteinase expression is regulated by zonula occludens-1 in human breast cancer cells. Cancer Res *65*, 7691-7698.
- Rahner, C., Mitic, L. L., and Anderson, J. M. (2001). Heterogeneity in expression and subcellular localization of claudins 2, 3, 4, and 5 in the rat liver, pancreas, and gut. Gastroenterology *120*, 411-422.
- Resnick, M. B., Konkin, T., Routhier, J., Sabo, E., and Pricolo, V. E. (2005). Claudin-1 is a strong prognostic indicator in stage II colonic cancer: a tissue microarray study. Mod Pathol *18*, 511-518.
- Riazuddin, S., Ahmed, Z. M., Fanning, A. S., Lagziel, A., Kitajiri, S., Ramzan, K., Khan, S. N., Chattaraj, P., Friedman, P. L., Anderson, J. M., *et al.* (2006). Tricellulin is a tight-junction protein necessary for hearing. Am J Hum Genet *79*, 1040-1051.
- Ridley, A. J., Paterson, H. F., Johnston, C. L., Diekmann, D., and Hall, A. (1992). The small GTP-binding protein rac regulates growth factor-induced membrane ruffling. Cell *70*, 401-410.

- Robenek, H., Schopper, C., Fasske, E., Fetting, R., and Themann, H. (1981). Structure and function of the junctional complement of spontaneous and transplanted murine mammary carcinomas. J Submicrosc Cytol *13*, 347-363.
- Rodewald, M., Herr, D., Duncan, W. C., Fraser, H. M., Hack, G., Konrad, R., Gagsteiger, F., Kreienberg, R., and Wulff, C. (2009). Molecular mechanisms of ovarian hyperstimulation syndrome: paracrine reduction of endothelial claudin 5 by hCG in vitro is associated with increased endothelial permeability. Hum Reprod *24*, 1191-1199.
- Rodewald, M., Herr, D., Fraser, H. M., Hack, G., Kreienberg, R., and Wulff, C. (2007). Regulation of tight junction proteins occludin and claudin 5 in the primate ovary during the ovulatory cycle and after inhibition of vascular endothelial growth factor. Mol Hum Reprod *13*, 781-789.
- Saeki, R., Kondoh, M., Kakutani, H., Matsuhisa, K., Takahashi, A., Suzuki, H., Kakamu, Y., Watari, A., and Yagi, K. (2010). A claudin-targeting molecule as an inhibitor of tumor metastasis. J Pharmacol Exp Ther
- Saeki, R., Kondoh, M., Kakutani, H., Tsunoda, S., Mochizuki, Y., Hamakubo, T., Tsutsumi, Y., Horiguchi, Y., and Yagi, K. (2009). A novel tumor-targeted therapy using a claudin-4-targeting molecule. Mol Pharmacol *76*, 918-926.
- Saitou, M., Furuse, M., Sasaki, H., Schulzke, J. D., Fromm, M., Takano, H., Noda, T., and Tsukita, S. (2000). Complex phenotype of mice lacking occludin, a component of tight junction strands. Mol Biol Cell *11*, 4131-4142.
- Sakaguchi, T., Suzuki, S., Higashi, H., Inaba, K., Nakamura, S., Baba, S., Kato, T., and Konno, H. (2008). Expression of tight junction protein claudin-

5 in tumor vessels and sinusoidal endothelium in patients with hepatocellular carcinoma. J Surg Res *147*, 123-131.

- Sanders, A. J., Guo, X., Mason, M. D., and Jiang, W. G. (2010). IL-17B Can Impact on Endothelial Cellular Traits Linked to Tumour Angiogenesis. J Oncol.
- Sauer, T., Pedersen, M. K., Ebeltoft, K., and Naess, O. (2005). Reduced expression of Claudin-7 in fine needle aspirates from breast carcinomas correlate with grading and metastatic disease. Cytopathology *16*, 193-198.
- Scanlan, M. J., Ritter, G., Yin, B. W., Williams, C., Jr., Cohen, L. S., Coplan, K. A., Fortunato, S. R., Frosina, D., Lee, S. Y., Murray, A. E., *et al.* (2006). Glycoprotein A34, a novel target for antibody-based cancer immunotherapy. Cancer Immun *6*, 2.
- Schneeberger, E. E. (2003). Claudins form ion-selective channels in the paracellular pathway. Focus on "Claudin extracellular domains determine paracellular charge selectively and resistance but not tight junction fibril architecture". Am J Physiol Cell Physiol *284*, C1331-1333.
- Seo, K. W., Kwon, Y. K., Kim, B. H., Kim, C. I., Chang, H. S., Choe, M. S., and Park, C. H. Correlation between Claudins Expression and Prognostic Factors in Prostate Cancer. Korean J Urol *51*, 239-244.
- Seo, K. W., Kwon, Y. K., Kim, B. H., Kim, C. I., Chang, H. S., Choe, M. S., and Park, C. H. (2010). Correlation between Claudins Expression and Prognostic Factors in Prostate Cancer. Korean J Urol *51*, 239-244.
- Sheehan, G. M., Kallakury, B. V., Sheehan, C. E., Fisher, H. A., Kaufman, R. P., Jr., and Ross, J. S. (2007). Loss of claudins-1 and -7 and expression of

claudins-3 and -4 correlate with prognostic variables in prostatic adenocarcinomas. Hum Pathol *38*, 564-569.

- Shin, K., Wang, Q., and Margolis, B. (2007). PATJ regulates directional migration of mammalian epithelial cells. EMBO Rep *8*, 158-164.
- Short, S. M., Talbott, G. A., and Juliano, R. L. (1998). Integrin-mediated signaling events in human endothelial cells. Mol Biol Cell *9*, 1969-1980.
- Singh, A. B., and Harris, R. C. (2004). Epidermal growth factor receptor activation differentially regulates claudin expression and enhances transepithelial resistance in Madin-Darby canine kidney cells. J Biol Chem *279*, 3543-3552.
- Sirotkin, H., Morrow, B., Saint-Jore, B., Puech, A., Das Gupta, R., Patanjali, S. R., Skoultchi, A., Weissman, S. M., and Kucherlapati, R. (1997). Identification, characterization, and precise mapping of a human gene encoding a novel membrane-spanning protein from the 22q11 region deleted in velo-cardio-facial syndrome. Genomics *42*, 245-251.
- Soini, Y. (2004). Claudins 2, 3, 4, and 5 in Paget's disease and breast carcinoma. Hum Pathol *35*, 1531-1536.
- Soini, Y., Tommola, S., Helin, H., and Martikainen, P. (2006). Claudins 1, 3, 4 and 5 in gastric carcinoma, loss of claudin expression associates with the diffuse subtype. Virchows Arch *448*, 52-58.
- Soler, A. P., Laughlin, K. V., and Mullin, J. M. (1993). Effects of epidermal growth factor versus phorbol ester on kidney epithelial (LLC-PK1) tight junction permeability and cell division. Exp Cell Res *207*, 398-406.

- Soler, A. P., Miller, R. D., Laughlin, K. V., Carp, N. Z., Klurfeld, D. M., and Mullin, J. M. (1999). Increased tight junctional permeability is associated with the development of colon cancer. Carcinogenesis *20*, 1425-1431.
- Soma, T., Chiba, H., Kato-Mori, Y., Wada, T., Yamashita, T., Kojima, T., and Sawada, N. (2004). Thr(207) of claudin-5 is involved in size-selective loosening of the endothelial barrier by cyclic AMP. Exp Cell Res *300*, 202-212.
- Staehelin, L. A. (1973). Further observations on the fine structure of freeze-cleaved tight junctions. J Cell Sci *13*, 763-786.
- Suen, D., and Chow, L. W. (2006). Prognostic contribution of the HER-2 oncogene overexpression to the Nottingham Prognostic Index in breast cancer. Biomed Pharmacother *60*, 293-297.
- Swift, J. G., Mukherjee, T. M., and Rowland, R. (1983). Intercellular junctions in hepatocellular carcinoma. J Submicrosc Cytol *15*, 799-810.
- Taddei, A., Giampietro, C., Conti, A., Orsenigo, F., Breviario, F., Pirazzoli, V., Potente, M., Daly, C., Dimmeler, S., and Dejana, E. (2008). Endothelial adherens junctions control tight junctions by VE-cadherin-mediated upregulation of claudin-5. Nat Cell Biol *10*, 923-934.
- Tanaka, M., Kamata, R., and Sakai, R. (2005). EphA2 phosphorylates the cytoplasmic tail of Claudin-4 and mediates paracellular permeability. J Biol Chem *280*, 42375-42382.
- Tassi, R. A., Bignotti, E., Falchetti, M., Ravanini, M., Calza, S., Ravaggi, A., Bandiera, E., Facchetti, F., Pecorelli, S., and Santin, A. D. (2008). Claudin-7

expression in human epithelial ovarian cancer. Int J Gynecol Cancer *18*, 1262-1271.

- Tatum, R., Zhang, Y., Lu, Q., Kim, K., Jeansonne, B. G., and Chen, Y. H. (2007). WNK4 phosphorylates ser(206) of claudin-7 and promotes paracellular Cl(-) permeability. FEBS Lett *581*, 3887-3891.
- Tobioka, H., Isomura, H., Kokai, Y., Tokunaga, Y., Yamaguchi, J., and Sawada, N. (2004a). Occludin expression decreases with the progression of human endometrial carcinoma. Hum Pathol *35*, 159-164.
- Tobioka, H., Tokunaga, Y., Isomura, H., Kokai, Y., Yamaguchi, J., and Sawada, N. (2004b). Expression of occludin, a tight-junction-associated protein, in human lung carcinomas. Virchows Arch *445*, 472-476.
- Tokes, A. M., Kulka, J., Paku, S., Szik, A., Paska, C., Novak, P. K., Szilak, L., Kiss, A., Bogi, K., and Schaff, Z. (2005). Claudin-1, -3 and -4 proteins and mRNA expression in benign and malignant breast lesions: a research study. Breast Cancer Res *7*, R296-305.
- Tokunaga, Y., Tobioka, H., Isomura, H., Kokai, Y., and Sawada, N. (2004). Expression of occludin in human rectal carcinoid tumours as a possible marker for glandular differentiation. Histopathology *44*, 247-250.
- Tsukita, S. (1989). Isolation of cell-to-cell adherens junctions from rat liver. J Cell Biol *108*, 31-41.
- Tsukita, S., and Furuse, M. (2000). Pores in the wall: claudins constitute tight junction strands containing aqueous pores. J Cell Biol *149*, 13-16.
- Tsukita, S., Furuse, M., and Itoh, M. (2001). Multifunctional strands in tight junctions. Nat Rev Mol Cell Biol *2*, 285-293.

- Tsukita, S., Yamazaki, Y., Katsuno, T., and Tamura, A. (2008). Tight junction-based epithelial microenvironment and cell proliferation. Oncogene *27*, 6930-6938.
- Turunen, M., Talvensaari-Mattila, A., Soini, Y., and Santala, M. (2009). Claudin-5 overexpression correlates with aggressive behavior in serous ovarian adenocarcinoma. Anticancer Res *29*, 5185-5189.
- Umeda, K., Ikenouchi, J., Katahira-Tayama, S., Furuse, K., Sasaki, H., Nakayama, M., Matsui, T., Tsukita, S., and Furuse, M. (2006). ZO-1 and ZO-2 independently determine where claudins are polymerized in tight-junction strand formation. Cell *126*, 741-754.
- Usami, Y., Chiba, H., Nakayama, F., Ueda, J., Matsuda, Y., Sawada, N., Komori, T., Ito, A., and Yokozaki, H. (2006). Reduced expression of claudin-7 correlates with invasion and metastasis in squamous cell carcinoma of the esophagus. Hum Pathol *37*, 569-577.
- Van Itallie, C. M., and Anderson, J. M. (2004). The role of claudins in determining paracellular charge selectivity. Proc Am Thorac Soc *1*, 38-41.
- Van Itallie, C. M., and Anderson, J. M. (2006). Claudins and epithelial paracellular transport. Annu Rev Physiol *68*, 403-429.
- Van Itallie, C. M., Gambling, T. M., Carson, J. L., and Anderson, J. M. (2005). Palmitoylation of claudins is required for efficient tight-junction localization. J Cell Sci *118*, 1427-1436.
- Van Itallie, C. M., Holmes, J., Bridges, A., and Anderson, J. M. (2009). Claudin-2-dependent changes in noncharged solute flux are mediated by the

extracellular domains and require attachment to the PDZ-scaffold. Ann N Y Acad Sci *1165*, 82-87.

- Van Itallie, C. M., Rogan, S., Yu, A., Vidal, L. S., Holmes, J., and Anderson, J. M. (2006). Two splice variants of claudin-10 in the kidney create paracellular pores with different ion selectivities. Am J Physiol Renal Physiol *291*, F1288-1299.
- Wan, H., Winton, H. L., Soeller, C., Tovey, E. R., Gruenert, D. C., Thompson, P. J., Stewart, G. A., Taylor, G. W., Garrod, D. R., Cannell, M. B., and Robinson, C. (1999). Der p 1 facilitates transepithelial allergen delivery by disruption of tight junctions. J Clin Invest *104*, 123-133.
- Wang, Z., Mandell, K. J., Parkos, C. A., Mrsny, R. J., and Nusrat, A. (2005). The second loop of occludin is required for suppression of Raf1-induced tumor growth. Oncogene *24*, 4412-4420.
- Weber, C., Fraemohs, L., and Dejana, E. (2007). The role of junctional adhesion molecules in vascular inflammation. Nat Rev Immunol *7*, 467-477.
- Weigelt, B., Peterse, J. L., and van 't Veer, L. J. (2005). Breast cancer metastasis: markers and models. Nat Rev Cancer *5*, 591-602.
- Weiner, O. D., Marganski, W. A., Wu, L. F., Altschuler, S. J., and Kirschner, M. W. (2007). An actin-based wave generator organizes cell motility. PLoS Biol *5*, e221.
- Wilcox, E. R., Burton, Q. L., Naz, S., Riazuddin, S., Smith, T. N., Ploplis, B., Belyantseva, I., Ben-Yosef, T., Liburd, N. A., Morell, R. J., *et al.* (2001). Mutations in the gene encoding tight junction claudin-14 cause autosomal recessive deafness DFNB29. Cell *104*, 165-172.

- Wolburg, H., Wolburg-Buchholz, K., Kraus, J., Rascher-Eggstein, G., Liebner, S., Hamm, S., Duffner, F., Grote, E. H., Risau, W., and Engelhardt, B. (2003). Localization of claudin-3 in tight junctions of the blood-brain barrier is selectively lost during experimental autoimmune encephalomyelitis and human glioblastoma multiforme. Acta Neuropathol *105*, 586-592.
- Wu, Q., Liu, Y., Ren, Y., Xu, X., Yu, L., Li, Y., and Quan, C. (2010). Tight junction protein, claudin-6, downregulates the malignant phenotype of breast carcinoma. Eur J Cancer Prev *19*, 186-194.
- Yamamoto, M., Ramirez, S. H., Sato, S., Kiyota, T., Cerny, R. L., Kaibuchi, K., Persidsky, Y., and Ikezu, T. (2008). Phosphorylation of claudin-5 and occludin by rho kinase in brain endothelial cells. Am J Pathol *172*, 521-533.
- Yamauchi, K., Rai, T., Kobayashi, K., Sohara, E., Suzuki, T., Itoh, T., Suda, S., Hayama, A., Sasaki, S., and Uchida, S. (2004). Disease-causing mutant WNK4 increases paracellular chloride permeability and phosphorylates claudins. Proc Natl Acad Sci U S A *101*, 4690-4694.
- Yang, J., Mani, S. A., and Weinberg, R. A. (2006). Exploring a new twist on tumor metastasis. Cancer Res *66*, 4549-4552.
- Ye, L., Martin, T. A., Parr, C., Harrison, G. M., Mansel, R. E., and Jiang, W. G. (2003). Biphasic effects of 17-beta-estradiol on expression of occludin and transendothelial resistance and paracellular permeability in human vascular endothelial cells. J Cell Physiol *196*, 362-369.
- Zeissig, S., Burgel, N., Gunzel, D., Richter, J., Mankertz, J., Wahnschaffe, U., Kroesen, A. J., Zeitz, M., Fromm, M., and Schulzke, J. D. (2007). Changes in

expression and distribution of claudin 2, 5 and 8 lead to discontinuous tight junctions and barrier dysfunction in active Crohn's disease. Gut *56*, 61-72.

- Zen, K., Yasui, K., Gen, Y., Dohi, O., Wakabayashi, N., Mitsufuji, S., Itoh, Y., Zen, Y., Nakanuma, Y., Taniwaki, M., *et al.* (2009). Defective expression of polarity protein PAR-3 gene (PARD3) in esophageal squamous cell carcinoma. Oncogene *28*, 2910-2918.
- Zhan, L., Rosenberg, A., Bergami, K. C., Yu, M., Xuan, Z., Jaffe, A. B., Allred, C., and Muthuswamy, S. K. (2008). Deregulation of scribble promotes mammary tumorigenesis and reveals a role for cell polarity in carcinoma. Cell *135*, 865-878.
- Zheng, J., Xie, Y., Campbell, R., Song, J., Massachi, S., Razi, M., Chiu, R., Berenson, J., Yang, O. O., Chen, I. S., and Pang, S. (2005). Involvement of claudin-7 in HIV infection of CD4(-) cells. Retrovirology *2*, 79.
- Zimmerli, S. C., Kerl, K., Hadj-Rabia, S., Hohl, D., and Hauser, C. (2008). Human epidermal Langerhans cells express the tight junction protein claudin-1 and are present in human genetic claudin-1 deficiency (NISCH syndrome). Exp Dermatol *17*, 20-23.
- Zuker, M. (2003). Mfold web server for nucleic acid folding and hybridization prediction. Nucleic Acids Res *31*, 3406-3415.

- **Electronic references**

Office for National Statistic (2006) Cancer statistics

http://www.statistics.gov.uk/StatBase/Product.asp?vlnk=14209